

629

APPLICATIONS OF NUCLEAR MAGNETIC RESONANCE SPECTROSCOPY
IN ORGANIC AND BIOLOGICAL CHEMISTRY

Submitted in fulfilment of the degree of
Doctor of Philosophy
University of Stirling

Manajit Kaur Hayer

Chemistry Department
University of Stirling

October 1984

4/85

ABSTRACT

Monocyclic derivatives of hydroxylamines were synthesised to investigate their conformations and conformational rate processes. Derivatives of 1,4,2-oxathiazine(1-oxa-4-thia-2-azacyclohexane) were prepared, their conformational equilibria investigated and their rates of nitrogen and ring inversion measured. N-carbethoxy-1-oxa-2-azacyclooctane was prepared and reduced to N-methyl-1-oxa-2-azacyclooctane, whose nitrogen inversion rate was measured. N-carbethoxy-5,5-dimethyl-1-oxa-2-azacyclooctane and N-carbethoxy-6,6-dimethyl-1-oxa-2-azacyclononane were also prepared. Treatment of these compounds led to the formation of N-carbethoxy-2-(aminohydroxy)-3,3-dimethylhexane and N-carbethoxy-2-(aminohydroxy)-4,4-dimethylheptane respectively instead of the N-methyl derivatives. Other attempts to make the N-methyl derivatives also failed.

An investigation of aqueous lanthanide shift reagents for ^{23}Na and ^{39}K was undertaken. The best combinations were found with tripolyphosphate as the ligand in combination with Dysprosium or Terbium. Isotropic hyperfine shifts of up to ca 40 ppm (^{23}Na) and ca 13 ppm (^{39}K) are reported. The shift reagents were used to investigate intracellular Na^+ and K^+ in cellular systems. A quantitation of intracellular ^{39}K in human erythrocytes is reported. The use of these shift reagents in combination with large unilamellar vesicles of egg-yolk phosphatidylcholine is demonstrated to be a viable technique for measuring ionophore mediated membrane transport of Na^+ and K^+ . The monensin mediated transport of Na^+ was studied and shown to be first order in monensin. The transport was inhibited by the substrate itself, in a concentration dependent manner. Two related [15]-crown-5 derivatives were also investigated. The result indicated that anionic ionophores are more efficient in membrane transport than neutral ionophores.

ACKNOWLEDGEMENTS

I wish to thank my supervisor, Dr F G Riddell, for his invaluable patience, guidance and encouragement throughout the past three years.

I also take this opportunity to express my thanks to the members of the Chemistry Department for their interest and helpful suggestions during my period of studies at Stirling. I must also thank the technical staff of the department for being supportive and to Mr G Castle for supplying me with much needed glassware and valuable reagents.

I would also like to thank Dr P Brophy, Dr M North and Dr N J Dix of the Biological Sciences Department for their assistance in the preparation of the cellular systems investigated in this work. Dr Brophy has also to be thanked for his generous donation of egg-yolk phosphatidylcholine, guidance in the preparation of large unilamellar vesicles and numerous helpful discussions.

My thanks are also due to Mr Dance for the recording of mass spectral data, Mr T Forrest for the electron microscopy work, Dr I Sadler and Dr D Reed of the SERC Regional NMR Service of University of Edinburgh for time and assistance with the Bruker WP360 spectrometer and SERC for some nmr financial support.

Especial thanks is due to Mrs P Brown for painstakingly and efficiently typing this manuscript.

Finally, I wish to express my sincere gratitude to my mother for her encouragement and I dedicate this thesis to the memory of my late father, Chain Singh Hayer (1926-1982).

SECTION I APPLICATION OF NUCLEAR MAGNETIC RESONANCE SPECTROSCOPY IN
ORGANIC CHEMISTRY

CHAPTER 1: CONFORMATIONAL ANALYSIS OF SIX-MEMBERED AND LARGER
RING HYDROXYLAMINE DERIVATIVES

	<u>Page</u>
1.1 Introduction	1
1.2 Conformation Directing Forces	2
1.3 Nitrogen Inversion	5
1.4 The Conformations of Hydroxylamine Derivatives	8
1.4.1 Acyclic Compounds	9
1.4.2 Cyclic Derivatives	12
a. Three-membered Rings	12
b. Four-membered Rings	12
c. Five-membered Rings	13
d. Six-membered Rings	
(i) Tetrahydro-1,2-Oxazine	13
(ii) Tetrahydro-1,4,2-Dioxazine	16
(iii) Tetrahydro-1,2,4-Oxadiazine	17
(iv) Tetrahydro-1,2,5-Oxadiazine	17
e. Seven-membered Rings	18
1.5 Eight-membered Rings	20
1.6 Nine-membered Rings	21
1.7 Conclusion	22

CHAPTER 2: RESULTS, ANALYSIS AND DISCUSSION OF SYNTHESSES, ^1H and ^{13}C NUCLEAR MAGNETIC RESONANCE SPECTRA AND CONFORMATIONAL EQUILIBRIA OF HYDROXYLAMINE DERIVATIVES

	<u>Page</u>	
2.1	Synthesis of Hydroxylamine Derivatives	
2.1.1	1-Oxa-4-Thia-2-Azacyclohexanes	24
2.1.2	Eight- and Nine-membered Hydroxylamine Derivatives	25
	a. Bromination of α - or β -substituted dimethyl diols	26
	b. Baeyer Villiger Oxidation	26
	c. Reactions of N-Hydroxyurethane with Dibromides	27
	d. Reduction of the N-Carbethoxy Group	30
	e. Acid Hydrolysis of the N-Carbethoxy Group	31
	f. Base Hydrolysis of the N-Carbethoxy Group	31
2.1.3	Conclusion	32
2.2	Nuclear Magnetic Resonance Spectroscopy in Conformational Analysis	
2.2.1	Introduction	33
2.2.2	^1H Nuclear Magnetic Resonance Spectroscopy	34
	a. Proton-Proton Coupling	35
	b. Lineshape Analysis	37
2.2.3	^{13}C Nuclear Magnetic Resonance Spectroscopy	40
2.2.4	Conclusion	42
2.3	The ^1H and ^{13}C Nuclear Magnetic Resonance Spectra and Conformational Equilibria of Hydroxylamine Derivatives: Results, Analysis and Discussion	43
2.3.1	Introduction	43
2.3.2	1-Oxa-4-Thia-2-Azacyclohexanes	
	a. Spectral Assignments	44
	b. Coupling Constants	46
	c. Conformational Equilibria	47

	<u>Page</u>
2.3.3 N-Methyl-1-Oxa-2-Azacyclooctane	
a. Spectral Assignments	52
b. Conformational Equilibria	52
2.3.4 Conclusion	53
<u>CHAPTER 3:</u> EXPERIMENTAL	
3.1 General Notes	56
3.2 Synthesis of 1-Oxa-4-Thia-2-Azacyclohexanes	57
3.3 Synthesis of N-Methyl-1-Oxa-2-Azacyclooctane	75
3.4 Synthesis of N-Carbethoxy-5,5-Dimethyl-1-Oxa-2-Azacyclooctane	80
3.5 Synthesis of N-Carbethoxy-6,6-Dimethyl-1-Oxa-2-Azacyclononane	87
REFERENCES	100
<u>SECTION II</u> <u>APPLICATION OF NUCLEAR MAGNETIC RESONANCE SPECTROSCOPY IN</u> <u>BIOLOGICAL CHEMISTRY</u>	
<u>CHAPTER 1:</u> BIOLOGICAL MEMBRANES AND PARAMAGNETIC LANTHANIDE SHIFT REAGENTS IN NUCLEAR MAGNETIC RESONANCE SPECTROSCOPY	
1.1 Introduction	113
1.2 Biological Membranes	
1.2.1 The Molecular Organisation of Membranes	115
1.2.2 Chemical Composition	118
a) Membrane Lipids	118
b) Membrane Proteins	121

	<u>Page</u>
1.2.3 Membrane Transport	122
a) Passive Diffusion	124
b) Facilitated Diffusion	127
(i) Protein Carriers	128
(ii) Non-Protein Carriers - Ionophores	129
c) Active Transport	135
1.3 Paramagnetic Lanthanide Shift Reagents in Nuclear Magnetic Resonance Spectroscopy	140
1.3.1 Induced Shifts and Complex Formation Equilibria	144
1.3.2 Chemical Shifts in Paramagnetic Lanthanide Complexes	145
1.3.3 Nuclear Relaxation in Lanthanide Complexes	149
1.4 Conclusion	150

CHAPTER 2: DISCUSSION

2.1 Shift Reagents for ^{23}Na and ^{39}K NMR.	
2.1.1 Introduction	152
2.1.2 Discussion of Results	153
2.1.3 Conclusion	160
2.2 ^{23}Na NMR Studies of Ion Transport across the Membrane of Large Unilamellar Phosphatidylcholine Vesicles.	
2.1.1 Introduction	164
2.1.2 Discussion of Monensin Mediated Transport	168
2.2.3 Discussion of Crown-ether Mediated Transport	174
2.2.4 Conclusion	177

CHAPTER 3: EXPERIMENTAL

3.1 General Notes	180
-------------------	-----

	<u>Page</u>	
3.2	Lanthanide Induced Shifts	
3.2.1	Dysprosium as the Lanthanide	181
3.2.2	Lanthanum as the Lanthanide	187
3.2.3	Praseodymium as the Lanthanide	187
3.2.4	Terbium as the Lanthanide	187
3.2.5	Ytterbium as the Lanthanide	188
3.3	Attempted Synthesis of the Hexasodium Chelidamate Complex of Dysprosium: $\text{Na}_6\text{Dy}(\text{CA})_3 \cdot 3\text{NaCl}$	189
3.4	Measurement of Intracellular Concentrations: Cellular Systems	189
3.4.1	Human Erythrocytes	190
3.4.2	Baker's yeast (<u>Saccharomyces cerevisiae</u>)	192
3.4.3	<u>Escherichia coli</u>	193
3.4.4	<u>Tetrahymena pyriformis</u>	193
3.5	Measurement of Ionophore Mediated Sodium Ion Transport in Large Unilamellar Phospholipid Vesicles	194
3.5.1	Monensin Mediated Sodium Ion Transport	
	(a) Lineshape Analysis	196
	(b) Magnetization Transfer	197
3.5.2	[15]-Crown-5 Derivatives Mediated Sodium Ion Transport	199
3.6	Electron Microscopy	200
	REFERENCES	201

SECTION I

APPLICATION OF NUCLEAR MAGNETIC RESONANCE SPECTROSCOPY
IN ORGANIC CHEMISTRY

CHAPTER 1

Conformational Analysis of Six-membered and Larger Ring
Hydroxylamine Derivatives

CHAPTER 1

1.1 INTRODUCTION

What is conformational analysis? The fundamental tenet of conformational analysis, as suggested by Barton and Cookson,¹ is that the chemical and physical properties of organic molecules depend not only on their gross structure and stereochemistry but also on the conformations they prefer to adopt.

The origins of conformation analysis, which is considered as one of the most important branches of stereochemistry, may be found in the work of Sachse.^{2,3} He was the first to suggest that cyclohexane could exist in two possible arrangements, free from angle strain, and which were later named chair and boat conformations. Sachse's theories were confirmed by the work of Hückel on cis and trans decalins and later by the work of Hassel on X-ray and electron diffraction of substituted cyclohexanes, and by the work of Pitzer⁶ on the shape and thermodynamic properties of cyclohexane derivatives. However, the actual start of conformational analysis may be considered to be the classical paper of Barton⁷ in 1950, which introduced the concept of conformational analysis and pointed out some basic relationship between conformation and chemical reactivity.

What then are conformations? This question is best answered by placing the term "conformation" in the context of stereochemistry as a whole. The most adequate definition of what constitutes a conformation is that given by Riddell.⁸ It states that, "Conformations are stereoisomers that can be interconverted either by rotation about bonds of order approximately one, with any concomitant small distortions of bond lengths and angles, or by inversion at a three-coordinate centre in the molecule, or by pseudorotation on phosphorus." This definition

allows us to treat conformations in the same light as stereoisomers - as an assembly of molecules occupying a potential energy minimum. Those forms of molecules which do not have a finite existence,^{9,10} and in fact correspond to transition states, for example eclipsed ethane, do not fall under the definition.

The above definition includes not only conformational inter-conversions based on bond rotation, but also those which involve ring or nitrogen inversion, and applies equally to alicyclic and heterocyclic compounds.¹¹⁻¹³

1.2 CONFORMATION DIRECTING FORCES

The conformations of molecules, and the shapes and magnitudes of the barriers separating these conformations, depend on several factors. In six-membered ring systems the preferred conformation is commonly determined by the following factors:

- i) Torsional forces
- ii) Non-bonded interactions
- iii) Bond-stretching
- iv) Bond-angle deformation
- v) Electrostatic interactions
- vi) Solvent effects
- vii) Hydrogen bonding
- viii) Resonance effects

Considerable effort has been put into devising functions which describe the way molecular energy varies with headings (i)-(iv).¹⁴⁻¹⁹ Although functions are available for electrostatic interactions, they are mainly useful for qualitative rather than quantitative interpretation. Progress is being made on the evaluation of solvent effects on conformational equilibria. However, attempts at estimations of hydrogen

bonding and resonance effects are at present strictly enlightened guesses, although some molecular orbital (MO) calculations on hydrogen bonding have been successful.²⁰

The discussion which follows is an attempt to give a general picture of the way in which molecular energy changes with geometry.

The torsional strain is the 1,2-interaction between non-bonded atoms or groups which arises in less energetically favourable conformations. In butane, for example, the gauche conformation is less energetically favourable than the staggered conformation (Fig. 1.1). The energy difference between the more and less energetically favoured conformations implies a torsional potential opposing rotation about individual bonds in the ring skeleton. The torsional energy ($E(\theta)$) is a function of the torsion angle (θ) (dihedral angle) or projected valency angles between bonds attached to adjacent linked atoms (Fig. 1.1). For example, the torsion angles (θ) in staggered and eclipsed ethane are 60° and 0° respectively.

Non-bonded interactions, usually observed as 1,3-interactions between atoms or groups that are not directly bonded, will lead to relatively strong repulsion if the intermolecular distance between these atoms is smaller than the sum of the van der Waals radii of the atoms concerned. It should be noted, however, that the van der Waals radius of an atom is affected by the other atoms to which it is bonded and the nature of the bonding.

Deformations of conformations due to bond stretching are generally very small due to the large force constant involved. Bond length changes, due to conformational strains, are proportionately smaller than other molecular deformations; for example, it may be calculated¹⁶ that a stretching of 1 picometer (1pm) in a C-C bond (ca 0.7% change) would introduce ca $0.3 \text{ kcal mol}^{-1}$ strain. A similar amount of strain would

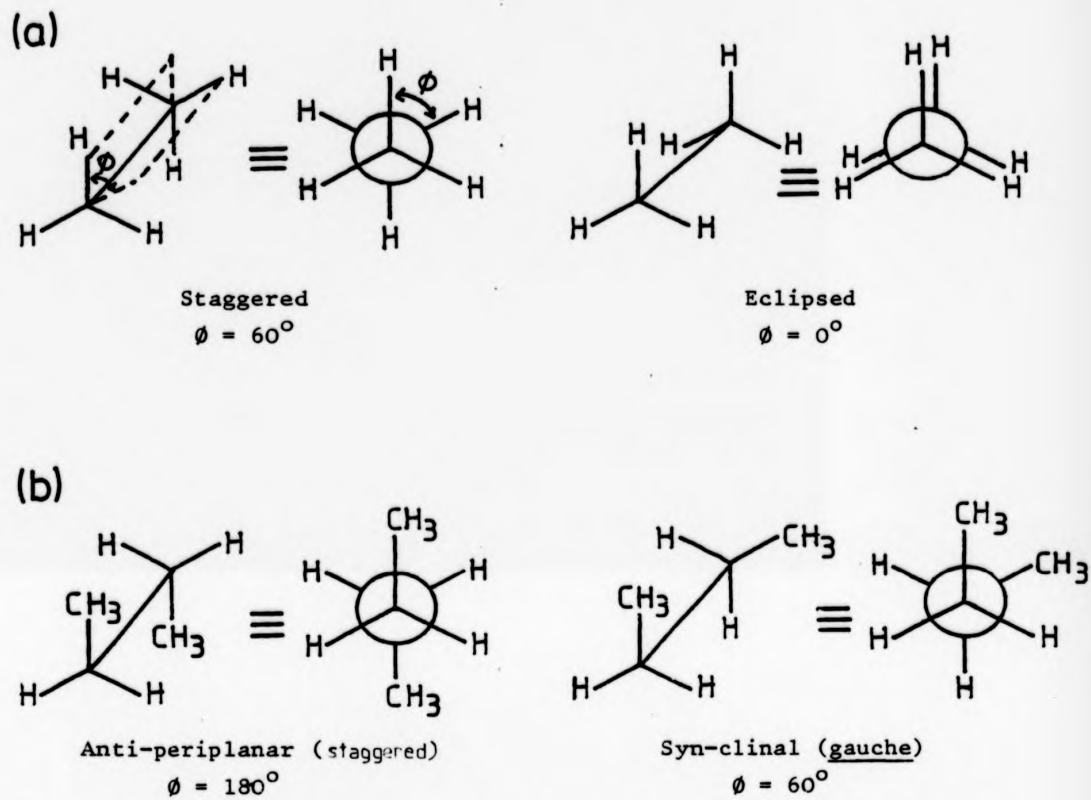


Fig 1.1 Saw-horse and Newman projection formulae for (a) ethane and (b) butane, demonstrating torsion angle (ϕ).

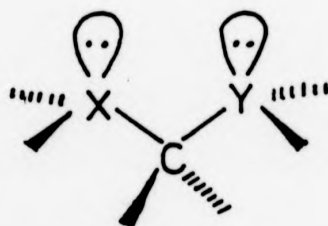


Fig 1.2 The "Rabbit Ear" Effect (X and Y are heteroatoms).

change a C-C-C bond angle by a much larger proportion (ca 4%). Thus strain induced bond length changes are proportionately smaller than other deformations.

Bond angle strain is usually associated with a potential energy increase which arises from the deformation of the valence angle from the angle preferred in unstrained acyclic hydrocarbons (ca 112.7°). It is commonly accepted for C-C-C angles that the original undeformed angle is not taken as tetrahedral (109.5°), but rather as the angle in acyclic hydrocarbons (ca 112.7°), as this tends to give better agreement between calculation and experiment.¹⁶ It is reasonably cheap in energy to deform bond angles, and as shown above proportionately considerably cheaper than stretching bonds. Much of the conformational strain in a molecule will thus be accommodated, if possible, in the form of deformed bond angles.

In conformational analysis, the two main types of polar groupings are: charged atoms or groups as in an ammonium ion, and polar bonds as in C-halogen. These different charged entities give rise to three main types of electrostatic interaction: charge-charge, charge-dipole, and dipole-dipole. The higher the order of the pole involved the more rapidly the interactions fall off with distance.

The presence of more than one heteroatom in a system gives rise to interactions between the dipoles of the heteroatomic lone pairs. The interactions resulting from the conformation in Fig. 1.2, which has two syn-axial lone pairs, the "rabbit ear" effect,²¹ is unfavoured. Eliel suggests the principal cause of this effect to be electrostatic dipole-dipole interactions,²¹ but this view has been questioned by Wolfe et al²² who say "analyses of the phenomenon in terms of 'dipole-dipole' repulsive interactions are without theoretical justification", and consider such phenomena in terms of the total potential energy of the

system.

The overall dipole moment of a molecule, however, can provide information about its conformation.²³ Conformations that lack any symmetry, or fall into point groups C_n , C_{nv} or C_s , must possess permanent dipole moments. Conformations in other point groups can have no dipole moment. The time average of the conformations determines the observed dipole moment. Conformational results derived from dipole moment studies must be treated with some caution as dipole moment technique has given results that have been shown to be quantitatively or even qualitatively incorrect.²⁴

Torsional potentials about heteroatom-heteroatom bonds are very different from those about carbon-carbon or carbon-heteroatom bonds. Thus, the introduction of a heteroatom-heteroatom bond into a molecule will have two possible conformational effects; first, the barrier to any torsional processes about the bond will be raised, and secondly, the torsion angle about these bonds when incorporated into molecules will be altered to accommodate the different position of minimum strain energy. Both the enhancement of the ring inversion barrier and the alteration of ring dihedral angle from "normal" values are shown very nicely in the studies of cyclic hydrazines by Nelson and co-workers.²⁵ However, the presence of the heteroatom nitrogen introduces, in addition, the conformational effect of nitrogen inversion which is discussed in the following sub-section.

1.3 NITROGEN INVERSION

The tri-coordinate nitrogen atom, possessing one unshared lone pair of electrons, has an overall pyramidal geometry (sp^3) in the ground state, and can exist in two potentially enantiomeric forms which may interconvert at room temperature by passing over an energy barrier

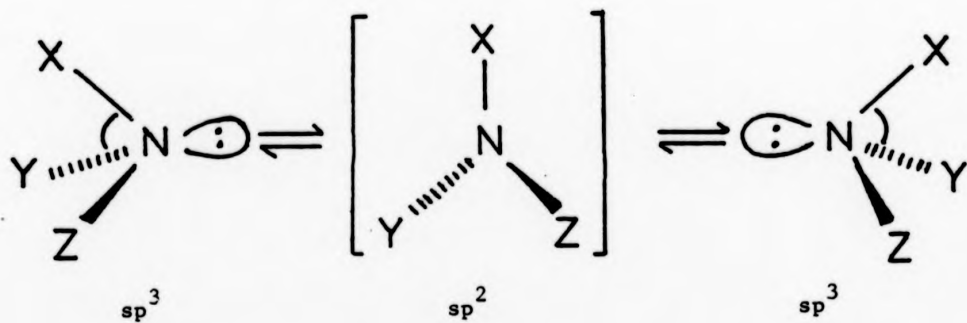
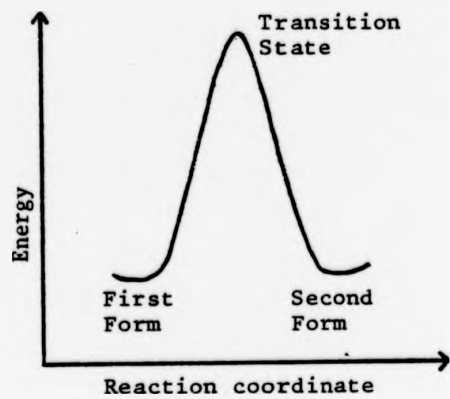
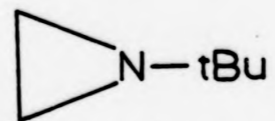


Fig 1.3 Nitrogen inversion and the potential energy profile for nitrogen inversion.

(transition state) in which the nitrogen is planar (sp^2).²⁶⁻³¹ This process, known as nitrogen inversion, has been called "pyramidal atomic inversion" by J B Lambert³² (Fig. 1.3).

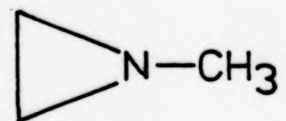
Both steric and electronic factors influence nitrogen inversion barriers. Steric effects stem mainly from non-bonded interactions in the ground state (GS) causing a decrease in the inversion barrier. A good example being the N-tert butyl group in the aziridine (1) which has greater repulsive interactions with the ring hydrogens in the ground state than the corresponding methyl derivative (2). Such repulsions are partially relieved in the transition state (TS) by the opening of the angle θ .³³ On the other hand, angular strain increases the inversion barrier (compare the derivatives 2 and 3). Since the inversion process has a planar transition state, the angle, θ in Fig. 1.3 must open to ca 120° . In the three-membered aziridine ($\theta \sim 60^\circ$) such an opening is prevented, whereas in the five-membered ring ($\theta \sim 105 - 110^\circ$)^{30,34} it is not. Thus the value of the angle at the nitrogen atom depends on the nature of the cyclic system.^{33,35-38} In these cases, the barrier increase in three- and four-membered rings is due to enhanced strain in the transition state compared to larger rings or to acyclic systems.

Electronic changes brought about by atoms or groups directly linked to the inverting nitrogen atom can affect the inversion barrier significantly. The principal electronic factors influencing barrier heights are conjugation and heteroatom substitution.³⁹ Both (p-p) π conjugation of, for example, a carbonyl or aromatic system, or (p-d) π conjugation of a second row element having low lying d orbitals, with the nitrogen atom lowers the inversion barrier, since the p orbital of the transition state can overlap with such systems to a greater extent than an sp^3 hybridised lone pair. As a result, the nitrogen site becomes less pyramidal and consequently the nitrogen inversion barrier



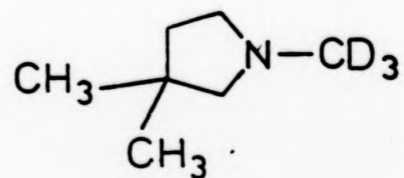
(1)

$$\Delta G_{NI}^{\ddagger} = 17.0 \text{ kcal mol}^{-1}$$



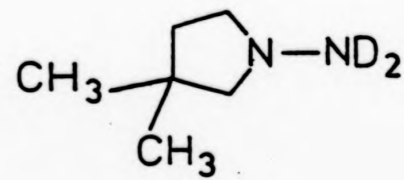
(2)

$$\Delta G_{NJ}^{\ddagger} = 22.3 \text{ kcal mol}^{-1}$$



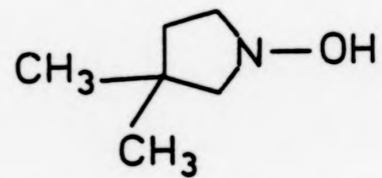
(3)

$$\Delta G_{NI}^{\ddagger} = 7.4 \text{ kcal mol}^{-1}$$



(4)

$$\Delta G_{NI}^{\ddagger} = 8.5 \text{ kcal mol}^{-1}$$



(5)

$$\Delta G^{\ddagger} = 13.0 \text{ kcal mol}^{-1}$$

decreases. The amount of this decrease depends on the size and conjugative ability of the group.^{40,41}

Heteroatom substitution, on the other hand, gives rise to electronegativity and electron repulsive effects both of which can increase the barrier (3, 4, 5).⁴²⁻⁴⁴ If the substituent is more electronegative than nitrogen an increase in the 's' character of the nitrogen lone pair results from a negative inductive effect, and since the lone pair passes through a 'p' orbital in the TS, a barrier increase occurs. Similarly, an electropositive substituent leads to a barrier decrease.⁴²

The nature of the medium may also affect the height of a nitrogen inversion barrier. As the ground state for a simple amine is more polar than the transition state, increasing the solvent polarity should stabilize the ground state and increase the inversion barrier.^{29,30} An increase of the inversion barrier due to a change in the polarity of the solvent is also evidence that the observed conformational change is nitrogen inversion and not ring inversion.⁴⁵ This criterion should, however, be applied with caution as it has been observed that the barrier to nitrogen inversion sometimes decreases with polarity or is relatively insensitive to solvent.²⁷ In solvents capable of hydrogen bonding such as water or methanol, the formation of a hydrogen bond to the nitrogen lone pair should also stabilize the GS and increase the inversion barrier.^{29,39} This may be used to identify the observed conformational process.³⁰ During nitrogen inversion a hydrogen bond must be broken but not necessarily in the case of ring inversion.²⁸

The magnitude of nitrogen inversion barriers have a wide range and can be measured by a variety of techniques. Nuclear magnetic resonance (nmr) spectroscopy involving line-shape changes with temperature probably

provides the greatest amount of information on barriers in the 6-25 kcal mol⁻¹ range.^{46,47}

1.4 THE CONFORMATIONS OF HYDROXYLAMINE DERIVATIVES

There are two fundamental sources of difference between heterocyclic and carbocyclic conformational analysis. Firstly, a change in the geometry of the ring is expected from the different bond angles and lengths involved, and secondly the substitution of a heteroatom has several electronic effects, including for nitrogen containing compounds the phenomenon of nitrogen inversion.

On the basis of experimental data obtained from investigated oxygen,^{48,49} nitrogen,^{27,45,50,51} and sulphur^{52,53} containing compounds, it has been shown that the energy barrier to ring inversion in six-membered heterocyclic compounds depended on several different factors. In fact, the kind of heteroatom, the number and relative position of heteroatoms in the ring, as well as the number and nature of the substituents attached to carbon atoms in the ring, play significant roles in the determination of the energy barrier. In the case of nitrogen heterocycles an additional factor is also the nature and size of the substituent attached to the nitrogen atom.

The presence of the oxygen atom adjacent to nitrogen in the tetrahydro-1,2-oxazine ring system serves to slow the rate of nitrogen inversion. This has had two important uses. Firstly, six-membered rings containing an N-O bond and a further heteroatom have proved valuable for examining the effects of heteroatoms at various positions in the ring on the rates of nitrogen inversion.⁵⁴ Secondly, due to the high conformational free energy difference of the N-methyl group arising in large measure from torsion about the N-O bond (vide infra), freezing out of the N-methyl inversion is a convenient way to obtain slow

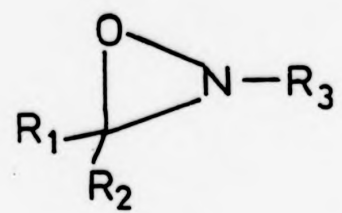
conformational exchange. This results in the observation of cis and trans isomers with equatorial N-methyl groups, allowing studies of individual conformers and positions of conformational equilibria to be made. Hydroxylamine derivatives have thus contributed considerably to our knowledge of the conformational analysis of both acyclic and cyclic systems.

Experimental⁵⁵ and theoretical⁵⁶⁻⁶¹ investigations of barriers to conformational changes in acyclic and cyclic hydroxylamines have been extensively carried out. In essence two conformational processes are important, namely, inversion at the nitrogen atom and rotation about the N-O bond. In the case of three-, four- and five-membered cyclic hydroxylamines, this latter process cannot be rate-determining since almost all rotation about the N-O bond is prohibited by the geometric constraints of these ring systems. Numerous nitrogen inversion barriers have been measured in these ring systems, particularly for substituted oxaziridines (6);^{55,62-64} which exhibit the largest nitrogen inversion barrier of 25-32 kcal mol⁻¹. In the case of tetrahydro-1,2-oxazolidines (7) which have been measured, the barriers to nitrogen inversion are much lower, in the range of 11-16 kcal mol⁻¹.^{35,65}

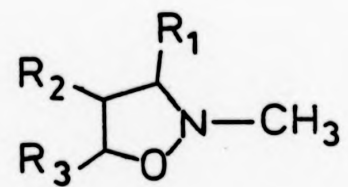
It is the purpose of this sub-section to review ring size effects, substituent effects and heteroatom effects on the conformational analysis of organic derivatives of hydroxylamine.

1.4.1 Acyclic Compounds

When dealing with hydrocarbons the concept of three-fold barrier to rotation is so deeply implanted in the minds of organic chemists, that many automatically assume the anti-periplanar and syn-clinal conformations as in butane (Fig 1.1) must inevitably be involved, and that perfectly staggered conformations are invariably energy minima,



(6)



(7)

whenever rotation about a single bond in an organic molecule occurs.

However, evidence for the conformational behaviour of hydroxylamine, from both molecular orbital calculations and experiments show that hydroxylamine has two maxima and two minima on its potential function for N-O bond rotation and the barrier is several times larger than in ethane and related compounds.

In 1967, Pedersen and Morukama,⁵⁶ and Fink, Pan and Allen⁵⁷ published results of MO calculations which were similar and showed that the molecular energy varied with N-O bond rotation as shown in Fig 1.4. The barriers to rotation were calculated to be 11.95 kcal mol⁻¹ and 1.16 kcal mol⁻¹. The two conformations were thus calculated to be 10.79 kcal mol⁻¹ apart.⁵⁷ The stable conformation was seen to be (8), with the lone pairs and bonds formally eclipsed, in which lone pair - lone pair electron repulsions are minimised. While the less stable conformation (10) has the formal bonds and lone pairs staggered. The other staggered arrangement (9) does not occupy a potential energy minimum. Experimental evidence on hydroxylamine qualitatively confirms the result of the MO calculations. The infrared (IR) study by Giguere and Liu⁶⁶ and the microwave investigation by Tsunekawa⁶⁷ are both in accord with the trans conformation (8) being strongly preferred for the parent compound. This preferred rotamer is also in complete accord with dipole moment measurements⁶⁸ and with electron diffraction study on N,N,O-trimethyl-, N,O-dimethyl-, and O-methylhydroxylamines.⁶⁹ The electron diffraction⁶⁹ study shows the N-O bond lengths in the three hydroxylamines to be 150.0 (+0.8), 148 (+0.8) and 146.4 (+0.3) pm respectively, which are only slightly longer than the value of 145pm reported from the X-ray analysis of N-methylhydroxylamine hydrochloride.⁷⁰

The nmr spectra of many derivatives of hydroxylamine show a

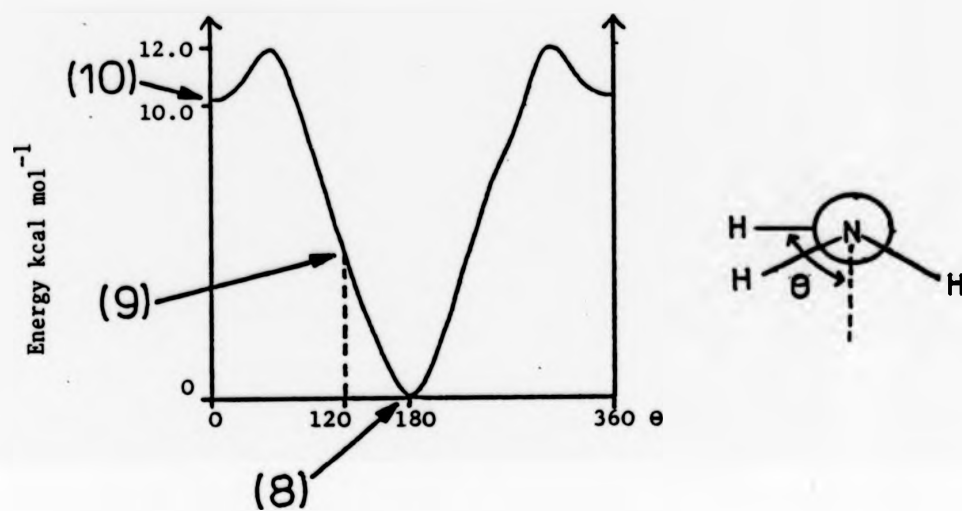
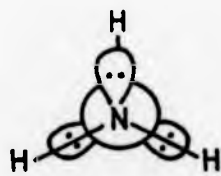
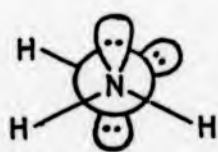


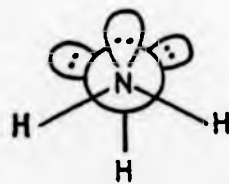
Fig 1.4 Barrier to rotation about the N-O bond in hydroxylamine from MO calculations.⁵⁷



(8)



(9)

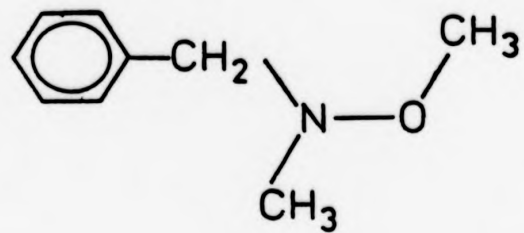


(10)

temperature dependence attributable either to N-O bond rotation or to inversion at nitrogen. Griffith and Roberts⁷¹ studied the process observed in (11) and ascribed it to nitrogen inversion. Other workers^{72,73} questioned this view and with the earlier sets of MO calculations^{56,57} to refer to, they pointed out that the total inversion path is as in Fig 1.5. The observed conformers a and a* are enantiomeric and therefore the methylene hydrogens in the benzyl group become diastereotopic when either nitrogen inversion (NI) or N-O bond rotation (BR) becomes slow on the nmr time scale. They observed a small steric retardation of the rate-limiting process which was consistent with it being bond rotation.

Work by Fletcher and Sutherland⁷⁴ supported the view for nitrogen inversion as the origin of the observed process. They noted that the observed barrier changed very little when the size of the O-substituent was reduced from alkyl or acyl to hydrogen. Such changes would be expected to cause substantial variations in the barrier were it due to N-O bond rotation. These views were also supported by a subsequent publication from Roberts' group.⁷⁵ The most recent work on trialkylhydroxylamines also comes down firmly on the side of nitrogen inversion being a slower process than bond rotation.⁷⁶

Although the above results for trialkyl derivatives point strongly to a slow nitrogen inversion process, inclusion of the nitrogen atom in a conjugated system such as an amide, a urethane or a pyridone causes N-O bond rotation to become the rate-limiting step. Price and Sutherland⁷⁷ found a barrier of 10 kcal mol⁻¹ for the compounds (12) while Raban and Kost⁷⁸ found a barrier of 10 kcal mol⁻¹ for (13a) and estimated barriers of 8-9 kcal mol⁻¹ for (13b) and (14). Work by Riddell and Turner⁷⁹ on N-O bond rotation gave barriers of ca 15 kcal mol⁻¹ for compounds of the type (15) and demonstrated that steric



(11)

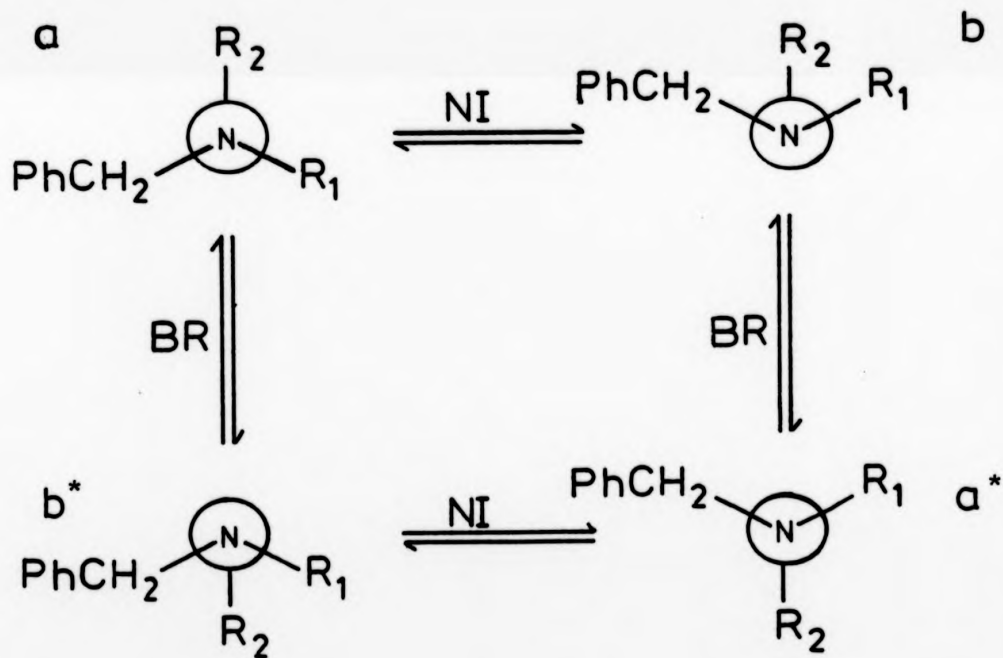
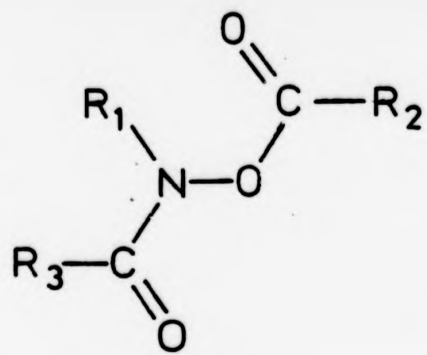
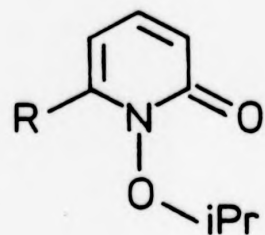


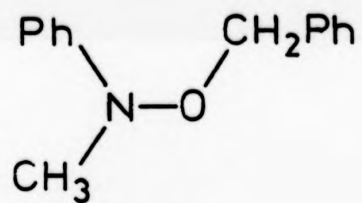
Fig 1.5 Bond rotation and nitrogen inversion pathways in N-benzyl-N,O-dialkylhydroxylamines.^{70,71}



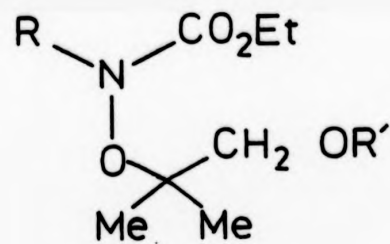
(12)



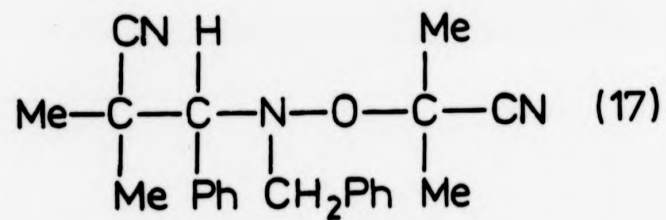
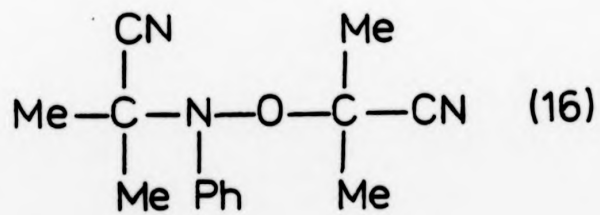
(13) a R=Cl
b R=H



(14)



(15)



effects were important in increasing the barrier. The most recent work on N-O bond rotation barriers comes from Iwamura and coworkers⁸⁰ who found barriers of 12.5 kcal mol⁻¹ and 15.2 kcal mol⁻¹ for the compounds (16) and (17) respectively.

1.4.2 Cyclic Derivatives

In cyclic derivatives of hydroxylamine, nitrogen inversion becomes the dominating slow rate process. Considerable work has been carried out in recent years in the field of cyclic hydroxylamine derivatives, ranging from three-membered rings up to seven-membered rings, their barrier to nitrogen inversion being analysed and recorded.^{8,81-86} Table 1.1 illustrates a limited number of the cyclic derivatives that have been investigated whose barriers are of relevance to this thesis.

a) Three-membered Rings

Oxidation of imines with optically pure peracids such as (+)-peroxycamphoric acid gives rise to optically active oxaziridines such as (18) and (19).^{37,87} These compounds were optically active because nitrogen inversion is slowed both by the adjacent O atom and by inclusion in a three-membered ring.³² It proved possible to study the rate of inversion of the N atom by following the racemisation of (18) at elevated temperatures.³⁷ The rate of the inversion process is appreciably more rapid when the N-alkyl group is tertiary-butyl ($\Delta H^\ddagger = 27.7$ kcal mol⁻¹) rather than a methyl group ($\Delta H^\ddagger = 34.1$ kcal mol⁻¹), a result attributed to steric hindrance in the ground state of the tertiary-butyl derivative raising its energy and lowering the barrier.

(b) Four-membered Rings

Lee and Orrell⁸⁸ studied the nitrogen inversion barriers in the fluorinated oxazetidines (20-23) and free energies of activation of ca 10 kcal mol⁻¹ were deduced. From studying the ¹⁹F nmr and comparing this with other species it was shown that fluoroalkyl groups tend to

TABLE 1.1 Energies of Activation for a Series of Cyclic Derivatives of Varying Ring Size.

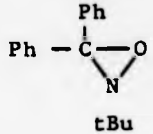
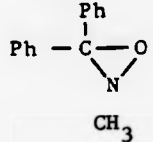
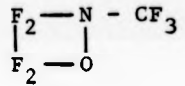
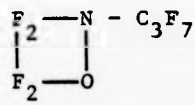
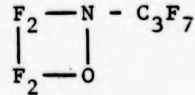
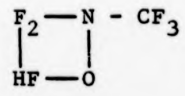
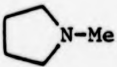
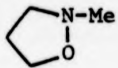
Compound	Number	Solvent	NI Barrier kcal mol ⁻¹	RI Barrier kcal mol ⁻¹	T _G ^o C	Ref
	18		$\Delta H^\ddagger = 27.7$			37
	19		$\Delta H^\ddagger = 34.1$			37
	20		$\Delta G^\ddagger = 10.0$		ca -30	32,88
	21		$\Delta G^\ddagger = 10.0$		ca -30	
	22		$\Delta G^\ddagger = 10.0$		ca -30	
	23		$\Delta G^\ddagger = 10.0$		ca -30	
	24		$\Delta G^\ddagger = 8.1$		-100	89,90
	25	CDCl ₃	$\Delta G^\ddagger = 15.6 \pm 0.5$		42 [±] 5	65

TABLE 1.1 (contd.)

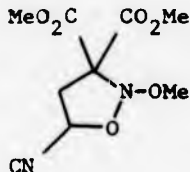
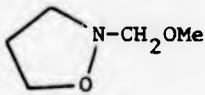
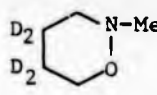
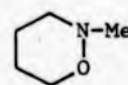
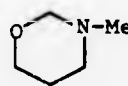
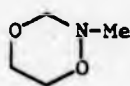
Compound	Number	Solvent	NI Barrier kcal mol ⁻¹	RI Barrier kcal mol ⁻¹	T _G ^o C	Ref
	26		E _a = 29.2			44
	27		ΔG [‡] = 10.3		-74	36
	28		ΔH [‡] = 15.1 [±] 0.4 ΔS [‡] = 2.3 [±] 1.5 cal mol ⁻¹ K ⁻¹		-18	65,97
	29	CH ₂ Cl ₂	ΔG [‡] = 13.7 [±] 0.5		5 [±] 5	65,97
	30	CF ₂ Cl ₂	ΔG ^o = 0.0 [±] 0.35 ΔG [‡] = 7.6		-85	107 8
				ΔG [‡] = 10.0		96,152
	31	CDCl ₃	ΔG [‡] = 11.4 [±] 0.2 ΔG ^o = 0.93 [±] 0.05 or 1.03	ΔG [‡] = 10.9 [±] 0.2	-39 [±] 3 -61 [±] 3 -80 -82	106 106 } 105,106

TABLE 1.1 (contd.)

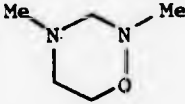
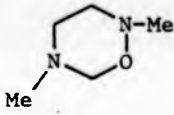
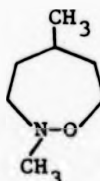
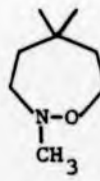
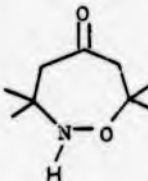
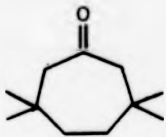

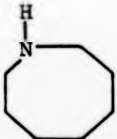
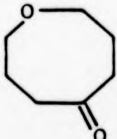

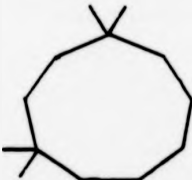
Compound	Number	Solvent	NI Barrier kcal mol ⁻¹	RI Barrier kcal mol ⁻¹	T _G ^o C	Ref
	32	CDCl ₃	N ₂ inversion:- ΔG ^o =1.6 [±] 1 (ax→ts)ΔG [‡] =11.3 [±] 2 ∴(eq→ts)ΔG [‡] =12.9		-20 -20 -8 [±] 3	111,115
			N ₄ inversion:- ΔG ^o =0.6-0.9 (ax→ts)ΔG [‡] =7.0 [±] 2 ∴(eq→ts)ΔG [‡] =7.4-7.9		-112 -112	
	33	Toluene-D ₈	ΔH [‡] =14.4 [±] 0.1 ΔS [‡] =-1.2 [±] 0.4 cal mol ⁻¹ K ⁻¹ ΔG [‡] =14.6 [±] 0.2		22 [±] 2	111,112 115-117
	34	CDCl ₃	ΔG [‡] =12.85		-18	129
	35	CDCl ₃	ΔG [‡] =12.09		-18	129
	36			ΔG [‡] =19.2 [±] 0.5	+101	126

TABLE 1.1 (contd.)

Compound	Number	Solvent	NI Barrier kcal mol ⁻¹	RI Barrier kcal mol ⁻¹	T _G ^o C	Ref
	37			$\Delta G^\ddagger = 8.5$	-80	126
	38			Boat-chair to crown:- $\Delta H^\circ = 1.9$ $\Delta G^\ddagger = 11.2$ $\Delta S = 1^\ddagger \text{leu}$	-45	135
	39			Boat-chair to crown: $\Delta G^\ddagger = 10.5 \pm 0.2$ $\Delta G^\circ = 1.2 \pm 0.1$ $\Delta G_{RI}^\circ = 7.3 \pm 0.2$		138
	40			$\Delta G_{RI}^\ddagger = 37.6$		147
	41			$\Delta G_{RI}^\ddagger = 9.0$		48
	42			$\Delta G_{RI}^\ddagger = 14.0$		151

increase the rate of nitrogen inversion and lower the barrier.³²

(c) Five-membered Rings

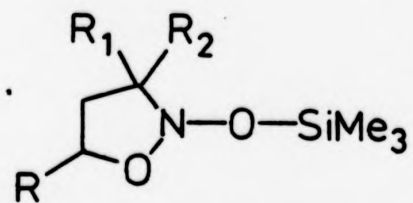
Interest in five-membered rings containing an N-O bond has largely centred around the measurement of nitrogen inversion rates and a study of the effects of substituents on such a process.⁸ α -Oxygen atoms tend to raise the barrier and hence slow its rate, which is well illustrated by a comparison of the barriers in (24) ΔG^\ddagger ca 8.1 kcal mol⁻¹,^{89,90} (25) ΔG^\ddagger ca 15.6 kcal mol⁻¹,⁶⁵ and (26) E_a ca 29.2 kcal mol⁻¹.⁴⁴

In the former cases the barrier is between two equi-energetic conformations. In the latter, two diastereoisomeric forms are involved. When the methyl group in (24) is replaced by the more bulky isopropyl group, the rate is found to decrease as is also the case with the β -oxygen atom in (27) ΔG^\ddagger ca 10.3 kcal mol⁻¹.³⁶ Conformational studies on some N-trimethylsilyoxy-isoxazolidines (43) have also been reported.⁹¹

(d) Six-membered Rings

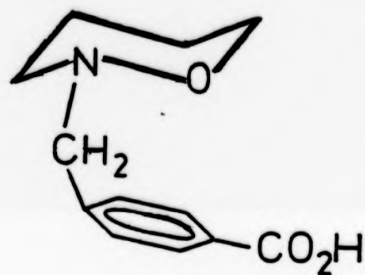
(i) Tetrahydro-1,2-Oxazine

The parent six-membered ring system containing an N-O bond is tetrahydro-1,2-oxazine, which has been extensively investigated by the groups in Stirling^{28,65,92-97} and Norwich.^{68,98} In an X-ray crystallographic study of the derivative (44), it was shown that the ring has a well-defined chair conformation. The conformation of the ring can be considered in two parts (CNO) and (CCCC). The first has the shorter bond lengths and greater torsion angle, whilst the second is more nearly cyclohexane-like in character with normal C-C bond lengths and torsion angles of ca 55°⁹⁵ (Table 1.2). The torsion angle about the N-O bond, whose length is 146pm, is 67° and is the largest in the ring. . From a knowledge of the torsional behaviour of cyclic compounds containing N-O bonds (Fig. 1.4) it can be seen that if the internal



R = CO₂Me, Me
 R₁ = CO₂Me, Me, H
 R = CO₂Me, Ph

(43)



(44)

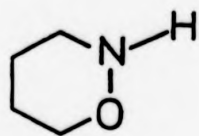
TABLE 1.2 Typical bond lengths, angles and van der Waals radii.¹⁰³

Bond Length (pm)		Bond Angles (in degrees)	
C - C	153	C - C - C	113.0
C - N	148	C - N - C	112.6
C - O	142	C - O - C	110.0
C - S	181	C - S - C	ca 100.0
N - N	145		
N - O	146	Van der Waals radii (pm)	
O - O	148	-CH ₂	200
O - S	160	O	140
S - S	203	N	150
		S	185

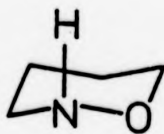
torsion angle in the ring were 55° , as in cyclohexane, there would be considerable residual torsional strain. This strain is in some measure relieved by opening the ring internal torsion angle to 67° .

Further evidence of the importance of torsional strain about the N-O bond is obtained from studies of axial-equatorial equilibria of groups on nitrogen. In piperidine and many other saturated heterocyclic systems there is much evidence for the N-H axial conformation being appreciably populated,⁹⁹ or even the most abundant conformation,¹⁰⁰ whereas the N-H group is almost exclusively equatorial in tetrahydro-1,2-oxazine (45).^{68,98} Similarly, ^1H nmr studies show no evidence for an axial N-methyl group in the 2-methyl derivative at temperatures where both nitrogen and ring inversion would be expected to be slow,²⁸ and this comes about because the axial conformation (45a) has the same rotational arrangement about the N-O bond as (9) which is in the higher energy minimum on the N-O rotation pathway. The equatorial conformation (45b) on the other hand corresponds to (10) which is certainly lower in energy than (9) even though it does not occupy a potential energy minimum (Fig 1.4). The above argument applies even more strongly for the N-methyl (or alkyl) derivatives where non-bonded interactions across the top of the ring will raise the energy of the axial conformation even more (46). There is thus expected to be a very strong tendency for N-substituents to be equatorial in tetrahydro-1,2-oxazine derivatives. However, in compounds such as the tetrahydro-1,4,2-dioxazines (47), where these syn-diaxial interactions are minimised and there are favourable anomeric interactions, the energy of the axial conformation is lowered sufficiently for it to be observed.

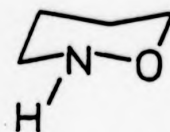
The presence of the oxygen atom adjacent to the nitrogen in a tetrahydro-1,2-oxazine ring slows down the rate of nitrogen inversion to such an extent that its rate becomes measurable by nmr spectroscopy at



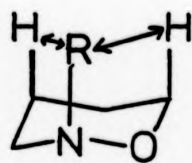
(45)



(45a)

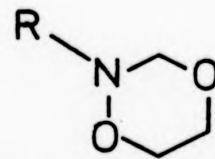


(45b)



(46)

R = CH₃



(47)

coalescence temperatures (T_c) of around 0° .^{65,96,97,101,102} Observed activation parameters are $\Delta H^\ddagger = 15.1 \pm 0.4 \text{ kcal mol}^{-1}$, $\Delta S^\ddagger = 2.3 \pm 1.5 \text{ cal mol}^{-1} \text{ K}^{-1}$, obtained from studies on the heptadeuterio derivative (28).^{65,97} Below that temperature (at ca -40°C), conformations separated by nitrogen inversion barriers are observable. Thus, slowing of the nitrogen inversion in 2,5-dimethyltetrahydro-1,2-oxazine^{94,98} (Fig 1.6) separates (a) and (d) from (b) and (c). At low temperatures two sets of signals are observed which are attributed to the diequatorial conformation (a) (major component) and the N-equatorial-5-axial conformation (c) (minor component). Conformations (b) and (d) with axial N-methyl groups will not contribute significantly to the equilibria since the axial N-methyls will considerably raise the energy of these species. The observed free energy difference, which corresponds to the equatorial-axial change of a 5-methyl group is $1.36 \pm 0.1 \text{ kcal mol}^{-1}$ (-35°C).

Analogous experiments allowed the determination of the free energy differences of methyl groups at all four ring C atoms (Fig 1.7).⁹³ From the X-ray crystallographic work discussed earlier⁹⁵ it had proved possible to estimate the distances between axial C-methyl and other atoms on the ring causing steric hindrance (Fig 1.8). Methyl groups at C4 and C5 are seen to be at almost identical distances from the hindering atoms yet experimentally C5 axial methyl is found to experience smaller interactions. These values confirm the view that at similar distances repulsions from nitrogen (van der Waals radius 150 pm) are greater than those from oxygen (van der Waals radius 140pm).¹⁰³ Similar comparison of positions 3 and 6 in the ring also reveals the same trend with the group forced against oxygen being less hindered than the group forced into nitrogen despite almost identical trans-annular distances. Experimentally, as expected, the hindrance to the axial substituents at 3

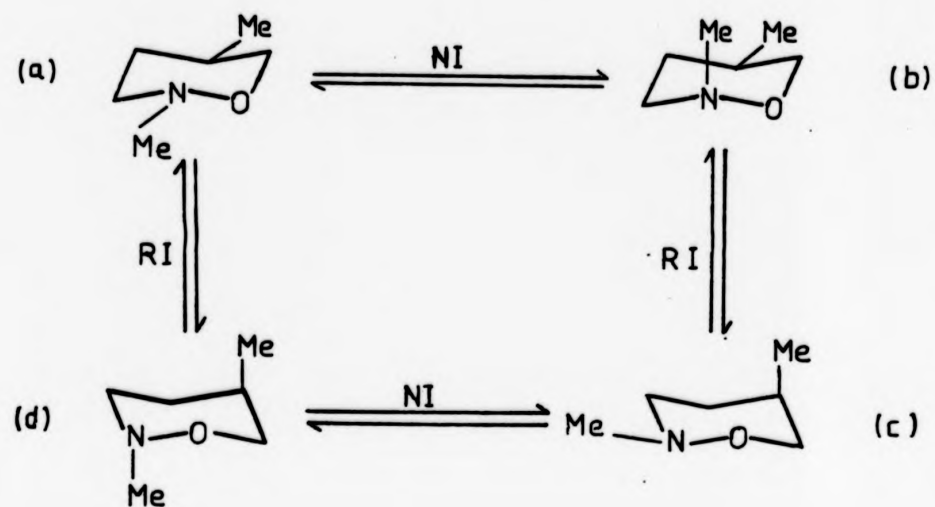


Fig 1.6 Ring and nitrogen inversion in 2,5-dimethyl-tetrahydro-1,2-oxazine.^{94,98}

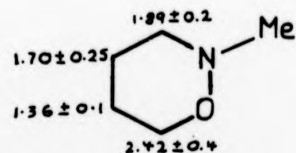


Fig 1.7 Free energy differences (kcal mol^{-1}) of methyl groups at positions 3, 4, 5 and 6 in the tetrahydro-1,2-oxazine ring.⁹³

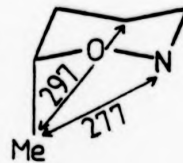
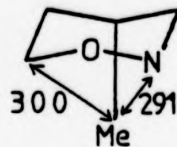
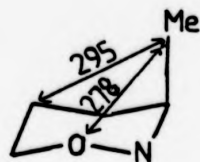


Fig 1.8 Distances separating methyl carbon atoms from other ring atoms in tetrahydro-1,2-oxazines (pm).

and 6 position is found to be greater than for positions 4 and 5 because of the closer proximity of the hindering groups. These experiments show the importance of the relative size of O and N atoms in determining conformational preferences.

(11) Tetrahydro-1,4,2-Dioxazine

The conformational behaviour of tetrahydro-1,4,2-dioxazine ring (47) is modified compared to the 1,2-oxazine ring by the introduction of an oxygen atom β to the nitrogen. The ring displays a fascinating fusion of the conformational properties of tetrahydro-1,2-⁹⁷ and -1,3-oxazine rings.^{101,104-106}

NMR spectral evidence on derivatives of the basic ring system (31) shows that there are two distinct inversion phenomena observable: nitrogen inversion $\Delta G^\ddagger = 11.4 \pm 0.2 \text{ kcal mol}^{-1}$ and ring inversion $\Delta G^\ddagger = 10.9 \pm 0.2 \text{ kcal mol}^{-1}$.¹⁰⁶ The barrier to inversion of an equatorial N-methyl group is clearly intermediate between the barriers in the 1,2-oxazine (29) and 1,3-oxazine (30) (ΔG^\ddagger ca $13.75 \pm 0.5 \text{ kcal mol}^{-1}$ ^{65,97} and $7.6 \text{ kcal mol}^{-1}$ ⁷ respectively). The effect of the β -oxygen atom is to lower the barrier to inversion of the equatorial N-methyl group, and the effect of the α -oxygen atom is clearly seen to raise this barrier.

The conformational free energy difference of a methyl group on nitrogen in the 1,3-oxazine ring is ca $0.0 \text{ kcal mol}^{-1}$, because of lower non-bonded interactions on the axial methyl group and a favourable anomeric interaction,¹⁰⁷⁻¹¹⁰ giving roughly equal amounts of axial and equatorial conformation. In the 1,2-oxazine ring only the equatorial conformation can be detected. In the tetrahydro-1,4,2-dioxazine ring this free energy difference is found to be ca 1 kcal mol^{-1} allowing ready detection of the axial conformation. This value is again intermediate between the two model systems.

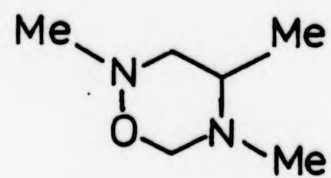
(iii) Tetrahydro-1,2,4-Oxadiazine

This series of compounds combines the conformational tendencies of the tetrahydro-1,2-oxazine and hexahydropyrimidine rings.¹¹¹⁻¹¹³ In the 2,4-dimethyl derivative (32) a detailed conformational analysis has been made by making use of a combination of ^1H and ^{13}C nmr spectra.¹¹³ Two nitrogen inversion barriers are observed. The equatorial N(4)-methyl inversion barrier is 7.4-7.9 kcal mol⁻¹ with a free energy difference of 0.6-0.9 kcal mol⁻¹. These values are very similar to those observed for N,N'-dimethylhexahydropyrimidine.^{114,115} The barrier to inversion of the equatorial N(2)-methyl group is ca 12.7-13.1 kcal mol⁻¹. This is higher than in the 1,2,4-dioxazine but lower than in the 1,2-oxazine series, reflecting the fact that the β -nitrogen atom lowers the N-inversion barrier, but by a smaller amount than a β -oxygen atom. The barrier to ring inversion is ca 12.7 kcal mol⁻¹.

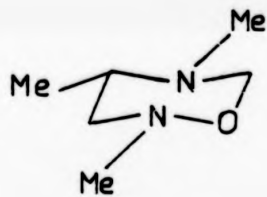
(iv) Tetrahydro-1,2,5-Oxadiazine

The "reference compounds" for this series of oxadiazines are the tetrahydro-1,2- and -1,3-oxazines. In the ^1H nmr spectrum of the dimethyl derivative (33) a kinetic process is observed with activation parameters so similar to those for 2-methyltetrahydro-1,2-oxazine (28) (ΔH^\ddagger 14.4 \pm 0.1, 15.1 \pm 0.4 kcal mol⁻¹; ΔS^\ddagger -1.2 \pm 0.4, 2.3 \pm 1.5 cal mol⁻¹ K⁻¹ respectively)^{111,112,115-117} as to strongly suggest N(2) inversion as a common origin. The effect of the γ -N atom on the N-inversion barrier is therefore negligible.

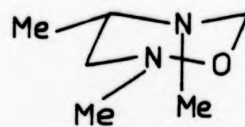
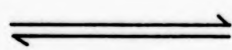
On freezing out of N(2) inversion in the 2,4,5-trimethyl derivative (48) some interesting observations are recorded.¹¹⁸ Below coalescence the ^1H spectra shows peaks associated with a major conformation (48a and 48b) and a minor conformation (48c). In the major set with the 4-methyl group equatorial, the N(5) methyl group equally populates the axial and equatorial positions. This agrees with the known behaviour of



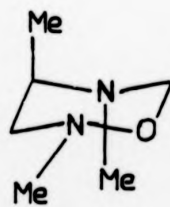
(48)



(48a)



(48b)



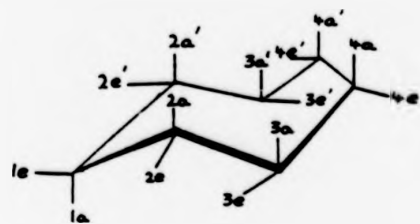
(48c)

the 1,3-oxazine moiety if the gauche-butane interactions about the C(4)-(C)5 bond are roughly equal for axial and equatorial N-methyl groups. The minor conformation (48c) has its C(4) and C(5) methyl groups axial. Here the N-methyl group goes axial as it forms part of a 1,3-oxazine-like end of the ring at minimal expense in energy, to avoid the gauche-butane repulsion it would experience were it equatorial.

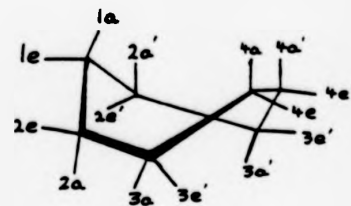
(e) Seven-membered Rings

Molecular mechanic calculations of Hendrickson¹⁵ and of Bixon and Lifson¹⁶ on cycloheptane show the main conformational features to be expected in seven-membered rings. There are two forms of cycloheptane which are flexible with respect to dihedral angles and may undergo pseudorotation, these being a chair (with C_s symmetry) (49) and a boat form (50). To overcome serious torsional and non-bonded repulsions, they may pseudorotate to a more energetically stable conformer, this being a twist-chair (C_2 symmetry) (51) with bond angles opened to 112° . The twist-chair can pseudorotate very easily, crossing a low energy barrier of ca $2.16 \text{ kcal mol}^{-1}$ to a chair, or ring invert to a twist-boat (52) conformation over a barrier of ca $8.5 \text{ kcal mol}^{-1}$, which is ca $2.5 \text{ kcal mol}^{-1}$ less stable than the twist-chair conformation. This is illustrated in Fig 1.9. Since the barrier to pseudorotation of the chair is only $2.16 \text{ kcal mol}^{-1}$, the ring can easily pseudorotate to relieve any unfavourable interaction, and the exact rotational arrangement of a substituted ring is therefore quite difficult to specify without a detailed calculation. This pseudorotation interconverts all substituent positions on the ring, giving, in the case of rapid pseudorotation, a completely time-averaged nmr spectrum. The process occurs extremely rapidly even at very low temperatures.

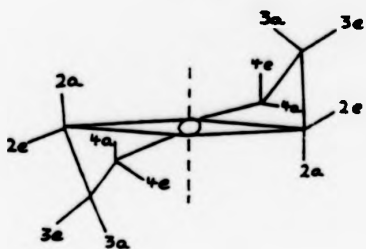
The pseudorotation and ring inversion can, however, be slowed down by the introduction of suitable substituents. Conformational



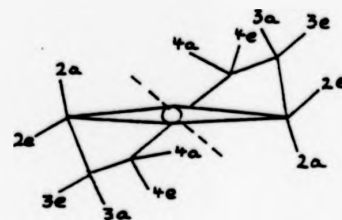
(49)



(50)



(51)



(52)

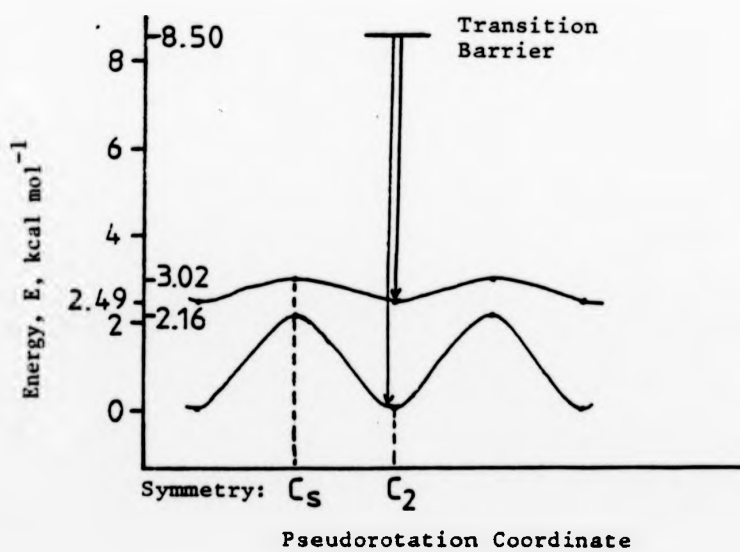


Fig 1.9 Calculated energies of pseudorotation of cycloheptanes.¹⁵

calculations on cycloheptane and some related oxepanes have been reported by Bocian and Strauss.¹¹⁹ The results of the calculations are compared with nmr information and with rotational Raman spectra. The available evidence leads to a consistent picture of the seven membered rings having twist chairs as the lowest energy conformations. Much work has also been done using heteroatom-heteroatom bond effects on rates of conformational interchange in seven-membered systems.¹²⁰⁻¹²⁹

In small rings, it would seem likely that the N-O bond would not be able to adopt the preferred conformation (8) because of restraints from the rest of the ring, so as the ring size increases and constraints due to molecular geometry decrease, the N-O bond should be freer to adopt the preferred conformation. Thus, in seven-membered cyclic hydroxylamine derivatives, it might be expected that one could have almost the preferred rotational arrangement about the N-O bond. The bond angles about nitrogen give these compounds a reasonably close resemblance to open-chain systems.

A comparison of the rates of conformational interchange found in the rings (34) and (35)¹²⁹ and rings (36) and (37)¹²⁶ provide us with the only data about the rate processes taking place in seven-membered hydroxylamine compounds (Table 1.1). For the hydroxylamine (36) a process with ΔG^\ddagger ca 19.2 ± 0.5 kcal mol⁻¹ at ca +100°C was observed which was ca 10 kcal mol⁻¹ greater than in the hydrocarbon (37). This very large increase in activation energy possibly arises because the presence of the gem-dimethyl groups in the ring restricts the number of possible conformations on the pseudorotation circuit, thus placing the N-O bond rotation into the rate-determining step and giving a very high barrier increase. The free energy of activation for the observed processes in compounds (34) and (35) presumed to arise from nitrogen inversion are very similar, indicating that the presence of the

gem-dimethyl group and C-methyl group do not seem to interfere with the inversion process being observed.

1.5 EIGHT-MEMBERED RINGS

There are generally two conformations considered to be important for cyclooctane, the crown (53) and the boat-chair (54). Molecular mechanics calculations on cyclooctane are in agreement with the boat-chair conformation of C_8 symmetry being slightly more stable than the crown.^{15,16,130-134} These calculations reveal that there are many low activation energy ring inversion and pseudorotation processes possible in cyclooctane. These processes have been discussed in some detail by Anet.¹³⁵

More recent nmr results are in accordance with cyclooctane (38) (Table 1.1) existing as a 95:5 mixture of boat-chair and crown conformations with $\Delta H^\circ = 1.9 \text{ kcal mol}^{-1}$, $\Delta S^\circ = 1.1 \text{ eu}$ and $\Delta G^\ddagger = 11.2 \text{ kcal mol}^{-1}$ at -45° (for boat-chair \rightarrow crown).¹³⁶ In an elegant study of partially deuterated cyclooctane dissolved in a nematic solvent the direct coupling constants between proton pairs and between ^{13}C and ^1H have been measured and assigned by Meiboom, Hewitt and Luz.¹³⁷ The boat-chair conformation is the only one capable of giving calculated couplings to reproduce the experimental data.

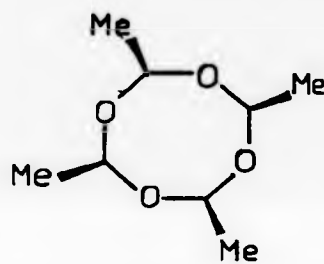
A ^1H and ^{13}C nmr study of azocane (azacyclooctane) (39) by Anet et al.¹³⁸ has clarified the conformational analysis of this compound. The compound exists predominantly in a boat-chair conformation with a small amount of a crown conformation present. Ring inversion of the boat-chair conformation has a free energy of activation of $7.3 \pm 0.2 \text{ kcal mol}^{-1}$. The boat-chair to crown interconversion has thermodynamics and kinetic parameters of $\Delta G^\circ = 1.2 \pm 0.1$ and $\Delta G^\ddagger = 10.5 \pm 0.2 \text{ kcal mol}^{-1}$.¹³⁸



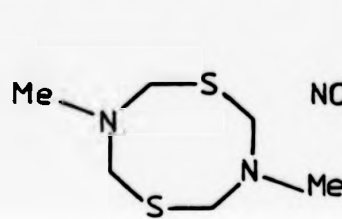
(53)



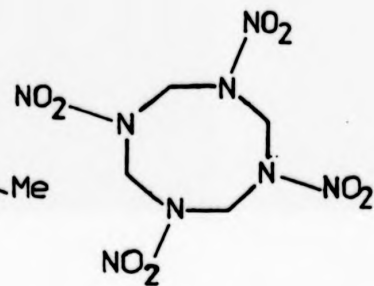
(54)



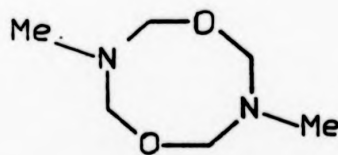
(55)



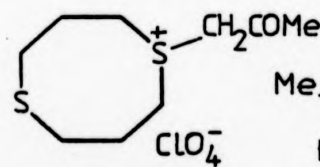
(56)



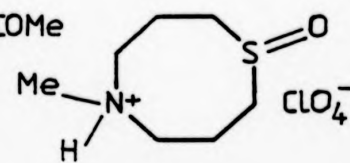
(57)



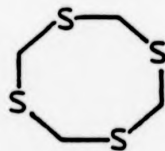
(58)



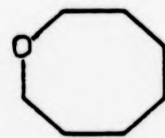
(59)



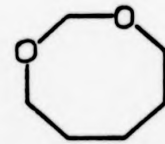
(60)



(61)



(62)



(63)

A ^{19}F variable temperature nmr study of fluorocyclooctane shows evidence of two conformational processes.¹³⁹ These are assigned to be ring inversion and pseudorotation amongst non-equivalent boat-chairs.

Finally, X-ray diffraction studies on heterocyclic eight-membered rings show that the molecules either adopt the crown (55 - 58)¹⁴⁰⁻¹⁴³ or boat-chair (59 - 63)¹⁴⁴⁻¹⁴⁹ conformation.

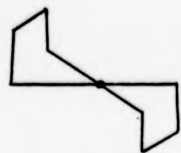
As far as it is possible to ascertain, no work prior to this thesis has been done on eight-membered cyclic hydroxylamines.

1.6 NINE-MEMBERED RINGS

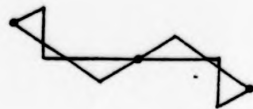
The two main conformations found for nine-membered rings have symmetry C_2 and D_3 and have been called the twist-chair-boat, TCB (64), and twist-boat-chair, TBC (65), respectively.

The low-temperature ^{13}C nmr spectrum of cyclononane at -162° shows two distinct types of carbon atom in the integrated ratio of 2:1.⁴⁸ This result is entirely consistent with the D_3 TBC conformation, and is unlikely for any conformation of lower symmetry (eg C_2 TCB). Moreover, the splitting arises from a conformational process of activation energy ca 6 kcal mol^{-1} , which is in reasonable agreement with calculations on processes that would lead to exchange between the two sites.¹⁵⁰

As with other ring systems, the introduction of geminal dimethyl groups can reduce or alternatively reinforce conformational preferences of rings. The preference for the TBC conformations in 1,1-dimethylcyclononane (41),⁴⁸ and in 1,1,4,4-tetramethylcyclononane (42)¹⁵¹ are inferred from nmr data. The presence of the gem-dimethyl groups lowers the overall molecular symmetry from D_3 to C_2 in both cases, and the central ring retains approximate D_3 symmetry. The activation energies for the observed conformational processes also



(64)



(65)

increase from 9 kcal mol⁻¹ (41)⁴⁸ to 14-20 kcal mol⁻¹ (42 and some derivatives).¹⁵¹ (Table 1.1).

Again, for nine-membered rings, no work dealing with hydroxylamine derivatives appears to have been published.

1.7 CONCLUSION

In view of the results presented above, it seemed well worthwhile investigating the conformations of, and conformational rate processes in several systems: Firstly, tetrahydro-1,2-oxazine derivatives containing a sulphur atom in the 4 position. Since no conformational equilibrium studies have been reported on 4-thia-1-oxa-2-azacyclohexane derivatives, it seems useful to look at conformational preferences in this series and to compare the result with model "reference compounds" for this system, namely, tetrahydro-1,2-oxazine, tetrahydro-1,3-thiazine and tetrahydro-1,4,2-dioxazines.

Secondly, in eight- and nine-membered ring systems the conformations and conformational processes are much less well understood than for the smaller ring systems. As the ring size increases, the degrees of freedom associated with the ring increase and so therefore does the conformational complexity. There is at present no conformational information on eight and nine-membered hydroxylamine cyclic derivatives. A study of these heterocyclic systems may shed some light on the conformational behaviour of these larger ring systems and demonstrate the effect of different magnitude and shape of the N-O rotational barrier.

It is thus hoped that these studies will let us gain insight into the conformations of the respective ring systems, to determine whether axial or equatorial N-methyl groups are preferred, to investigate the

non-bonded interactions that can arise and to investigate the nature of the observed processes in such ring systems.

CHAPTER 2

Results, Analysis and Discussion of Syntheses, ^1H and ^{13}C
Nuclear Magnetic Resonance Spectra and Conformation Equilibria
of Hydroxylamine Derivatives

2.1 SYNTHESIS OF HYDROXYLAMINE DERIVATIVES

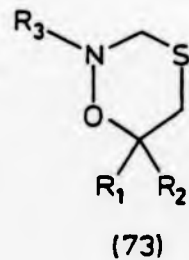
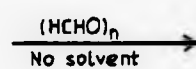
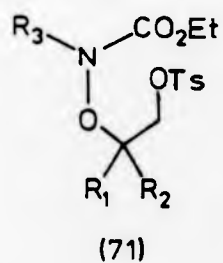
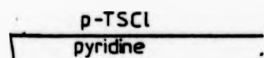
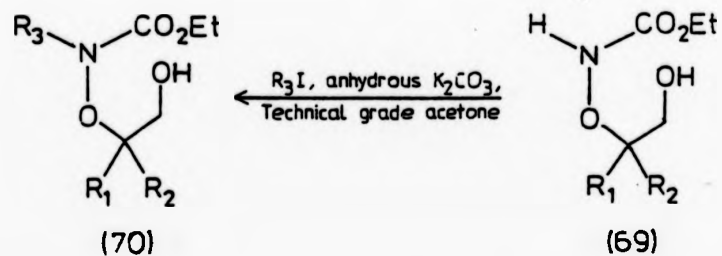
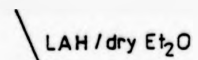
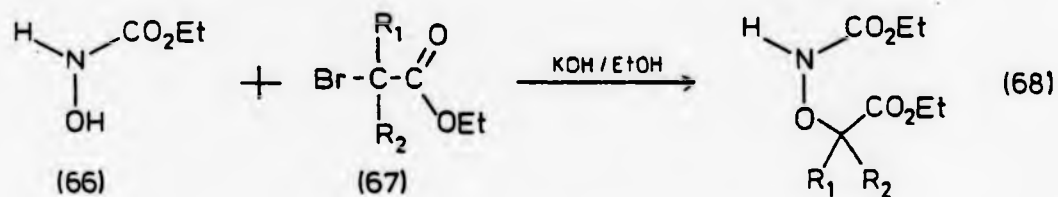
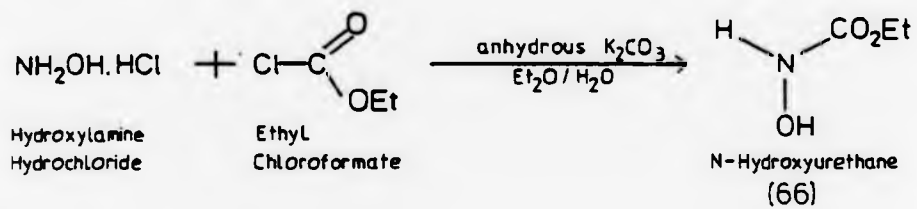
2.1.1 1-Oxa-4-Thia-2-Azacyclohexanes

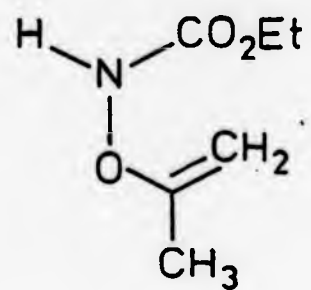
The syntheses were all accomplished by the general route shown in Scheme 1 and each reaction stage is assigned a reference number.

Reaction of N-hydroxyurethane (66) with an α -bromoester (67) in ethanolic potassium hydroxide leads to the esters (68). These compounds may be reduced selectively by lithium aluminium hydride at ca 0°C to the alcohols (69).¹⁰⁶ Reduction of the derivative (68, $R_1=CH_3$, $R_2=R_3=H$) also resulted in the formation of N-carbethoxy-2-(amino-hydroxy)-2-propene (74) as a major by-product (ca 30%). It is presumed that the hydroxy compound (73, $R_1=CH_3$, $R_2=R_3=H$) formed undergoes elimination to give the undesired by-product (74). While reduction of the derivative (68, $R_1=R_2=CH_3$, $R_3=H$) gave the corresponding hydroxy compound (69, $R_1=R_2=CH_3$, $R_3=H$) only as a minor component (23%). The major component was a white crystalline product identified as 6,6-dimethyl-4-dioxo-2-azin-3-one (75). A steric hindrance effect appears to be important in the 6,6-dimethyl substituted derivative (68; $R_1=R_2=CH_3$, $R_3=H$) and repeated attempts to obtain the amino-thiol derivative (72, $R_1=R_2=R_3=CH_3$) failed.

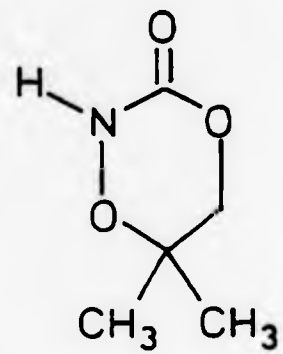
Alkylation of the hydroxy compounds (69) under standard conditions using carefully dried acetone as solvent, leads to the derivatives (70) with 4-hydroxy-4-methyl-2-pentanone (76) produced as a major by-product, forming an azeotropic mixture thus making it very difficult to obtain the desired product pure. An attempt to get rid of the diacetone alcohol by converting it to mesityl oxide (77), using iodine as catalyst,¹⁵³ failed. The diacetone alcohol was formed in much smaller quantities when technical grade acetone was used and it was possible to obtain the desired products in a pure state.

Scheme 1

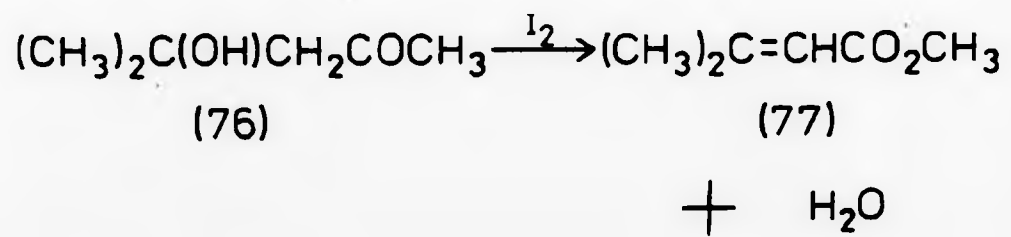




(74)



(75)



The derivatives (70) can be tosylated by the method employed by Bussert et al¹⁵⁴ to the N-carbethoxy tosylates (71). Reaction of these tosylates in ethanolic potassium hydroxide solution saturated with hydrogen sulphide leads to the amino-thiols (72). The amino-thiols condense with paraformaldehyde to form the 1-oxa-4-thia-2-azacyclohexanes (73).

2.1.2 Eight- and Nine-membered Hydroxylamine Derivatives

King,¹⁵⁵ in 1942, showed that alkyl halides in the presence of a strong base reacted with N-hydroxyurethane to give O-alkyl hydroxyurethanes, which upon acid hydrolysis gave the corresponding O-alkyl hydroxylamines.¹⁵⁶ Hydrolysis with hydrochloric acid and subsequent basification yield the free bases.

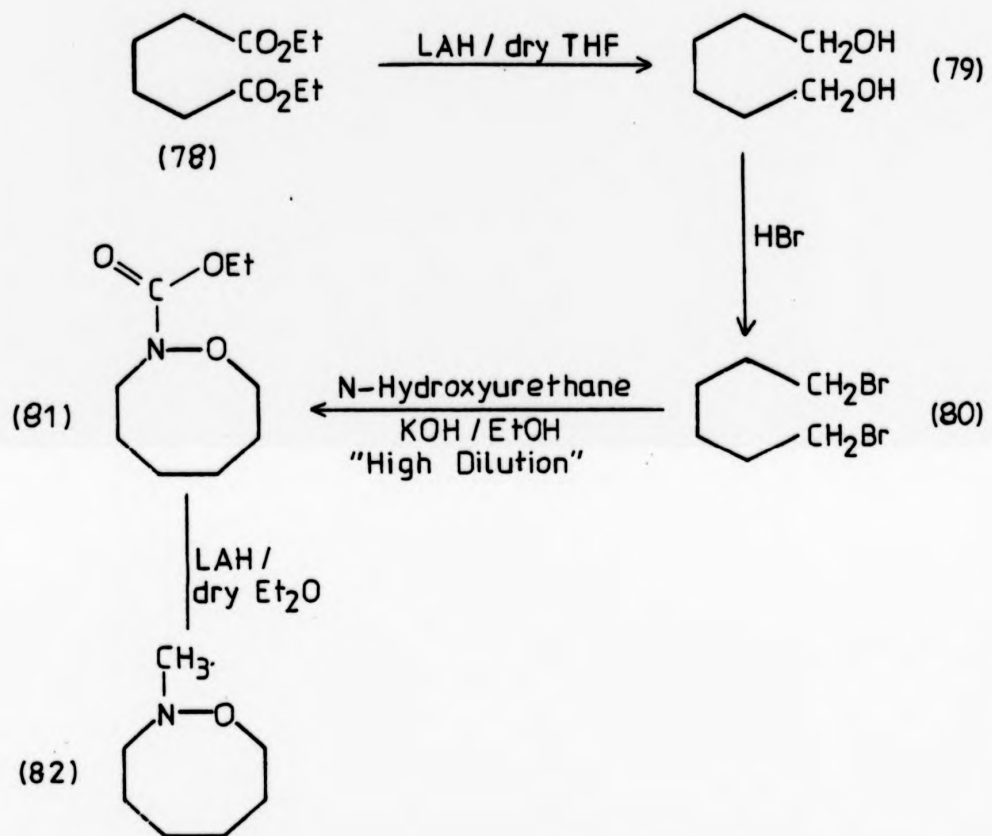
The present work required the preparations of 1-oxa-2-azacyclooctane (82, 92) derivatives and 6,6-dimethyl-1-oxa-2-azacyclononane derivative (104). The synthesis of the eight- and nine-membered hydroxylamine derivatives are illustrated in Schemes 2-4. The dibromides required for the preparation of the N-carbethoxy cyclic hydroxylamines, by an extension of King's¹⁵⁵ method, were all prepared from the appropriate diols which were synthesised by standard procedures. Most of these synthetic steps do not require discussion and are outlined in the Experimental section.

Since the reduction of N-carbethoxy groups with lithium aluminium hydride (LAH) is known to give N-methyl groups,¹⁵⁷ it was hoped that the cyclised hydroxylamines made by adopting King's¹⁵⁵ method would give the desired compounds upon LAH reduction.

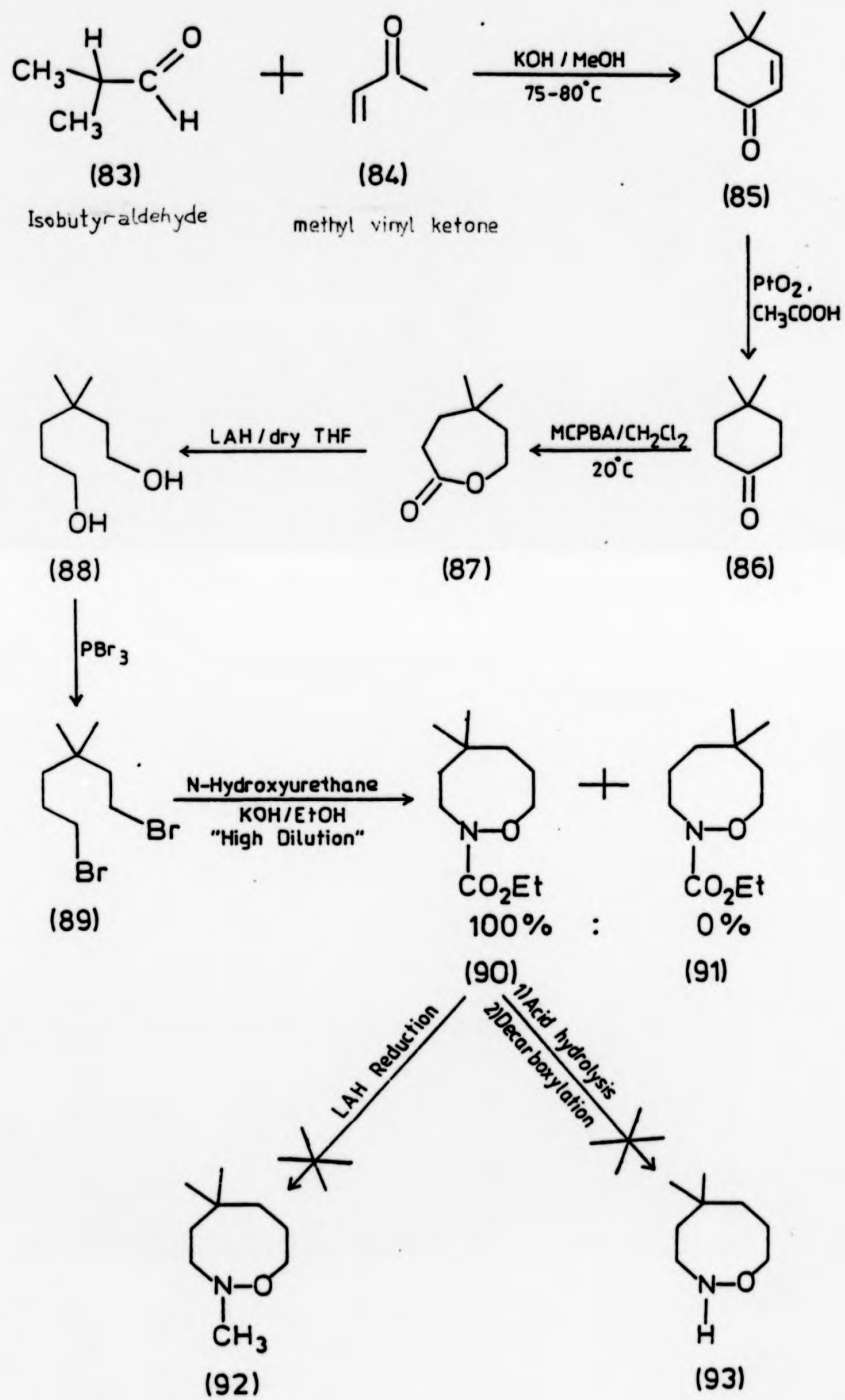
The principal points of discussion are:

- (1) bromination of β - or γ -substituted dimethyl diols

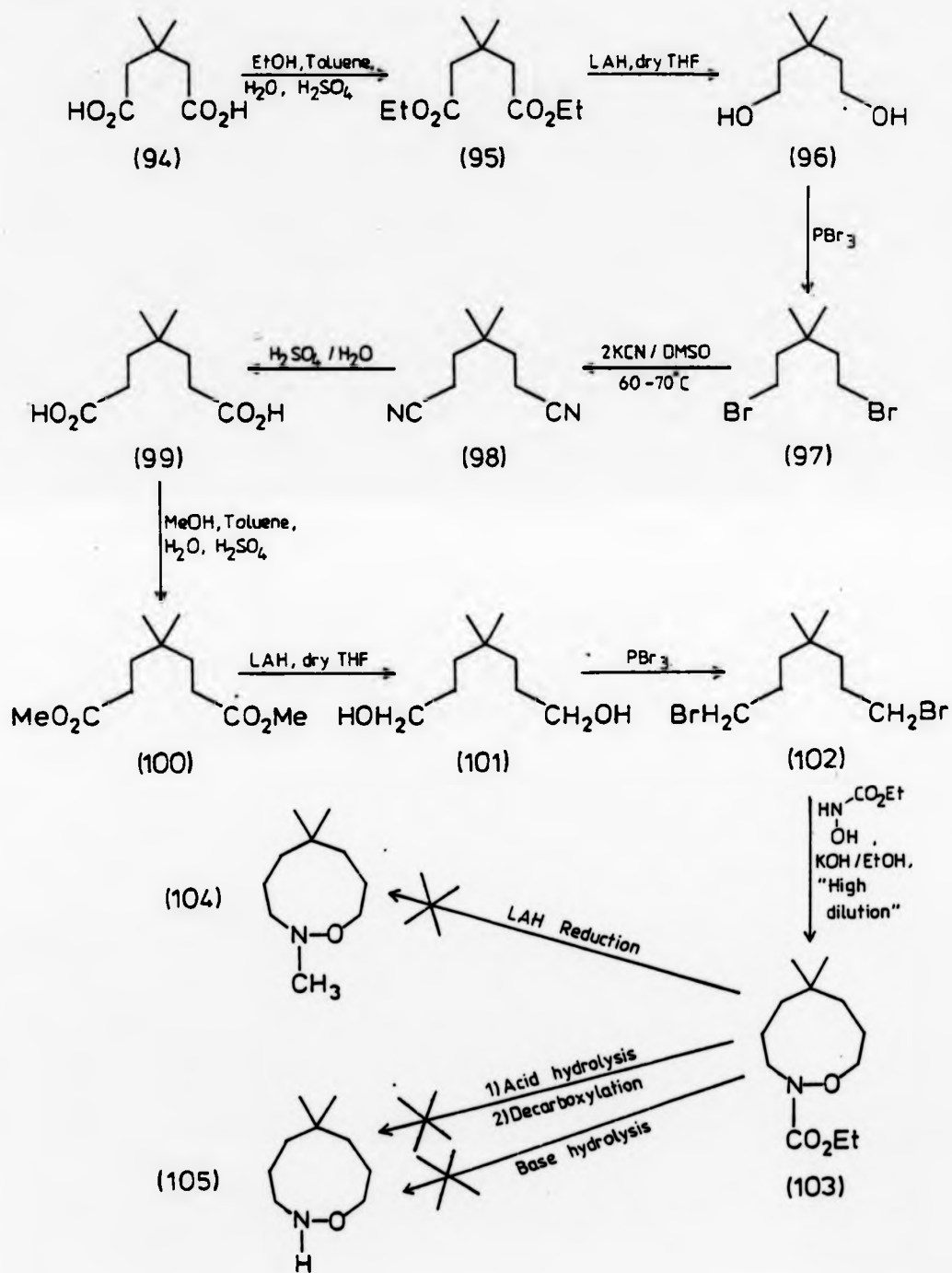
Scheme 2



Scheme 3



Scheme 4



- (ii) by-product formation in Baeyer-Villiger oxidation and its implication in subsequent steps
- (iii) the stereochemical and mechanistic implications of the condensation of N-hydroxyurethane with the dibromides and
- (iv) the failure of both reduction and hydrolysis of the N-carbethoxydimethyl substituted compounds to give the expected products.

(a) Bromination of β - or γ -substituted Dimethyl Diols

The bromination of 3,3-dimethyl-1,5-pentanediol (96) using the standard method as adopted by Van Heyningen¹⁵⁸ (conc. aq. HBr) resulted in the formation of 4,4-dimethyltetrahydropyran (106) in 44% yield, while the desired dibromide (97) was only obtained in 40% yield. Bromination using phosphorus tribromide method as adopted by Blomquist and Verdol,¹⁵⁹ gave the desired dibromide (97) in very much better yield (58%), so this method of bromination was finally adopted.

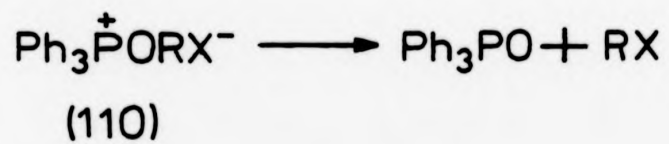
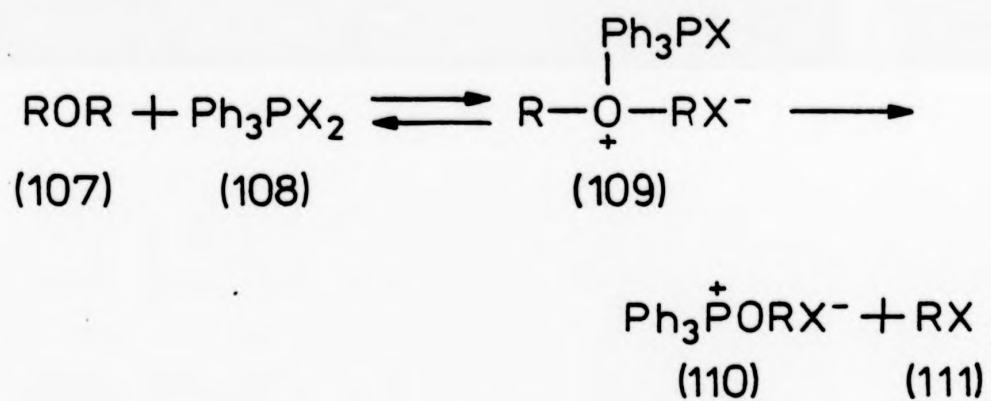
Attempts to cleave 4,4-dimethyltetrahydropyran (106) to give 3,3-dimethyl-1,5-dibromopentane (97), in the first instance, using concentrated hydrobromic acid (48% w/v)¹⁵⁸ and in the second instance using triphenyldibromophosphorane¹⁶⁰ failed. With the use of concentrated hydrobromic acid the cyclic ether (106) was recovered, while with the phosphorane reagent the product obtained was not identifiable. Anderson and Freenor¹⁶⁰ showed that ethers (107) reacted with tertiary phosphine dihalides (108) to form an oxonium intermediate (Scheme 5). This conjugate-Lewis (109) acid of the ether then reacts in the usual manner to give alkyl halide (111) and a quasiphosphonium ion intermediate (110) corresponding to that proposed for phenols and alcohols,¹⁶¹⁻¹⁶⁴ which, for dialkyl ethers, could afford a second molecule of alkyl halide.

(b) Baeyer-Villiger Oxidation



(106)

Scheme 5

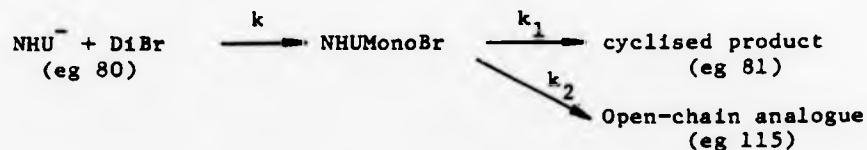


The mechanism of the oxidation reaction of 4,4-dimethyl-cyclohexanone (86) using *m*-chloroperoxybenzoic acid (MCPBA) as the oxidizing agent is believed to be as shown in Scheme 6. The benzoic acid (111a) is produced as a by-product in the reaction. If during workup it is not washed out completely it goes through subsequent reaction steps to form the product (114) (Scheme 7). This appears as a major impurity in the preparation of *N*-carbethoxy-5,5-dimethyl-1-oxa-2-azacyclooctane (90) and is removed by column chromatography (silica gel) only with great care, as it runs down the column just behind the desired product.

(c) Reactions of *N*-Hydroxyurethane with Dibromides

In previous experiments using 1,4-dibromides⁴⁷ it was found that a 3:1 molar ratio of *N*-hydroxyurethane and base to the dibromide gave reasonable yields, so this ratio was adopted with the condensation reaction of 1,6-dibromohexane (80) with *N*-hydroxyurethane. However, it resulted in the formation of an open-chain analogue with *N*-hydroxyurethane groups attached to both ends of the hexane chain (115). At this point an elementary analysis of the probable kinetics of the various competing reactions was made.

In considering the rates of the expected reactions;



it is assumed that the rate expression in the reaction of the *N*-hydroxyurethane anion (NHU^-) and a dibromide (DiBr) is:

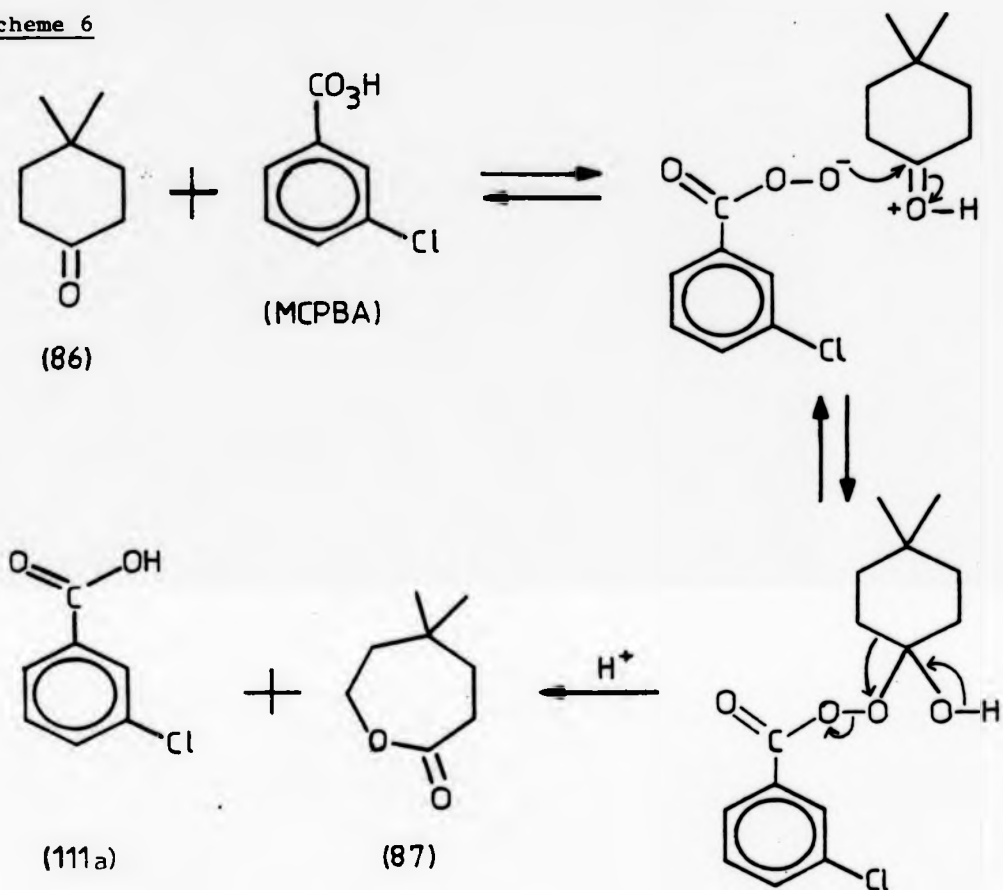
$$\text{rate} = k[\text{NHU}^-][\text{DiBr}]$$

The rate of cyclisation to give (eg 81) will be

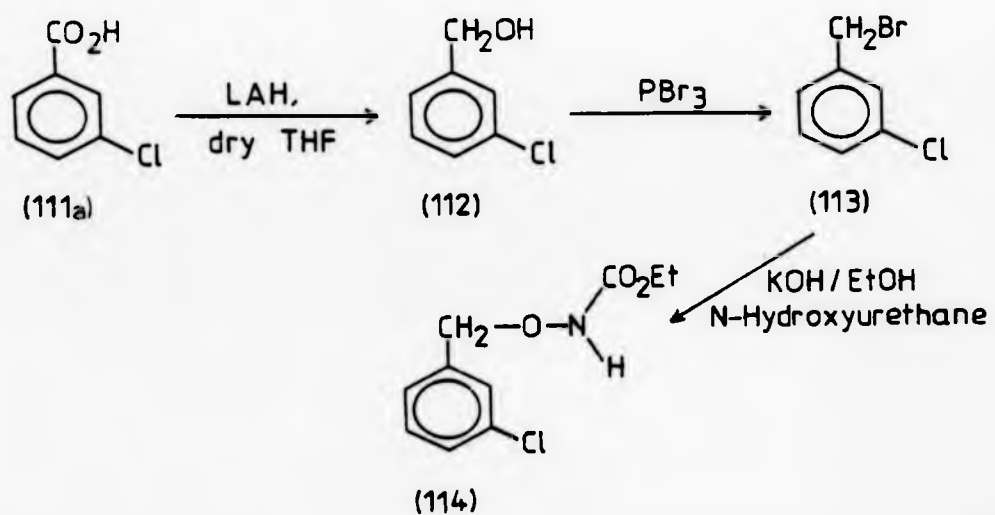
$$\text{rate} = k_1[\text{NHUMonoBr}]$$

and the rate of formation of the undesired product (eg 115) is given by

Scheme 6



Scheme 7



$$\text{rate} = k_2[\text{NHU}^-][\text{NHUMonoBr}]$$

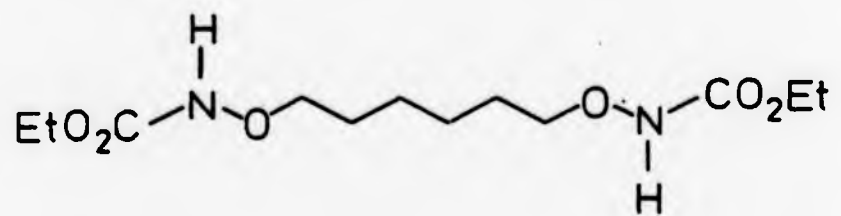
The ratio of the desired to the undesired reaction rate is thus equal to;

$$\text{Rate} = \frac{k_1[\text{NHUMonoBr}]}{k_2[\text{NHU}^-][\text{NHUMonoBr}]} = \frac{k_1}{k_2[\text{NHU}^-]}$$

that is, it is inversely proportional to the concentration of N-hydroxyurethane. Thus, in order to promote cyclisation at the expense of intermolecular reaction, the 'high-dilution' technique was used, ie low concentrations of N-hydroxyurethane were used. In subsequent reactions the concentration of N-hydroxyurethane was kept at least fourteen times less at any one time than in the previous experiment. Therefore the rate of the undesired reaction should be at least fourteen times slower relative to cyclisation.

An analysis of the synthetic difficulty of medium and large rings was made by L Ruzicka and coworkers.^{165,166} For a typical simple ring closure reaction in solution, both the enthalpy and the entropy of ring closure must be considered. In Fig 2.1 the effects of these two quantities on the yield of the ring closure reaction as a function of ring size are indicated. Low yields in the small rings were then predicted because of the very unfavourable enthalpy change. The five- and six-membered rings had less favourable entropies of ring closure than did the small rings, but very much more favourable enthalpies, and are both obtained in good yield. The rings containing seven or more atoms were expected to be obtained in steadily decreasing yields. The ring closure reactions investigated at the time appeared to fulfil the simple predictions quite well, with the glaring exception of rings containing from eight to twelve carbons. With these compounds the yields were exceedingly poor, indicating a "medium ring effect".¹⁶⁷

The effect of substituents in promoting cyclizations was noted as



(115)

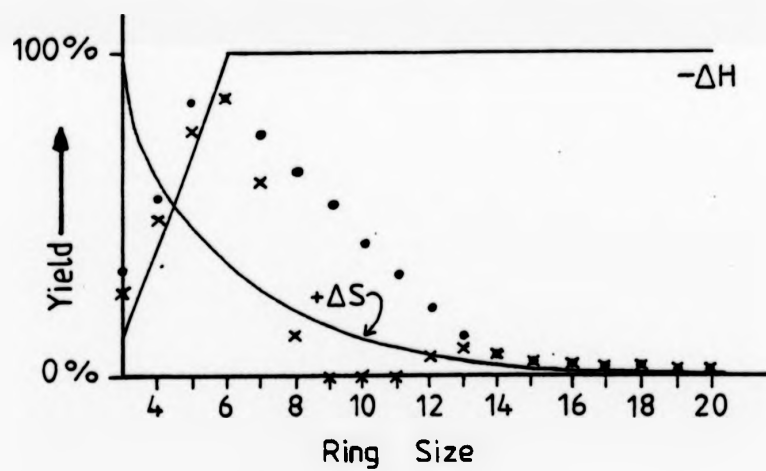


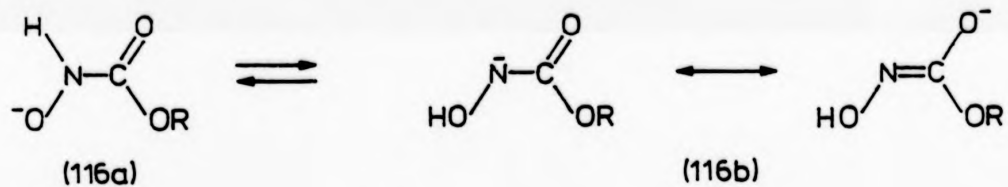
Fig 2.1 Thermodynamic parameters for ring closure as a function of ring size (schematic). Dots represent predicted yields; crosses experimental yields.

early as 1915;¹⁶⁸⁻¹⁷⁰ it has been referred to as the "gem-dimethyl effect". This can be quantitatively explained in terms of the thermodynamics of the conformations involved.^{171,172} An ordinary unsubstituted hydrocarbon chain exists predominantly in an extended (zig-zag) form, and energy is required to introduce the gauche interactions necessary to put the molecule into the proper conformation necessary for cyclization. The energy difference between the ground state (zig-zag) and the transition state thus includes this conformational energy. If one or more substituents are present on the hydrocarbon chain, the transition state may contain no additional gauche interactions (or it may contain some smaller number) beyond those present in the unsubstituted case. The groundstate necessarily will contain some (or many) additional gauche interactions, and hence upon substitution the energy of the ground state is raised in relation to that of the transition state. Substitution consequently encourages cyclization,¹⁷¹⁻¹⁷³ with regard to both rate and equilibrium. Yields of the respective eight- and nine-membered N-carbethoxy hydroxylamine rings synthesised are shown in Table 2.1.

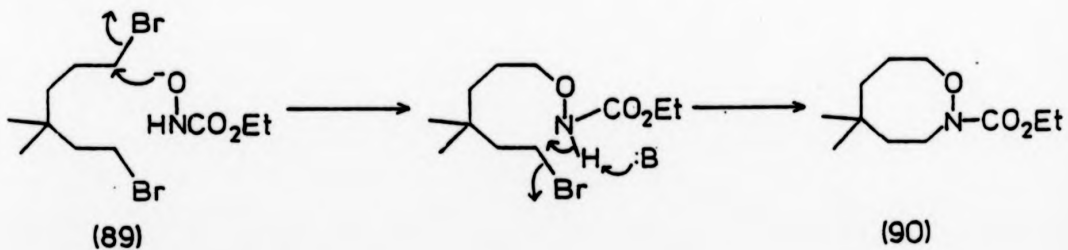
In the condensation of 3,3-dimethyl-1,6-dibromohexane (89) with N-hydroxyurethane (66), the cyclised product (90) was formed in absolute bias. The result seems to suggest a possible mechanism of ring formation. The suggested mechanism being that in the strongly basic conditions used (potassium hydroxide in ethanol), the N-hydroxyurethane loses a proton from one of the two possible sites to give tautomers (116a) and (116b) (R=Et). Several pieces of evidence^{156,174-177} show that although the two tautomers appear to exist in approximately equal concentrations, the nucleophilicity of tautomer (116a) is far greater than (116b), and hence the initial attack is by oxygen. This idea was

TABLE 2.1 Percentage yields of eight- and nine-membered N-carbethoxy hydroxylamine rings.

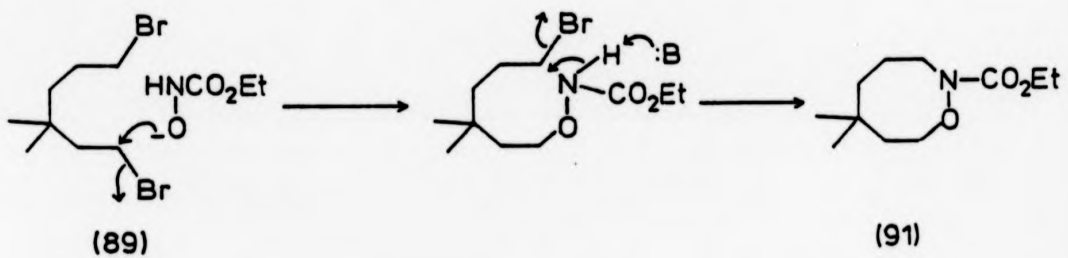
N-Carbethoxy Compound	% Yield
1-Oxa-2-Azacyclooctane (81)	54
5,5-Dimethyl-1-Oxa-2-Azacyclooctane (90)	49
6,6-Dimethyl-1-Oxa-2-Azacyclononane (103)	58



Scheme 8



Scheme 9



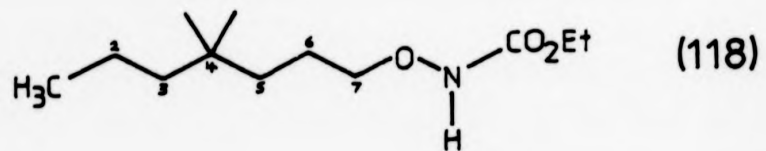
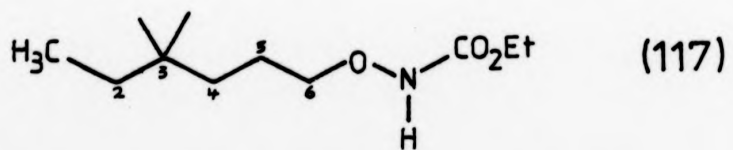
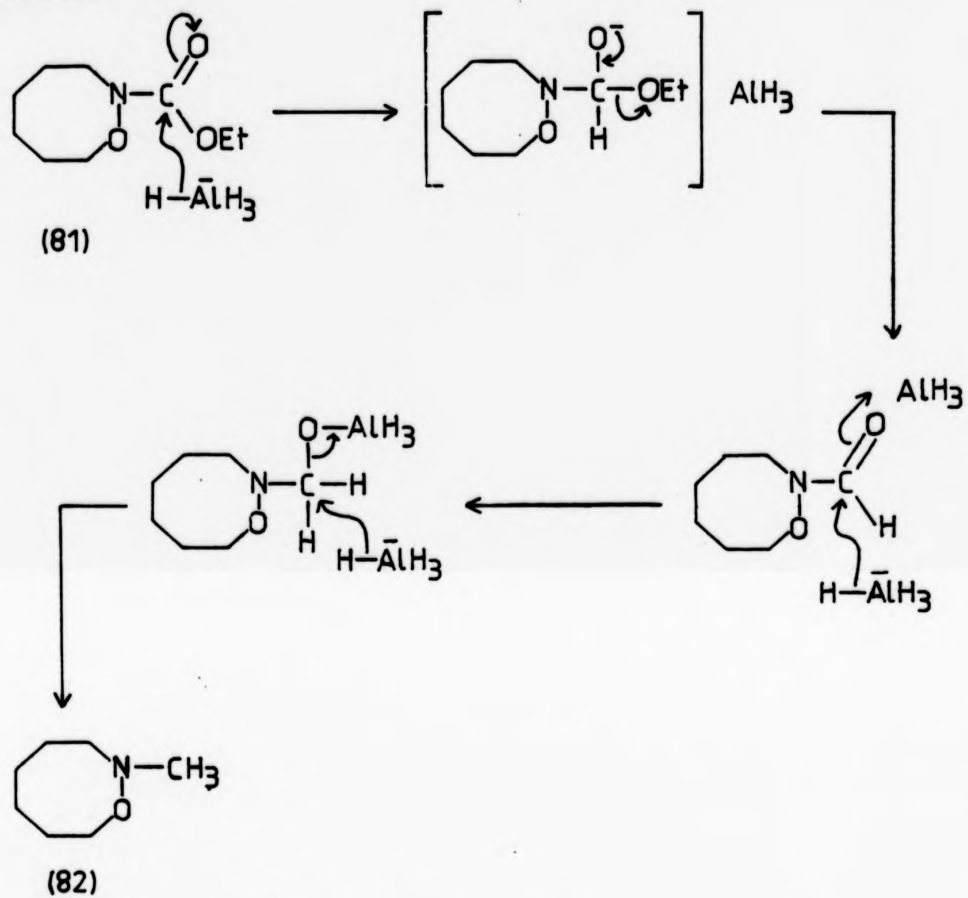
confirmed for the reaction of N-hydroxyurethane with 1,4-dibromides where the results are consistent with bimolecular nucleophilic substitution, S_N2 , attack by oxygen being more rapid than attack by nitrogen.⁴⁷ Thus for an unsymmetrically substituted dibromide, assuming the same molecularity (S_N2) at each site, the relative rates of reaction at each centre will determine the relative amounts of the alternative products. The mechanism in the condensation of 3,3-dimethyl-1,6-dibromohexane (89) with N-hydroxyurethane (66), for ring formation could proceed by either of the routes shown in Schemes 8 and 9 which involve initial attack by oxygen. The very strong bias in favour of the compound (90) in the ring formation is probably due to steric hindrance effect of the dimethyl substituent at carbon-3 of the dibromide (89). This is an example of a γ substituent effect in nucleophilic reactions.¹⁷⁸ Reaction at the more hindered bromide is much slower than reaction at the other bromide. Thus initial attack determines which isomer is formed.

(d) Reduction of the N-Carbethoxy Group

The reduction of N-carbethoxy-1-oxa-2-azacyclooctane (81) with lithium aluminium hydride¹⁴⁶ gave a comparatively low yield (33%) of the N-methyl derivative (82), compared to previously prepared six-membered hydroxylamine derivatives.⁴⁷ A probable mechanism is outlined in Scheme 10. Reduction does not stop at the alcohol and the C-O bond is cleaved more readily than the C-N bond.

The reduction of the eight- and nine-membered N-carbethoxy dimethyl hydroxylamine derivatives (90 and 103 respectively) gave the corresponding open-chain compounds (117) and (118), and not the expected cyclic N-methyl derivatives (92) and (104). Presumably the reduction of the carbethoxy group is hindered by the gem-dimethyl groups giving rise to the undesired products (117 and 118). The probable mechanism is

Scheme 10



indicated in Scheme 11. Hydride ion attack at carbon-3 results in opening the ring and forming the resonance stabilised nitrogen anion which readily picks up a proton. On examining the two possible competing reactions, ie attack by hydride at carbon-3 or attack by hydride at C-carbonyl, it is noted that the formation of the products (117 and 118 respectively) indicates that the attack by hydride at 3-position is most probably due to relief of strain, caused by the presence of the gem-dimethyl, in the ring. A further component of the driving force for this bimolecular nucleophilic displacement (S_N2) reaction is thought to be the formation of the resonance stabilized amide ion. Furthermore, the conformation of the ring could be such that the presence of the gem-dimethyl hinders hydride attack at the carbonyl.

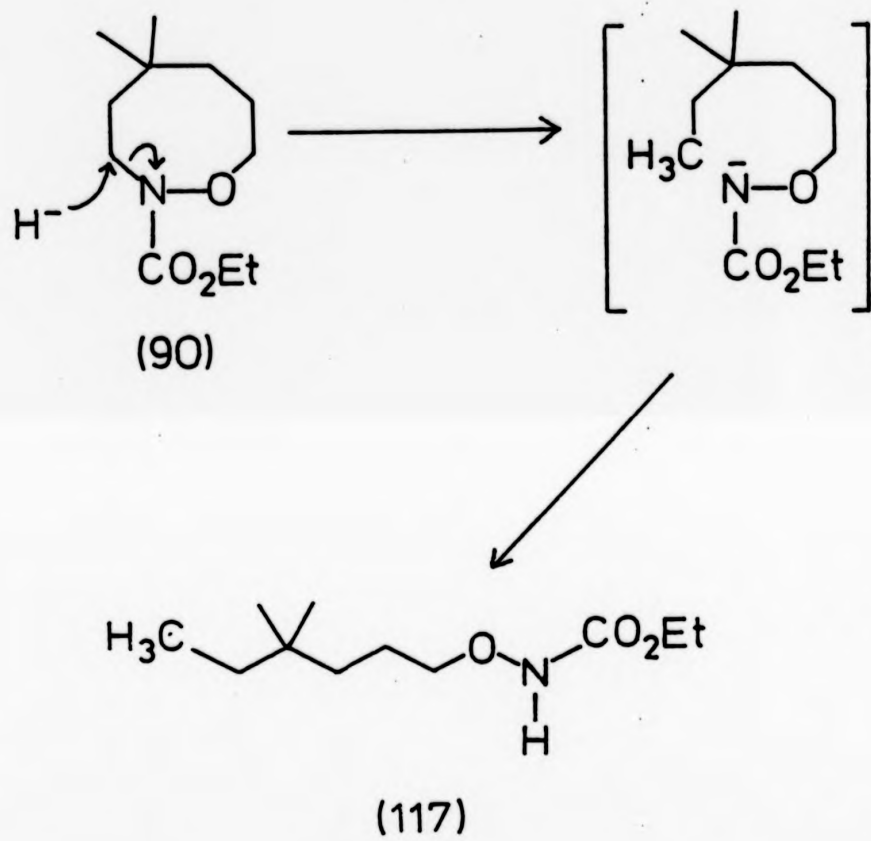
(e) Acid Hydrolysis of the N-Carbethoxy Group

Because of the failure of the above reductions to prepare the desired N-methyl derivatives, an attempt was made to prepare the secondary amines (93) and (105) by acid hydrolysis followed by decarboxylation. Standard literature methods were used. Repeated attempts to hydrolyse the N-carbethoxy group in both eight- and nine-membered dimethyl hydroxylamine rings failed and the respective starting compounds (90 and 103) were recovered from the reaction mixture indicating steric hindrances at the CO_2Et groups.

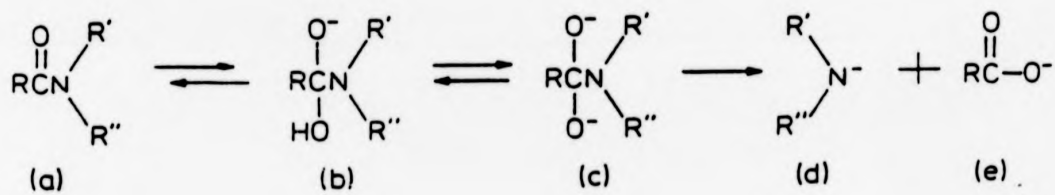
(f) Base Hydrolysis of the N-Carbethoxy Group

In a second attempt to prepare compound (105), the method of base hydrolysis of amides at ambient temperature as employed by P G Gassmann et al¹⁷⁹ was used. They reasoned that base hydrolysis of amides is frequently an inefficient process. While the addition of hydroxide ion to an amide of general formula (a) (Scheme 12) should occur with relative ease to produce (b), the thermodynamically preferred route for the

Scheme 11



Scheme 12



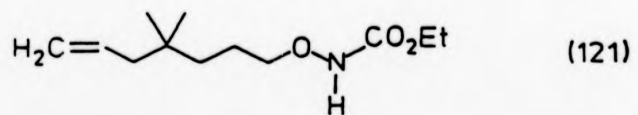
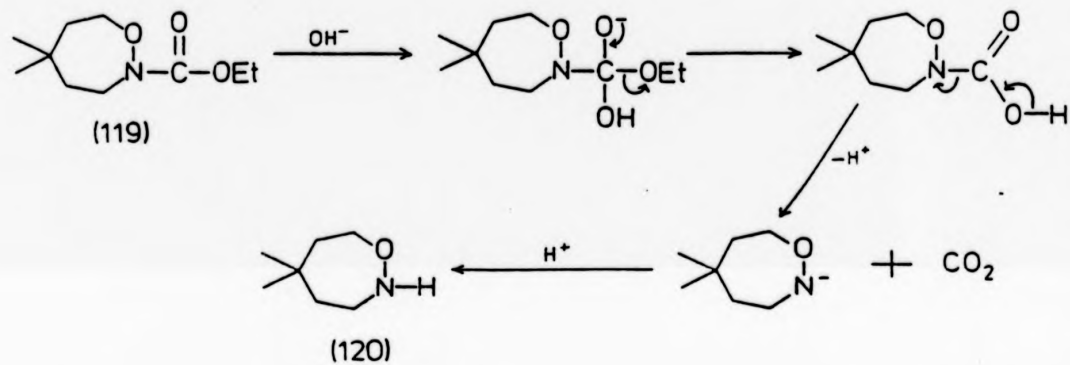
breakdown of (b) involves loss of hydroxide to regenerate (a).¹⁸⁰⁻¹⁸⁵
In principle, if the hydroxylic proton of (b) could be removed by a
second strong base (c) should be generated.¹⁸⁶⁻¹⁸⁸ Cleavage of (c)
with loss of amide anion would generate (d) and (e).

The details of the method are given in the Experimental section.
The base hydrolysis was first attempted on a model compound,
N-carbethoxy-5,5-dimethyl-1-oxa-2-azacycloheptane (119), and the
mechanism of the hydrolysis is believed to proceed as shown in Scheme
13. The hydrolyzed product, 2,5,5-dimethyl-1,2-oxazepane (120), was
obtained in 85% yield. However, on repeating the base hydrolysis with
N-carbethoxy-6,6-dimethyl-1-oxa-2-azacyclononane (103) the product
obtained was identified as N-carbethoxy-2-(aminohydroxy)-4,4-
dimethylheptene (121). It is presumed that the product was formed by
bimolecular elimination (E2). Once again, it is noted that under high
concentration of a strong base, the attack on a proton to give the
elimination product is favoured, rather than a nucleophilic attack on the
C-carbonyl. This result further supports the arguments presented above
that the strain in the ring, probably due to the presence of the
gem-dimethyl grouping, is relieved by an S_N2 or E2 mechanism depending
on the experimental conditions to form the resonance stabilized amide
which readily picks up a proton. Finally, the conformation of the ring
(103) could be such as to make the carbethoxy group very hindered to
attack by a nucleophile.

2.1.3 Conclusion

The preparative method to give N-alkyl-2-(aminohydroxy)-
alkyl-1-thiols (72) from the corresponding tosylates (71) gave yields
over a range of 30-90%; no consistency was observed. While the ring

Scheme 13



formation reaction of the thiols with paraformaldehyde gave consistently very low yields of 10-30% of the 1-oxa-4-thia-2-azacyclohexanes (73).

The "high-dilution" (ie low concentrations of N-hydroxyurethane) method gave yields of 50-60% in the preparations of the N-carbethoxy eight- and nine-membered hydroxylamine rings. The ring formation reaction of the dibromides with N-hydroxyurethane appears to go by way of the oxy-anion tautomer (116a). The lithium aluminium hydride reduction and acid or base hydrolysis of the N-carbethoxy group is hindered by the presence of gem-dimethyl groupings in the rings.

2.2 NUCLEAR MAGNETIC RESONANCE SPECTROSCOPY IN CONFORMATIONAL ANALYSIS

2.2.1 Introduction

Nuclear magnetic resonance spectroscopy is undoubtedly the most powerful technique commonly used for the determination of the conformation of heterocyclic molecules in solution. The nuclei most widely used have been ^1H and ^{13}C . Several reviews exclusively devoted to such application of the nmr technique have appeared.^{8,167,189,191} Conventional methods for measuring rates of chemical exchange by nmr methods have been reported.¹⁹²⁻¹⁹⁴ Roberts has reviewed the line-shape method for determining rates of chemical and conformational exchange.¹⁹²

The presence of electronegative heteroatoms give heterocycles a much wider range of chemical shifts in both ^1H and ^{13}C spectra than is possible for alicyclic compounds. This is because deshielding of the observed nuclei can be caused by a neighbouring electronegative atom through the inductive effect, resulting in a shift to lower field. The anisotropy of the π -electron system (double bond, carbonyl or aromatic system) can also cause a similar field effect. It thus gives spectra

that are far more readily interpreted and also minimizes the problems due to second-order splitting patterns in ^1H spectra.

In the course of this work ^1H and ^{13}C nmr were extensively employed, therefore discussion of their use in conformational analysis is warranted.

2.2.2 ^1H nmr Spectroscopy

In spite of its rather limited range of chemical shifts (ca 10ppm for most organic compounds) the proton is the nucleus most studied by magnetic resonance. Both of the readily available nmr parameters, viz the chemical shift (δ), and the coupling constant (J), are influenced by stereochemical factors.

Spin-spin coupling is the indirect interaction of proton spins through the intervening bonding electrons. It occurs because there is some tendency for a bonding electron to pair its spin with the spin of the nearest proton. A measure of the energy of the interactions of two nuclei, for example, A and B in the molecule, is known as a coupling constant and is given the symbol J_{AB} . Chemically equivalent protons do not show spin-spin coupling due to interaction among themselves. Couplings are divided into geminal, vicinal and long range couplings etc, and will be discussed in more detail below.

Simple splitting patterns which are produced by the coupling of protons which have very different chemical shifts ($\Delta\nu/J \gg 10$) are called first order splitting patterns.¹⁸⁹ When $\Delta\nu/J \leq 10$ the spectra cease to obey simple first order rules and are known as second order spectra. In the case of a complex spectrum the spin-spin decoupling method,¹⁹⁶ for simplifying the spectrum can be used. It involves irradiation of a nucleus with a strong radiofrequency signal at its resonance frequency.

This removes all couplings on the other nuclei due to this nucleus.

(a) Proton-Proton Coupling

Geminal Coupling (2J)

Measurements of geminal couplings^{189,196,197} are especially useful in case of cyclic molecules as they give information about the orientation of groups near a CH_2 -fragment. However, the major limitation of the use of such couplings is experimental as in many cases the two protons are magnetically equivalent and only the replacement of one of the equivalent protons by deuterium enables one to observe H-D coupling. From this value the proton-proton coupling may be calculated by means of equation $J_{\text{H,H}} = 6.55 J_{\text{H,D}}$.

Recently, considerable interest has been displayed in the influence of the lone pair of electrons, present on heteroatoms on the nmr parameters. Variation in the geminal coupling constant between the protons of a methylene group adjacent to a heteroatom have been interpreted in terms of the dihedral angle between lone pair and the CH_2 bonds.¹⁹⁸⁻²⁰¹

Anteunis¹⁹³ has proposed that an increase of 1.8 Hz be added to J_{HH} each time an α -oxygen or α -nitrogen atom has one of its lone pair p-orbitals parallel to the C-H bond for one of the protons involved in the coupling.

In many six-membered nitrogen containing systems there has been observed large chemical shift difference between geminal protons adjacent to nitrogen^{26,45,202} and this has been attributed to the effect of the axial lone-pair of electrons on nitrogen shielding the axial protons in the adjacent methylene group. Thus, the sym-hexahydrotriazines^{26,45} show differences for the ring protons of about 1ppm. A large geminal chemical shift difference for C-(2),(6) protons (0.94 ppm) in N-methyl

piperidine was reported by Lambert and Keske,²⁰³ while in case of N-methyl quinolizidine²⁰² the difference is 0.92 ppm. The increase in the geminal chemical shift difference on changing the N-substituent suggests that the N-substituent plays an important role in determining the magnitude of this difference.²⁰⁴

Vicinal coupling (³J)

The values of these couplings are always positive and range in six-membered ring systems from 1 to 14 Hz. This includes couplings through both double and single bonds and also couplings via atoms other than carbon.^{189,205}

The coupling constant (³J) is related to the dihedral angle (ϕ) (Fig 1.1) in the ethane molecule by the approximated Karplus equation

$$J = A \cos^2 \phi \quad \text{eq 1}$$

where A is a constant and depends on the precise nature of the fragment H-C-C-H, ie A is only constant for a restricted set of compounds.¹⁷⁹

In heterocyclic systems, however, the constant A in equation 1 is often unknown. The constant A varies with the electronegativity of the substituent on the C-C bond. Lambert^{206,207} solved this problem and made vicinal coupling constants a useful conformational tool by taking ratios of coupling constants (R value) for the couplings in the vicinal fragment (Fig 2.2). This eliminates the constant A.

$$R = \frac{J_{\text{trans}}}{J_{\text{cis}}} \quad \text{eq 2}$$

For rapidly inverting six-membered rings R values near 2.0 are indicative of an almost perfect chair conformation, whilst lower R values nearer to 1.0 suggest the presence of flattened chairs or even non-chair conformations. Highly puckered chairs have $R > 2$. The R value method, however, has severe limitations when applied to larger or smaller ring

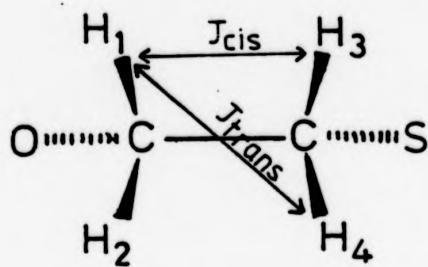


Fig 2.2 Couplings in the vicinal fragment.

systems.^{208,209}

Buys²¹⁰ has shown that for many six-membered rings the internal ring dihedral angle (ϕ) can be related to R by the equation 3.

$$R = \frac{J_{\text{trans}}}{J_{\text{cis}}} = \frac{(3 - 2 \cos^2 \phi)}{4 \cos^2 \phi} \quad \text{eq 3}$$

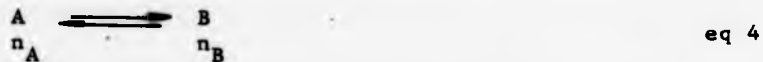
This appears to be a good way for determination of dihedral angles in saturated heterocyclic rings. Values of dihedral angles obtained by this method generally agree to within 2° of those found by other methods.²¹¹

(b) Lineshape Analysis

Analysis of nmr lineshapes for systems undergoing chemical exchange, a technique sometimes referred to as 'Dynamic Nuclear Magnetic Resonance' yields rate constants for the exchange process.²¹²⁻²¹⁴ In practice, the rate constant expressed in sec^{-1} for the exchange process must be round about the value of the chemical shift difference measured in Hertz (Hz) between the exchanging sites. Generally, to bring the rate of exchange into the observable range, the temperature of the sample is varied. Accessible temperatures range from ca 100K to ca 500K, giving a variation in free energies of activation from ca 5 kcal mol^{-1} to ca 25 kcal mol^{-1} . This technique has proved valuable in the measurement of rates of conformational interchange, for example the rates of processes such as restricted rotation and ring and nitrogen inversion,^{26,33} and in determining the proportions of various conformations present at the slower exchange rates (slow exchange limit) when the spectrometer "sees" all of the slowly interconverting conformations.

Consider a molecule which is interconverting between two states A and B, or a nucleus exchanging between two molecules A and B. The

equilibrium,



is obtained in which n_A and n_B are the mole fractions of A and B.

Any equilibrium is characterized by two parameters.

Firstly, the position of the equilibrium is determined by ΔG , the free energy of the process ie

$$n_B/n_A = \exp(-\Delta G/RT) \quad \text{eq 5}$$

and

$$n_A + n_B = 1$$

Secondly, the rate of interconversion is determined by the Gibbs free energy of activation (ΔG^\ddagger), ie the rate of the reaction $A \rightarrow B$. The rate theory developed by Eyring^{215,218} gives the Eyring equation (eq 6) which is used to calculate Gibbs free energy of activation when the rate constant (k) and coalescence temperature (T_c) (vide infra) are known.

$$K = \bar{K} \frac{k_B T_c}{h} \exp \frac{-\Delta G^\ddagger}{RT_c} \quad \text{eq 6}$$

\bar{K} is the transmission coefficient and is assumed to be unity. On giving the Boltzmann (k_B) and Planck (h) constants their numerical values in equation 6, equation 7 in terms of decimal logarithms is obtained. (ΔG^\ddagger units in kcal mol⁻¹).

$$\begin{aligned} \Delta G^\ddagger &= -RT_c [\ln k - \ln (k_B/h) - \ln T_c] \\ &= RT_c [\ln (k_B/h) + T_c/k] \\ \therefore \Delta G^\ddagger &= 4.575 \times 10^{-3} T_c [10.319 + \log (T_c/k)] \quad \text{eq 7} \end{aligned}$$

Now consider a nucleus in the molecule. In state A it has chemical shift ν_A and coupling J_A and in state B shift ν_B and coupling J_B . Note that all these quantities are measured in Hertz. There are three cases to consider.

SLOW EXCHANGE: If the rate of interconversion of A and B is slow (on the nmr time scale) then the nmr spectra of the two separate species A and B will be observed, ie the signals at ν_A and ν_B with couplings J_A and J_B and the relative intensities of the signals give directly n_A and n_B and therefore ΔG .

FAST EXCHANGE: If the rate of interconversion is fast, the nmr spectrum observed is one 'averaged' spectrum in which the chemical shifts and couplings are the weighted averages of the values in A and B. That is, the nucleus will give rise to one signal with the protons (ν_{AV}) given by

$$\nu_{AV} = n_A \nu_A + n_B \nu_B \quad \text{eq 8}$$

and coupling (J_{AV}) by

$$J_{AV} = n_A J_A + n_B J_B \quad \text{eq 9}$$

INTERMEDIATE RATES OF EXCHANGE: In this case broad lines are observed in the nmr spectrum, and is indicative of a rate process. This is one of the few cases in which the resolution of an nmr spectrum is not due solely to the spectrometer. The other common examples are the presence of quadrupolar nuclei (in particular ^{14}N) and paramagnetic species, the latter often as impurity; and poor sample preparation, resulting in solid impurities being present.

Generally, to observe the rate of exchange, the temperature of the sample is varied. The position where separate resonances just merge into one is called the coalescence point and the temperature at which this occurs is known as the coalescence temperature (T_c).

Exchange-broadened spectra of systems, which contain nuclei that are spin-spin coupled to one another, in general cannot be calculated by the Bloch equations.²¹⁷ For such systems (an AB system) a quantum-mechanical technique, based on the density matrix method, has been developed. The rate constant (k)²¹⁸⁻²²⁰ at the coalescence

temperature (T_c) for an AB spectrum with exchange between A and B is given by:

$$k = \frac{\pi}{\sqrt{2}} (\delta_{AB}^2 + 6J_{AB}^2)^{1/2} \quad \text{eq 10}$$

$$\text{where } \delta_{AB} = (\delta_{13}^2 - J_{AB}^2)^{1/2} \quad \text{eq 11}$$

the chemical shift difference between the two coupled nuclei (Fig 2.3). These equations (eq 10 and 11) used in conjunction with eq 7 derive the expression (eq 12) to calculate the free energy of activation at the temperature of coalescence of an AB system (ΔG^\ddagger in kcal mol⁻¹).

$$\Delta G^\ddagger = 4.575 \times 10^{-3} T_c \left[9.972 + \log \frac{T_c}{(\delta_{AB}^2 + 6 J_{AB}^2)^{1/2}} \right] \quad \text{eq 12}$$

2.2.3 ¹³C nmr Spectroscopy

The first observation of conformational effects by ¹³C nmr (cmr) was by Stothers,²²¹ who examined the shift of the carbinol carbon atoms in a series of conformationally biased 4-tert-butyl-cyclohexanols (Fig 2.4). He noted that for the isomer with an axial hydroxyl group the carbinol carbon resonated ca 5ppm to higher field of that in the isomer with an equatorial hydroxyl group.

However, the first lineshape kinetic analyses by cmr were reported in 1971²²²⁻²²⁵ and showed that cmr is particularly useful in studies of rapid chemical processes. Several factors cause dynamic cmr studies to be distinctly advantageous relative to analogous proton nmr studies:

1. Frequency differences between "exchanging" sites are generally far greater in ¹³C nmr.
2. Carbon resonance bandshapes that are not undergoing exchange can be easily controlled; most resonances are singlets.
3. The relative simplicity of ¹³C spectra facilitates interpretation

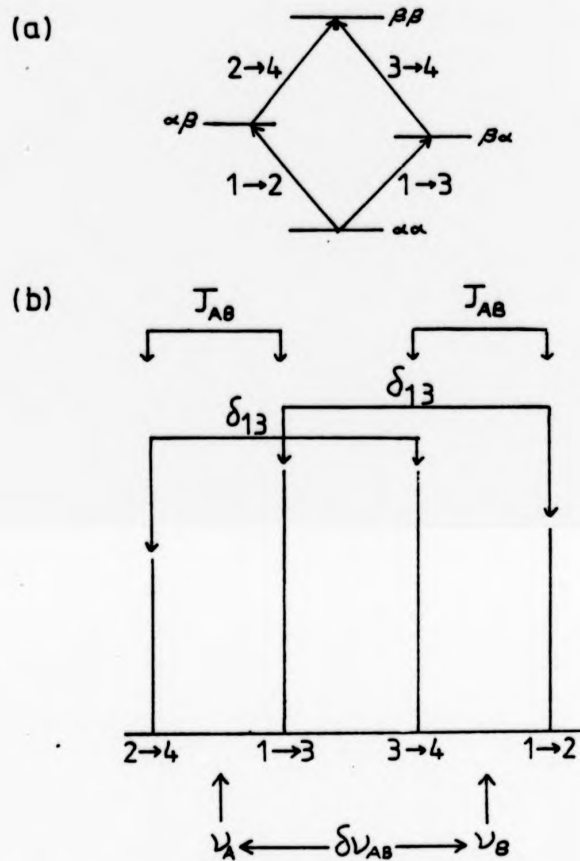


Fig 2.3 (a) Scheme of the transitions in an AB system.
 (b) Exchange between the A and B sites of an AB system, indicating the apparent site exchanges.

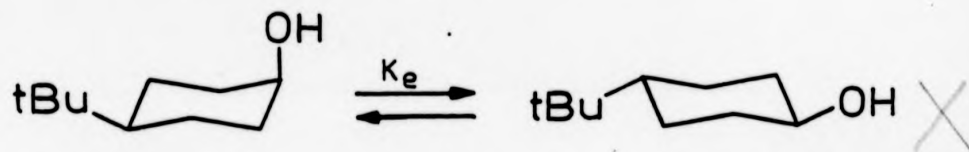


Fig 2.4 The Conformational Equilibrium in 4-tert-butyl-cyclohexanol.

of complex situations, for example, sorting out two or more frozen configurations..

Anet had used ^{13}C nmr extensively to evaluate conformational dynamics of alicyclic systems.^{48,135,136,148,226-229} Other groups have also discussed the methods and advantages of dynamic ^{13}C nmr.²³⁰⁻²³² Equations developed by Anet et al²³³ for exchange between two unequally populated sites give:

$$\nu_{(1/2 \text{ max})} = P \times \delta\nu \quad \text{eq 13*}$$

$$k = 2\pi\delta\nu \quad \text{eq 14*}$$

Equation 13 gives the population of a minor form from the maximum line broadening provided that the chemical shift difference is known.

Equation 14 gives the rate constant for exchange at maximum broadening and hence the free energy of activation. Then the free energy of activation, ΔG^\ddagger is found using the standard kinetic expression as developed by Eyring;^{215,216} equations 6 and 7. The free energy, ΔG° , of the observed process defined by the equation,²³⁴

$$\Delta G^\circ = -RT \ln K \quad \text{eq 15}$$

may also be calculated by estimating the equilibrium constant K from the approximate digital integrals of the 'major' and 'minor' peaks under study. This, thus gives the free energy difference between the conformations observed.

These equations were first used in the study of 1,2,2,6-tetramethylpiperidine²³³ and have subsequently been used by other workers, proving

* $\nu_{(1/2 \text{ max})}$ is the maximum broadening at half height of the signal; P is the population of the minor form; $\delta\nu$ is the chemical shift difference in hertz (Hz), and k is the rate constant in s^{-1} for the temperature of maximum broadening in the direction minor to major. These equations are applicable for conformer ratios greater than 10:1 and can be obtained mathematically from the Gutowsky-Holm lineshape equation for two sites.

to be extremely valuable especially for ^{13}C studies of low barriers not accessible to ^1H nmr spectrometers.

The problems with the use of ^{13}C nmr spectra can be summed up as being due to low sensitivity of natural abundance spectra, to differences in intensity response in different sites, and to resolution problems inherent in the Fourier Transform technique.

2.2.4 Conclusion

In dynamic nmr studies, the major problems are the relatively small range in temperature over which meaningful values of the rate can be measured, the difficulty in measuring the sample temperature accurately in the probe and the errors involved in the estimation of the nmr parameters needed for the calculations. A reasonable error in T_c is $\pm 2^\circ$ and this corresponds to an error in ΔG^\ddagger of $\pm 0.12 \text{ kcal mol}^{-1}$. In order to cause a similar error in ΔG^\ddagger , k has to be in error by ca $\pm 20\%$. If larger errors in ΔG^\ddagger can be accepted, say $\pm 0.48 \text{ kcal mol}^{-1}$, errors in k as large as 100% can be allowed. Undoubtedly, the most accurate molecular parameter obtained from such experiments is the value of the free energy of activation (ΔG^\ddagger) at the coalescence temperature, and this is the parameter we shall be most concerned with in the first section of this thesis.

The combined use of ^1H and ^{13}C nmr has, however, considerably extended the temperature range investigated and, in principle, provided a method whereby more accurate values may be obtained. In many cases a clearer insight into mechanisms of intermolecular exchange processes can be obtained by using a combination of ^1H and ^{13}C nmr spectroscopy. This is, for example, the case when two processes with rather similar barriers occur in the same molecule, and both of them affect the ^1H

spectrum and only one of them affects the ^{13}C spectrum.

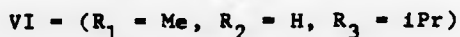
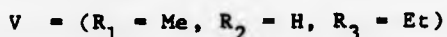
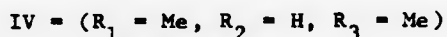
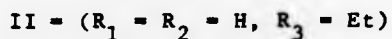
2.3 THE ^1H AND ^{13}C NUCLEAR MAGNETIC RESONANCE SPECTRA AND CONFORMATIONAL EQUILIBRIA OF HYDROXYLAMINE DERIVATIVES: RESULTS, ANALYSIS AND DISCUSSION

2.3.1 Introduction

The ^1H and ^{13}C nmr spectra run at ambient and low temperatures are analysed and discussed in this section. They provide information about the following:

- i) The chemical shifts and coupling constants
- ii) The nitrogen and/or ring inversion barriers
- iii) The conformational equilibria.

For simplification in the following discussion the 1-oxa-4-thia-2-azacyclohexane derivatives (73) have been assigned reference numbers as follows:



The chemical shift differences of the ring protons in the hydroxylamine derivatives were very much greater than the coupling constants, hence the ^1H nmr spectra were virtually first order. The chemical shifts of ^1H and ^{13}C nmr of the 1-oxa-4-thia-2-azacyclohexane derivatives are reported in Tables 2.2 and 2.3 respectively and the coupling constants in Table 2.4. The ^1H and/or ^{13}C nmr spectra of the cyclic hydroxylamine derivatives were found to be temperature

dependent showing effects due to both ring and/or nitrogen inversion. The details of the spectral measurements for the 1-oxa-4-thia-2-azacyclohexane derivatives are given in Tables 2.5 and 2.6 respectively.

2.3.2 1-Oxa-4-Thia-2-Azacyclohexanes

(a) Spectral Assignments

The ^1H nmr spectra of derivatives I, II and III run at ca 35°C show the following principal resonances: the $-\text{NCH}_2\text{S}$ as a singlet and approximate triplets for the $-\text{CH}_2\text{O}-$ and $-\text{CH}_2\text{S}-$ protons (actually AA'BB' spectrum) with splitting of ca. 5.0 Hz ($J_{5,6}$) due to vicinal coupling. The $-\text{NCH}_3$ signal for I is a sharp singlet of relative intensity three and appears at lower field compared to a $-\text{CMe}$ signal because of the deshielding effect of the nitrogen. The N-ethyl group in II is characterized by two resonances. The $-\text{NCH}_2-$ resonance of relative intensity two appears as a quartet due to coupling to the hydrogen of the methyl group. The $-\text{NCH}_2\text{CH}_3$ resonance of relative intensity three is shown as a triplet due to splitting by the two hydrogens of the methylene group. Two resonances again characterize the N-isopropyl group in III. A septet of relative intensity one corresponds to the methine group [$-\text{NCH}(\text{CH}_3)_2$] coupled to six hydrogens of the two methyl groups. On the other hand, a doublet of relative intensity six is consistent with the methyl groups [$-\text{NCH}(\text{CH}_3)_2$] split by the proton of the methine group.

While, the ^1H nmr spectra of derivatives IV, V and VI run at ca 35°C show the following principal resonances: the $-\text{NCH}_2\text{S}-$ as an AB quartet, multiplets for the C(5)-H's and C(6)-H and the C(6)-Me as a doublet. The N-alkyl resonances for N-Me in IV and N-Et in V are identical to those described above. However, in the case of these

C(6)-methyl substituted derivatives where the C(6) carbon atom now becomes asymmetric, the two methyl groups in $[-NCH(\underline{CH}_3)_2]$ are diastereotopic and appear in the spectrum as two pairs of doublets.

The ^{13}C off resonance decoupled nmr spectra of the derivatives I, II and III run at ca $30^\circ C$ show the following principal resonances: the C(3), C(5) and C(6) carbon resonances as triplets. The $-NCH_3$ signal for I as a quartet, for II the $-NCH_2-$ signal is a triplet and $-NCH_2CH_3$ is a quartet and for III $-NCH-$ is a doublet and $-NCH(\underline{CH}_3)_2$ is a quartet.

The ^{13}C off resonance decoupled nmr spectra of the derivatives IV, V and VI run at ca $30^\circ C$ show the following resonances: the C(3) and C(5) resonances as triplets. The C(6) as a doublet and C(6)- \underline{CH}_3 substituent as a quartet. The N-alkyl carbon resonances for N-Me in IV and N-Et in V are identical to those described above. The two diastereotopic methyl groups in N-iPr for VI appear as two pairs of quartets.

The chemical shift values from 1H and ^{13}C nmr are reported in Tables 2.2 and 2.3 respectively. All these values are consistent with the structures for the respective 1-oxa-4-thia-2-azacyclohexane derivatives and are consistent with rapid inversion of both ring and the nitrogen atom. When, however, the temperature is lowered all the 1H nmr resonances of compounds I, II and III remain essentially unchanged except the singlet due to the C(3)-H's, which broadens and then splits into an AB quartet. In the low temperature lineshape kinetic analysis by cmr the carbon resonances due to the C(3) and C(6) were observed to broaden reaching a maximum at temperatures of about -58 to $-63^\circ C$ and then sharpen again below this range. Coalescence temperatures, coupling constants, rate constants and free energies of activation for the

TABLE 2.2 Proton chemical shifts for 10% w.v solutions of 1-oxa-4-thia-2-azacyclohexanes in CDCl_3 , 35°C (δ scale, relative to internal TMS).

PROTONS	COMPOUND (73)					
	I	II	III	IV	V	VI
C(3)H	3.80	3.85	3.95	3.75	3.77	3.85
C(5)H	2.70	2.70	2.65	2.45	2.45	2.50
C(6)H	4.10	4.10	4.15	4.15	4.05	4.15
C(6)CH ₃	-	-	-	1.15	1.13	1.15
N.CH ₃	2.60	-	-	2.60	-	-
N. <u>CH</u> ₂ .CH ₃	-	2.75	-	-	2.73	-
N.CH ₂ . <u>CH</u> ₃	-	1.15	-	-	1.10	-
N. <u>CH</u> .(CH ₃) ₂	-	-	3.00	-	-	3.00
N.CH.(<u>CH</u> ₃) ₂	-	-	1.10	-	-	1.10

TABLE 2.3 The ^{13}C chemical shift data and spectral assignments for some 1-oxa-4-thia-2-azacyclohexanes (ppm downfield from TMS), measured at ambient temperature.

Substituents	C3	C5	C6	N-C	N-C-C	C6(Me)
2-Methyl	58.18	26.42	69.81	46.07	-	-
2-Ethyl	52.80	26.90	69.80	56.50	11.90	-
2-Isopropyl	53.70	27.02	70.14	56.46	19.05	-
2-Methyl-6-methyl	57.04	32.00	74.20	45.95	-	20.62
2-Ethyl-6-methyl	55.41	32.54	74.16	52.52	11.90	20.56
2-Isopropyl-6-methyl	52.53	32.72	74.52	56.10	18.93 and 19.30	20.54

processes involved in the derivatives I, II and III are listed in Tables 2.5 and 2.6.

In the case of the compounds IV, V and VI the C(3)-H's in ^1H nmr appear as a quartet at nmr probe temperature (ca 35°C), because the C(3)- protons are diastereotopic with respect to the C(6)-methyl substituent.

Low temperature cmr analysis of resonances C(3) and C(6) in compounds IV, V and VI showed maximum line broadening in the temperature range -25 to -54°C (Table 2.6). The proton-proton coupling constants are listed in Table 2.4.

(b) Coupling Constants

The ^1H nmr spectra of the 1-oxa-4-thia-2-azacyclohexanes provide useful information about the kind and the variation in range of the coupling constants in this series of compounds.

The vicinal couplings are found to be between 3.0 ± 0.2 to 7.0 ± 0.3 Hz. In the case of the C(6)-methyl substituted derivatives (IV-VI) there was observed geminal coupling ($J_{3,3}$) due to the presence of two chemically different protons in the position C(3) the range being 11.7 to 12.0 Hz. In the case of N-alkyl-1-oxa-4-thia-2-azacyclohexanes (I-III) the geminal coupling ($J_{3,3}$) observed at low temperatures (from -75° to -80°C) is similar 12.0 ± 0.3 Hz to the C(6)-methyl substituted derivatives.

From Lambert's^{206,207} and Buys',²¹⁰ equations (eq 2 and 3 respectively), the dihedral angle (θ) of the ring was calculated using derivative I as the model compound. Analysis of the AA'BB' multiplets for the C(5) and C(6) hydrogens gives $J_{\text{cis}} = 1/2(J_{\text{ea}} + J_{\text{ae}}) = 2.8$ Hz and $J_{\text{trans}} = 1/2(J_{\text{ee}} + J_{\text{aa}}) = 6.9$ Hz. Then using Lambert's equation, we have

TABLE 2.4 Coupling constants (Hz) in the 1-oxa-4-thia-2-azacyclohexane derivatives measured at ca +35°C.

Substituents	Vicinal Coupling		Geminal Coupling	
	$J_{5,6}$	$J_{N-Alkyl}$	$J_{6,6}$	$J_{A,B}$
N-Me	5.0 \pm 0.2	-	-	-
N-Et	5.0 \pm 0.2	7.0 \pm 0.3	-	-
N-iPr	5.0 \pm 0.2	6.5 \pm 0.3	-	-
N-Me; 6-CH ₃	3.2 \pm 0.2	-	6.4 \pm 0.2	12.0 \pm 0.2
N-Et; 6-CH ₃	3.2 \pm 0.2	7.0 \pm 0.3	6.4 \pm 0.2	12.0 \pm 0.3
N-iPr; 6-CH ₃	3.2 \pm 0.2	6.3 \pm 0.3	6.4 \pm 0.2	11.7 \pm 0.3

TABLE 2.5 The barrier to nitrogen inversion in 1-oxa-4-thia-2-azacyclohexanes from measurements on the C3 hydrogens by low-temperature proton nuclear magnetic resonance.

N-substitution	J_{AB} ± 0.2 Hz	δ_{13} Hz	$\delta_{\nu AB}$ ± 0.2 Hz	k s ⁻¹	T_c °C	ΔG^\ddagger kcal mol ⁻¹
Methyl	12.2	20.5	16.47	75.80	-40 \pm 5	11.52
Ethyl	12.1	20.0	15.92	74.74	-51 \pm 3	10.96
Isopropyl	12.3	20.7	16.65	76.47	-57 \pm 2	10.64

TABLE 2.6 The barriers to inversion in 1-oxa-4-thia-2-azacyclohexanes from measurements on the carbon (6) by low temperature ^{13}C nuclear magnetic resonance.

Substituents	$T_c \pm 5K$	ν_i ($\frac{1}{2}$ max)	If $P \leq 10\%$			If $\delta\nu \leq 400$ Hz			Average ΔG^\ddagger ± 0.15 kcal mol $^{-1}$
			P	lower limit for k s $^{-1}$	$\therefore \Delta G^\ddagger$ kcal mol $^{-1}$	P	upper limit for k s $^{-1}$	$\therefore \Delta G^\ddagger$ kcal mol $^{-1}$	
2-Methyl	215	18.9	0.1	1187.52	9.42	0.047	2526.64	9.10	9.26
2-Ethyl	215	23.8	0.1	1495.40	9.32	0.060	2492.33	9.10	9.21
2-Isopropyl	210	31.0	0.1	1947.79	8.98	0.078	2497.16	8.88	8.93
2-Methyl-6-Methyl	248	30.0	0.1	1884.96	10.71	0.075	25.3.27	10.57	10.64
2-Ethyl-6-Methyl	223	30.51	0.1	1917.00	9.57	0.076	2522.37	9.45	9.51
2-Isopropyl-6-Methyl	219	49.5	0.1	3110.18	9.18	0.123	2528.60	9.27	9.23

$$R = \frac{J_{\text{trans}}}{J_{\text{cis}}} = \frac{6.9}{2.8} = 2.46$$

An R value greater than 2 is indicative of a more puckered chair than in cyclohexane. Also the fact that the bond lengths C-C, C-O, C-S, C-N and N-O are different (Table 1.2) suggest that the ring will have an unsymmetrical puckering. On substituting ϕ as 59° , 60° and 61° respectively into Buys' equation

$$R = \frac{J_{\text{trans}}}{J_{\text{cis}}} = \frac{(3-2 \cos^2 \phi)}{4 \cos^2 \phi}$$

we obtain R values of 2.33, 2.50 and 2.69 respectively. Thus, on comparison with the R value measured, the internal dihedral angle about the C(5) to C(6) bond in the ring may be assumed to be $60 \pm 2^\circ$, taking into consideration error estimates on J values. This is in keeping with the internal ring torsion angles of most bonds in saturated six-membered rings. Torsion angles about the C(5) to C(6) bond in the closely related tetrahydro-1,4,2-dioxazine and -1,2-oxazines have been measured^{95,106} and found to be $56 \pm 2^\circ$ and $56.2 \pm 0.4^\circ$ respectively, and the value for cyclohexane is ca 55° .

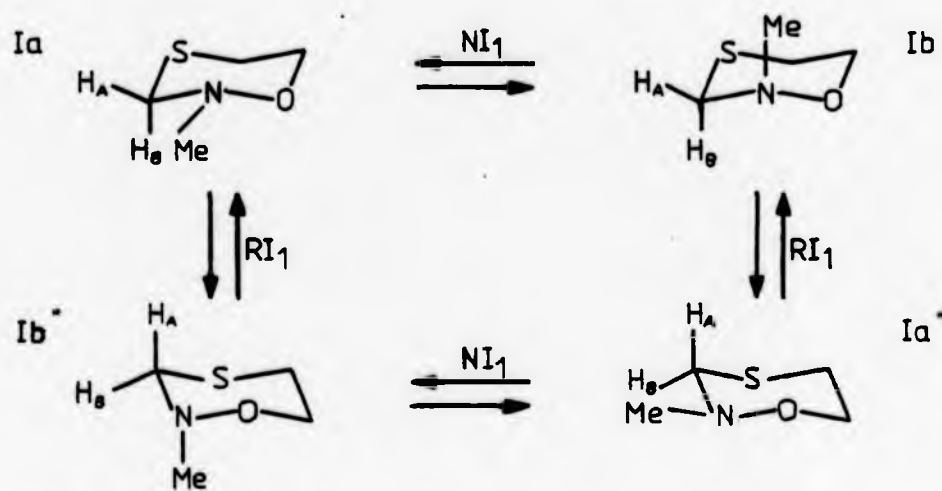
If the torsion angle about the N-O bond is 67° as in the tetrahydro-1,2-oxazine ring, this oxathiazine ring system can be described as considerably puckered.

(c) Conformational Equilibria

As was shown in the introduction the different conformations of 2,5-dimethyltetrahydro-1,2-oxazine (Fig. 1.6) are in equilibrium through a series of ring and nitrogen inversions. The same idea can be applied to the N-alkyl-1-oxa-4-thia-2-azacyclohexanes (I, II and III), and a representative equilibrium scheme, for compound I, is shown in Scheme

14. Assuming a preference for an equatorial N-methyl group, the equilibrium reduces to that between conformations Ia and Ib. One of these processes, probably nitrogen inversion, was slowed down in the ^1H spectra (Table 2.5). The decrease in the free energy of activation barrier (ΔG^\ddagger) observed as R_3 (73) is changed in the series Me, Et, iPr may be explained in terms of increase in the size of the substituent on nitrogen. The effect of the size of the substituent on nitrogen has been found to lower the barrier significantly as the alkyl group changes from methyl to isopropyl. The nitrogen inversion barriers of the closely related tetrahydro-1,4,2-dioxazines were found to be 11.4, 11.0 and ca 10.2 kcal mol $^{-1}$ for the N-Me, N-Et and N-iPr substituted derivatives respectively. The corresponding values in the current work were 11.5, 11.0 and 10.6 kcal mol $^{-1}$ indicating that β -sulphur has a similar effect to β -oxygen on nitrogen inversion barriers.

A low temperature study was also done using ^{13}C nmr. The temperature dependence of the cmr spectrum clearly shows that one of the processes shown in Scheme 14 is being 'frozen out' at temperatures very much lower than for the ^1H spectra. Furthermore, the changes involved are those consistent with sites of very different populations and thus consistent with the freezing out of the second, lower activation energy process. The changes are therefore presumed to arise from a ring inversion process. The temperature of maximum broadening seems hardly to vary along the series indicating that the N-substituent does not affect the barrier to the process. Again this is consistent with slowing of ring inversion giving rise to the observation. As this barrier to ring inversion involves the dynamics between two unequally populated sites the equations developed by Anet et al²³³ are employed



Scheme 14 Equilibrium Scheme for N-methyl-1-Oxa-4-Thia-2-Azacyclohexane (I).

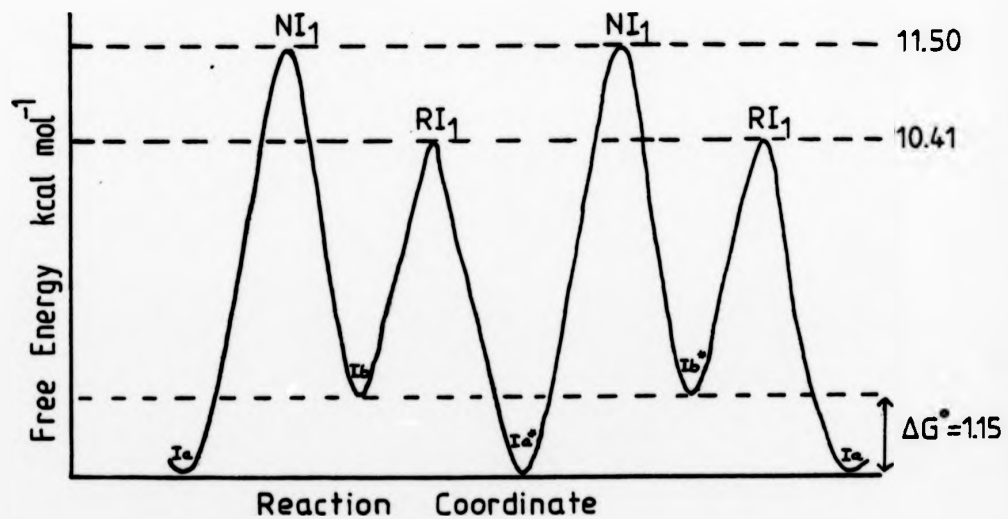


Fig 2.5 Free energy changes associated with ring and nitrogen inversion in N-methyl-1-oxa-4-thia-2-azacyclohexane, corresponding to Scheme 14.

(Section 2.33).

$$\nu_{(1/2\max)} = P \times \delta\nu \quad \text{eq 13}$$

$$k = 2\pi\delta\nu \quad \text{eq 14}$$

$$\therefore k = \frac{2\pi \nu_{(1/2\max)}}{P} \quad \text{eq 16}$$

Since the peaks from the minor conformations at low temperatures could not be observed, the values of $\delta\nu$ or P could not thus be determined. Estimated limits may however be set and ranges for k calculated from a knowledge of $\nu_{(1/2\max)}$. Hence ranges for ΔG^\ddagger can be estimated.

It was estimated that the population of the minor conformation (P) was <10% giving a lower limit for k (eq 16). The upper limit for k was calculated by assuming that the chemical shift difference between the minor and major conformation is less than or equal to 400 Hz (eq 13) (Table 2.6). In these cases of unequally populated sites, the ΔG^\ddagger values correspond to the process of lower activation energy.

In the dynamic nmr experiment for exchange between two sites, A and B, the rate constant measured, k_{obs} , is the sum of the forward and reverse rate constants ($k_f + k_r$). If A and B are equally populated $k_f = k_r = k_{\text{obs}}/2$. If however the populations differ by a factor of (say) ten or more, then $k_r \gg k_f$ and $k_r = k_{\text{obs}}$. The observed free energy of activation at coalescence therefore corresponds to the change least stable conformer \rightarrow transition state. In order to make the free energy of activation correspond to the change more stable conformer \rightarrow transition state, the free energy difference (ΔG°) between the conformers must be added to the observed barrier. This point is of direct relevance in the 1-oxa-4-thia-2-azacyclohexanes where all barriers are most sensibly related to the change equatorial N-alkyl \rightarrow transition state. Thus, the free energy difference ΔG° should be added to the

observed ΔG^\ddagger values to correct for equally populated sites giving a value for the barrier equatorial N-alkyl \rightarrow transition state. This gives us a value for ring inversion barrier. ΔG° can now be estimated from limits set on P in Table 2.6. The ΔG° values estimated are listed in Table 2.7.

Figure 2.5 shows schematically the energy barrier changes around the ring and nitrogen inversion route map for I presented in Scheme 14. In this graph, following the argument above, nitrogen inversion is shown as the larger barriers and ring inversion as the smaller.

The possible conformations of compound IV and the route map arising from ring and nitrogen inversions are shown in Scheme 15. The following discussion of compound IV is also applicable to compounds V and VI.

The cmr spectrum of the compound IV shows temperature dependence. The high field carbon-(6) resonance broadens as the temperature is lowered, but resharpenes at -30°C . The N-methyl signal also broadens as the temperature is lowered, resharpening at -40°C , but all other resonances remain essentially unchanged. Again assuming a preference for an equatorial N-methyl group, the equilibrium scheme probably reduces to a virtual equilibrium between conformations IVa and IVb.

There is no steric or electronic reason to expect that in Scheme 15 the energy change from IVa to the transition state NI_1 should differ much from the energy state IVc \rightarrow transition state NI_2 . Since IVc is presumed to be higher than IVa the transition state NI_2 should therefore be higher than NI_1 . The energy changes for ring and nitrogen inversion in C(6)-methyl substituted derivatives are shown schematically in Fig 2.6. The first process to be frozen out involves passage over the barrier NI_2 . This is not observable by nmr spectroscopy because all conformations continue to interconvert via the

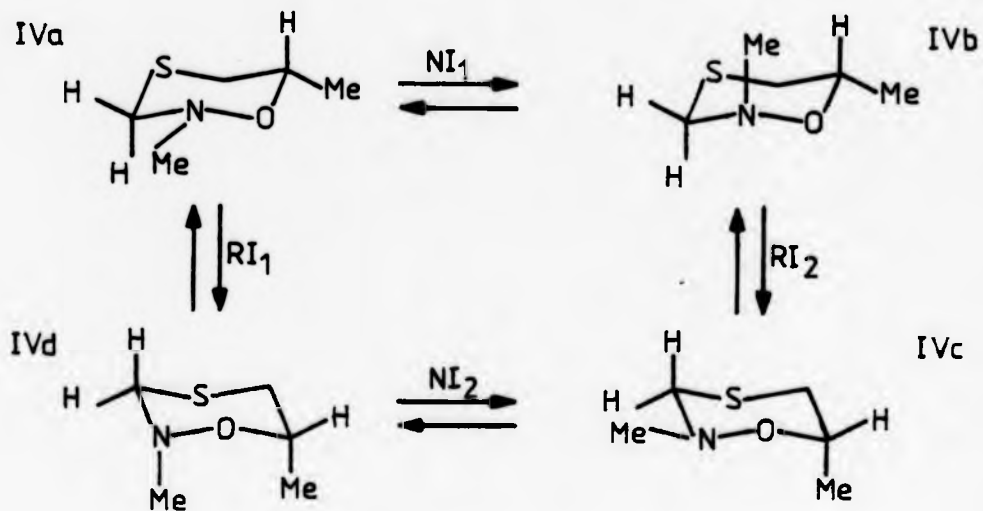
TABLE 2.7 Conformational free energy differences on nitrogen calculated from the approximate digital integrals of the 'minor' peak ie $\Delta G^\circ = RT_c \ln P$.

Substituent	T _c K	If P < 10% ΔG° kcal mol ⁻¹	If $\delta\nu \leq 400$ Hz ΔG° kcal mol ⁻¹	Average $\Delta G^\circ \pm 0.2$ kcal mol ⁻¹
2-Methyl	215	0.98	1.31	1.15
2-Ethyl	215	0.98	1.20	1.09
2-Isopropyl	210	0.96	1.06	1.01
2-Methyl-6-Methyl	248	1.13	1.28	1.21
2-Ethyl-6-Methyl	223	1.02	1.14	1.08
2-Isopropyl-6-Methyl	219	1.00	0.91	0.96

lower barriers RI_1 , RI_2 and NI_1 . The next process to be frozen out is NI_1 which separates (IVa and IVd) from (IVb and IVc). The rate constant observed from the coalescence measurements corresponds to $IVb \rightarrow NI_1$, therefore the observed barrier and the free energy difference between IVa and IVb must be added to measure the barrier height relative to IVa. Freezing out of the ring inversions $IVa \rightarrow IVd$ and $IVb \rightarrow IVc$ will give rise to no spectral changes because of the low amounts of IVd and IVc present. Thus slowing of any one of the four different processes in Scheme 15 will lead to no spectral changes as all conformers may still interconvert rapidly. Two processes are required to be slow for the observed change which separates IVa and IVb to be explained. The only compatible pairs of slow rates are NI_1RI_1 , NI_1RI_2 and NI_1NI_2 . In all cases NI_1 plus one other process must be slow on the nmr scale if IVa and IVb are to be observed separately at low temperature.

As for the parent N-alkyl compounds, no peaks from the minor conformation at low temperature cmr could be observed. The following limits as above were set; $p \leq 10\%$ and $\delta\nu < 400$ Hz, which allowed us to put upper and lower limits to the population of the minor conformation. Hence ranges for ΔG^\ddagger were estimated (Table 2.6). These values of observed free energy of activation at coalescence have, as before, to be corrected to make the free energy of activation correspond to the more stable conformer \rightarrow transition state. The free energy difference ΔG° may again be estimated from the limits set on P in Table 2.6. The ΔG° values calculated from the values of P are listed in Table 2.7.

On examining the coalescence temperatures and the observed ΔG^\ddagger values of these C(6)-methyl substituted rings, a distinct variation is noted as the N-alkyl group is altered. Furthermore, the corrected



Scheme 15 Equilibrium Scheme for 6-Methyl-N-Methyl-1-Oxa-4-Thia-2-azacyclohexane (IV).

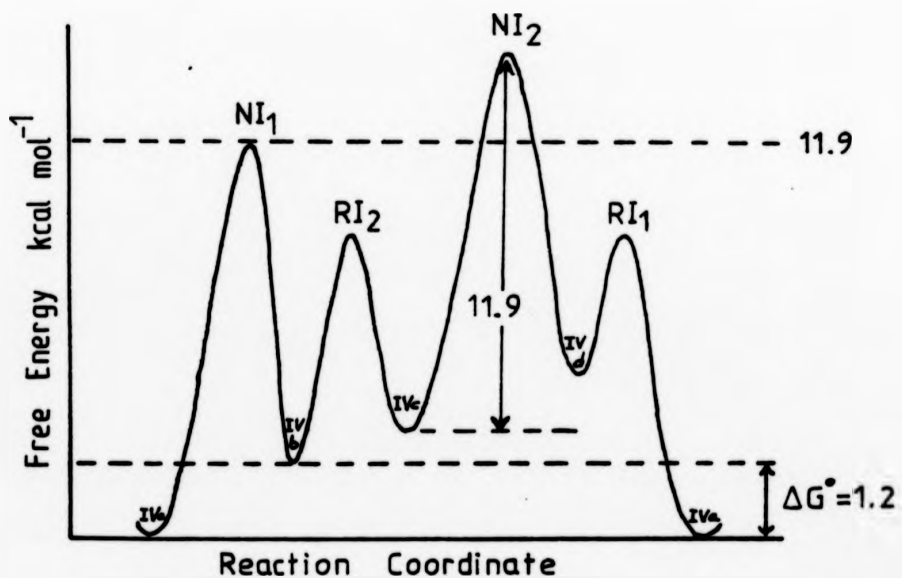


Fig 2.6 Free energy changes associated with ring and nitrogen inversions in N-methyl-6-methyl-1-oxa-4-thia-2-azacyclohexane, corresponding to Scheme 15.

values for the derivatives IV, V and VI are 11.8, 10.6 and 10.2 ± 0.2 kcal mol⁻¹ respectively. These values are in close agreement with the nitrogen inversion barriers of the respective parent N-alkyl derivatives (I-III) (Table 2.5). Thus the origin of the observed process appear to be nitrogen inversion, and consistency is obtained between the series I, II, III and the series IV, V, VI.

2.3.3 N-Methyl-1-Oxa-2-Axacyclooctane

(a) Spectral Assignments

The chemical shifts of ¹H and ¹³C nmr are reported in the experimental section.

The ¹H nmr spectrum run at ca 35°C show the following principal resonances: the N-methyl as a sharp singlet of relative intensity three and C(3)-protons as a kinetically broader peak of relative intensity two. The C(4), C(5), C(6) and C(7) protons appear as a singlet of relative intensity eight. The C(8)-protons appear at highest frequency as a broadened triplet.

(b) Conformational Equilibria

In the low temperature lineshape kinetic analysis by ¹H nmr, the C(3)-proton resonance was observed to broaden reaching a maximum broadening at coalescence temperature ca $9 \pm 3^\circ\text{C}$ giving a complex multiplet on further cooling (Fig 2.7). On closer examination of the complex splitting pattern, it may be noted that the left hand side (ie high frequency end) looks like the left hand side of an AB quartet with additional small triplet couplings superimposed on it. While the right-hand side (ie lower frequency) of the splitting pattern appears to have a larger additional triplet coupling on it. Thus, the multiplet was approximately treated as a AB quartet in order to obtain a value for

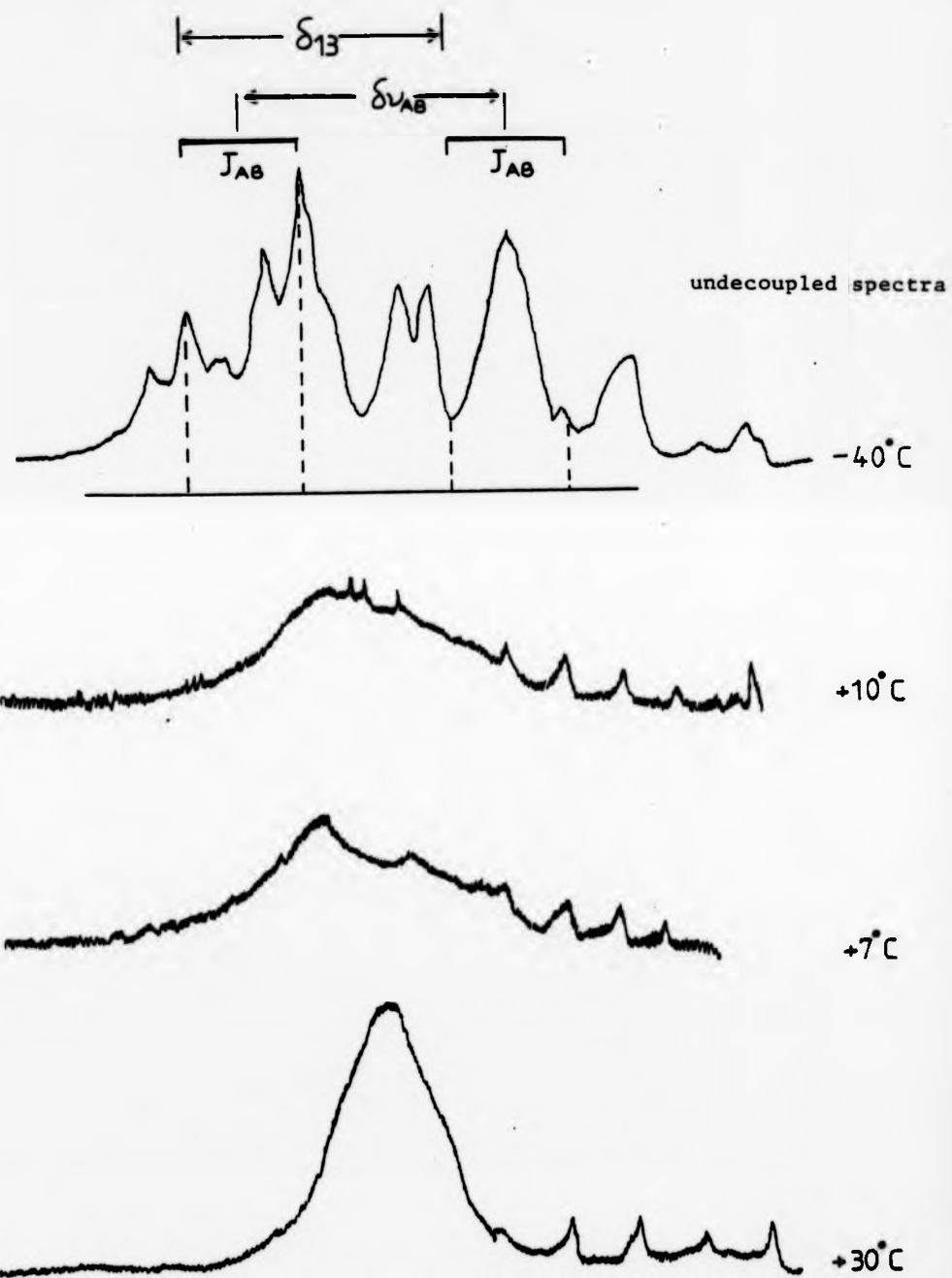


Fig 2.7 Spectra of C3-protons in 1-oxa-2-azacyclooctane obtained by decoupling the ring protons, C4, C5, C6 and C7, at various temperatures. The coalescence temperature is $+9\pm 3^{\circ}\text{C}$.

the chemical shift difference and geminal coupling constant. These values were then used in the AB quartet coalescence equation to obtain the rate constant and the free energy of activation.

The coalescence temperature of the C(3)-protons is $9 \pm 3^\circ\text{C}$, $\delta_{AB} = 26.1$ Hz and $J_{AB} = 11.5$ Hz. The rate constant, k , is then 85.3 sec^{-1} giving a free energy of activation at 9°C of $14.0 \pm 0.3 \text{ kcal mol}^{-1}$.

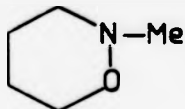
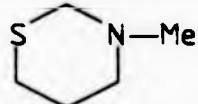
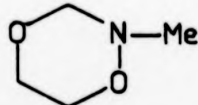
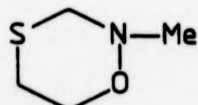
This high value of the free energy of activation is assumed to be the barrier to nitrogen inversion. The ^{13}C nmr spectrum for N-methyl-1-oxa-2-azacyclooctane was found not to be temperature dependent which is clearly consistent with the process being observed in ^1H nmr as slow inversion at the nitrogen atom.

2.3.4 Conclusion

The results from the 1-oxa-4-thia-2-azacyclohexanes lead us inescapably to the conclusion that the barrier to N-alkyl inversion is greater than the barrier to ring inversion, for example, the N-Me inversion in the N-methyl-1-oxa-4-thia-2-azacyclohexane is $11.5 \pm 0.2 \text{ kcal mol}^{-1}$ and that the barrier to ring inversion is somewhat less than this, ca $10.4 \pm 0.2 \text{ kcal mol}^{-1}$.

A comparison of the results obtained from N-methyl-1-oxa-4-thia-2-azacyclohexane with model "reference compounds" for this system, namely, tetrahydro-1,2-oxazine, tetrahydro-1,3-thiazine and tetrahydro-1,4,2-dioxazine, is shown in Table 2.8. The barrier to nitrogen inversion in N-methyl-piperidine, taken as a base to construct an empirical scheme of factors affecting nitrogen inversion barriers in six-membered rings, was found to be $8.7 \text{ kcal mol}^{-1}$.^{235,236} The effects of α -oxygen^{65,97} are to increase the energy barrier (ca $+5.0 \text{ kcal mol}^{-1}$) presumably due to an effect of an adjacent strongly electronegative atom which according

TABLE 2.8 A comparison of dihedral angle (C5-C6) and energies of activation with model "reference compounds" for the system 1-oxa-4-thia-2-azacyclohexane.

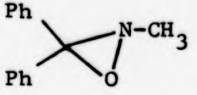
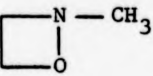
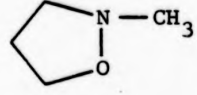
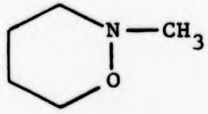
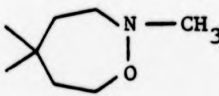
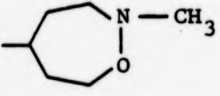
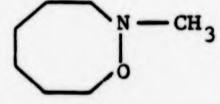
Compound	Dihedral angle ϕ (C5-C6)	NI Barrier ΔG^\ddagger kcal mol ⁻¹	RI Barrier $\Delta G^\ddagger + \Delta G^\circ$ ± 0.2 kcal mol ⁻¹	Reference
 N-Methyltetrahydro-1,2-Oxazine	56.2 [±] 0.4	13.7 [±] 0.5 H = 15.1 [±] 0.4 S = 2.3 [±] 1.5 cal mol ⁻¹ K ⁻¹	-	65,97
 N-Methyltetrahydro-1,3-thiazine	-	7.1	-	237
 N-Methyltetrahydro-1,4,2-dioxazine	56.5 [±] 2	11.4 [±] 0.2	9.95±0.93 = 10.88	106
 N-Methyl-1-oxa-4-thia-2-azacyclohexane	60 [±] 2	11.5 [±] 0.2	9.26±1.15 = 10.41	This work

to the orbital theory increases the 's'-character of the lone-pair orbital of nitrogen atom. Since the lone-pair in the transition state is in a 'p'-orbital such a substituent would be expected to increase the barrier to nitrogen inversion.

The β -sulphur effects to lower the energy barrier (-1.6 kcal mol⁻¹).²³⁷ Thus the barrier in N-methyl-tetrahydro-1,3-thiazine is 6.6 kcal mol⁻¹ lower than that of N-methyltetrahydro-1,2-oxazine.^{65,97} The barrier lowering effect of β -heteroatoms may result at least in part from relief of dipolar interactions in the transition state.¹⁰² Alternatively, 'charge alternation', the effect of an β -electronegative atom in raising the electron density, previously shown by quantum mechanical calculations may be implicated.¹⁰² Thus, the introduction of two heteroatoms, one α and the other β to nitrogen atom results in a conformational behaviour that is intermediate with respect to their individual conformational tendencies. As there was observed no marked difference between N-methyltetrahydro-1,4,2-dioxazine (11.4 ± 0.2 kcal mol⁻¹)¹⁰⁶ and N-methyl-1-oxa-4-thia-2-azacyclohexane (11.5 ± 0.2 kcal mol⁻¹) it is concluded that changing the β -heteroatom from oxygen to sulphur has practically no effect on nitrogen inversion. However, an increase in the size of the substituent on nitrogen was found to lower the barrier significantly (Tables 2.5 and 2.6) according to the sequence: Me < Et < iPr.

We now compare the nitrogen inversion barrier value obtained for N-methyl-1-oxa-2-azacyclooctane with those obtained for similar cyclic hydroxylamines of varying ring size (Table 2.9). At a glance, it can be seen that the value of ΔG^\ddagger decreases as the ring size increases from three to seven-membered illustrating one of the effects of nitrogen inversion (see above), whereby increasing the 'p' character of the

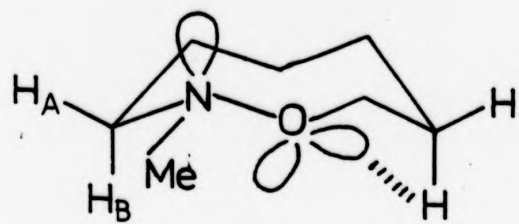
TABLE 2.9 Energies of activation for a series of cyclic hydroxylamine derivatives of varying ring size.

Compound	ΔG^\ddagger kcal mol ⁻¹	T_c °C	Reference
	$\Delta H^\ddagger = 34.1$	-	37
	N.A.	N.A.	
	15.6 ± 0.5	$42 \pm 5^\circ$	65
	$\Delta H^\ddagger = 15.1 \pm 0.4$ $\Delta S^\ddagger = 2.3 \pm 1.5$ cal mol ⁻¹ K ⁻¹	$5 \pm 5^\circ$	65, 97
	12.09	-18°	129
	12.85	-18°	129
	14.0 ± 0.3	$+9 \pm 3$	this work

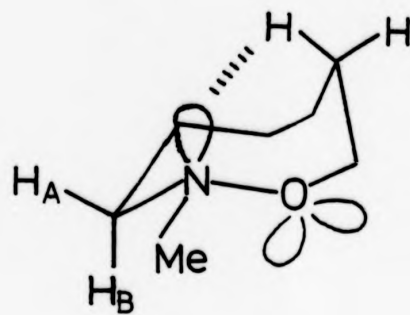
nitrogen ground state, in this case by angle opening, will tend to lower the barrier to nitrogen inversion. The barrier to nitrogen inversion seems to increase again in the eight-membered hydroxylamine derivative.

As was shown in the introduction (Chapter 1), cyclooctane exists as a 95:5 mixture of boat-chair and crown conformations,¹³⁶ with boat-chair conformation being more stable than the crown.^{15,16,130-134} Anet et al¹³⁸ have shown that azacyclooctane exists predominantly in a boat-chair conformation with only a small amount of the crown conformation present. Thus, the two possible conformational families for N-methyl-1-oxa-2-azacyclooctane are the boat-chair or crown. Each family has different members depending upon the location of the N-O bond. A probable major member of the crown family is (122) and a probable major member of the boat-chair family is (123).

It can be seen that in eight-membered rings it is possible for the N-O bond to attain a rotational arrangement much closer to the ideal for minimum torsional energy than in six-membered and smaller rings. If the N-inversion barrier is dependent on the rotational arrangement about the N-O bond this might account for the differences observed (Table 2.9).



(122)



(123)

CHAPTER 3

Experimental

3.1 GENERAL NOTES

Kieselgel 60 GF₂₅₄ (MERCK, Art. 7730) silica was used for column chromatography throughout and is referred to as silica gel. The column was packed with silica gel on the basis of 0.5g of crude product to ca 20g of silica gel. Thin-layer chromatography (tlc) was used to monitor column chromatography. The tlc plastic sheets used were bought from MERCK and are pre-coated with silica gel 60F₂₅₄ (Art. 5735). Solvent system used was ethylacetate-petroleum ether (60-80°) unless otherwise stated. Analytical tlc plates were developed either with ceric ammonium sulphate in dilute sulphuric acid²³⁸ or iodine vapour.

All organic layers were dried over anhydrous magnesium sulphate (MgSO₄) or anhydrous sodium sulphate (Na₂SO₄) unless otherwise stated. Tetrahydrofuran (THF) and diethyl ether (Et₂O) were dried with lithium aluminium hydride (LAH) and sodium metal respectively.

Melting points are determined on a Kofler hot-stage apparatus and are uncorrected. Infrared spectra (IR) were recorded on a Perkin-Elmer 577 grating infrared spectrometer and Mass spectra were determined on a Jeol JMS D100 mass spectrometer.

Nuclear magnetic resonance (nmr) spectra were recorded on a Hitachi Perkin-Elmer R24 (60 MHz), a Perkin-Elmer R32 (90 MHz) or a Bruker WP80 (80 MHz) nmr spectrometer using tetramethylsilane (TMS) as internal standard. The deuterated solvents used were deuteriochloroform (CDCl₃), deuterated dichloromethane (CD₂Cl₂) or deuteriomethanol (MeOH-d₄). The following notation is used in presenting nmr data: s = singlet; d = doublet; t = triplet; m = multiplet; q = quartet. The scale is quoted in parts per million (ppm) chemical shift (δ) scale. The ¹³C nmr assignment of the resonances was carried out for the uncoupled spectra and these conclusions applied to the noise

decoupled spectra.

A two feet Nester-Faust annular spinning band column with manual reflux ratio adjustment was used for separation of azeotropic mixtures of compounds, collecting fractions as little as 2°C apart was possible.

Hydrogenation was carried out on a 'Cook' - Heated Type Low Catalytic Hydrogenation Apparatus.

3.2 SYNTHESIS OF 1-OXA-4-THIA-2-AZACYCLOHEXANES

The synthesis of substituted 1-oxa-4-thia-2-azacyclohexanes are illustrated in Scheme 1. Each reaction stage is numbered and the experimental details are recorded in numerical order. A typical example is given:

N-Hydroxyurethane²³⁹

Finely powdered hydroxylamine hydrochloride (160g, 2.3 mol) and anhydrous potassium carbonate (290g, 2.1 mol) were added to diethyl ether (1.2 litre) and water (15 cm^3). This mixture was stirred vigorously while ethyl chloroformate (270g, 2.5 mol) was added dropwise over ca 2.5hr. Heat and carbon dioxide were evolved during the addition, and the mixture turned slightly yellow over the 48hr of stirring. The ether layer was decanted and the remaining sludge washed with ether (3x500 cm^3). The combined ether extracts were dried over anhydrous magnesium sulphate and evaporated. The product, N-hydroxyurethane (66) distilled at $110^{\circ}\text{--}113^{\circ}\text{C}/3\text{mm}$ (literature bp $113^{\circ}\text{--}116^{\circ}/3\text{mm}$). Yield - 140g (57%).

Rf (EtOAc: Petrol 60-80 $^{\circ}$; 1:3) = 0.67.

^1H nmr (CDCl_3): δ = 1.27 (3H, t, CH_3 - ethyl ester group); 4.20 (2H, q, CH_2 - ethyl ester group); 7.90 (1H, s, NH).

Preparation of N-Carboethoxy-2-(Aminohydroxy)-Ethyl-Alkanoates¹⁰⁶

Illustrated by the preparation of the diester (68: $R_1 = \text{Me}$, $R_2 = R_3 = \text{H}$), N-carboethoxy-2-(aminohydroxy)-ethyl propionate, from N-hydroxyurethane and ethyl-2-bromopropionate.

A solution of N-hydroxyurethane (84g, 0.8 mol) in technical grade ethanol (100 cm³) was added to a well stirred solution of potassium hydroxide (45g, 0.8 mol) in technical grade ethanol (150 cm³). To the resultant solution was added a solution of ethyl-2-bromopropionate (145g, 0.8 mol) in technical grade ethanol (150 cm³); and the solution was heated under reflux for 3hr. The cooled solution was decanted from the precipitate of potassium bromide which was washed with ethanol (2 x 75 cm³). The mixture and extracts were combined and solvent was removed on a rotary evaporator to leave a yellow oil. This oil was washed with water (75 cm³) and the aqueous washings extracted with diethyl ether (2 x 75 cm³). The combined organic fractions were dried over anhydrous sodium sulphate and the solvent evaporated. Distillation afforded the diester, N-carboethoxy-2-(aminohydroxy)-ethylpropionate, as a colourless oil bp 118-120°C/2mm. Yield - 110g (67%).

¹H nmr (CDCl₃): δ = 1.30 (6H, two t's, CH₃-ethyl ester groups);
1.45 (3H, d, $R_1 = \text{CH}_3$); 4.25 (4H, two q's, CH₂ - ethyl ester groups); 4.50 (1H, q, $R_2 = \text{H}$); 8.40 (1H, s, NH).

N-Carboethoxy-2-(Aminohydroxy)-Ethylacetate

Ethyl-2-bromoacetate (117g, 0.7 mol) added to a solution of N-hydroxyurethane (75g, 0.7 mol) and potassium hydroxide (40g, 0.7 mol) in technical grade ethanol (140 cm³) was heated under reflux for 3hr. Work up as described above gave the product (68: $R_1 = R_2 = R_3 = \text{H}$) bp 106-108°C/4mm. Yield 75.5g (57%).

^1H nmr (CDCl_3): $\delta = 1.30$ (6H, two t's, CH_3 - ethyl ester groups); 4.25 (4H, two q's, CH_2 - ethyl ester groups); 6.46 (2H, s, $\text{R}_1 = \text{R}_2 = \text{H}$); 8.80 (1H, s, NH).

N-Carbethoxy-2-(Aminohydroxy)-Isobutyrate

Ethyl-2-bromoisobutyrate (153g, 0.78 mol) added to a solution of N-hydroxyurethane (82g, 0.78 mol) and potassium hydroxide (44g, 0.78 mol) in technical grade ethanol (260 cm^3) was heated under reflux for 4hr. Workup as described above gave the product (68: $\text{R}_1 = \text{R}_2 = \text{CH}_3$, $\text{R}_3 = \text{H}$) bp $80-90^\circ\text{C}/0.7\text{mm}$. Yield - 111g (65%).

^1H nmr (CDCl_3) $\delta = 1.30$ (6H, two t's, CH_3 - ethyl ester groups); 1.50 (6H, s, $\text{R}_1 = \text{R}_2 = \text{CH}_3$); 4.20 (4H, two q's, CH_2 - ethyl ester groups); 8.10 (1H, s, NH).

Reduction of N-Carbethoxy-2-(Aminohydroxy)-Ethyl-Alkanoates¹⁰⁶

Reduction of the diesters (68) with lithium aluminium hydride to give the alcohols (69) is illustrated by the reduction of the diester (68: $\text{R}_1 = \text{Me}$, $\text{R}_2 = \text{R}_3 = \text{H}$) to the corresponding alcohol.

A solution of the diester (68: $\text{R}_1 = \text{Me}$, $\text{R}_2 = \text{R}_3 = \text{H}$) (73g, 0.395 mol) in anhydrous diethyl ether (150 cm^3) was added slowly to a mechanically stirred cooled suspension of lithium aluminium hydride (31g, 0.82 mol) in anhydrous diethyl ether (800 cm^3). Addition was controlled so as to maintain the mixture below 5°C . After stirring for 5hr, solid carbon dioxide (100g) and then water (60 cm^3) were added very cautiously and the mixture stirred until the separated solids were completely white (ca 2hr). The ethereal layer was decanted and the residue washed with diethyl ether ($3 \times 300 \text{ cm}^3$). The combined organic fractions were evaporated and distilled. The resulting pale yellow oil

boiled at 123°C/2mm. Yield - 40g (62%).

¹H nmr (CDCl₃): δ = 1.20 (3H, d, R₁ = CH₃); 1.30 (3H, t, CH₃ - ethyl ester group); 3.60 (1H, m, R₂ = H); 3.90 (2H, m, -CH₂OH); 4.20 (2H, q, CH₂-ethyl ester group); 8.90 (1H, s, NH).

The major by-product of the reaction boiled at 100-110°C/3mm and was identified by ¹H nmr as N-carbethoxy-2-(aminohydroxy)-2-propene (74) due to the presence of an AB quartet at 6.45 and 7.00 and absence of a 2H multiplet at 3.90 .

N-Carbethoxy-2-(Aminohydroxy)-Ethan-1-ol

Reduction of the diester (68: R₁ = R₂ = R₃ = H) (55g, 0.3 mol) with lithium aluminium hydride (20g, 0.5 mol) in anhydrous diethyl ether (770 cm³) gave the product (69: R₁ = R₂ = R₃ = H) bp 116°C/1mm, on workup as described above. Yield - 22.8g (50%).

¹H nmr (CDCl₃): δ = 1.30 (3H, t, CH₃ - ethyl ester group); 3.75 (2H, t, R₁=R₂=H); 3.95 (2H, t, -CH₂OH); 4.20 (2H, q, CH₂-ethyl ester group); 9.00 (1H, s, NH).

N-Carbethoxy-2-(Aminohydroxy)-2-Methyl-Propan-1-ol

Reduction of the diester (69: R₁ = R₂ = CH₃, R₃ = H) (100g, 0.46 mol) with lithium aluminium hydride (27.4g, 0.72 mol) in anhydrous diethyl ether on workup as described above gave two products. The minor product, distilled at 130°C/3mm, was identified by ¹H nmr to be N-carbethoxy-2-(aminohydroxy)-2-methyl-propan-1-ol. Yield - 17g (23%).

¹H nmr (CDCl₃): δ = 1.30 (3H, t, CH₃-ethyl ester group); 1.20 (6H, s, R₁ = R₂ = CH₃); 4.17 (2H, s, -CH₂OH); 4.20 (2H, q, CH₂-ethyl ester group).

The major product of the reaction distilled at 160°C/3mm. The resulting white crystalline solid was identified by its ^1H and ^{13}C nmr spectra, IR spectra and by mass spectroscopy to be the cyclic dioxazinone (75). Recrystallized from toluene. Yield - 45g (74g). mp 132-134°C.

IR (CH_2Cl_2): 1700 (C=O) cm^{-1} .

^1H nmr (CDCl_3): δ = 1.36 (6H, s, $\text{R}_1 = \text{R}_2 = \text{CH}_3$); 4.12 (2H, s, $-\text{OCH}_2$).

^{13}C nmr (CDCl_3): ppm = 21.40(q), 72.65(s), 75.43(t), 152.44(s).

m/e: M^+ (found) = 131.0575, M^+ (calc.) for $\text{C}_5\text{H}_9\text{O}_3\text{N}$ = 131.0582.

N-Alkylation of N-Carboethoxy-2-(Aminohydroxy)-Alkan-1-ol¹⁰⁶

The alcohols (69) were converted to their corresponding N-alkyl derivatives (70) by treatment with alkyl halides and anhydrous potassium carbonate in technical grade acetone. Riddell et al¹⁰⁶ in their method used dry acetone. Use of dry acetone resulted in the formation of 4-hydroxy-4-methyl-2-pentanone (76) in a large quantity so much so that it formed an azeotropic mixture with the produce. This azeotropic mixture was practically impossible to separate even by spinning-band distillation. An attempt was made to get rid of the diacetone alcohol by converting it to mesityl oxide (77), using iodine as catalyst.¹⁵⁴ The alkylated crude product was refluxed with a crystal of iodine using an oil bath (150°C). The mesityl oxide (bp 126-131°C)¹⁵⁴ distilled off at atmospheric pressure and the residue was micro-distilled. ^1H nmr of the distillate showed the presence of the alkylated alcohol plus other unidentified materials. The diacetone alcohol was formed in much smaller quantities when technical grade acetone was used and it was possible to obtain the desired products in a pure state.

Alkylation with iodomethane generally required under 48hr reflux, with iodoethane and 2-iodopropane correspondingly longer periods (up to one week with 2-iodopropane) were required. A typical alkylation is the conversion of the alcohol (69; $R_1 = \text{Me}$, $R_2 = R_3 = \text{H}$) into the corresponding N-ethyl compound (70; $R_1 = \text{Me}$, $R_2 = \text{H}$, $R_3 = \text{Et}$).

A mixture of the alcohol (10g, 0.06 mol), anhydrous potassium carbonate (50g, 0.36 mol), iodoethane (50g, 0.36 mol) and technical grade acetone (150 cm³) was heated under reflux using an oil bath for 48hr. The hot suspension was filtered and the solid residue washed with warm technical grade acetone (2 x 100 cm³). The combined organic fractions were evaporated and the residual pale yellow oil distilled. The product, N-carbethoxy-N-ethyl-2-(aminohydroxy)-propan-1-ol boiled at 86-90°C/2.0mm. Yield - 9.8g (83%).

¹H nmr (CDCl₃): $\delta = 1.20$ (3H, t, -CH₃: N-ethyl group); 1.25 (3H, d, $R_1 = \text{CH}_3$); 1.30 (3H, t, CH₃-ethyl ester group); 3.55 (2H, q, -CH₂-: N-ethyl group); 3.68 (1H, m, $R_2 = \text{H}$); 4.00 (2H, m, -CH₂OH); 4.25 (2H, q, CH₂-ethyl ester group).

N-Carbethoxy-N-Methyl-2-(Aminohydroxy)-Ethan-1-ol

The reaction of the alcohol, (69: $R_1 = R_2 = R_3 = \text{H}$) (5g, 0.03 mol), anhydrous potassium carbonate (25g, 0.18 mol), and iodomethane (23g, 0.16 mol) heated under reflux in technical grade acetone (75 cm³) for 24hr, was worked up as described above. The product (70: $R_1 = R_2 = \text{H}$, $R_3 = \text{Me}$) distilled at 78-82°C/1.2mm. Yield - 10.33g (94%).

¹H nmr (CDCl₃): $\delta = 1.30$ (3H, t, CH₃-ethyl ester group); 3.17 (3H, s, $R_3 = \text{Me}$); 3.70 (2H, t, $R_1 = R_2 = \text{H}$); 3.95 (2H, t, -CH₂OH); 4.20 (2H, q, CH₂-ethyl ester group).

N-Carbethoxy-N-Ethyl-2-(Aminohydroxy)-Ethan-1-ol

The reaction, of the alcohol (69: $R_1 = R_2 = R_3 = H$) (5g, 0.033 mol), anhydrous potassium carbonate (28g, 0.2 mol), and iodoethane (28g, 0.18 mol) heated under reflux in technical grade acetone (100 cm³) for 36hr, was worked up as described above. The product (70: $R_1 = R_2 = H$, $R_3 = Et$) distilled at 82-84°C/0.6mm. Yield - 10.8g (91%).

¹H nmr (CDCl₃): $\delta = 1.20$ (3H, t, -CH₃: N-ethyl group); 1.30 (3H, t, CH₃-ethyl ester group); 3.55 (2H, q, -CH₂-: N-ethyl group); 3.70 (2H, t, $R_1 = R_2 = H$); 3.95 (2H, t, -CH₂OH); 4.20 (2H, q, CH₂-ethyl ester group).

N-Carbethoxy-N-Isopropyl-2-(Aminohydroxy)-Ethan-1-ol

The reaction, of the alcohol (69: $R_1 = R_2 = R_3 = H$) (10g, 0.067 mol), anhydrous potassium carbonate (56g, 0.4 mol), and 2-iodopropane (61g, 0.34 mol) heated under reflux in technical grade acetone (200 cm³) for 48hr, was worked up as described above. The product (70: $R_1 = R_2 = H$, $R_3 = iPr$) distilled at 84°C/1.1mm. Yield - 9.5g (75%).

¹H nmr (CDCl₃): $\delta = 1.25$ (6H, d, (CH₃)₂-: N-isopropyl group); 1.30 (3H, t, CH₃-ethyl ester group); 3.70 (2H, t, $R_1 = R_2 = H$); 4.00 (2H, t, -CH₂OH); 4.20 (1H, m, -CH-: N-isopropyl group); 4.20 (2H, q, CH₂-ethyl ester group).

N-Carbethoxy-N-Methyl-2-(Aminohydroxy)-Propan-1-ol

The reaction, of the alcohol (69: $R_1 = Me$, $R_2 = R_3 = H$) (10g, 0.06 mol), anhydrous potassium carbonate (50g, 0.4 mol), and iodomethane (50g, 0.35 mol) heated under reflux in technical grade acetone (150 cm³) for 36hr, was worked up as described above. The product (70:

$R_1 = R_3 = \text{Me}$, $R_2 = \text{H}$) distilled at 88-90°C/1.5mm. Yield - 10.1g (95%).

^1H nmr (CDCl_3): $\delta = 1.25$ (3H, d, $R_1 = \text{CH}_3$); 1.30 (3H, t, CH_3 -ethyl ester group); 3.18 (3H, s, $R_3 = \text{CH}_3$); 3.60 (1H, m, $R_2 = \text{H}$); 3.90 (2H, m, $-\text{CH}_2\text{OH}$); 4.25 (2H, q, CH_2 -ethyl ester group).

N-Carbethoxy-N-Isopropyl-2-(Aminohydroxy)-Propan-1-ol

The reaction, of the alcohol (69: $R_1 = \text{Me}$, $R_2 = R_3 = \text{H}$) (10g, 0.06 mol), anhydrous potassium carbonate (50g, 0.4 mol) and 2-iodopropane (60g, 0.35 mol) heated under reflux in technical grade acetone (150 cm^3) for one week, was worked up as described above. The product (70: $R_1 = \text{Me}$, $R_2 = \text{H}$, $R_3 = \text{iPr}$) distilled at 86-90°C/2mm. Yield -10.56 (86%).

^1H nmr (CDCl_3): $\delta = 1.20$ (6H, d, $(\text{CH}_3)_2$ -: N-isopropyl group); 1.25 (3H, d, $R_1 = \text{CH}_3$); 1.30 (3H, t, CH_3 -ethyl ester group); 3.60 (1H, m, $R_2 = \text{H}$); 4.00 (2H, m, $-\text{CH}_2\text{OH}$); 4.20 (1H, m, $-\text{CH}$ -: N-isopropyl group); 4.25 (2H, q, CH_2 -ethyl ester group).

N-Carbethoxy-N-Methyl-2-(Aminohydroxy)-2-Methyl-Propan-1-ol

The N-alkylated product (70: $R_1 = R_2 = R_3 = \text{Me}$) was obtained from another worker and used for the next reaction step.

^1H nmr (CDCl_3): $\delta = 1.25$ (6H, s, $R_1 = R_2 = \text{CH}_3$); 1.30 (3H, t, CH_3 -ethyl ester group); 3.15 (3H, s, $R_3 = \text{CH}_3$); 4.25 (2H, q, CH_2 -ethyl ester group); 4.30 (2H, m, $-\text{CH}_2\text{OH}$).

Tosylation of N-Carboethoxy-N-Alkyl-2-(Aminohydroxy)-Alkan-1-ol¹⁵⁴

Illustrated by the preparation of the tosylate (71: $R_1 = \text{Me}$, $R_2 = \text{H}$, $R_3 = \text{Et}$), N-carboethoxy-N-ethyl-2-(aminohydroxy)-propan-1-ol-(p-toluenesulphonate), from the corresponding alcohol and toluene-4-sulphonyl chloride in dry pyridine.

Toluene-4-sulphonyl chloride (20.4g, 0.11 mol) was added to a solution of the alcohol, N-carboethoxy-N-ethyl-2-(aminohydroxy)-propan-1-ol (9.8g, 0.05 mol), in dry pyridine (150 cm³) cooled in ice. The mixture was left to stand overnight. Long needle-like crystals of pyridine hydrochloride were observed. The reaction product was then poured onto ice-water mixture and extracted with diethyl ether (3 x 100 cm³). The combined organic extracts were washed with hydrochloric acid (1.1d: 2 x 100 cm³), followed by water (100 cm³). The organic layer was dried over anhydrous sodium sulphate and the diethyl ether evaporated to give the product (71: $R_1 = \text{Me}$, $R_2 = \text{H}$, $R_3 = \text{Et}$) as a yellow oil. This crude product was used directly in the next stage. Yield - 16.0g (93%).

¹H nmr (CDCl₃): $\delta = 1.10$ (3H, t, -CH₃: N-ethyl group); 1.25 (3H, t, CH₃ - ethyl ester group); 1.25 (3H, t, $R_1 = \text{CH}_3$); 2.45 (3H, s, CH₃-phenyl); 3.45 (2H, q, -CH₂-: N-ethyl group); 4.15 (2H, q, CH₂ - ethyl ester group); 4.20 (3H, m, $R_2 = \text{H}$ & -CH₂OTs); 7.68 (4H, A₂X₂ q, phenyl protons).

N-Carboethoxy-N-Methyl-2-(Aminohydroxy)-Ethyl-1-(p-Toluenesulphonate)

Reaction of the alcohol (70: $R_1 = R_2 = \text{H}$, $R_3 = \text{Me}$) (10g, 0.06 mol) and toluene-4-sulphonyl chloride (24.5g, 0.13 mol) in dry pyridine (185 cm³) on workup as described above gave the product (71: $R_1 =$

$R_2 = H, R_3 = Me$) as a yellow oil. This crude product was used directly in the next stage. Yield - 16.02g (83%).

1H nmr ($CDCl_3$): $\delta = 1.25$ (3H, t, CH_3 - ethyl ester group); 2.45 (3H, s, CH_3 - phenyl); 3.10 (3H, s, $R_3 = CH_3$); 4.15 (2H, q, CH_2 - ethyl ester group); 4.20 (4H, m, $-OCH_2CH_2OTs$); 7.60 (4H, A_2X_2 q, phenyl protons).

N-Carbethoxy-N-Ethyl-2-(Aminohydroxy)-Ethyl-1-(p-Toluenesulphonate)

Reaction of the alcohol (70: $R_1 = R_2 = H, R_3 = Et$) (10.62g, 0.06 mol) and toluene-4-sulphonyl chloride (24.5g, 0.13 mol) in dry pyridine (185 cm^3) on workup as described above gave the product (71: $R_1 = R_2 = H, R_3 = Et$) as a yellow oil. This crude product was used directly in the next stage. Yield - 18.73g (94%).

1H nmr ($CDCl_3$): $\delta = 1.15$ (3H, t, $-CH_3$: N-ethyl group); 1.25 (3H, t, CH_3 - ethyl ester group); 2.45 (3H, s, CH_3 -phenyl); 3.45 (2H, q, $-CH_2-$: N-ethyl group); 4.15 (2H, q, CH_2 - ethyl ester group); 4.20 (4H, m, $-OCH_2CH_2OTs$); 7.60 (4H, A_2X_2 q, phenyl protons).

N-Carbethoxy-N-Isopropyl-2-(Aminohydroxy)-Ethyl-1-(p-Toluenesulphonate)

Reaction of the alcohol (70: $R_1 = R_2 = H, R_3 = iPr$) (11.8g, 0.06 mol) and toluene-4-sulphonyl chloride (24.5g, 0.13 mol) in dry pyridine (185 cm^3) on workup as described above gave the product (71: $R_1 = R_2 = H, R_3 = iPr$) as an orange oil. This crude product was used directly in the next stage. Yield - 16.7g (81%).

^1H nmr (CDCl_3): δ = 1.15 (6H, d, $(\text{CH}_3)_2$ -: N-isopropyl group);
 1.25 (3H, t, CH_3 - ethyl ester group); 2.45
 (3H, s, CH_3 -phenyl); 4.15 (2H, q, CH_2 -
 ethyl ester group); 4.20 (5H, m,
 $-\text{OCH}_2\text{CH}_2\text{OTs}$ & $-\text{CH}-$: N-isopropyl group);
 7.60 (4H, A_2X_2 q, phenyl protons).

N-Carbethoxy-N-Methyl-2-(Aminohydroxy)-Propan-1-(p-Toluenesulphonate)

Reaction of the alcohol (70: $\text{R}_1 = \text{Me}$, $\text{R}_2 = \text{H}$, $\text{R}_3 = \text{Me}$)
 (10.62g, 0.06 mol) and toluene-4-sulphonyl chloride (24.5g, 0.13 mol) in
 dry pyridine (185 cm^3) on workup as described above gave the product
 (71: $\text{R}_1 = \text{Me}$, $\text{R}_2 = \text{H}$, $\text{R}_3 = \text{Me}$) as a yellow oil. This crude
 product was used directly in the next stage. Yield - 14.23g(72%).

^1H nmr (CDCl_3): δ = 1.25 (3H, t, CH_3 - ethyl ester group); 1.25
 (3H, d, $\text{R}_1 = \text{CH}_3$); 2.45 (3H, s, CH_3 -
 phenyl); 3.05 (3H, s, $\text{R}_3 = \text{CH}_3$); 4.15 (2H,
 q, CH_2 - ethyl ester group); 4.20 (3H, m,
 $\text{R}_2 = \text{H}$ & $-\text{CH}_2\text{OTs}$); 7.60 (4H, A_2X_2 q,
 phenyl protons).

N-Carbethoxy-N-Isopropyl-2-(Aminohydroxy)-Propan-1-(p-Toluenesulphonate)

Reaction of the alcohol (70: $\text{R}_1 = \text{Me}$, $\text{R}_2 = \text{H}$, $\text{R}_3 = \text{iPr}$)
 (10.56g, 0.05 mol) and toluene-4-sulphonyl chloride (20.4g, 0.11 mol) in
 dry pyridine (185 cm^3) on workup as described above gave the product
 (71: $\text{R}_1 = \text{Me}$, $\text{R}_2 = \text{H}$, $\text{R}_3 = \text{iPr}$) as an orange oil. This crude
 product was used directly in the next stage. Yield - 16.22g (90%).

^1H nmr (CDCl_3): δ = 1.15 (6H, d, $(\text{CH}_3)_2$ -: N-isopropyl group);
 1.25 (3H, t, CH_3 - ethyl ester group); 1.25
 (3H, d, $\text{R}_1 = \text{CH}_3$); 2.45 (3H, s,
 CH_3 -phenyl); 4.10 (3H, m, $\text{R}_2 = \text{H}$ &
 $-\text{CH}_2\text{OTs}$); 4.15 (2H, q, CH_2 - ethyl ester
 group); 4.20 (1H, m, $-\text{CH}-$: N-isopropyl group);
 7.60 (4H, A_2X_2 q, phenyl protons).

N-Carboethoxy-N-Methyl-2-(Aminohydroxy)-2-Methyl-Propan-1-(p-Toluene
 -sulphonate)

Reaction of the alcohol (70: $\text{R}_1 = \text{R}_2 = \text{R}_3 = \text{Me}$) (10g, 0.05
 mol) and toluene-4-sulphonyl chloride (21g, 0.11 mol) in dry pyridine
 (187 cm^3) on workup as described above gave the product (71: $\text{R}_1 =$
 $\text{R}_2 = \text{R}_3 = \text{Me}$) as a yellow oil. This crude product was used directly
 in the next stage. Yield - 15g (91%).

^1H nmr (CDCl_3): δ = 1.22 (6H, s, $\text{R}_1 = \text{R}_2 = \text{CH}_3$); 1.25 (3H,
 t, CH_3 - ethyl ester group); 2.45 (3H, s,
 CH_3 -phenyl); 3.05 (3H, s, $\text{R}_3 = \text{CH}_3$);
 3.92 (2H, s, $-\text{CH}_2\text{OTs}$); 4.15 (2H, q, CH_2 -
 ethyl ester group); 7.60 (4H, A_2X_2 q,
 phenyl protons).

Preparation of N-Alkyl-2-(Aminohydroxy)-Alkyl-1-Thiols

Generally, thiol group formation required hydrogen sulphide to be
 passed through the reaction mixture for a period of 4-6hr. A typical
 amino-thiol formation is illustrated by the preparation of
 N-ethyl-2-(aminohydroxy)-propyl-1-thiol (72: $\text{R}_1 = \text{Me}$, $\text{R}_2 = \text{H}$, $\text{R}_3 =$
 Et).

A solution of potassium hydroxide (2.8g, 0.05 mol) in water (1.2
 cm^3) and ethanol (15 cm^3) was cooled to 0°C . The vigorously

stirred solution was saturated with hydrogen sulphide gas (Kipps Apparatus: Ferric sulphide/50% concentrated hydrochloric acid) at ca 0°C. A solution of the tosylate (71: R₁ = Me, R₂ = H, R₃ = Et) (5.55g, 0.016 mol) in ethanol (7.5 cm³) was added and the reaction mixture heated to 60°C with gentle stirring. Hydrogen sulphide gas was bubbled through the system. The reaction mixture was heated at 60°C for a further 1.5hr after addition of more potassium hydroxide (5g, 0.09 mol). On completion the reaction mixture was made acidic with concentrated hydrochloric acid and heated for a further 1.5hr. The mixture was then allowed to come to room temperature and the ethanol was evaporated, leaving a white damp solid. At this point the reaction mixture was left to stand overnight. The white damp solid was dissolved in water (ca 10 cm³) and made basic by addition of solid potassium carbonate. The solution was then filtered and the filtrate extracted with diethyl ether (3 x 50 cm³). The combined organic extracts were dried over anhydrous sodium sulphate and the solvent evaporated. Microdistillation afforded the amino-thiol, (72: R₁ = Me, R₂ = H, R₃ = Et), as a yellow oil bp 120-130°C/2mm. Yield - 0.75g (35%).

¹H nmr (CDCl₃): δ = 1.10 (3H, t, -CH₃: N-ethyl group); 1.25 (3H, d, R₁ = CH₃); 2.85 (2H, m, -CH₂SH); 2.95 (2H, q, -CH₂-: N-ethyl group); 3.90 (1H, m, R₂ = H); 5.40 (1H, broad s, SH).

¹³C nmr (CDCl₃): ppm = 12.55 (q), 19.61 (q), 44.78 (t), 46.80 (t), 77.30 (d).

m/e: M⁺ (found) = 133.0555; M⁺(calc.) for C₅H₁₁NOS = 133.0561.

N-Methyl-2-(Aminohydroxy)-Ethyl-1-Thiol

Reaction of the tosylate (71: R₁ = R₂ = H, R₃ = Me) (6g, 0.019 mol) in a solution of potassium hydroxide (3.3g, 0.06 mol), water (1.5

cm³) and ethanol (15 cm³) saturated with hydrogen sulphide, on workup as described above gave the product (72: R₁ = R₂ = H, R₃ = Me) as an orange oil. This crude product was used directly in the next stage. Yield - 0.55g (30%).

¹H nmr (CDCl₃): δ = 2.70 (3H, s, R₃ = CH₃); 2.93 (2H, t, -CH₂SH); 3.98 (2H, t, R₁ = R₂ = H); 5.45 (1H, broad s, SH).

¹³C nmr (CDCl₃): ppm = 31.1 (t), 39.35 (q), 71.50 (t).

m/e : M⁺ (found) = 105.0225, M⁺ (calc.) for C₃H₇NOS = 105.0249.

N-Ethyl-2-(Aminohydroxy)-Ethyl-1-Thiol

Reaction of the tosylate (71: R₁ = R₂ = H, R₃ = Et) (5.3g, 0.016 mol) in a solution of potassium hydroxide (2.8g, 0.05 mol), water (1.2 cm³) and ethanol (15 cm³) saturated with hydrogen sulphide, on workup as described above gave the product (72: R₁ = R₂ = H, R₃ = Et) as an orange oil. This crude product was used directly in the next stage. Yield - 1.63g (84%).

¹H nmr (CDCl₃): δ = 1.10 (3H, t, -CH₃: N-ethyl group); 2.93 (2H, t, -CH₂SH); 2.95 (2H, q, -CH₂-: N-ethyl group); 3.90 (2H, t, R₁ = R₂ = H); 5.20 (1H, broad s, SH).

m/e: M⁺ (found) = 119.0409, M⁺ (calc.) for C₄H₉NOS = 119.0405.

N-Isopropyl-2-(Aminohydroxy)-Ethyl-1-Thiol

Reaction of the tosylate (71: R₁ = R₂ = H, R₃ = iPr) (5.5g, 0.016 mol) in a solution of potassium hydroxide (2.8g, 0.05 mol), water (1.2 cm³) and ethanol (15 cm³) saturated with hydrogen sulphide, on workup as described above gave the product (72: R₁ = R₂ = H, R₃ = iPr) as an orange oil. This crude product was used directly in the next stage. Yield - 1.06g (49%).

^1H nmr (CDCl_3): $\delta = 1.05$ (6H, d, $(\text{CH}_3)_2$ -: N-isopropyl group);
 2.93 (2H, t, $-\text{CH}_2\text{SH}$); 3.10 (1H, septet,
 $-\text{CH}-$: N-isopropyl group); 3.90 (2H, t, $\text{R}_1 =$
 $\text{R}_2 = \text{H}$); 5.40 (1H, broad s, SH).

m/e: M^+ (found) = 134.0633, M^+ (calc.) for $\text{C}_5\text{H}_{12}\text{NOS} = 134.0639$.

N-Methyl-2-(Aminohydroxy)-Propyl-1-Thiol

Reaction of the tosylate (71: $\text{R}_1 = \text{Me}$, $\text{R}_2 = \text{H}$, $\text{R}_3 = \text{Me}$) (5.3g, 0.016 mol) in a solution of potassium hydroxide (2.8g, 0.05 mol), water (1.2 cm^3) and ethanol (15 cm^3) saturated with hydrogen sulphide, on workup as described above gave the crude product (72: $\text{R}_1 = \text{Me}$, $\text{R}_2 = \text{H}$, $\text{R}_3 = \text{Me}$) as a yellow oil. Microdistillation of a small amount of the crude oil in a Kugelrohr apparatus gave the pure product (72: $\text{R}_1 = \text{Me}$, $\text{R}_2 = \text{H}$, $\text{R}_3 = \text{Me}$) bp $100^\circ\text{C}/3\text{mm}$, and from its ^1H nmr spectra was found to be of equivalent purity as the crude. The crude product was thus used directly in the next stage. Yield - 1.92g (99%).

^1H nmr (CDCl_3): $\delta = 1.25$ (3H, d, $\text{R}_1 = \text{CH}_3$); 2.70 (3H, s, $\text{R}_3 = \text{CH}_3$); 2.90 (2H, m, $-\text{CH}_2\text{SH}$); 3.90 (1H, m, $\text{R}_2 = \text{H}$); 4.80 (1H, broad s, SH).

m/e: M^+ (found) = 119.0396, M^+ (calc.) for $\text{C}_4\text{H}_9\text{NOS} = 119.0405$.

N-Isopropyl-1-(Aminohydroxy)-Propyl-1-Thiol

Reaction of the tosylate (71: $\text{R}_1 = \text{Me}$, $\text{R}_2 = \text{H}$, $\text{R}_3 = \text{iPr}$) (2.3g, 0.0064 mol) in a solution of potassium hydroxide (1.16g, 0.02 mol), water (0.5 cm^3) and ethanol (4.5 cm^3) saturated with hydrogen sulphide, on workup as described above gave the product (72: $\text{R}_1 = \text{Me}$, $\text{R}_2 = \text{H}$, $\text{R}_3 = \text{iPr}$) as a yellow oil. This crude product was used directly in the next stage. Yield - 0.43g (45%).

^1H nmr (CDCl_3): δ = 1.05 (6H, d, $(\text{CH}_3)_2$ -: N-isopropyl group);
 1.20 (3H, d, $\text{R}_1 = \text{CH}_3$); 2.85 (2H, m,
 $-\text{CH}_2\text{SH}$); 3.15 (1H, septet, $-\text{CH}-$: N-isopropyl
 group); 3.90 (1H, m, $\text{R}_2 = \text{H}$); 5.10 (1H,
 broad s, SH).

^{13}C nmr (CDCl_3): ppm = 18.51 (q), 20.17 (t), 20.29 (t), 44.80 (t),
 51.65 (d), 77.55 (s).

m/e: M^+ (found) = 147.0721, M^+ (calc.) for $\text{C}_6\text{H}_{13}\text{NOS}$ = 147.0718.

N-Methyl-2-(Aminohydroxy)-2-Methyl-Propan-1-Thiol

Reaction of the tosylate (71: $\text{R}_1 = \text{R}_2 = \text{R}_3 = \text{Me}$) (5g, 0.015 mol) in a solution of potassium hydroxide (2.8g, 0.05 mol), water (1.4 cm^3) and ethanol (15 cm^3) saturated with hydrogen sulphide on workup as described above failed to give the desired amino-thiol (72: $\text{R}_1 = \text{R}_2 = \text{R}_3 = \text{Me}$). Repeated attempts failed to obtain the thiol.

Preparation of 1-Oxa-4-Thia-2-Azacyclohexanes

The amino-thiols (72) condense with paraformaldehyde when heated in a Kugelrohr apparatus to form 1-oxa-4-thia-2-azacyclohexanes. These reactions were carried out in the absence of any solvent. A typical example is illustrated by the preparation of N-ethyl-6-methyl-1-oxa-4-thia-2-azacyclohexane.

A mixture of N-ethyl-2-(aminohydroxy)-propyl-1-thiol (0.44g, 3.26×10^{-3} mol) and paraformaldehyde (0.2g) was heated to 100°C and the temperature slowly raised to 130°C on a Kugelrohr apparatus. Excess paraformaldehyde sublimed out. Vacuum was applied and the product (73: $\text{R}_1 = \text{Me}$, $\text{R}_2 = \text{H}$, $\text{R}_3 = \text{Et}$) distilled at ca $140^\circ\text{C}/80\text{mm}$. Yield - 0.2g (37%).

^1H nmr (CDCl_3): δ = 1.10 (3H, t, $-\text{CH}_3$: N-ethyl group); 1.13 (3H, d, $\text{R}_1 = \text{CH}_3$); 2.45 (2H, m, C(5) protons); 2.73 (2H, q, $-\text{CH}_2-$: N-ethyl group); 3.77 (2H, AA' q, N- CH_2 -S); 4.05 (1H, m, $\text{R}_2 = \text{H}$).

^{13}C nmr (CDCl_3): ppm = 11.90 (q), 20.56 (q), 32.54 (t), 52.52 (t), 55.41 (t), 74.16 (d).

m/e: M^+ (found) = 147.0717, M^+ (calc.) for $\text{C}_6\text{H}_{13}\text{NOS}$ = 147.0718.

N-Methyl-1-Oxa-4-Thia-2-Azacyclohexane

The reaction of the amino thiol (72: $\text{R}_1 = \text{R}_2 = \text{H}$, $\text{R}_3 = \text{Me}$) (0.5g, 4.67×10^{-3} mol) with paraformaldehyde (0.2g) on distillation gave the product (73: $\text{R}_1 = \text{R}_2 = \text{H}$, $\text{R}_3 = \text{Me}$) at $100^\circ\text{C}/50\text{-}60\text{mm}$. Yield - 0.048g (9%).

^1H nmr (CD_2Cl_2): δ = 2.60 (3H, s, $\text{R}_3 = \text{CH}_3$); 2.70 (2H, t, C(5) protons); 3.85 (2H, s, C(3) protons); 4.10 (2H, t, $\text{R}_1 = \text{R}_2 = \text{H}$).

^{13}C nmr (CD_2Cl_2): ppm = 26.42 (t), 46.97 (q), 58.18 (t), 69.81 (t).

m/e: M^+ (found) = 119.0400, M^+ (calc.) for $\text{C}_4\text{H}_9\text{NOS}$ = 119.0405.

N-Ethyl-1-Oxa-4-Thia-2-Azacyclohexane

The reaction of the amino-thiol (72: $\text{R}_1 = \text{R}_2 = \text{H}$, $\text{R}_3 = \text{Et}$) (0.5g, 4.13×10^{-3} mol) with paraformaldehyde (0.2g) on distillation gave the product (73: $\text{R}_1 = \text{R}_2 = \text{H}$, $\text{R}_3 = \text{Et}$) at $150\text{-}170^\circ\text{C}/100\text{mm}$. Yield - 0.103g (19%).

^1H nmr (CD_2Cl_2): δ = 1.15 (3H, t, $-\text{CH}_3$: N-ethyl group); 2.70 (2H, t, C(5) protons); 2.75 (2H, t, $-\text{CH}_2-$: N-ethyl group); 3.85 (2H, s, C(3) protons); 4.10 (2H, t, $\text{R}_1 = \text{R}_2 = \text{H}$).

^{13}C nmr (CD_2Cl_2) ppm = 11.90 (q), 26.90 (t), 52.80 (t), 56.5 (t), 69.8 (t).

m/e: M^+ (found) = 133.0554, M^+ (calc.) for $\text{C}_5\text{H}_{11}\text{NOS}$ = 133.0561

N-Isopropyl-1-Oxa-4-Thia-2-Azacyclohexane

The reaction of the amino-thiol (72: $\text{R}_1 = \text{R}_2 = \text{H}$, $\text{R}_3 = \text{iPr}$) (0.5g, 3.7×10^{-3} mol) with paraformaldehyde (0.2g) on distillation gave the product (73: $\text{R}_1 = \text{R}_2 = \text{H}$, $\text{R}_3 = \text{iPr}$) at $150\text{-}160^\circ\text{C}/100\text{mm}$. Crude yield - 0.75g. Crude yields from two experiments were combined and microdistilled to give the product at $40^\circ\text{C}/2.5\text{mm}$. Yield - 0.2g (18%).

^1H nmr (CD_2Cl_2): δ = 1.10 (6H, d, $(\text{CH}_3)_2$ -: N-isopropyl group); 2.65 (2H, t, C(5) protons); 3.00 (1H, septet, -CH-: N-isopropyl group); 3.95 (2H, s, C(3) protons); 4.15 (2H, t, $\text{R} = \text{R}_2 = \text{H}$).

^{13}C nmr (CD_2Cl_2): ppm = 19.05 (q), 27.02 (t), 53.76 (t), 56.46 (d), 70.14 (t).

m/e: M^+ (found) = 147.0731, M^+ (calc.) for $\text{C}_6\text{H}_{13}\text{NOS}$ = 147.0718.

N-Methyl-6-Methyl-1-Oxa-4-Thia-2-Azacyclohexane

The reaction of the amino-thiol (72: $\text{R}_1 = \text{Me}$, $\text{R}_2 = \text{H}$, $\text{R}_3 = \text{Me}$) (0.5g, 4.1×10^{-3} mol) with paraformaldehyde (0.25g) on distillation gave the product (73: $\text{R}_1 = \text{Me}$, $\text{R}_2 = \text{H}$, $\text{R}_3 = \text{Me}$) at $150^\circ\text{C}/50\text{mm}$. Crude yield - 0.7g. Crude yields from two experiments were combined and microdistilled to give the product at $100^\circ\text{C}/10\text{mm}$. Yield - 0.19g (17%).

^1H nmr (CD_2Cl_2): δ = 1.15 (3H, d, $\text{R}_1 = \text{CH}_3$); 2.45 (2H, m, C(5) protons); 2.60 (3H, s, $\text{R}_3 = \text{CH}_3$); 3.75 (2H, AA' q, N- CH_2 -S); 4.15 (1H, m, $\text{R}_2 = \text{H}$).

^{13}C nmr (CD_2Cl_2): ppm = 20.62 (q), 32.00 (t), 45.95 (q), 57.04 (t), 74.20 (d).

m/e: M^+ (found) = 133.0558, M^+ (calc.) for $C_5H_{11}NOS$ = 133.0561.

N-Isopropyl-6-Methyl-1-Oxa-4-Thia-2-Azacyclohexane

The reaction of the amino-thiol (72: $R_1 = Me$, $R_2 = H$, $R_3 = iPr$) ($0.5g$, 2.68×10^{-3} mol) with paraformaldehyde ($0.16g$) on distillation gave the product (73: $R_1 = Me$, $R_2 = H$, $R_3 = iPr$) at $120^\circ C/50mm$. Yield - $0.12g$ (28%).

1H nmr (CD_2Cl_2): $\delta = 1.10$ (6H, two d's, $(CH_3)_2$ -: N-isopropyl group); 1.15 (3H, d, $R_1 = CH_3$); 2.50 (2H, m, C(5) protons); 3.00 (1H, septet, -CH-: N-isopropyl group); 3.85 (2H, AA'q, N- CH_2 -S); 4.15 (1H, m, $R_2 = H$).

^{13}C nmr (CD_2Cl_2): ppm = 18.93 (q), 19.30 (q), 20.54 (q), 32.72 (t), 52.53 (t), 56.10 (d), 74.54 (d).

m/e: M^+ (found) = 161.0866, M^+ (calc.) for $C_7H_{15}NOS$ = 161.0874.

3.3 SYNTHESIS OF N-METHYL-1-OXA-2-AZACYCLOOCTANE

The synthesis of N-methyl-1-oxa-2-azacyclooctane is illustrated in Scheme 2. Each reaction stage is numbered and the experimental details are recorded in numerical order..

1,6-Hexanediol

Diethyladipate (78) ($31g$, 0.15 mol) in dry tetrahydrofuran ($45 cm^3$) was added dropwise to a stirred suspension of lithium aluminium hydride ($6.3g$, 0.17 mol) in dry tetrahydrofuran ($50 cm^3$). The grey solid formed was broken up carefully with a spatula and another $100 cm^3$ dried tetrahydrofuran added. The reaction mixture was heated under reflux for 2hr. The cooled solution was quenched with 50% sodium hydroxide solution ($10 cm^3$), followed by water ($40 cm^3$) which was added slowly over a period of an hour and the mixture stirred until the

separated solids were completely white. The tetrahydrofuran layer was decanted and the residue washed with a fair amount of diethyl ether (3 x 200 cm³). The combined organic fractions were evaporated under reduced water pressure on the rotary evaporator and the residual oil was distilled. The distillate crystallized to give a white crystalline solid. The product, 1,6-hexanediol (79), boiled at 108°C/0.7mm. Yield - 15.1g (85%).

m.p: 37.5 - 38.5°C [lit. val. = 42°; 36.8°; 47°, 59°].

¹H nmr (CDCl₃): δ = 1.25 - 1.85 (8H, m, C(2), C(3), C(4), & C(5) protons); 3.65 (4H, t, C(1) & C(6) protons).

¹³C nmr (CDCl₃): ppm = 25.54 (t), 32.69 (t), 62.77 (t).

1,6-Dibromohexane¹⁵⁸

A solution of 1,6-hexanediol (79) (13.8g, 0.117 mol) and concentrated hydrobromic acid 48% w/v (92 cm³) was left to stand stirring overnight. The mixture was then heated under reflux for 1.5hr. Two distinct layers were observed at this point, a lower dark brown layer and an upper almost colourless layer. Hydrogen bromide gas, generated by the action of concentrated sulphuric acid on hydrobromic acid, was passed into the reaction mixture until saturation of the mixture was considered complete. The mixture was then heated under reflux for a further 2.5 hr. On cooling, the reaction mixture was poured onto ice (ca 50g) and extracted with chloroform (3 x 50 cm³). The combined chloroform extracts were washed with water (1 x 80 cm³), dried over anhydrous magnesium sulphate and evaporated. The residue gave on distillation 1,6-dibromohexane (80), b.p. 71°C/1.1mm [lit. val. = 63-64°C/3mm]. Yield - 24.7g (95%).

¹H nmr (CDCl₃): δ = 1.50 (4H, m, C(3) and C(4) protons); 1.89 (4H, m, C(2) and C(5) protons); 3.40 (4H, t, C(1) and C(6) protons).

Attempted Condensation of N-Hydroxyurethane with 1,6-Dibromohexane

The condensation of 1,6-dibromohexane was carried out using the same procedure as that adopted by D Williams⁴⁷ for 1,4,-dibromobutane.

A solution of N-hydroxyurethane (66) (7.5g, 0.07 mol), potassium hydroxide (4g, 0.07 mol), and 1,6-dibromohexane (4.1g, 0.017 mol) in technical grade ethanol (80 cm³) was heated under reflux, using an oil bath, for 4 hr. On cooling the ethanol layer was decanted from the pale yellow precipitate and the residue washed with ethanol (3 x 20 cm³). The combined extracts were evaporated and the residual oil washed with an equal volume of water. The two resulting layers were separated and the aqueous layer washed once with an equal volume of diethyl ether. The ether extract and the organic layer were combined, dried over anhydrous magnesium sulphate and evaporated. The resulting oil was purified by column chromatography (100g silica gel, eluting with EtOAc:Petrol 60-80°C, 3:7 increasing the polarity slowly to 1:2). This yielded two products, the more polar compound was identified to be unreacted or excess N-hydroxyurethane. The less polar compound was believed to be the product (115), produced in 90% yield (4.5g).

¹H nmr (CDCl₃): δ = 1.27 (6H, t, -CH₃, ethyl ester groups);
 1.15 - 1.82 (8H, m, C(2), C(3), C(4), & C(5)
 protons); 3.74 (4H, t, C(1) & C(6) protons);
 4.17 (4H, q, -CH₂-: ethyl ester groups); 7.30
 (2H, broad s, NH groups).

¹³C nmr (CDCl₃): ppm = 14.54 (q), 25.69 (t), 27.93 (t), 61.74 (t),
 76.70 (t), 158.00 (s).

Successful Condensation of N-hydroxyurethane with 1,6-Dibromohexane

In order to promote cyclisation at the expense of intermolecular reaction, the 'High-Dilution' technique was used. The dibromide was

introduced slowly into the vigorously stirred reaction medium. Here the concentration of N-hydroxyurethane is fourteen times less than in the previous unsuccessful attempt at cyclisation. At this concentration the undesired reaction is therefore at least fourteen times slower relative to cyclisation and thus the probability of intermolecular reaction is greatly reduced.

The following general procedure, illustrated by the reaction of 1,6-dibromohexane with N-hydroxyurethane, for the preparation of medium size hydroxylamine rings was finally adopted.

A solution of N-hydroxyurethane (1.05g, 0.01 mol) in ethanol (50 cm³) was added to a well stirred solution of potassium hydroxide (0.56, 0.01 mol) in ethanol (140 cm³); 1,6-Dibromohexane (2.44g, 0.01 mol) in ethanol (25 cm³) was then added dropwise to the reaction flask. The mixture was heated under reflux for 2hr and left to stir at room temperature for 48hr. The ethanol solution was decanted and the pale yellow residue washed with ethanol (3 x 50 cm³). The combined washings were evaporated and the resulting residual oil washed with water (50 cm³). The organic layer was separated and the aqueous layer extracted with diethyl ether (3 x 50 cm³). The combined organic phase was then dried over anhydrous magnesium sulphate and evaporated to give a yellow oil (crude yield ca 2g) which was purified by column chromatography (60g silica gel, eluting with EtOAc:Petrol 60-80°C; 1:9 increasing the polarity slowly to 1:4). This produced the product, N-carbethoxy-1-oxa-2-azacyclooctane (81), as a yellow oil. Yield - 1.0g (54%).

Rf (EtOAc:Petrol 60-80°C; 1:4) = 0.34.

^1H nmr (CDCl_3): δ = 1.28 (3H, t, $-\text{CH}_3$ -: ethyl ester group);
 1.72 (8H, s, C(4), C(5), C(6) and C(7)
 protons); 3.37 (2H, broad t, $-\text{CH}_2\text{N}$); 3.87
 (2H, broad t, $-\text{CH}_2\text{O}$); 4.07 (2H, q, $-\text{CH}_2$ -:
 ethyl ester group).

^{13}C nmr (CDCl_3): ppm = 14.69 (q), 25.45 (t), 26.22 (t), 27.04 (t),
 50.45 (t), 61.84 (t), 74.74 (t), 158.39 (s).

m/e: M^+ (found) = 187.1202, M^+ (calc.) for $\text{C}_9\text{H}_{17}\text{NO}_3$ = 187.1208.

N-Methyl-1-Oxa-2-Azacyclooctane

A solution of N-carbethoxy-1-oxa-2-azacyclooctane (0.7g, 3.74×10^{-3} mol) in dry diethyl ether (3 cm^3) was added very slowly (over 1hr) to a vigorously stirred suspension of lithium aluminium hydride (0.56g, 0.015 mol) in dry diethyl ether (10 cm^3). The mixture was left stirring at room temperature (ca 20°C) for an hour. On completion the reaction mixture was quenched cautiously with technical grade diethyl ether followed by water and stirred until the separated solids were completely white. The ether was decanted off and the residual sludge washed with ether ($3 \times 20 \text{ cm}^3$). The ether was then distilled using a Vigreux column until ca 2 cm^3 of the reaction mixture was left. The residue gave on distillation, in a Kugelrohr apparatus, the product (82) bp $100^\circ\text{C}/760 \text{ mm}$. Yield - 0.16g (33%).

^1H nmr (CDCl_3): δ = 1.68 (8H, broad s, C(4), C(5), C(6) & C(7)
 protons); 2.52 (3H, s, N- CH_3); 2.55 (2H,
 broad t, $-\text{CH}_2\text{N}$); 3.71 (2H, broad t, $-\text{CH}_2\text{O}$).

^{13}C nmr (CDCl_3): ppm = 26.11 (t), 26.49 (t), 27.05 (t), 46.63 (q),
 60.93 (t), 71.98 (t).

m/e: M^+ (found): = 129.1159, M^+ (calc.) for $\text{C}_7\text{H}_{15}\text{NO}$ = 129.1154.

3.4 SYNTHESIS OF N-CARBETHOXY-5,5-DIMETHYL-1-OXA-2-AZACYCLOOCTANE

The synthesis of N-Carbethoxy-5,5-dimethyl-1-oxa-2-azacyclooctane is illustrated in Scheme 3. Each reaction stage is numbered and the experimental details are recorded in numerical order.

4,4-Dimethylcyclohex-2-enone

The method of Eliel and Lukach,²⁴⁰ modified by using 90% methyl vinyl ketone-water and correspondingly less water, was scaled up to twice molar proportions to give the product (85).

A mixture of 90% fresh methyl vinyl ketone (140g, 2.0 mol; 15g water) and freshly distilled isobutyraldehyde (145g, 2.014 mol) was dissolved in water (185 cm³) and sufficient methanol (ca. 100 cm³) to ensure homogeneity. The solution was then added slowly to a well-stirred solution of potassium hydroxide (7.5g, 0.13 mol) in methanol (45 cm³) whose temperature was raised slowly to 75-80°C by external heating. At the end of the addition, the mixture was cooled and extracted seven times with 200 cm³ portions of diethyl ether. The combined extracts were washed with water (3 x 200 cm³), dried over anhydrous sodium sulphate and concentrated. Distillation yielded a fraction boiling at 90-94°C/20mm (lit.val. = 72.5-73.5/20mm;²⁴¹ 72-73/15mm;²⁴² 54-56/4mm²⁴³), considered to be the product, 4,4-dimethylcyclohex-2-enone. Yield - 120g (48%).

¹H nmr (CDCl₃): δ = 1.15 (6H, s, C(4): gem-dimethyl); 1.85 (2H, t, C(5) protons); 2.42 (2H, t, C(6) protons); 5.75 (1H, d, C(3) proton), 6.55 (1H, d, C(2) proton).

¹³C nmr (CDCl₃): ppm = 27.66 (q), 32.70 (s), 34.31 (t), 36.13 (t), 126.79 (d), 159.27 (d), 198.47 (s).

m/e: M⁺ (found): = 124.0894, M⁺(calc.) for C₈H₁₂O = 124.0889.

4,4-Dimethylcyclohexanone²⁴⁰

A solution of 4,4-dimethylcyclohex-2-enone (77g, 0.62 mol) in glacial acetic acid (225 cm³) was hydrogenated, using a low pressure hydrogenator, over platinum oxide (0.54g) at room temperature until one equivalent of hydrogen gas had been taken up (ca 24hr). On completion the reaction mixture was filtered, poured into water and extracted with diethyl ether (5 x 200 cm³). The combined ether extracts were washed with water, followed by aqueous sodium bicarbonate and again by water. The organic layer was dried over anhydrous sodium sulphate and evaporated to yield crude 4,4-dimethylcyclohexanone. The pale yellow solid was purified by crystallisation from petroleum ether (40-60°C) to obtain white needle-like crystals. Yield - 49g (63%).

mp: 39-40°C (lit. val. = 42°C;²⁴² 39-40°C²⁴³).

Rf (EtOAc:Petrol 60-80°C; 1:5.7) = 0.53.

¹H nmr (CDCl₃): δ = 1.10 (6H, s, C(4): gem-dimethyl); 1.67 (4H, t, C(3) & C(5) protons); 2.35 (4H, t, C(2) & C(6) protons).

¹³C nmr (CDCl₃): ppm = 27.52 (q), 29.85 (s), 37.96 (t), 39.20 (t), 212.19 (s).

m/e: M⁺ (found): = 126.1042, M⁺(calc.) for C₈H₁₄O = 126.1044.

γ,γ-Dimethyl-ε-Caprolactone

A solution of 4,4-dimethylcyclohexanone (10.0g, 0.08 mol) in dichloromethane (15 cm³) was added dropwise over a period of 15 minutes to a solution of m-chloroperoxybenzoic acid (13.8g, 0.08 mol) in dichloromethane (150 cm³). The reaction mixture was left to stir at room temperature (ca 20°C) and the course of the reaction was followed by tlc. A white precipitate of benzoic acid was observed to form. On completion, the mixture was made neutral with aqueous sodium hydrogen

carbonate, washed with water, followed by saturated sodium chloride solution and extracted with dichloromethane (3 x 100 cm³). The combined extracts were dried over anhydrous magnesium sulphate and the dichloromethane was removed on a rotary evaporator. On cooling in ice, white needle-like crystals were obtained. The small amount of residual dichloromethane was removed under high vacuum. The white crystalline product, γ,γ -dimethyl- ϵ -caprolactone (87), was produced in 92.5% (10.5g) yield.

mp: 29-31°C.

Rf (EtOAc:Petrol 60-80°C; 1:5.7) = 0.1.

¹H nmr (CDCl₃): δ = 1.00 (6H, s, C(5): gem dimethyl); 1.60 (4H, C(4) & C(6) protons); 2.60 (2H, t, C(7) protons); 4.15 (2H, t, C(3) protons).

¹³C nmr (CDCl₃): ppm = 28.38 (q), 29.97 (t), 31.89 (s), 35.71 (t), 41.93 (t), 64.73 (t), 176.01 (s).

m/e: M⁺ (found) = 142.0990, M⁺(calc.) for C₈H₁₄O₂ = 142.0994.

It should be noted that if all of the byproduct *m*-chlorobenzoic acid is not washed out, it goes through subsequent reaction steps (Scheme 7) to finally form the product (114), which appears as an impurity in the preparation of *N*-carbethoxy-5,5-dimethyl-1-oxa-2-azacyclooctane (90). The impurity can then be removed by column chromatography only with great care, as it runs down the column just behind the desired product.

Compound (114).

¹H nmr (CDCl₃): δ = 1.25 (3H, t, -CH₃: ethyl ester group); 4.18 (2H, q, -CH₂-: ethyl ester group); 6.80 (2H, s, -CH₂- phenyl); 7.20 - 7.55 (4H, m, phenyl protons and NH).

^{13}C nmr (CDCl_3): ppm = 14.46 (q), 62.11 (t), 77.78 (t), 127.06 (d),
128.70 (d), 129.03 (d), 129.79 (d), 137.76 (s),
157.90 (s).

An accurate mass measurement on the molecular ion could not be obtained,
instead measurement on the expected major fragment, $\text{C}_7\text{H}_6\text{Cl}$, was done.

For $\text{C}_7\text{H}_6\text{Cl}$: m/e (found) = 125.0159

m/e (calc.) = 125.0158

3,3-Dimethyl-1,6-Hexanediol

A solution of γ,γ -dimethyl- ϵ -caprolactone (7g, 0.05 mol) in dry tetrahydrofuran (20 cm^3) was added cautiously to a well stirred suspension of lithium aluminium hydride (2.5g, 0.06 mol) in dry tetrahydrofuran (40 cm^3). The reaction mixture was heated under reflux for 1.5hr. The cooled solution was quenched with 50% sodium hydroxide solution (5 cm^3), followed by water and the mixture was stirred until the separated solids were completely white (ca 1 hr). The tetrahydrofuran layer was decanted and the residue washed with ether ($3 \times 100\text{ cm}^3$). The combined organic fractions were evaporated and the residual crude oil distilled to give the product, 3,3-dimethyl-1,6-hexanediol, as a colourless oil, at bp $128^\circ\text{C}/1.5\text{mm}$. Yield - 6.6g (90%).

^1H nmr (CDCl_3): δ = 0.90 (6H, s, C(3): gem-dimethyl); 1.15 - 1.75 (6H, m, C(2), C(4) & C(5) protons); 3.60 & 3.68 (4H, two t's, C(1) & C(6) protons).

^{13}C nmr (CDCl_3): ppm = 27.35 (t), 27.63 (q), 31.90 (s), 38.14 (t),
43.92 (t), 59.22 (t), 63.19 (t).

An accurate mass measurement on the molecular ion could not be obtained,
instead measurement on the expected major fragment, $\text{C}_6\text{H}_{13}\text{O}$ was done.

For $\text{C}_6\text{H}_{13}\text{O}$: m/e (found) = 101.0958

m/e (calc.) = 101.0966.

3,3-Dimethyl-1,6-Dibromohexane¹⁵⁹

Phosphorous tribromide (22.7g, 0.084 mol; ca 8 cm³) was added cautiously to 3,3-dimethyl-1,6-hexanediol (88) (10.6g, 0.073 mol), cooled to ca -10°C in an ice/salt bath. The reaction mixture was stirred and allowed to come to room temperature. Hydrogen bromide gas was evolved at this point. The mixture was then heated using a water bath (40-50°C) until no further hydrogen bromide gas was liberated. On completion, water (25 cm³) was added very cautiously dropwise to quench the reaction and the product was extracted with dichloromethane (3 x 50 cm³). The combined extracts were washed with 10% aqueous sodium carbonate (50 cm³), followed by water (50 cm³) and were then dried over anhydrous magnesium sulphate and evaporated. The crude product was examined by tlc to check that the reaction had gone to completion. Distillation afforded the dibromide, 3,3-dimethyl-1,6-dibromohexane (89), as a yellow oil bp 120°C/6mm. Yield - 12.7g (64%).

¹H nmr (CDCl₃): δ = 0.90 (6H, s, C(3): gem-dimethyl); 1.35 (2H, m, C(4) protons); 1.85 (4H, m, C(2) & C(5) protons); 3.40 (4H, t, C(1) & C(6) protons).

¹³C nmr (CDCl₃): ppm = 26.75 (q), 27.66 (t), 28.91 (t), 34.09 (s), 34.23 (t), 40.26 (t), 45.44 (t).

An accurate mass measurement on the molecular ion could not be obtained, instead measurement on the expected major fragment, C₆H₁₂Br, was done.

For C₆H₁₂Br: m/e (found) = 165.0101

m/e (calc.) = 165.0103

N-Carbethoxy-5,5-Dimethyl-1-Oxa-2-Azacyclooctane

The condensation of 3,3-dimethyl-1,6-dibromohexane with N-hydroxyurethane was carried out by using the 'High Dilution' technique adopted for the preparation of N-carbethoxy-1-oxa-2-azacyclooctane (90).

3,3-Dimethyl-1,6-dibromohexane (3g, 0.011 mol) in ethanol (50 cm³) was added dropwise to a well stirred solution of N-hydroxyurethane (1.2g, 0.011 mol) and potassium hydroxide (0.63g, 0.011 mol) in ethanol (200 cm³). The reaction mixture was refluxed for 2-3 hrs and left to stir at room temperature (ca 20°C) for one week. On workup as described previously, the resulting oil was purified by column chromatography (70g silica gel, eluting with EtOAc:Petrol 60-80°C, 1:13.3 increasing the polarity slowly to 1:4) to give a product presumed to be (90) rather than the product (91) on the basis of its ¹H nmr spectrum. Yield - 1.16g (49%).

Rf (EtOAc:Petrol 60-80°C; 1:4) = 0.32.

¹H nmr (CDCl₃): δ = 0.90 (6H, s, C(5): gem-dimethyl); 1.29 (3H, t, -CH₃: ethyl ester group); 1.40 - 1.70 (4H, m, C(6) & C(7) protons); 1.82 (2H, m, C(4) protons); 3.38 (2H, m, -CH₂N); 3.85 (2H, m, -CH₂O); 4.19 (2H, q, -CH₂=: ethyl ester group).

¹³C nmr (CDCl₃): ppm = 14.51 (q), 22.72 (t), 26.70 (q), 29.18 (t), 34.12 (s), 37.71 (t), 45.44 (t), 61.86 (t), 77.40 (t), 157.85 (s).

An accurate mass measurement on the molecular ion could not be obtained, instead measurement on the expected major fragment, C₈H₁₅, was done.

For C₈H₁₅: m/e (found) = 111.1175

m/e (calc.) = 111.1174

Attempted Reduction of N-Carbethoxy-5,5-Dimethyl-1-Oxa-2-Azacyclooctane Using Lithium Aluminium Hydride

The reduction of N-carbethoxy-5,5-dimethyl-1-oxa-2-azacyclooctane was carried out using the same procedure as that adopted for

N-carbethoxy-1-oxa-2-azacyclooctane.

A solution of N-carbethoxy-5,5-dimethyl-1-oxa-2-azacyclooctane (90) (lg, 4.6×10^{-3} mol) in dry diethyl ether (2 cm^3) was added very slowly to a vigorously stirred suspension of lithium aluminium hydride (0.60g, 0.016 mol) in dry diethyl ether (5 cm^3). The reaction mixture was stirred at ambient temperature for three hours. The course of the reaction was followed by tlc. After workup as described previously, the ether was distilled using a Vigreux column until ca 2 cm^3 of residue was left. The residue on being distilled, on a Kugelrohr apparatus, failed to give a clean separation of the products. The distillation fractions were then combined and purified by column chromatography (70g silica gel, eluting with EtOAc:Petrol 60-80°C; 1:15 increasing the polarity slowly to 1:4) to give a product which did not contain a N-methyl moiety. The product was identified to be N-carbethoxy-2-(aminohydroxy)-3,3-dimethylhexane (117). Yield - 0.85g (85%).

Rf (EtOAc:Petrol 60-80°C; 1:4) = 0.36.

^1H nmr (CDCl_3): δ = 0.85 (6H, s, C(3): gem-dimethyl); 1.15 - 1.80 (9H, m, C(1), C(2), C(4) & C(5) protons); 1.38 (3H, t, $-\text{CH}_3$: ethyl ester group); 3.90 (2H, t, $-\text{CH}_2\text{O}$); 4.25 (2H, q, $-\text{CH}_2-$: ethyl ester group); 7.64 (1H, broad s, NH).

^{13}C nmr (CDCl_3): ppm = 8.74 (q), 14.87 (q), 23.19 (t), 26.92 (q), 32.90 (s), 34.43 (t), 37.65 (t), 62.17 (t), 78.30 (t), 158.23 (s).

m/e: M^+ (found) = 218.1775, M^+ (calc.) for $\text{C}_{11}\text{H}_{24}\text{NO}_3$ = 218.1757.

Attempted Acid Hydrolysis of N-Carbethoxy-5,5-Dimethyl-1-Oxa-2-Azacyclooctane

Using 50% Concentrated Hydrochloric Acid

N-Carbethoxy-5,5-dimethyl-1-oxa-2-azacyclooctane (90) (0.62g, 2.88×10^{-3} mol) in 50% concentrated hydrochloric acid (10 cm^3) was heated under reflux for 3 hr. On cooling, the reaction mixture was made basic using sodium hydroxide pellets and extracted with diethyl ether to remove any unreacted reactants. The aqueous layer was acidified and extracted with dichloromethane ($3 \times 30 \text{ cm}^3$). The combined extracts were dried over anhydrous sodium sulphate and evaporated. The resulting yellow oil (ca 20mg) was identified by ^1H nmr as the starting compound. From the diethyl ether extract above, practically all of the starting material was recovered.

3.5 SYNTHESIS OF N-CARBETHOXY-6,6-DIMETHYL-1-OXA-2-AZACYCLONONANE

The synthesis of N-carbethoxy-6,6-dimethyl-1-oxa-2-azacyclononane is illustrated in Scheme 4. Each reaction stage is numbered and the experimental details are recorded in numerical order.

Diethyl-3,3-Dimethylglutarate

3,3-Dimethylglutaric acid (94) (73.5g, 0.46 mol), technical grade ethanol (184 cm^3), toluene (92 cm^3) and concentrated sulphuric acid (0.8g) were placed in a 500 cm^3 round-bottomed flask equipped with a coiled air condenser, thermometer, distillation head and a Liebig condenser. The reaction mixture was heated under reflux using an oil-bath, and when the acid had dissolved an azeotropic mixture of alcohol, toluene and water commenced to distil at 78°C . The distillate was collected in a flask containing anhydrous potassium carbonate (50g, 0.36 mol). Distillation was continued until the

temperature at the top of the column began to fall below 78°C. The distillate was shaken thoroughly with anhydrous potassium carbonate, then filtered through a fluted filter paper back into the reaction flask. The mixture was then reheated until the temperature at the stillhead rose to 78°C and stopped when the temperature fell below 78°C. On cooling, anhydrous potassium carbonate was added to the flask to neutralize the sulphuric acid. After 15 minutes the mixture was filtered and the residue washed with toluene. The filtrate was then distilled under reduced pressure on the rotary evaporator to remove ethanol and toluene to yield a pale yellow oil. Finally, vacuum distillation yielded the pure product, diethyl-3,3-dimethylglutarate (95), as a colourless oil. bp 100-104°C/3mm. Yield - 85.5g (84%).

^1H nmr (CDCl_3): δ = 1.14 (6H, s, C(3): gem-dimethyl); 1.25 (6H, t, $-\text{CH}_3$: ethyl ester groups); 2.42 (4H, s, C(2) & C(4) protons); 4.09 (4H, q, $-\text{CH}_2-$: ethyl ester groups).

^{13}C nmr (CDCl_3): ppm = 14.3 (q), 27.67 (q), 32.58 (s), 45.36 (t), 59.98 (t), 171.82 (s).

m/e: M^+ (found) = 216, 1371, M^+ (calc.) for $\text{C}_{11}\text{H}_{20}\text{O}_4$ = 216.1362.

3,3-Dimethyl-1,5-Pentanediol

The reduction of diethyl-3,3-dimethylglutarate was carried out using the same procedure as that adopted for the preparation of 1,6-hexanediol (79). A solution of diethyl-3,3-dimethylglutarate (50g, 0.23 mol) in dry tetrahydrofuran (100 cm^3) was added dropwise to a stirred suspension of lithium aluminium hydride (10g, 0.26 mol) in dry tetrahydrofuran (150 cm^3). The reaction mixture was heated under reflux for 4hr. After workup as described previously, distillation afforded the diol, 3,3-dimethyl-1,5-pentanediol (96), as a colourless

oil, bp 124-125°C/2.5 cm³. Yield - 28g (92%).

¹H nmr (CDCl₃): δ = 0.95 (6H, s, C(3): gem-dimethyl); 1.68 (4H, t, C(2) & C(4) protons); 7.20 (4H, t, C(1) & C(5) protons).

¹³C nmr (CDCl₃): ppm = 28.18 (q), 31.64 (s), 44.05 (t), 59.20 (t).

3,3-Dimethyl-1,5-Dibromopentane

1) Bromination using Concentrated Hydrobromic Acid¹⁵⁸

The bromination of 3,3-dimethyl-1,5-pentanediol was carried out using the same procedure as that adopted for the preparation of 1,6-dibromohexane (80). A solution of 3,3-dimethyl-1,5-pentanediol (10g, 0.076 mol) and concentrated hydrobromic acid 48% w/v (70 cm³). The reaction mixture was heated under reflux for 3hr. and on cooling, the hydrogen bromide gas was passed for approximately 3hr. The mixture instead of being refluxed again was left to stand over the weekend. After workup as described previously, the residue gave on distillation two fractions. The higher boiling fraction was identified as 3,3-dimethyl-1,5-dibromopentane (97), obtained as a pale yellow oil. bp 104-107°C/7mm. Yield - 7.7g (40%).

¹H nmr (CDCl₃): δ = 0.98 (6H, s, C(3): gem-dimethyl); 1.91 (4H, BB'm, C(2) & C(4) protons); 3.44 (4H, AA'm, C(1) & C(5) protons).

¹³C nmr (CDCl₃): ppm = 26.48 (q), 28.32 (t), 35.68 (s), 45.35 (t).

An accurate mass measurement on the molecular ion could not be obtained, instead measurement on the expected major fragment, C₅H₁₀Br, was done.

For C₅H₁₀Br: m/e (found) = 148.9964

m/e (calc.) = 148.9966.

The lower boiling fraction obtained as a colourless oil was identified to be 4,4-dimethyltetrahydropyran (106), bp 20-25°C/7mm. Yield - 3.8g (44%).

^1H nmr (CDCl_3): δ = 0.98 (6H, s, C(4): gem-dimethyl); 1.37 (4H, t, C(3) & C(5) protons); 3.62 (4H, t, C(2) & C(6) protons).

^{13}C nmr (CDCl_3): ppm = 38.00 (s), 39.24 (q), 64.29 (t), 77.48 (t).

m/e: M^+ (found) = 114.1055, M^+ (calc.) for $\text{C}_7\text{H}_{14}\text{O}$ = 114.1045.

ii) Bromination using Phosphorus Tribromide¹⁵⁹

The bromination of 3,3-dimethyl-1,5-pentanediol (96) was carried out using the same procedure as that adopted for the preparation of 3,3-dimethyl-1,6-dibromohexane (97). Phosphorus tribromide (50g, 0.18 mol ca 18 cm³) was added cautiously to 3,3-dimethyl-1,5-pentanediol (21g, 0.16 mol) cooled to ca -10°C in an ice/salt bath. After workup as described previously, distillation afforded the dibromide (97) as a pale yellow oil. Yield - 24g (58%).

Attempted Cleavage of 4,4-Dimethyltetrahydropyran to 3,3-Dimethyl-1,5-Dibromopentane

i) Using Concentrated Hydrobromic Acid

The cleavage of 4,4-dimethyltetrahydropyran was attempted using the same experimental conditions adopted for the bromination of the alcohol (96) with concentrated hydrobromic acid (48% w/v). On workup only the starting material was recovered. The reaction was then repeated except this time it was heated under reflux for 5hr. The starting material still remained and no new product had appeared.

ii) Using Triphenyldibromophosphorane¹⁶⁰

Triphenyldibromophosphorane was prepared by the method of Schaefer and Higgins²⁴⁴ using a 200 cm³ oven dried flask, a positive pressure O₂-free N₂ atmosphere, 14.5g (0.055 mol) of triphenylphosphine, 8.8g (0.055 mol) of bromine, and 75 cm³ of dry chlorobenzene. Colourless crystalline phosphorane precipitated when the addition of bromine was ca

one-half complete. This phosphorane reagent was prepared immediately prior to use.

A solution of the phosphorane reagent (0.055 mol), 80 cm³ of chlorobenzene and 4,4-dimethyltetrahydropyran (4.0g, 0.035 mol) was heated at 126°C for 1 hr and left overnight. Diphenylmethane (75 cm³) was added prior to distillation. The product that distilled at bp 130°C/10mm was not identifiable.

Attempted Bromide Ion Displacement Reaction with Model Compound,
3-Methyl-1,5-Dibromopentane, with Cyanide Ion¹⁵³

Potassium cyanide (2.67g, 0.041 mol) in dry dimethylsulphoxide (20 cm³) was heated using a water bath until most of the solid had dissolved. A solution of 3-methyl-1,5-dibromopentane (5.0g, 0.02 mol) in dry dimethylsulphoxide (2 cm³) was added dropwise to the well stirred solution over a period of 30 minutes.

The reaction mixture was left to stir for 18 hr at water-bath temperature 60-70°C. The course of the reaction was followed by tlc. On completion, the reaction mixture was poured into water (500 cm³) and extracted with diethyl ether (3 x 300 cm³). The combined organic extracts were dried over anhydrous magnesium sulphate and evaporated. The resulting oil was microdistilled to yield 4-methyl-1,7-heptanedinitrile, bp 120°C/0.9mm. Yield - 1.5g (55%). Rf (EtOAc/Petrol 60-80°C; 1:2) = 0.30.

¹H nmr (CDCl₃): δ = 0.98 (3H, d, C(4)-methyl); 1.30-2.20 (5H, m, C(3), C(4) & C(5) protons); 2.39 (4H, t, C(2) & C(6) protons).

¹³C nmr (CDCl₃): ppm = 14.85 (t), 18.02 (q), 31.60 (d), 31.80 (t), 119.31 (s).

m/e: M⁺ (found) = 135.0923, M⁺ (calc.) for C₈H₁₂N₂ = 135.0923.

4,4-Dimethyl-1,7-Heptanedinitrile

The displacement reaction of the dibromide (97) to the corresponding dinitrile was thus carried out using the same procedure adopted for 3-methyl-1,5-dibromopentane as shown above. A solution of potassium cyanide (5.2g, 0.08 mol), 3,3-dimethyl-1,5-dibromopentane (97) (9g, 0.035 mol) in dry dimethylsulphoxide (44 cm³) was stirred for 48 hr at 60-65°C using an oil-bath. After workup as described above, distillation afforded the product, 4,4-dimethyl-1,7-heptanedinitrile (98), at 130°C/0.6mm. Yield - 3.75 (71%).

¹H nmr (CDCl₃): δ = 0.95 (6H, s, C(4): gem-dimethyl); 1.65 (4H, BB'm, C(3) & C(5) protons); 2.32 (4H, AA'm, C(2) & C(6) protons).

¹³C nmr (CDCl₃): ppm = 12.28 (t), 25.49 (q), 32.80 (s), 36.79 (t), 120.08 (s).

An accurate mass measurement on the molecular ion could not be obtained, instead measurement on the expected major fragment, C₆H₁₀N, was done.

For C₆H₁₀N: m/e (found) = 96.0813

m/e (calc.) = 96.0813

4,4-Dimethyl-1,7-Heptanedioic Acid²⁴⁵

To a vigorously stirred solution of concentrated sulphuric acid (90g) in water (110 cm³) at 50°C was added dropwise 4,4-dimethyl-1,7-heptanedinitrile (7g, 0.046 mol). The mixture was heated under reflux for 5 hr. On cooling, the reaction mixture was poured onto an equal volume of ice and water, and extracted with diethyl ether (3 x 50 cm³). The combined organic extracts were dried over anhydrous magnesium sulphate and evaporated to leave a white solid. The crude product was recrystallized from diethyl ether to give the product (99) as a white crystalline powder. Yield - 7.92 (91%).

mp : 82-85°C.

^1H nmr (CDCl_3): δ = 0.90 (6H, s, C(4): gem-dimethyl); 1.59 (4H, BB'm, C(3) & C(5) protons); 2.36 (4H, AA'm, C(2) & C(6) protons).

^{13}C nmr (CDCl_3): ppm = 26.35 (q), 29.38 (t), 32.23 (s), 35.93 (t), 180.66 (s).

An accurate mass measurement on the molecular ion could not be obtained. Instead, measurement on the expected major fragment, $\text{C}_6\text{H}_{11}\text{O}_2$, was done.

For $\text{C}_6\text{H}_{11}\text{O}_2$: m/e (found) = 115.0786
m/e (calc.) = 115.0760

Diethyl-3,3-Dimethylpimelate

The esterification of 3,3-dimethylpimelic acid (99) was carried out using the same procedure adopted for the preparation of diethyl-3,3-dimethylglutarate (100), using methanol rather than ethanol. The methanol-toluene azeotropic mixture distilled at 63-64°C. The reaction of 3,3-dimethylpimelic acid (7g, 0.037 mol), technical grade methanol (20 cm^3), toluene (10 cm^3) and concentrated sulphuric acid (0.5 cm^3) on workup as described previously gave on distillation the product (100) as a colourless oil, bp 117°C/4mm. Yield - 7.0g (87.6%).

^1H nmr (CDCl_3): δ = 0.89 (6H, s, C(4) gem-dimethyl); 1.55 (4H, BB'm, C(3) & C(5) protons); 2.30 (4H, AA'm, C(2) & C(6) protons); 3.68 (6H, s, $-\text{OCH}_3-$: methyl ester groups).

^{13}C nmr (CDCl_3): ppm = 26.39 (q), 29.35 (t), 32.24 (s), 36.28 (t), 51.56 (q), 174.48 (s).

An accurate mass measurement on the molecular ion could not be obtained,

instead measurement on the expected major fragment, $C_7H_{13}O_2$, was done.

For $C_7H_{13}O_2$: m/e (found) = 129.0918

m/e (calc.) = 129.0916

4,4-Dimethyl-1,7-Heptanediol

A solution of the diester (100) (6.0g, 0.028 mol) in dry tetrahydrofuran (30 cm³) was added cautiously to a well stirred suspension of lithium aluminium hydride (2g, 0.05 mol) in dry tetrahydrofuran (100 cm³). The reaction mixture was heated under reflux for 3 hr. The workup was carried out using the same procedure adopted for the preparation of 3,3-dimethyl-1,6-hexanediol (88). The crude product on distillation afforded the product, 4,4-dimethyl-1,7-heptanediol (101), as a colourless viscous oil at bp 125°C/1mm. Yield - 4.0g (71%).

¹H nmr (CDCl₃): δ = 0.90 (6H, s, C(4): gem-dimethyl); 1.10 - 1.75 (8H, m, C(2), C(3), C(5) & C(6) protons); 3.65 (4H, t, C(1) & C(7) protons).

¹³C nmr (CDCl₃): ppm = 27.32 (q), 32.17 (s), 37.56 (t), 63.43 (t).

An accurate mass measurement on the molecular ion could not be obtained, instead measurement on the expected major fragment, $C_6H_{13}O$, was done.

For $C_6H_{13}O$: m/e (found) = 101.0967

m/e (calc.) = 101.0967

4,4-Dimethyl-1,7-Dibromoheptane¹⁵⁹

Phosphorus tribromide (7g, 0.026 mol ca 2.6 cm³) was added cautiously to 4,4-dimethyl-1,7-heptanediol (101) (2.5g, 0.016 mol) cooled to ca -10°C in an ice/salt bath. The workup was carried out using the same procedure adopted for the preparation of 3,3-dimethyl-1,6-dibromohexane (89). The crude product (102) was used

directly in the next stage. Yield - 4.0g (87%).

^1H nmr (CDCl_3): δ = 0.90 (6H, s, C(4): gem-dimethyl); 1.19-1.50 (4H, m, C(3) & C(5) protons); 1.60-2.05 (4H, m, C(2) & C(6) protons); 3.40 (4H, t, C(1) & C(7) protons).

^{13}C nmr (CDCl_3): ppm = 27.08 (q), 27.85 (t), 32.41 (s), 34.53 (t), 40.36 (t).

An accurate mass measurement on the molecular ion could not be obtained, instead measurement on the expected major fragment, $\text{C}_6\text{H}_{12}\text{Br}$, was done.

For $\text{C}_6\text{H}_{12}\text{Br}$: m/e (found) = 163.0120 & 165.0113

m/e (calc.) = 163.0123 & 165.0103

N-Carbethoxy-6,6-Dimethyl-1-Oxa-2-Azacyclononane

The condensation of N-hydroxyurethane with 4,4-dimethyl-1,7-dibromoheptane was carried out by using the 'High Dilution' technique adopted for the preparation of N-carbethoxy-1-oxa-2-azacyclooctane (81).

4,4-Dimethyl-1,7-dibromoheptane (1.9g, 6.64×10^{-3} mol) in ethanol (50 cm^3) was added dropwise to a well stirred solution of N-hydroxyurethane (0.70g, 6.6×10^{-3} mol) and potassium hydroxide (0.37g, 6.61×10^{-3} mol) in ethanol (200 cm^3). The reaction mixture was refluxed for 3 hr and left to stir at room temperature (ca 20°C) for one week. The course of the reaction was followed by tlc. On workup as described previously, the resulting oil was purified by column chromatography (70g silica gel, eluting with EtOAc:Petrol 60- 80°C ; 1:13.3 increasing the polarity slowly to 1:4) to give the product (103) as a pale yellow oil. Yield - 0.88g (58%).
Rf (EtOAc:Petrol 60- 80°C ; 1:4) = 0.27.

^1H nmr (CDCl_3): δ = 1.85 (6H, s, C(6): gem-dimethyl); 1.10-2.05 (8H, m, C(4), C(5), C(7) & C(8) protons); 1.30 (3H, t, $-\text{CH}_3$: ethyl ester group); 3.38 (2H, t, C(3) protons); 3.35 (2H, t, C(9) protons); 4.20 (2H, q, $-\text{CH}_2-$: ethyl ester group).

^{13}C nmr (CDCl_3): ppm = 14.51 (q), 22.80 (t), 27.02 (q), 27.90 (t), 32.36 (s), 34.68 (t), 37.79 (t), 40.42 (t), 61.86 (t), 77.64 (t), 157.92 (s).

An accurate mass measurement on the molecular ion could not be obtained, instead measurement on the expected major fragment, C_9H_{17} , was done.

For C_9H_{17} : m/e (found) = 125.1336

m/e (calc.) = 125.1331

Attempted Reduction of N-Carboethoxy-6,6-Dimethyl-1-Oxa-1-Azacyclononane Using Lithium Aluminium Hydride

The reduction of N-carboethoxy-6,6-dimethyl-1-oxa-2-azacyclononane was carried out using the same procedure as that adopted for N-carboethoxy-1-oxa-2-azacylooctane.

A solution of N-carboethoxy-6,6-dimethyl-1-oxa-2-azacyclononane (0.88g, 3.5×10^{-3} mol) in dry ether (3 cm^3) was added slowly to a vigorously stirred suspension of lithium aluminium hydride (0.6g, 0.016 mol) in dry ether (5 cm^3). The reaction mixture was stirred at ambient temperature for 3 hr. After workup as described previously, the ether was distilled using a Vigreux column until ca 2 cm^3 of residue was left. The residue on being distilled on a Kugelrohr apparatus, failed to give a clean separation of the products. The distillation fractions were then combined and purified by column chromatography (70g silica gel, eluting with EtOAc: Petrol 60-80°C; 1:15 increasing the polarity slowly to 1:5) to give a product which did not contain a

N-methyl moiety. The product was identified to be N-carbethoxy-2-(aminohydroxy)-4,4-dimethylheptane (118). Yield - 0.65g (80%).

Rf (EtOAc): Petrol 60-80°C, 1:4) = 0.35.

^1H nmr (CDCl_3): δ = 0.85 (6H, s, C(4): gem-dimethyl); 1.10-1.85 (11H, m, C(1), C(2), C(3), C(5) & C(6) protons); 1.30 (3H, t, CH_3 : ethyl ester group); 3.87 (2H, t, C(7) protons); 4.25 (2H, q, $-\text{CH}_2-$: ethyl ester group).

^{13}C nmr (CDCl_3): ppm = 14.45 (q), 15.04 (t), 17.23 (t), 22.85 (t), 27.08 (q), 32.55 (s), 37.74 (t), 44.45 (t), 61.82 (t), 77.89 (t), 157.81 (s).

m/e: M^+ (found) = 232.1918, M^+ (calc.) for $\text{C}_{12}\text{H}_{26}\text{NO}_3$ = 232.1913.

Attempted Hydrolysis of N-carbethoxy-6,6-Dimethyl-1-Oxa-2-Azacyclononane

i) Using Deuterated Hydrogen Chloride

A solution of N-carbethoxy-6,6-dimethyl-1-oxa-2-azacyclononane (103) (0.1g, 4.37×10^{-4} mol), deuterated methanol (0.5 cm^3) and deuterated hydrogen chloride (in D_2O , 0.5 cm^3) was placed in a 5mm nmr tube and the reduction followed by its ^1H nmr spectrum. The temperature was slowly raised to 50°C. After 2 hr starting material still remained and no new product had appeared. On cooling, more deuterated hydrogen chloride (in D_2O , 0.5 cm^3) was added. After 2 days, starting material still remained.

ii) Using Potassium Tertiary Butoxide/Water, at Ambient Temperature¹⁷⁹

(a) Successful Base Hydrolysis of Model Compound, N-Carbethoxy-dimethyl-1-oxa-2-azacycloheptane (23)

A slurry of potassium tert-butoxide (0.74g, 6.6×10^{-3} mol), water ($36 \mu\text{litre}$ ie 0.036g , 1.99×10^{-3} mol) and

N-carbethoxy-5,5-dimethyl-1-oxa-2-azacycloheptane (23) (0.2g , 9.95×10^{-4} mol) in diethyl ether (5 cm^3) was stirred vigorously at room temperature (ca 20°C) under nitrogen atmosphere. The course of the reaction was followed by tlc. On completion the reaction was cooled in an ice-bath and ice was added to the reaction mixture until two layers were formed. The layers were separated and the products were isolated from the appropriate layers. The organic phase was identified by ^1H nmr to contain mainly tert-butanol with very little unreacted material. While, the aqueous layer contained the hydrolysed product. An attempt to extract the product into an ether layer by salting the aqueous layer failed. Distillation using a Kugelrohr apparatus also failed to obtain the product pure. Finally, a 24 hr continual extraction over dichloromethane managed to extract the product, 2,5,5-trimethyl-1,2-oxazepane (120), into the organic phase. Yield - 0.11g (85%).

^1H nmr (CDCl_3): δ = 1.75 (6H, s, C(5): gem-dimethyl); 1.15-1.65 (4H, m, C(4) & C(6) protons); 1.74 (2H, t, C(3) protons); 3.85 (2H, t, C(7) protons).

^{13}C nmr (CDCl_3): ppm = 28.54 (q), 29.71 (s), 40.51 (t), 43.72 (t), 50.29 (t), 69.56 (t).

(b) Attempted Base Hydrolysis of N-Carbethoxy-6,6-Dimethyl-1-Oxa-2-Azacyclononane

The same procedure as that outlined above was adopted. A slurry of potassium tert-butoxide (0.74g , 6.6×10^{-3} mol), water ($40 \mu\text{litre}$ ie 0.04g , 2.2×10^{-3} mol) and N-carbethoxy-6,6-dimethyl-1-oxa-2-azacyclononane (0.15g , 6.5×10^{-4} mol) was stirred vigorously at ambient temperature for 48 hr. On workup the organic phase was identified to be N-carbethoxy-2-(aminohydroxy)-4,4-dimethylheptane

(121). A continual extraction over dichloromethane for 48 hrs of the aqueous extract failed to yield any product. The product (121) was produced in 74% yield (0.11g).

^1H nmr (CDCl_3): δ = 0.85 (6H, s, C(4): gem-dimethyl); 1.10-1.28 (3H, t, $-\text{CH}_3$ -: ethyl ester group); 1.10-1.75 (4H, m, C(5) & C(6) protons); 1.95 (2H, d, C(3) protons); 3.82 (2H, t, C(7) protons); 4.20 (2H, q, $-\text{CH}_2$ -: ethyl ester group); 5.00 & 6.00 (3H, m, C(1) & C(2) olefinic protons).

^{13}C nmr (CDCl_3): ppm = 14.45 (q), 22.85 (t), 26.86 (q), 32.92 (s), 37.81 (t), 46.50 (t), 61.82 (t), 77.74 (t), 116.79 (t), 135.55 (d), 157.88 (s).

m/e: M^+ (found) = 230.1764, M^+ (calc.) for $\text{C}_{12}\text{H}_{24}\text{NO}_3$ = 230.1757.

REFERENCES

REFERENCES

1. D H R Barton and R C Cookson (1956) *Quart.Rev.*, 10, 44.
2. H Sachse (1890) *Ber.*, 23, 1363.
3. H Sachse (1892) *Z.Physik.Chem.*, 10, 203.
4. W Hückel (1925) *Liebigs Ann.Chem.*, 441, 1.
5. O Hassel (1953) *Quart.Rev.*, 7, 221.
6. C W Beckett, K S Pitzer and R Spitzer (1947) *J.Amer.Chem.Soc.*, 69, 2488.
7. D H R Barton (1950) *Experienta*, 6, 316; (1948) *J.Chem.Soc.*, 340.
8. F G Riddell (1980) "The Conformational Analysis of Heterocyclic Compounds", Academic Press, London.
9. M Hanack (1965) "Conformation Theory", Academic Press, New York and London.
10. W G Dauben and K S Pitzer (1965) in "Steric Effects in Organic Chemistry"; Ch. 1, Ed. M S Newman, Wiley, New York.
11. F G Riddell (1967) *Quart.Rev.*, 21, 364.
12. E L Eliel and N L Allinger (eds.) (1968) "Topics in Stereochemistry", Vol. 4, Interscience, New York.
13. K Pihlaja (1974) Reprint *Kemia-Kemi*, 8, 492.
14. S Weiss and G E Le Roi (1958) *J.Chem.Phys.*, 29, 340.
15. J B Hendrickson (1961) *J.Amer.Chem.Soc.*, 83, 4537.
16. M Bixon and S Lifson (1967) *Tetrahedron*, 23, 769.
17. J H Jeans (1925) "The Mathematical Theory of Electricity and Magnetism", 5th Ed., eq. 354 on p.379, Cambridge University Press, London.
18. C P Smyth, R W Dornie and E B Wilson Jr. (1931) *J.Amer.Chem.Soc.*, 53, 4242.

19. J M Lehn and G Ourisson (1963) Bull.Soc.Chim. France, 1113.
20. D N J White and M J Bovill (1977) J.Chem.Soc. Perkin Trans. II, 1610.
21. E L Eliel (1969) Kemisk Tidskrift, NR/6-7, 22.
22. S Wolfe, A Rauk, L M Tel and I G Csizmadia (1970) J.Chem.Soc. (B), 142.
23. R J W Le Fevre (1953) "Dipole Moments", Methuen.
24. N S Zefirov, L G Gurvich, A S Shashkov, M Z Krimer and E A Vorob'eva (1976) Tetrahedron, 32, 1211.
25. S F Nelson (1978) Acc.Chem.Res., 11, 14.
26. F G Riddell and J M Lehn (1966) J.Chem.Soc.Chem.Comm., 375.
27. J E Anderson (1969) J.Amer.Chem.Soc., 91, 6374.
28. F G Riddell, D A R Williams, C Hoctele and N Reid (1970) J.Chem.Soc. (B), 1739.
29. J M Lehn (1970) Fortschr.Chem.Forsch., 15, 313.
30. J M Lehn and J Wagner (1970), J.Chem.Soc. Chem.Comm., 414.
31. R A Y Jones, A R Katritzky and S Saba (1974) J.Chem.Soc. Perkin Trans. II, 1737.
32. J B Lambert (1971) in "Topics in Stereochemistry", Vol. 6, 19, Eds. N L Allinger and E L Eliel, Wiley Interscience.
33. M S Newman (ed.) (1956) "Steric Effects in Organic Chemistry", John Wiley and Sons, New York.
34. L Nygnard, J T Nielsen, J Kirchheiner, G Mattesen, J Rastrup-Andersen, and G O Srensen (1969) J.Mol.Struct., 3, 491.
35. E L Eliel (1962) "Stereochemistry of Carbon Compounds", McGraw Hill, New York.
36. D L Griffith and B L Olson (1968) J.Chem.Soc.Chem.Comm., 1682.
37. F Montanari, I Moretti and G Torre (1969) J.Chem.Soc.Chem.Comm., 1086.

38. M Jantelat and J D Roberts (1969) *J.Amer.Chem.Soc.*, 91, 642.
39. A Bottini and J D Roberts (1958) *J.Amer.Chem.Soc.*, 80, 5203.
40. F A L Anet and J M Osyanny (1957) *J.Amer.Chem.Soc.*, 89, 352.
41. G R Boggs and J T Gerig (1969) *J.Org.Chem.*, 34, 1484.
42. H A Bent (1961) *Chem.Rev.*, 61, 275.
43. R G Gillespie (1963) *J.Chem.Educ.*, 40, 295.
44. K Muller and A Eschenmoser (1969) *Helv.Chim.Acta*, 52, 1823.
45. J M Lehn, F G Riddell, B J Price and I O Sutherland (1967) *J.Chem.Soc. (B)*, 387.
46. A Rauk, L C Allen, K Mislow (1970) *Agnew.Chem.Internat. Ed.*, 9, 400.
47. D A R Williams (1971) "Conformational Studies on Some Nitrogen Containing Compounds", PhD Thesis, University of Stirling.
48. A L Anet and J Wagner (1971) *J.Amer.Chem.Soc.*, 93, 5266.
49. J B Lambert, R G Keske, D K Weary (1967) *J.Amer.Chem.Soc.*, 89, 5921.
50. R K Harris and R A Spray (1968) *J.Chem.Soc. (B)*, 684.
51. J B Lambert; R G Keske, R E Carhart and A P Javanovich (1969) *J.Amer.Chem.Soc.*, 91, 6374.
52. E L Eliel and R O Hutchins (1969) *J.Amer.Chem.Soc.*, 91, 2703.
53. K Pihlaja (1974) *J.Chem.Soc.Perkin Trans. II*, 890.
54. A R Katritzky, R C Patel and F G Riddell (1979) *J.Chem.Soc. Chem.Comm.*, 674.
55. I O Sutherland (1971) in "Annual Reports on NMR Spectroscopy", Vol. 4, p.71, ed. E F Mooney, Academic Press, London.
56. L Pedersen and K Morukama (1967) *J.Chem.Phys.*, 46, 3941.
57. W H Fink, D C Pan and L C Allen (1967) *J.Chem.Phys.*, 47, 895.
58. L Radom, W J Hehre and J A Pople (1972) *J.Amer.Chem.Soc.*, 94, 2371.
59. S Wolfe, L M Tel and I G Csizmadia (1973) *Canad.J.Chem.*, 51, 2423.

60. F Bernardi, I G Csizmadia, A Mangini, H B Sahlegel, M H Whangbo and S Wolfe (1975) *J.Amer.Chem.Soc.*, 97, 2209.
61. D Kost and M Raban (1976) *J.Org.Chem.*, 41, 1748.
62. D R Boyd and R Graham (1969) *J.Chem.Soc.(C)*, 2648.
63. J Bjorgo and D R Boyd (1973) *J.Chem.Soc.Perkin Trans. II*, 1575.
64. J Bjorgo, D R Boyd, R M Campbell, N J Thompson and W B Jennings (1976) *J.Chem.Soc. Perkin Trans. II*, 606.
65. F G Riddell, J M Lehn and J Wagner (1968) *J.Chem.Soc.Chem.Comm.*, 1403.
66. P A Giguere and I D Liu (1952) *Canad.J.Chem.*, 30, 948.
67. S Tsunekawa (1972) *J.Phys.Soc. Japan*, 33, 167.
68. R A Y Jones, A R Katritzky, S Saba and A J Sparrow (1974) *J.Chem.Soc. Perkin II*, 1554.
- 69a. F G Riddell, E S Turner, D W H Rankin and M R Todd (1979) *J.Chem.Soc. Chem.Comm.*, 72.
- 69b. D W H Rankin, M R Todd, F G Riddell and E S Turner (1981) *J.Mol.Struct.*, 71, 171.
70. L Toft and B Jerslev (1967) *Acta Chem.Scand.*, 21, 1383.
71. D L Griffith and J D Roberts (1965) *J.Amer.Chem.Soc.*, 87, 4089.
72. M Raban and G W J Kenney (1969) *Tetrahedron Lett.*, 1295.
73. W Walter and E Schaumaan (1971) *Liebigs.Ann.*, 747, 191.
74. J R Fletcher and I O Sutherland (1970) *J.Chem.Soc.Chem.Comm.*, 687.
75. D L Griffiths, B L Olson and J D Roberts (1971) *J.Amer.Chem.Soc.*, 93, 1648.
76. T B Posner, D A Couch and C D Hall (1978) *J.Chem.Soc. Perkin Trans. II*, 450.
77. B J Price and I O Sutherland (1967) *J.Chem.Soc.Chem.Comm.*, 1070.
78. M Raban and D Kost (1972) *J.Org.Chem.*, 37, 499.

79. F G Riddell and E S Turner (1978) *J.Chem.Soc. Perkin Trans. II*, 707.
80. M Iwamura, M Katos and H Iwanamura (1980) *Org.Magn.Reson.*, 14, 392.
81. F G Riddell (1979) in "Nuclear Magnetic Resonance" - Specialist Periodical Reports, Vol. 8, 285. The Chemical Society, London.
82. F G Riddell (1980) in "Nuclear Magnetic Resonance" - Specialist Periodical Reports, Vol. 9, 222. The Chemical Society, London.
83. F G Riddell (1981) in "Nuclear Magnetic Resonance" - Specialist Periodical Reports, Vol.10, 222. The Chemical Society, London.
84. F G Riddell (1982) in "Nuclear Magnetic Resonance" - Specialist Periodical Reports, Vol.11, 225. The Chemical Society, London.
85. F G Riddell (1983) in "Nuclear Magnetic Resonance" - Specialist Periodical Reports, Vol.12, 246. The Chemical Society, London.
86. F G Riddell (1980) in "Heterocyclic Chemistry" - Specialist Periodical Reports, Vol. 1, 469, The Royal Society of Chemistry, London.
87. A Mannschrek, J Lines and W Seitz (1969) *Liebigs.Ann.*, 727, 224.
88. J Lee and K G Orrell (1965) *Trans.Farad.Soc.*, 61, 2342.
89. J B Lambert and W L Oliver Jr (1969) *J.Amer.Chem.Soc.*, 91, 7774.
90. J B Lambert, W L Oliver Jr and B S Packard (1971) *J.Amer.Chem.Soc.*, 93, 933.
91. V M Shitkin, S L Ioffe, M V Kashutina and V A Tartakovski (1977) *Izv.Akad.Nauk.SSSR, Ser.Khim*, 226; *Chem.Abs.*, 88:50151n.
92. F G Riddell and D A R Williams (1974) *Tetrahedron*, 30, 1083.
93. F G Riddell and D A R Williams (1974) *Tetrahedron*, 30, 1097.
94. F G Riddell (1975) *Tetrahedron*, 31, 523.
95. F G Riddell, P Murray-Rust and J Murray-Rust (1974) *Tetrahedron*, 30, 1087.
96. F G Riddell and J E Anderson (1977) *J.Chem.Soc. Perkin Trans.II*, 588.

97. F G Riddell, E S Turner and A Boyd (1979) *Tetrahedron*, 35, 259.
98. R A Y Jones, A R Katritzky, A C Richards, S Saba, A J Sparrow and D L Trepanier (1972) *J.Chem.Soc. Chem.Comm.*, 673.
99. R W Baldock and A R Katritzky (1968) *J.Chem.Soc. (B)*, 1470.
100. H Booth and R U Lemieux (1971) *Canad.J.Chem.*, 49, 777.
101. I J Ferguson, A R Katritzky and D M Read (1975) *J.Chem.Soc. Chem.Comm.*, 255.
102. F G Riddell and H Labaziewicz (1975) *J.Chem.Soc. Chem.Comm.*, 766.
103. L Pauling (1960) "The Nature of the Chemical Bond", Cornell University Press, Ithaca.
104. R A Y Jones, A R Katritzky, A R Martin and S Saba (1973) *J.Chem.Soc. Chem.Comm.*, 908.
105. R A Y Jones, A R Katritzky, A R Martin and S Saba (1974) *J.Chem.Soc. Perkin Trans. II*, 1561.
106. F G Riddell, M H Berry and E S Turner (1978) *Tetrahedron*, 34, 1415.
107. F G Riddell and J M Lehn (1968) *J.Chem.Soc. (B)*, 1224.
108. Y Allingham, R C Cookson, T A Crabb and S Vary (1968) *Tetrahedron*, 24, 4625.
109. T A Crabb and R F Newton (1968) *Tetrahedron*, 24, 4423.
110. T A Crabb and S I Judd (1970) *Magn.Res.*, 2, 317.
111. F G Riddell and E S Turner (1978) *Heterocycles*, 9, 267.
112. F G Riddell and E S Turner (1979) *Tetrahedron*, 35, 1311.
113. F G Riddell, E S Turner, A R Katritzky, R C Patel and F M S Brito-Palma (1979) *Tetrahedron*, 35, 1391.
114. A R Katritzky, V J Baker, I J Ferguson and R C Patel (1979) *J.Chem.Soc. Perkin Trans. II*, 143.
115. A R Katritzky and R C Patel (1978) *Heterocycles*, 9, 263.
116. A R Katritzky and R C Patel (1979) *J.Chem.Soc. Perkin Trans. II*, 993.

117. F G Riddell and E S Turner (1978) *J.Chem.Res. (S)*, 476.
118. F G Riddell and E S Turner (1979) *Tetrahedron*, 35, 1131.
119. D F Bocian and H L Strauss (1977) *J.Amer.Chem.Soc.*, 99, 127.
120. H Friebohn, R Mecke, S Kabuss and A Luttringhaus (1964) *Tetrahedron Lett.*, 1929.
121. S Kabuss, H Friebohn and H G Schmid (1965) *Tetrahedron Lett.*, 469.
122. S Kabuss, A Luttringhaus, H Friebohn and R Mecke (1966) *Z.Naturforsch.*, 21b, 320.
123. S Kabuss, A Luttringhaus, H Friebohn, H G Schmid and R Mecke (1966) *Tetrahedron Lett.*, 719.
124. R M Moriarty, N Ishibe, M Kayser, K C Ramey and H J Gisler (1969) *Tetrahedron Lett.*, 4883.
125. M St Jacques and C Vaziri (1971) *Canad.J.Chem.*, 49, 1256.
126. R E Wasylshen, K C Rice and U Weiss (1975) *Canad.J.Chem.*, 53, 414.
127. P Ayras and A Partanen (1977) *Org.Magn.Res.*, 9, 379.
128. H Faucher, A Guimares and J B Lambert (1977) *Tetrahedron Lett.*, 1743.
129. C A MacCadie (1981) "Synthesis and Conformational Analysis of some Seven-Membered Cyclic Derivatives of Hydroxylamine" - BSc Honours Project, Stirling University, Chemistry Department.
130. J B Hendrickson (1963) *J.Amer.Chem.Soc.*, 85, 4059.
131. J B Hendrickson (1964) *J.Amer.Chem.Soc.*, 86, 4854.
132. J B Hendrickson (1967) *J.Amer.Chem.Soc.*, 89, 7036; * 7043; 7047.
133. W B Wilberg (1965) *J.Amer.Chem.Soc.*, 87, 1070.
134. N L Allinger, J A Hirsch, M Miller, J J Tyminski and F A van Catledge (1968) *J.Amer.Chem.Soc.*, 90, 1199.
135. F A L Anet (1974) *Fortschritte*, 45, 169.
136. F A L Anet and V J Basus (1973) *J.Amer.Chem.Soc.*, 95, 4424.

137. S Meiboom, R C Hewitt and Z Lux (1977) *J.Chem.Phys.*, 66, 4041.
138. F A L Anet, P J Degan and I Yavari (1978) *J.Org.Chem.*, 43, 3021.
139. F J Weigert and W J Middleton (1980) *J.Org.Chem.*, 45, 3289.
140. L Pauling and D L Carpenter (1937) *J.Amer.Chem.Soc.*, 58, 1274.
141. D Grandjean and H Lechaire (1967) *Compte.Rend.*, 265, 795.
142. H H Caldy, A C Larson and D T Comer (1963) *Acta.Cryst.*, 16, 617.
143. H Schenck (1971) *Acta.Cryst.*, B27, 185.
144. G W Frank, P J Degan and F A L Anet (1972) *J.Amer.Chem.Soc.*, 94, 4792.
145. K T Go and I C Paul (1965) *Tetrahedron Lett.*, 4265.
146. K T Go and I C Paul (1969) *J.Chem.Soc. (B)*, 33.
147. S M Johnson, C A Maier and I C Paul (1970) *J.Chem.Soc. (B)*, 1603.
148. F A L Anet and P J Degan (1972) *J.Amer.Chem.Soc.*, 94, 1390.
149. J Dale, J Ekeland and J Krane (1972) *J.Amer.Chem.Soc.*, 94, 1389.
150. J Dale (1973) *Acta.Chem.Scand.*, 27, 1130.
151. G Borgen and J Dale (1970) *J.Chem.Soc.Chem.Comm.*, 1105.
152. J M Lehn, P Linscheid and F G Riddell (1968) *Bull.Soc.Chim. France*, 1172.
153. A I Vogel (1978) "A Text-book of Practical Organic Chemistry, including Qualitative Organic Analysis", 4th Edition, Longmans, London.
154. J F Bussert, K W Greenlee, J M Derfer, C E Boord (1956) *J.Amer.Chem.Soc.*, 6076.
155. H King (1942) *J.Chem.Soc.*, 432.
156. L W Jones and R Oesper (1914) *J.Amer.Chem.Soc.*, 36, 730.
157. N G Gaylord (1956) "Reduction with Complex Metal Hydrides", Interscience.
158. E M van Heyningen (1952) *USP 2*, 183, 621.

159. A T Blomquist and J A Verdol (1955) *J.Amer.Chem.Soc.*, 77, 1806.
160. A G Anderson Jr and F J Freenon (1972) *J.Org.Chem.*, 37, 626.
161. L Horner, H Oediger and H Hoffman (1959) *Justus Liebigs Ann.Chem.*, 626, 26.
162. D B Denney and R R Dileone (1962) *J.Amer.Chem.Soc.*, 34, 4737.
163. G A Wiley, R L Hershkowitz, B M Rein and B C Chung (1964) *J.Amer.Chem.Soc.*, 86, 964.
164. G A Wiley, B M Rein and R L Hershkowitz (1964) *Tetrahedron Lett.*, 2509.
165. L Ruzicka, W Brugger, M Pfeiffer, N Schinz and M Stoll (1926) *Helv.Chem.Acta.*, 9, 499.
166. L Ruzicka (1935) *Chem. and Ind. London*, 54, 2.
167. E L Eliel, N L Allinger, S J Angyal and G A Morrison (1965) "Conformational Analysis", John Wiley and Sons, New York.
168. R M Beesley, C K Ingold and J F Thorpe (1915) *J.Chem.Soc.*, 107, 1080.
169. C K Ingold (1921) *J.Chem.Soc.*, 119, 305.
170. G S Hammond (1956) in "Steric Effects in Organic Chemistry", Ed. M S Newman, John Wiley and Sons, New York.
171. N L Allinger and V Zalkow (1960) *J.Org.Chem.*, 25, 701.
172. H Yumoto (1958) *J.Chem.Phys.*, 29, 1234.
173. J Dale (1963) *J.Chem.Soc.*, 93.
174. G M Steinberg and R Swidler (1965) *J.Org.Chem.*, 30, 2362.
175. L W Jones and L Neuffer (1914) *J.Amer.Chem.Soc.*, 36, 2208.
176. C Hecker (1913) *Amer.Chem.J.*, 50, 457.
177. L Neuffer and A L Hoffmann (1925) *J.Amer.Chem.Soc.*, 47, 1685.
178. P Sykes (1965) "A Guidebook to Mechanism in Organic Chemistry", Longmans, London.

179. P G Gassman, P K G Hodgson and R J Balchunis (1976)
J.Amer.Chem.Soc., 98, 1275.
180. M L Bender (1960) Chem.Rev., 60, 53.
181. M L Bender and R D Ginger (1955) J.Amer.Chem.Soc., 77, 348.
182. M L Bender, R D Ginger and J P Unik (1958) J.Amer.Chem.Soc., 80,
1044.
183. C A Bunton and D N Spatcher (1956) J.Chem.Soc., 1079.
184. M L Bender and R J Thomas (1961) J.Amer.Chem.Soc., 83, 4183, 4189.
185. C A Bunton, B Nayak and C O'Connor (1968) J.Org.Chem., 33, 572.
186. S S Biechler and R W Taft Jr (1957) J.Amer.Chem.Soc., 79, 4927.
187. R L Schowen, H Jayaraman and L Kershner (1966) J.Amer.Chem.Soc.,
88, 3373.
188. M T Behme and E H Cordes (1964) J.Org.Chem., 29, 1255.
189. H Booth (1969) in "Progress in NMR Spectroscopy", Chapter 3, Ed. T
W Emsley, Feeney and Sutcliffe, Pergamon Press, Oxford.
190. J E Anderson (1965) Quart.Rev., 14, 426.
191. W A Thomas (1970) in "Annual Reports of NMR Spectroscopy", Ed. E F
Mooney, Academic Press, London.
192. J D Roberts (1979) Pure Appl.Chem., 51, 1037.
193. W M M J Bovee (1979) Mol.Phys., 37, 1975.
194. D M Doddrell, M R Bendall, P F Barron and D T Pegg (1979)
J.Chem.Soc.Chem.Comm., 2, 77.
195. J D Baldeschwieler and E W Randall (1963) Chem.Rev., 63, 81.
196. J A Pople and A A Bothner-By (1965) J.Chem.Phys., 42, 1339.
197. M Barfield and B Chakrabarti (1969), Chem.Revs., 69, 757.
198. R J Abraham and W A Thomas (1965) J.Chem.Soc.Chem.Comm., 431.
199. R C Cookson, T A Crabb, J J Frankel and J Hudes (1966) Tetrahedron,
suppl., 7, 355.

200. T A Crabb and R F Newton (1966) Chem.and Ind., London, 339.
201. M Anteunis (1966) Bull.Soc.Chim.Belges., 75, 413.
202. H P Hamlov, S Okuda and N Nakagawa (1964) Tetrahedron Lett., 2553.
203. J B Lambert and R G Keske (1966) J.Amer.Chem.Soc., 88, 620.
204. W B Monitz and J A Dixon (1961) J.Amer.Chem.Soc., 83, 1671.
205. M Karplus (1963) J.Amer.Chem.Soc., 85, 2870.
206. J B Lambert (1967) J.Amer.Chem.Soc., 89, 1836.
207. J B Lambert (1971) Acc.Chem.Res., 4, 87.
208. J B Lambert, J J Papay, E S Magyar and M K Neuberger (1973)
J.Amer.Chem.Soc., 95, 4459.
209. J B Lambert, J J Papay, S A Khan, K A Kappauf and E S Magyar (1974)
J.Amer.Chem.Soc., 96, 6112.
210. H R Buys (1970) Rec.Trav.Chim., 89, 1244.
211. H R Buys (1970) Rec.Trav.Chim., 89, 1253.
212. J Sandström (1982) "Dynamic NMR Spectroscopy", Academic Press,
London.
213. A Steigel (1978) "NMR, Basic Principles and Progress", 15, 1.
214. L M Jackman and F A Cotton (1975) "Dynamic Nuclear Magnetic
Resonance Spectroscopy", Academic Press, London and New York.
215. H Eyring (1935) Chem.Revs., 17, 65.
216. S Glasstone, K J Laidler and H Eyring (1941) "The Theory of Rate
Processes", McGraw-Hill, New York.
217. F Bloch (1946) Phys.Rev., 70, 460.
218. G Claesson, G Androes and M Calvin (1961) J.Amer.Chem.Soc., 83, 4357.
219. M Oki, H Iwamura and N Hayakawa (1963) Bull.Chem.Soc.Japan, 36,
1542.
220. R J Kurland, M B Rubin and M B Wyse (1964) J.Chem.Phys., 40, 2426.

221. G W Buchanan, D A Ross and J B Stothers (1966) *J.Amer.Chem.Soc.*, 88, 4301.
222. O A Gansow, J Killough and A R Burke (1971) *J.Amer.Chem.Soc.*, 93, 4297.
223. S Masamune, K Hojo, G Bigam and D L Rabenstein (1971) *J.Amer.Chem.Soc.*, 93, 4966.
224. D K Dalling, D M Grant and L F Johnson (1971) *J.Amer.Chem.Soc.*, 93, 3678.
225. H J Schneider, R Price and T Keller (1971) *Angew.Chemie.*, 83, 759.
226. F A L Anet and R Anet (1975) in "Dynamic Nuclear Magnetic Resonance Spectroscopy", p.543, Eds. L M Jackman and F A Cotton, Academic Press, London and New York.
227. F A L Anet and I Yavari (1977) *J.Amer.Chem.Soc.*, 99, 7640.
228. F A L Anet and I Yavari (1978) *J.Amer.Chem.Soc.*, 100, 7814.
229. F A L Anet and T N Rawdah (1979) *J.Amer.Chem.Soc.*, 101, 1887.
230. Y K Grishin, N M Sergeev, D A Subbotin and Y A Ustynyuk (1973) *Mol.Phys.*, 25, 297.
231. C Piccinni-Leopardi, O Fabre and J Reisse (1976) *Org.Magn.Res.*, 8, 233.
232. A Blanchette, F Sauriol-Lord and M St Jacques (1978) *J.Amer.Chem.Soc.*, 100, 4055.
233. F A L Anet, I Yavari, I J Ferguson, A R Katritzky, M Moreno-Manas and M J T Robinson (1976) *Chem.Comm.*, 399.
234. N C Franklin and H Feltkamp (1965) *Angew.Chem.Int.Ed.*, 4, 774.
235. P J Crowley, M J T Robinson and M G Ward (1977) *Tetrahedron*, 33, 915.
236. A R Katritzky, R C Patel and F G Riddell (1981) *Angew.Chemie.Int.Ed.Engl.*, 20, 521.

237. A R Katritzky, V J Baker, F M S Brito-Palma, I J Ferguson, L Angiolini (1980) *J.Chem.Soc.Perkin Trans.II*, 1746.
238. A J Gordon and A F Richard (1972) "The Chemists's Companion - A Handbook of Practical Data, Techniques and References", John Wiley & Sons, New York.
239. R T Major, F Dürsch and H J Hess (1959) *J.Org.Chem.*, 24, 431.
240. E L Eliel and C A Lukach (1957) *J.Amer.Chem.Soc.*, 79, 5986.
241. E D Bergmann and R Corett (1958) *J.Org.Chem.*, 23, 1507.
242. J M Conia and A Le Craz (1960) *Bull.Soc.Chim.France*, 1934.
243. F G Bordwell and K M Wellman (1963) *J.Org.Chem.*, 28, 1347.
244. J P Schaefer and J Higgins (1967) *J.Org.Chem.*, 32, 1607.
245. A H Blatt (ed.) (1955) "Organic Synthesis - Collective Volume III", p557, John Wiley & Sons, New York.

SECTION II

APPLICATION OF NUCLEAR MAGNETIC RESONANCE SPECTROSCOPY
IN BIOLOGICAL CHEMISTRY

CHAPTER 1

Biological Membranes and Paramagnetic

Lanthanide Shift Reagents

CHAPTER 1: BIOLOGICAL MEMBRANES AND PARAMAGNETIC LANTHANIDE SHIFT REAGENTS1.1 INTRODUCTION

The alkali and alkali earth cations, especially sodium⁺ (Na⁺), potassium⁺ (K⁺), magnesium²⁺ (Mg²⁺) and calcium²⁺ (Ca²⁺) are present abundantly in living systems and occupy an important role in many processes^{1,2} eg Mg²⁺ and K⁺ are concentrated in the cytoplasm while Na⁺ and Ca²⁺ are rejected by the cell.

It has become increasingly clear that the ionic composition of the intracellular fluids is of enormous importance in regulating the activities of biological cells and tissues. Regulation of processes including excitability³ and mitosis and cell growth⁴⁻⁷ has been correlated with intracellular ion activities. The crucial roles played by intracellular Ca²⁺ have been particularly well defined⁸⁻¹¹ and Mg²⁺ ions have been shown to be involved in many enzymatic reactions. The intracellular roles of the monovalent cations have been far less clearly established, although several lines of evidence suggest their importance. The activities of a large number of enzymes are dependent upon the local Na⁺ and K⁺ concentrations.¹² The activity of isolated chromosomes has also been reported to depend upon the relative activities of Na⁺ and K⁺ in the medium.¹³ Possibly because of these dependences, protein synthesis appears to be directly dependent upon the intracellular K⁺.¹⁴ Shifts in the subcellular distribution of K⁺ may also be of importance, at least with respect to the process of fertilization.¹⁵ The intracellular K⁺ may be an important regulator of net K⁺ excretion by the kidney,¹⁶ and play a crucial role in the development of blast transformation.^{17,18}

The intracellular Na^+ also appears to be of specific importance in several ways. Its activity within transporting cells regulates, in part, the rate of transepithelial sodium chloride (NaCl) transport.¹⁹ Transport of amino acids and nucleotides across the membrane bounding the cell nucleus also seems to display a specific requirement for Na^+ .²⁰ Within the framework of the generally accepted ion gradient theory, the gradient in electrochemical activity for Na^+ across the external cell membrane assumes central importance in being coupled to a host of secondary electrochemical and chemical gradients via Na^+/H^+ , $\text{Na}^+/\text{Ca}^{2+}$, $\text{Na}^+/\text{Mg}^{2+}$ and Na^+ /substrate exchange or sugars and amino acids cotransport reactions.^{21,22} The control of these proton, divalent ion and substrate gradients in turn regulates many additional vital cell functions. There is evidence that cancer cells have abnormally high intracellular Na^+ concentrations.^{5,7,23} A number of recent reports have correlated abnormal ion fluxes in erythrocytes with the conditions of essential hypertension,²⁴⁻²⁸ affective disorders^{29,30} and myotonic dystrophy.³¹⁻³³

In view of the likely physiological importance of intracellular Na^+ and K^+ , considerable effort has been devoted not only to measuring the total contents and determining the state and subcellular distribution of these ions within the intracellular fluids but also to the problem of measurement of the rates of exchange between the intra- and extracellular fluids. Because ²³Na and ³⁹K are nuclear magnetic resonance (nmr) active nuclei, nmr is potentially a most attractive method for studying these ions in living systems and such investigations form the basis of Section II of this thesis. These studies, however, first require some knowledge of the nature and transport mechanisms of biological membranes.

1.2 BIOLOGICAL MEMBRANES

1.2.1 Molecular Organisation of Membranes

The cell membrane divides this universe into two parts, the "inside" and the "outside". By this the membrane becomes the most important organ of the cell for it is here where the two worlds, the inside and the outside, meet.

A Szent-Gyorgyi

In 1855 Karl Nageli³⁴ observed differences in the penetration of pigments into damaged and undamaged plant cells, and examined the cell boundary, to which he gave the name plasma membrane. These studies were extended by Overton³⁵ who observed that non-polar compounds more readily traversed the membranes of cells than polar compounds. These studies indicated, for the first time, that fatty materials might be an important constituent of biological membranes.³⁶ The physical chemist I Langmuir³⁷ demonstrated that molecules of amphipathic nature arrange themselves into monomolecular films at air-water interfaces. He proposed that the molecules in such films are all orientated with their polar ends into the water and their hydrophobic ends away from the water. Capitalizing on Langmuir's work, the Dutch scientists, E Gorter and F Grendel³⁸ set out to measure the total film size produced by the lipids extracted from human erythrocytes (red blood cells). They found that the extracted lipids covered twice the area of the cell surface and so proposed that the cell membrane was a lipid bilayer. The view that membranes consisted of lipid bilayers gained support until the

observation of Harvey, Cole and others^{39,40} in the early 1930s showed that biological membranes have a much lower surface tension than that displayed by oil or neutral lipid/water interfaces. This led Danielli and Davson⁴¹⁻⁴⁴ to propose that a stable membrane structure would be produced by a symmetrical arrangement of a lipid bilayer covered on either side by a layer of protein (Fig 1.1).⁴¹ The fundamentals of this structure are still accepted today, though there have been numerous proposals for modification.

Despite their insight, Gorter, Grendel, Danielli and all the membrane workers who had gone before had never seen the cell membrane. It was not until the development of electron microscope that it became possible to examine membranes directly, opening a new era in the study of membranes. Early electron micrographs suggested that all membranes have the same basic structure: a three-layered (trilaminar) structure approximately 7.5 to 10.0nm in thickness, composed of two dark electron dense lines, each 2.0 to 2.5nm thick, separated by a light electron-transparent region of 3.5 to 5.0nm (Fig 1.2). Robertson^{45a} termed this structure a "unit membrane" and was considered to represent a universal structure for all biological membranes - a generalization that became known as the unit membrane hypothesis.⁴⁶⁻⁵⁰

Over the years, however, it has become apparent that the original concept of a universal structure is inadequate^{51,52}. Current concepts of membrane structure were developed in large part from observation made on membranes after freeze-fracture and freeze-etching. The importance of this technique to the study of biological membranes became clear in 1967 when Daniel Branton⁵³⁻⁵⁵ demonstrated that the fracture line frequently follow the middle of a membrane, separating the two layers of the lipid leaflet from one another (Fig 1.3). This separation revealed

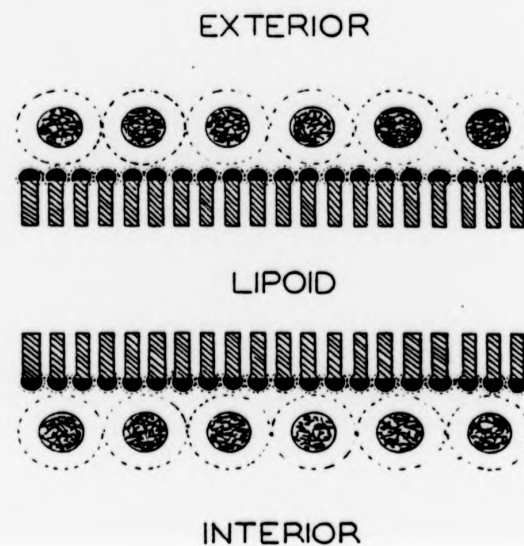


Fig 1.1 The original Danielli-Davson model of membrane structure. The bimolecular layer of lipid molecules is of undefined thickness and is covered on each side by a continuous layer of globular proteins.⁴¹

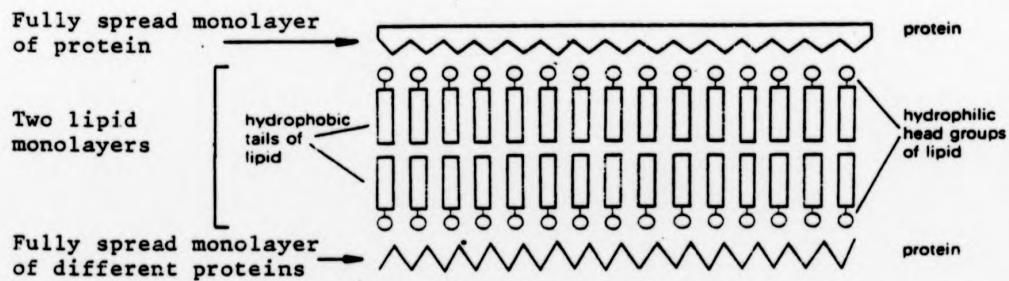


Fig 1.2 Schematic diagram of the Davson-Danielli-Robertson model.^{45b}

not a smooth lipid surface, as expected, but a surface that looked like cobble stones. The "stones" are membrane-associated proteins sitting not on the surface but within the lipid leaflets. In recent experiments, some of these proteins have been identified and there is evidence that some globular particles may span the entire membrane. The most favoured model for the plasma membrane was amplified by Singer and Nicolson^{56b} in 1972 when they stressed the dynamic aspects of membrane structure in describing the fluid mosaic model. The refined model is most aptly illustrated by their now classic diagram (Fig 1.4) in which globular proteins are shown to resemble 'icebergs' floating in a 'sea' of lipid bilayer. Both these components are capable of translational diffusion within an overall bilayer. The mosaic arrangement implies:

- (i) that the macromolecules have a characteristic asymmetry
- (ii) that they are orientated for carrying information across the bilayer, and
- (iii) that they have considerable freedom of movement within the bilayer (fluidity).

The concept of fluidity of phospholipid molecules in biological tissue was considered by Chapman et al⁵⁷ on the basis of phase transitions. The fluidity of the lipids depends on the temperature and degree of saturation. Most of the lipids of the membrane are fluid at body temperature. With freeze-fracturing it is possible to demonstrate the movement of protein particles in different experimental conditions.

The concept of hydrophobicity has been thoroughly discussed by Tanford.⁵⁸ Hydrophobicity contributes not only the cohesive force that stabilizes the phospholipid bilayer and holds the integral proteins (vide infra) in place; it also provides the energy barrier (entropy barrier) that prevents water from penetrating the fairly close-packed

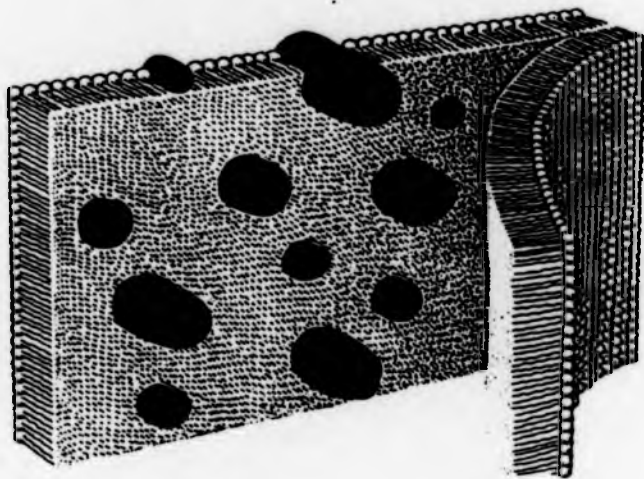


Fig 1.3

Replica of a freeze-fractured membrane. A lipid bilayer can be split between the hydrocarbon tails parallel to the surface of the membrane by freeze fracturing. Integral proteins are detected as protrusions or cavities in the replicas.^{56a}

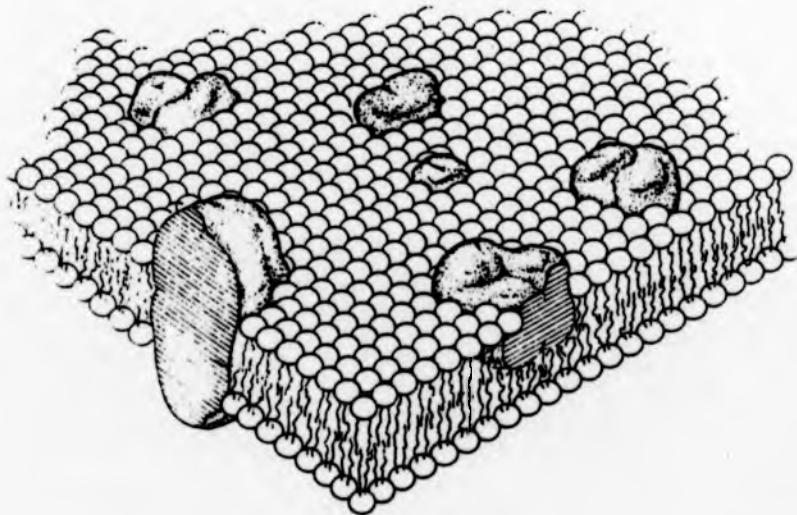


Fig 1.4

Diagram of Singer's fluid mosaic model of membrane structure. The large bodies are globular protein molecules which are embedded to varying degrees in a lipid bilayer.^{56b}

phospholipid tails of the bilayer.

There are many gaps in our knowledge of membrane structure. For example, the tertiary structure of proteins in membranes are unknown, as are the details of lipid-protein interactions although these are currently the subject of extensive research work. Inorganic ions seem to be required to maintain membrane structure, an observation not easily explained by the fluid mosaic model. It has been suggested that they might merely form ion pairs with the ionic heads to minimize electrostatic repulsion, thus stabilizing the bilayer.⁵⁹

1.2.2 Chemical Composition

Chemical analysis of membranes has been accomplished for a number of organelles, cells and organisms and it has been found that all cellular membranes, including the plasma membrane as well as those in the cell interior, are composed primarily of lipid and protein, although carbohydrate is often present covalently bonded either to lipid (as glycolipid) or to protein (as glycoprotein). The carbohydrate containing molecules will be considered here as lipids or proteins as appropriate. While the composition of membranes varies with their source (Table 1.1) they generally contain approximately 40% of their dry weight as lipid^{60,61} and 60% as protein,⁶² held together in a complex by non-bonded interactions. In addition to the above components, membranes contain some 20% of their total weight as water, which is tightly bond and essential to the maintenance of their structure. Membranes are among the most stable of cellular structures.⁶⁶

(a) Membrane Lipids

The lipid components of biological membranes can be divided into two broad classes, each having several subdivisions:

TABLE 1.1 Approximate Chemical Composition of Various Biological
Membranes⁶³⁻⁶⁵

	Percent of dry weight		
	Protein	Lipid	Carbohydrate
Myelin	18	79	3
Huran erythrocyte	49	43	8
Retinal rod outer segment	51	49	-
Rat liver mitochondria			
inner membrane	76	24	2
outer membrane	52	48	-
<u>Salmonella typhimurium</u>			
inner membrane	65	35	-
outer membrane	44	20	37 (lipopolysaccharide)

(i) THE AMPHIPHATHIC LIPIDS:

- are the phospholipids which include phosphoglycerides (and glycolipids) and sphingolipids.
- they have ionic or polar, water-soluble "heads" and non-polar hydrocarbon "tails", hence called amphipathic (Fig. 1.5).

(ii) THE STEROL FAMILY

- whose principal representative in animal membranes is cholesterol
- largely absent from prokaryotic cells and from certain intracellular organelles, such as the mitochondrial inner membrane
- it too, is amphipathic, since its hydroxyl group is polar and the steroid ring system and hydrocarbon "tail" are non-polar. However, the affinity of the hydroxyl group for water is much less than the affinity of an ionic head for water, and the amphipathic properties of cholesterol do not dominate its physical properties.

The phospholipids found in cellular membranes are of two general types. The most common type, the phosphoglycerides, includes the phosphatidic acids and their derivatives. The general structure of the glycerol phospholipids is illustrated in Fig 1.6. R_1 and R_2 are long fatty acids ranging in length from 12 to 24 carbon atoms. Whilst R_1 is generally saturated, R_2 (depending on its length) may contain up to six olefinic double bonds. A single phospholipid isolated from a homogeneous source may contain a great variety of fatty acids varying in both chain length and unsaturation.⁶⁷ The great majority of membrane phosphoglycerides are derivatives of phosphatidic acids. In these derivatives choline, ethanolamine, serine, inositol and sometimes other compounds are linked to one of the phosphate hydroxy groups of phosphatidic acids (Fig 1.6).

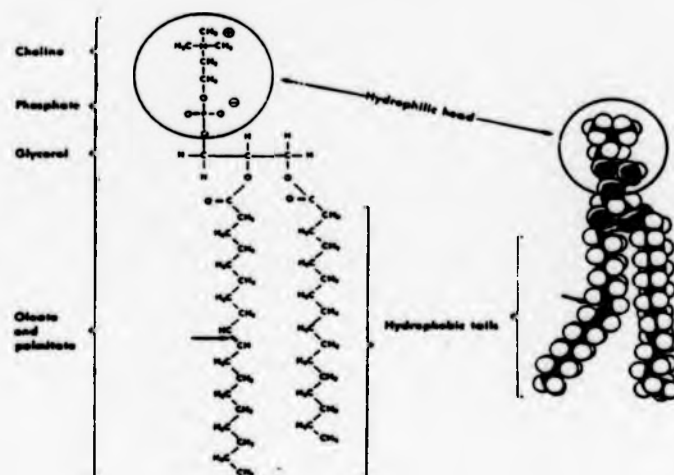
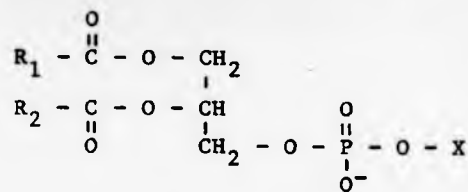


Fig. 1.5

A membrane phospholipid molecule has a hydrophilic head and two hydrophobic tails. The phospholipid represented here is palmitoyl-oleoyl-phosphatidyl-choline. Note that the double bond in the oleic acid produces a bend in the hydrocarbon chain (indicated by an arrow). Double bonds in the fatty acids increase cell membrane fluidity because unsaturated chains are more flexible (the rotation of the carbon-carbon single bonds on either side of the arrow is enhanced).

General structure of the
glycerol phospholipids



		net charge at neutral pH
X = -H	phosphatidic acid	negative
$ = -\text{CH}_2\text{CH}_2 - \begin{array}{c} \text{CH}_3 \\ \\ \text{N}^+ \\ \\ \text{CH}_3 \end{array} - \text{CH}_3 $	phosphatidyl choline (PC) (lecithin)	neutral
$ = -\text{CH}_2\text{CH}_2 - \text{N}^+\text{H}_3 $	phosphatidyl ethanolamine (PE)	neutral
$ = -\begin{array}{c} \text{N}^+\text{H}_3 \\ \\ \text{CH}_2\text{CH}_2 \end{array} - \text{COO}^- $	phosphatidyl serine (PS)	neutral
$ = -\begin{array}{c} \text{OH} \\ \\ \text{CH}_2\text{CH} \end{array} - \text{CH}_2\text{OH} $	phosphatidyl glycerol (PG)	negative
$ = \begin{array}{c} \text{OH} \quad \text{H} \\ \quad \\ \text{H} \quad \text{OH} \\ \quad \\ \text{H} \quad \text{H} \\ \quad \\ \text{OH} \quad \text{OH} \end{array} $	phosphatidyl inositol (PI)	negative

cardiolipin is diphosphatidyl glycerol, and has phosphatidic
esterified at the 1- and the 3-hydroxyl groups of glycerol negative

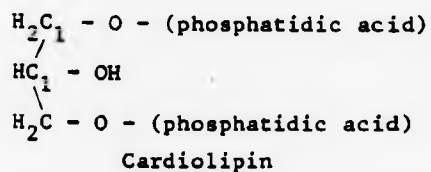
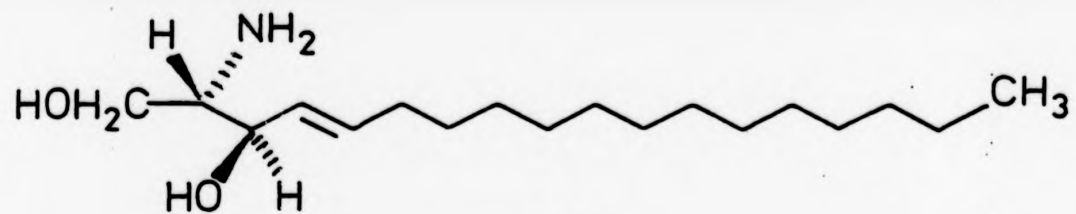


Fig 1.6 Structures of the glycerol phospholipids.

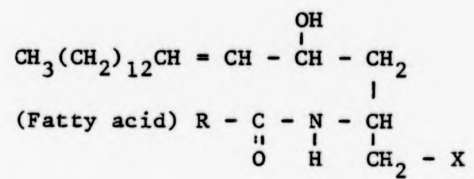
Sphingolipids are also common constituents of membranes. The generic structure of some sphingolipids are shown in Fig. 1.7. Their structure and properties are similar to the phosphoglycerides, though the "backbone" is not glycerol but the base sphingosine (1). This is best thought of as a straight chain alcohol (C_{18}) having a unique double bond and substituted with amino and hydroxyl groups at carbons 2 and 3. The sphingolipids carry only a single fatty acid residue and this is linked via an amide linkage at C(2) of the sphingosine. The parent molecule of this class is ceramide. When the free hydroxyl of C(1) of ceramide is esterified to phosphorycholine, the result is sphingomyelin. Note that sphingomyelin, like the phosphoglycerides, is a phospholipid. The cerebroside and gangliosides are derived by glycosidic linkage at C(1). The more complex carbohydrate structures attached to these molecules are antigenic in quality, and it is possible that they play a role in cell recognition, but of the precise role, little is known.

The "heads" of the phosphoglycerides and sphingomyelins are either neutral, dipolar ions or anionic. Cationic head groups are extremely rare, and have been found only in a few bacteria. The surfaces of biological membranes therefore bear a net negative charge. The chemistry and structure of phospholipids, sphingolipids and related materials is excellently presented in reference (68) and in standard textbooks.^{59,69,70}

The sterols constitute the second class of lipid component in biological membranes. They are fused ring systems and exert a stabilizing influence on the overall membrane structure. The most abundant sterol in animal tissues is cholesterol (Fig 1.8a). The fused rings of the steroid nucleus form a rigid plate-like structure, on which are mounted methyl groups at C(10) and C(13) (as can be seen in the model



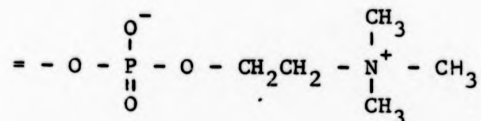
(1)



Sphingolipids

X = -OH

ceremide



sphingomyelin

= simple sugar of polysaccharide which may be N-acetylated

cerebroside

= polysaccharide containing N-acetylneuraminic acid (NANA, ie acetylated sialic acid)

ganglioside

Fig 1.7 Structures of the sphingolipids.

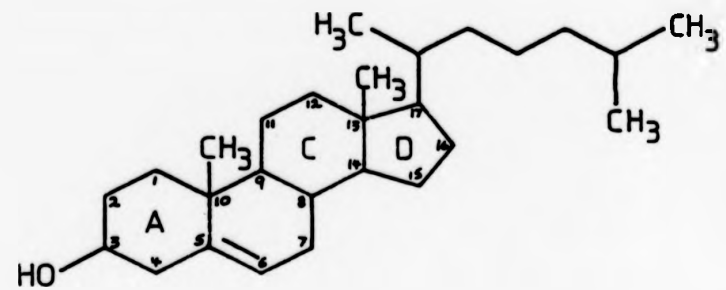
of cholesterol illustrated in Fig 1.8b), which confer a third dimension to this otherwise flat molecule. The aliphatic tail at C(17) is uncomplicated, and free to flex and rotate. Cholesterol is a highly hydrophobic molecule whose maximum solubility in water is 10^{-8} Moles. It reduces the permeability of phospholipid bilayers and enhances their stability. These effects have been attributed to the demonstrated ability of cholesterol to restrict the molecular mobility of hydrocarbon chains of phospholipids probably by way of an equimolar complex with phospholipid.

(b) Membrane Proteins

Biological membranes contain protein as well as lipids. Proteins represent the main component of most biological membranes. They play an important role, not only in the mechanical structure of the membrane, but also as carriers or channels, serving for transport; they may also be involved in regulatory or ligand recognition properties. In addition, numerous enzymes, antigens and various kinds of receptor molecules are present in plasma membranes. There is a rough correlation between the metabolic activity of a membrane and its protein content. The myelin sheath of nerves, for example, primarily serves as an insulator and contains relatively little protein, whereas the metabolically active inner mitochondrial membrane contains a large amount of protein (Table 1.1).

Membrane proteins have been classified as integral (intrinsic) or peripheral (extrinsic)^{56,64,71} according to the degree of their association with the membrane and the methods by which they can be solubilized. Peripheral proteins constitute about 25% of membrane proteins. They are bound electrostatically to the ionic head groups on the membrane surface.^{71,72} Therefore, they can be isolated in high

(a)



(b)

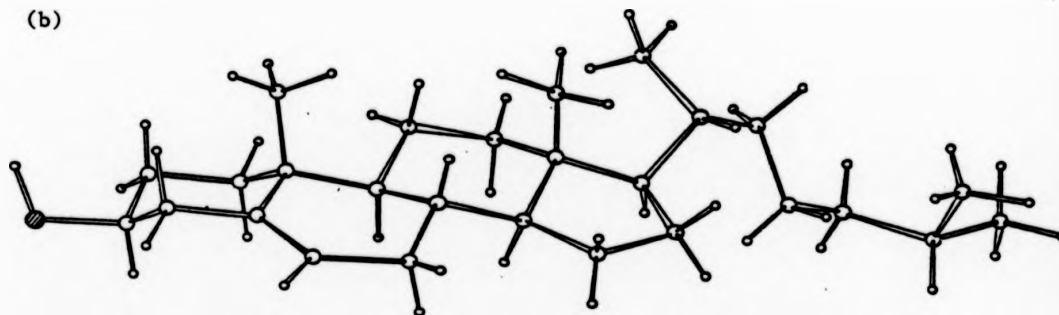


Fig 1.8

- a) The structure of cholesterol
b) A drawing of a molecular model of cholesterol

purity by mild treatment, such as increasing the ionic strength of the medium; are soluble in aqueous solutions and are usually free of lipids.

Integral proteins represent more than 70% of the two protein types and require drastic procedures for isolation. Draconian techniques that disrupt membranes, such as treatment with detergents or exposure of the membranes to ultrasonic vibrations, are required. Even then, the proteins isolated often have lipid tightly bound to them and are often denatured or otherwise significantly altered. To a large extent the function of integral membrane proteins depends upon the structural integrity of the membrane.

1.2.3 Membrane Transport

Research into membrane-associated phenomena has expanded greatly since the proposal of the fluid-mosaic model of membrane structure in the mid 1960s by Singer and Nicolson.⁵⁶ The fundamental function of the plasma membrane is that of protection. The cell has a different milieu from that of its external environment. For example, the ionic content of animal cells is quite dissimilar from that of the surrounding fluids (Table 1.2). The protoplasm of a plant or animal cell contains 75 to 85 per cent water, 10 to 20 per cent protein, 2 to 3 per cent lipid, 1 per cent carbohydrate and 1 per cent inorganic material. The cell has a high concentration of K^+ and Mg^{2+} while Na^+ and Cl^- are localized mainly in the interstitial fluid. The dominant anion in cells is phosphate; some bicarbonate is also present. The plasma membrane is thus essential to maintain a constant internal environment, irrespective of changes that may occur outside. However, the cell membrane, while protecting the cell from a variable external environment, must allow selective communication with the exterior, controlling which materials

TABLE 1.2 Concentrations of Na⁺ and K⁺ (in millimoles/litre) in various cell types*.

Cell	Intracellular		Fluid surrounding cells	
	Na ⁺	K ⁺	Na ⁺	K ⁺
Human erythrocyte	11	91	138	4.2
Rat erythrocyte	12	100	151	5.9
Frog muscle	16	127	106	2.6
Rat muscle	8	160	147	7.3
<u>Chara</u> cell sap	66	65	460	10.0
<u>Valonia</u> cell sap (marine alga)	35	576	460	10.0

* All data calculated from H B Steinbach (1963) in "Comparative Biochemistry" Vol 4, Part B, eds, M Florkin and H S Mason, Academic Press, Inc, New York, 677.

get in and out and the rate at which they do so. For example, the plasma membrane permits the entrance of water, nutrients, certain salts and other essential material into the cell while excluding unneeded or potentially harmful substances; it hinders the loss of metabolically useful substances and encourages the release of toxic or useless metabolic byproducts; at the same time it controls the concentration of intracellular substances at acceptable levels. The function of the plasma membrane of regulating this exchange between the cell and the medium is called permeability. The lipids and proteins play complementary roles in the control of membrane permeability.

Arrangement must thus be made for the controlled passage of nutrients into the cell, and the removal of waste products from it. Plasma membranes, therefore, have associated with them a range of transfer systems which enable molecules to pass through the membrane in a specific manner. Movement across a membrane may be dependent either only on concentration gradient (passive and facilitated transfer) or may require an energy supply (active transfer). Extensive literature on membrane permeability describes numerous mechanisms by which transport is accomplished.^{69,73-86}

In the following discussion of transport systems, reproducing pages of equations which describe the kinetic models, have deliberately been avoided. The reason for this is two-fold. Firstly, they have been adequately described in standard textbooks,^{81,83,85-91} but more importantly, they do not in fact define a unique physical model of a transport protein.⁹²

In their natural state, cell membranes are bounded on both sides by aqueous environments. Passage of a solute from one side of the membrane to the other can be considered to occur in three stages:

- (i) The solute must leave the aqueous phase and enter the hydrophobic lipid region of the membrane.
- (ii) The solute must transverse the lipid bilayer
- (iii) The solute must leave the lipid phase and return to an aqueous environment.

For most polar molecules stages (i) and (iii) represent a considerable barrier.

(a) Passive Diffusion

Random Brownian movements of molecules in solution cause a solute, over a period of time, to disperse from areas of high concentration to a region of lower concentration until the solution is homogeneous. This process of diffusion can also occur between compartments separated by a biological membrane. In this case the close packing and hydrophobic nature of the hydrocarbon chains in the centre of the membrane adds a constraint on the types of molecules that can diffuse into the cell at any meaningful rate. Overton and Collander⁹³ found a number of compounds which show marked deviations from the general rule that the rate of movement depends on lipid solubility (Fig 1.9). Thus water, methanol, formamide and ethylene glycol enter cells more rapidly than would be expected from a consideration of their oil-water coefficients.

Passive diffusion across a biological membrane obeys Fick's first law in which the flux per unit area (J) of a molecule through the membrane depends only on the diffusion coefficient of the molecule (D) and its concentration gradient (dc/dx) across that region.

$$J = D \frac{dc}{dx} \quad \text{eq 1}$$

No term is included for the binding of the substrate to the membrane since discrete binding sites are not involved. Consequently, passive

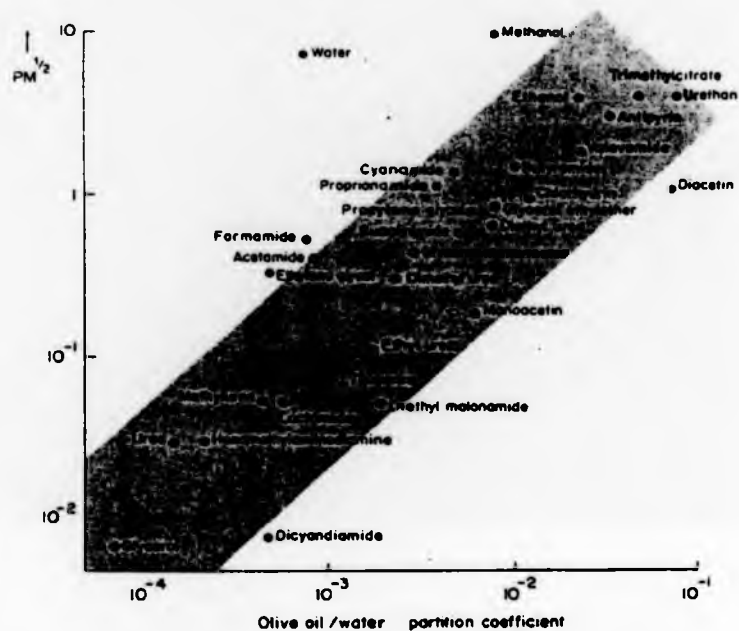


Fig 1.9

The correlation of diffusion with hydrophobicity. On the lattice model the rate of diffusion is predicted to be inversely proportional to the square root of the molecular weight for molecules smaller than the lattice dimensions. Thus, $PM^{1/2}$ is a constant. Data taken from the alga *C. ceratophylla* show however, that the value of this constant changes with the hydrophobicity of a molecule as measured by its oil:water partition coefficient. This suggests that a second factor determining the rate of diffusion is the lipid solubility of a molecule. It may also be seen that the molecules on the lower limit (like diacetin, monoacetin and malonamide) are all large molecules, whilst those with higher permeabilities than the average (like water, methanol, formamide and ethylene glycol) are all small molecules. A third factor influencing the rate of diffusion may therefore be the presence of pores of small diameter which span the bilayer. 93

diffusion does not saturate at high substrate concentration.

Table 1.3 gives the rates of passive diffusion of a few metabolites.⁵⁹ Data obtained from permeability measurements indicate that the penetration of biological membranes by molecules can be correlated with three major properties:⁷³ (1) Lipid solubility enhances penetration. For example, nonpolar compounds, which have a low solubility in water but a high solubility in fats or fat solvents, penetrate faster than polar compounds. (2) Molecular size is important. Large molecules do not enter as rapidly as do small molecules. (3) Permeation depends on the degree of ionization of the solute molecule. The stronger the charge on the permeant, the less rapidly the molecule will penetrate.

The presence of charges on ions, thus, adds another level of complexity to their transport across membranes. The difference in the permeability of electrolytes and non-electrolytes is mainly due to much lower partition coefficients of electrolytes. The monovalent alkali cations form a series in which the mass and charge on the atomic nucleus for unhydrated ions increase with increasing atomic number in the following order: $\text{Li}^+ < \text{Na}^+ < \text{K}^+ < \text{Rb}^+ < \text{Cs}^+$; hydrated ions form a series which increases in the reverse order: $\text{Cs}^+ < \text{Rb}^+ < \text{K}^+ < \text{Na}^+ < \text{Li}^+$. This difference may be attributed to the fact that water molecules which are close to the charged nucleus are bound more firmly and thus the hydration radius of the ion will be greater. Hence small atoms yield large hydrated ions (Fig 1.10). Absolute values of the hydrated radii of ions are difficult to estimate, but relative sizes are reflected in the observed values for ionic mobilities obtained when an electric field is applied to a solution. For instance, the mobilities of potassium, sodium and lithium at 25°C are 7.62, 5.19 and

TABLE 1.3 Diffusion coefficients for passage of ions and small molecules across lipid bilayers.

Ion or Molecule	Diffusion Coefficient ($\text{cm}^2 \text{sec}^{-1}$)
H_2O	5×10^{-3}
Indole	3×10^{-4}
Urea	3×10^{-6}
Glycerol	3×10^{-6}
Tryptophan	1×10^{-7}
Glucose	5×10^{-8}
Cl^-	7×10^{-10}
K^+	5×10^{-12}
Na^+	1×10^{-12}

Radii of ions
in crystal lattice

Hydration numbers
determined from diffusion

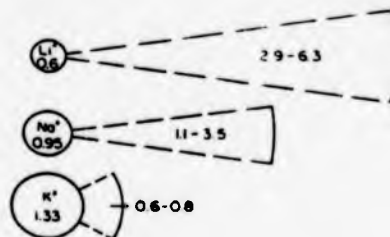
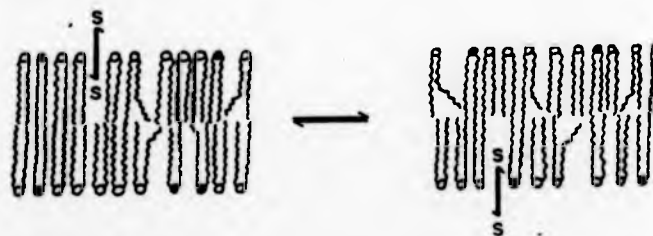


Fig 1.10

The relative size of some alkali cations. The radii of ions can be determined accurately from measurements of crystal lattices. The actual size of the hydration shells cannot be determined unambiguously or in absolute units. The numbers and the radii shown are therefore only relative.⁸³

(a) Lattice theory



(b) Membrane pores



Fig 1.11

Mechanisms of membrane diffusion. Biological membranes at 37°C are in a fluid state allowing small molecules to diffuse into, and out of, 'vacancies' in the outer leaflet of the bilayer (a). As they do so they move from an aqueous environment into the apolar interior of the membrane. If a 'vacancy' in the lattice of phospholipids in the inner leaflet becomes available the substrate can diffuse right across the membrane. Membrane pores (b) could be formed by a micellar rearrangement of the phospholipid bilayer or by proteins in the membrane. In both cases solutes pass into the cell without entering the hydrophobic core of the bilayer.⁹²

$4.01 \text{ m}^2 \text{ s}^{-1} \text{ V}^{-1}$, respectively: the smaller the non-hydrated ion the lower is the mobility.⁸³

Two theories describe the mechanism by which molecules can diffuse through biological membranes. For many non-electrolytes the lattice model adequately accounts for the rate of transport. In this model, diffusion occurs by the movement of the permeant molecule into a 'vacancy' in the lattice structure of the membrane (Fig. 1.11a). The principal energetic barrier to diffusion in this case is the activation energy required to move the substrate from the aqueous phase into the apolar environment of the phospholipid bilayer. This theory is in line with the permeability of the membrane of Chara ceratophylla⁹³ (Fig 1.9). The best correlation of permeability is in fact observed if it is expressed as a function of the number of hydrogen bonds that must be broken as molecules pass from aqueous solvent into the bilayer.

This still leaves the question of how the postulated 'vacancies' in the bilayer lattice arise. Most simply these are envisaged as temporary discontinuities created by the lateral movement of phospholipid molecules. This simple lattice theory cannot, however, account for the diffusion of all molecules through biological membranes. It may be seen in Fig 1.9 for example, that small molecules like water and methanol have a greater permeability than would be predicted on the basis of their partition coefficient or degree of hydrogen bonding. Furthermore, dissolved gases such as oxygen and carbon dioxide diffuse through biological membranes at a similar rate despite their large difference in size. Finally, since an electrolyte can only cross the membrane by losing its associated water, the activation energy for ion permeation is not high enough to include the energy which would be involved if dehydration were a prerequisite for ion movement through the membrane.

The inconsistencies between observation and hypothesis together with the realisation that the lipid bilayer is a highly fluid structure gave rise to the concept of the statistical pore (Fig 1.11b). The hydrophilic gaps or pores will arise spontaneously in a random fashion, and are transitory structures unlike the discrete protein-lined pores in a rigid bilayer that were proposed by earlier workers. But the existence of such pores has not been confirmed and furthermore not all small, lipid-insoluble substances penetrate the plasma membrane at equal rates - an observation that is difficult to rationalize with the presence of pores, which presumably could not display a great deal of selectivity. Many workers have concluded that if pores in fact exist, it is quite probable that only water normally penetrates the membranes through them. This conclusion would account for the extremely rapid penetration of water relative to that of most other substances.

Biological membranes are in general more permeable than synthetic phospholipid vesicles, showing that some of the ion-diffusion properties are a feature of the proteins in the membrane rather than on the phospholipids.

(b) Facilitated Diffusion

The carrier-assisted passive transfer of material is referred to as facilitated diffusion, a term preferred over the more ambiguous "mediated transport".⁷⁵ Facilitated diffusion systems can be identified by certain criteria:

1. The rate of transport of a substance down its gradient of electrochemical potential is more rapid than that predicted from its molecular size and lipid solubility.
2. Fick's law is not obeyed.
3. Competition occurs between structural analogues.

4. Denaturing of the carrier depresses the rate of transport.
5. Counter-transport in the opposite direction may take place simultaneously.

(1) PROTEIN CARRIERS

The precise nature of the carrier in biological membranes is not clear. However, a widely held view is that the ion carrier compounds are proteins and probably enzymes. Proteins have a number of properties which are suited to such a role in ion transport. They are invariably constituents of biological membranes; they are capable of combining reversibly with specific ions; and they are able to assume various configurations, thus altering their shape and position in the membrane from time to time.

Early models⁹⁴ of facilitated transport involved a shuttle of carriers between the two surfaces of the membrane (Fig 1.12a) or tumbling molecules which alternately revealed a substrate binding site at each surface (Fig 1.12b). Transport proteins are in general the largest proteins found in the membrane and contain hydrophilic regions which extend into the aqueous regions on both sides of the membrane. Thus, whilst both these models might aptly describe the kinetics of transport, they are unlikely to exist in vivo since the movement of large hydrophilic regions of proteins through the apolar core of the membrane is not thermodynamically feasible. Direct evidence against the models in Fig 1.12a and Fig 1.12b comes from measurements of the orientation of proteins in the membrane. Transport proteins like band 3 in the erythrocyte membrane, Ca^{2+} ATPase in sarcoplasmic reticulum, and the Na^+/K^+ ATPase (adenosine triphosphatase) are not found in random orientation as would be predicted by these models, but have all copies of the protein in the same direction.

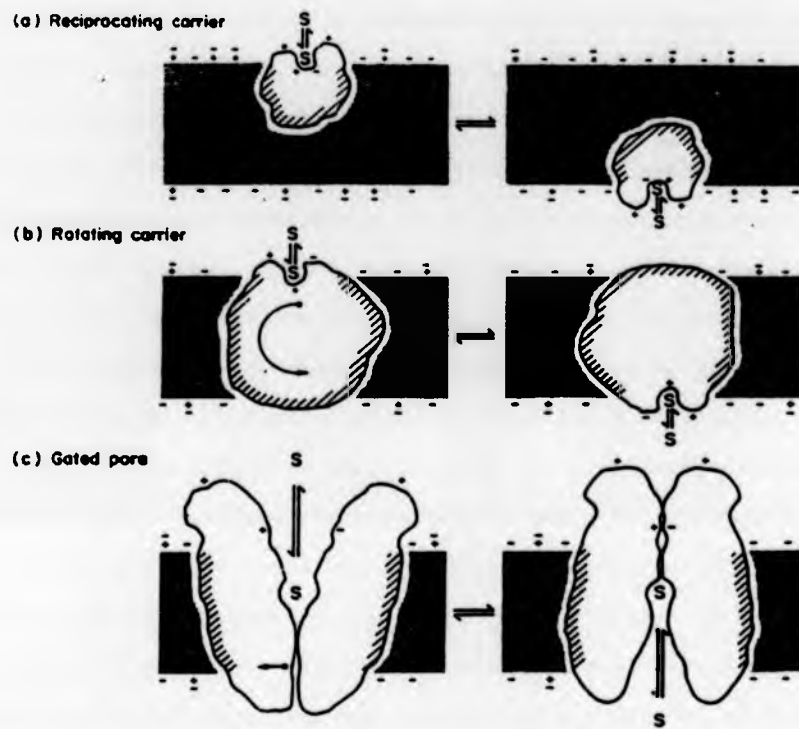


Fig 1.12

Models of membrane transport proteins. A polar substrate, S, cannot pass directly across the hydrophobic core of the membrane (shown in stipple) because of the high inactivation energy involved. The moving carrier models depicted in (a) and (b) account for the kinetics of facilitative diffusion, but are unlike the structures of known membrane transport proteins, and are energetically unlikely since they require hydrophilic regions (shown by + and - charges) of the protein to pass across the bilayer. All characterized transport proteins have a structure more akin to that shown in (c). In this model the protein does not move across the membrane but acts as a gated pore allowing substrate to pass across the membrane following a conformational change.⁵²

The current concept of a transport protein is shown in Fig 1.12c. This model proposes that the substrate passes through hydrophilic pores formed between the subunits of a multimeric membrane transport protein. Since the pore is not a fixed structure giving permanent access of substrate across the membranes, it is quite distinct from a membrane channel (vide infra), and has been described as a gated-pore. The model proposes that the transport protein can exist in two states which are interconvertible by a conformational change. One of the properties of a multimeric protein is that a relatively low input of energy can give rise to a large rearrangement of the subunits. It is quite conceivable, therefore, that the energy of substrate binding in the case of facilitative transport could be sufficient to achieve this.

An alternative gated-pore proposes that an 'arm' of the protein containing the substrate binding site moves across a narrow hydrophobic barrier in a fixed pore through the membrane. This is really a modification of the carrier theory except that the distance of 'carrier' movement has been reduced. In both cases the absolute asymmetry and thermodynamic stability of the membrane are maintained and kinetics identical to those of a moving carrier are generated.

Direct experimental tests of the gated-pore hypothesis are not easy. The best evidence comes from structural investigations of transport proteins. Glucose and glycerol are thought to be transported by facilitated diffusion. A number of recent reviews⁹⁵⁻⁹⁹ and papers 100-105 on the investigations of transport proteins are recommended for further reading.

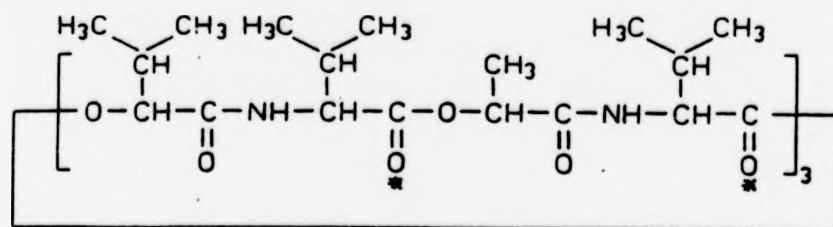
(11) NON-PROTEIN CARRIERS - IONOPHORES

The suitability and economy of using proteins as carriers does not preclude the use of other organic molecules, for we may easily imagine

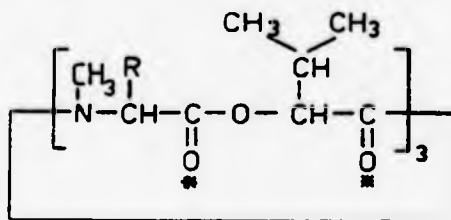
transport tasks for which proteins are not ideal. In recent years the study of ionophoric substances has provided a clue to the molecular basis of carrier transport of ions across membranes. An ionophore may be defined as a substance that enhances the movement or incorporation of an ion from the aqueous phase into the hydrophobic phase.¹⁰⁶ The ionophores were first recognised through their effect of stimulating energy-linked transport in mitochondria.¹⁰⁷⁻¹¹⁰ These ionophores are antibiotic molecules produced by bacteria and fungi and have been observed to increase greatly the permeability of artificial lipid bilayers and biological membranes to ions, in some cases in a selective manner.^{108,111-115} These substances are effective even when present at very low concentrations (10^{-8} - 10^{-3} mol m⁻³), and it has been speculated that molecules with similar properties may be carriers in biological membranes.

There appear to be two ways in which ionophores act. They either form a complex with the ions transported which diffuses through the lipid phase of the membrane in a facilitated manner,^{106,116,117} or they induce the formation of transient pores in the membrane through which ions enter.¹¹⁸ Ionophoric effects appear to be restricted largely to cations and protons although some anion selective molecules have been found.

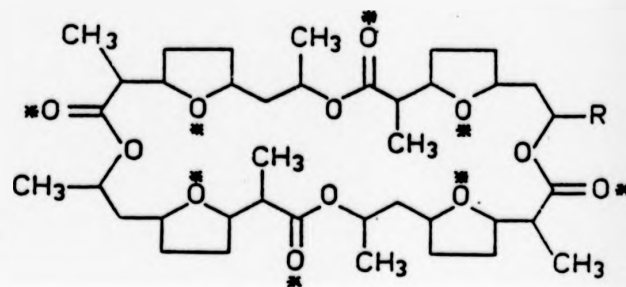
Fig. 1.13 shows the structures of some naturally occurring ion-carrying ionophores. The ion-carrying ionophores fall into two main classes: the valinomycin group and nigericin group. Members of the former are electrically neutral, mainly cyclic compounds and form a charged complex with alkali metal cations. The nigericin group compounds consist of a series of linked heterocyclic rings having a carboxyl group at one end and a hydroxyl group at the other (Fig 1.13).



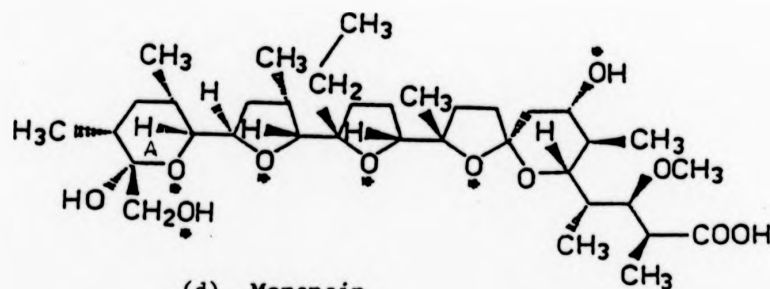
(a) Valinomycin



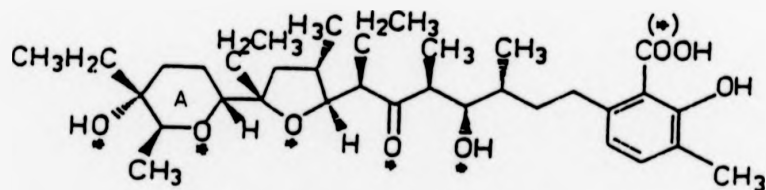
(b) Enniatin A, R = *sec* butyl
Enniatin B, R = *iso.* propyl
Beauvericin, R = $-\text{CH}_2\text{C}_6\text{H}_5$



(c) Nonactin



(d) Monensin



(e) Lasaloid (X-537A)

Fig 1.13 Structures of some naturally-occurring antibiotics: (a)-(c) of the valinomycin group (ie macrotetrolide antibiotics) and (d)-(e) of the nigericin group. The asterisks indicate the bonding oxygens.

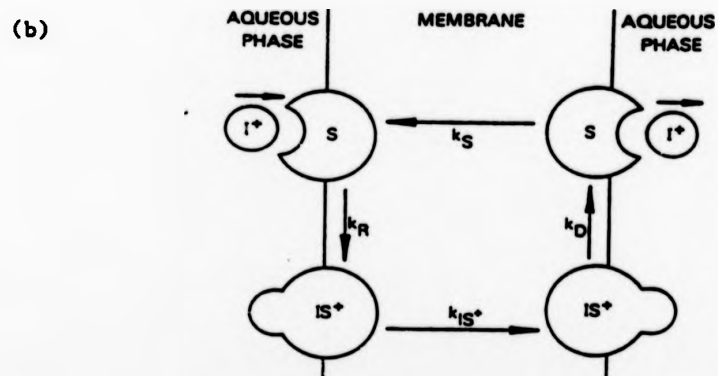
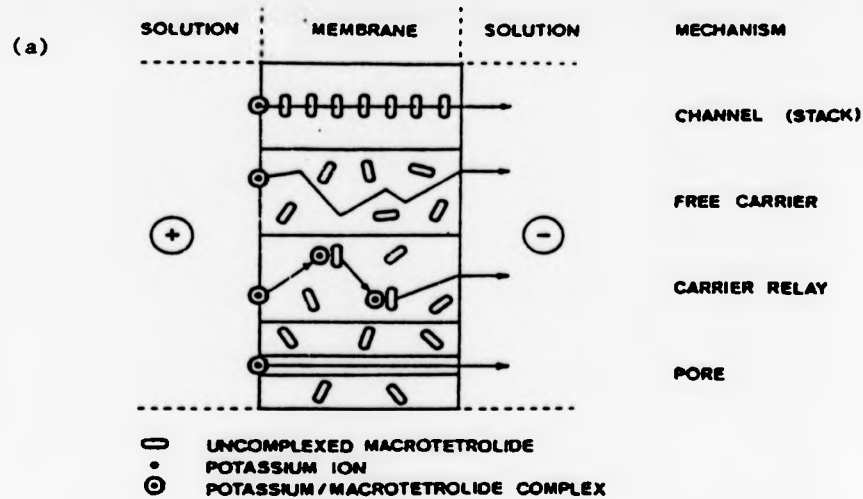


Fig 1.14

(a) Transport Mechanisms. 119

(b) Diagram of carrier-mediated ion translocation across a membrane. The rate constants k_R and k_D are the rates of ion (I^+)-carrier complex formation and dissociation respectively, and the constants k_{IS^+} and k_S represent the rates of transfer of the ion-carrier complex (IS^+) and the free carrier (S), respectively across the membrane. 120

The open-chain depiction is misleading since they all form rings via head-to-tail hydrogen bonding, i.e. hydrogen bonding between the carboxylate group and the hydroxyl group attached to the pyran ring A. Carriers of the nigericin class are electrically insensitive and only act to dissipate ion concentration gradients,¹² fulfilling the description of exchange diffusion carriers. The carboxylic acid grouping dissociates over the physiological pH range leading to the formation of electrically neutral complexes.

In spite of a large number of oxygen atoms, all of these compounds are extremely insoluble in water, and this must be due to the screening of the oxygens from the external environment which arises from the ring structures. The chemical groups situated on the outside of the ring are non-polar, accounting for the observed lipid-solubility of the molecule. On the inside of the ring the oxygen atoms provide a polar environment with sites for the electrostatic binding of cations. Thus an ion in this exchange site could cross the membrane surrounded by a hydrophobic layer.

Several different mechanisms have been suggested¹¹⁹ for the stimulating effect of ionophores on the alkali ion transport (Fig. 1.14a). Considerable evidence has, however, been cited for the currently accepted mechanism by which ion-carrying ionophores transport ions across biological membranes.¹²⁰ According to this model the ionophore at one membrane-solution interface envelops an ion so as to form an ionophore-ion complex with all polar or hydrophilic moieties of the carrier and ion "hidden" on the inside of the complex, so that the exterior of the ionophore-ion complex is lipophilic. This complex is free to traverse the membrane by random walk. At the other interface dissociation of the complex may occur and the ion may be released to the

aqueous phase. The free carrier in its "protected" lipophilic configuration diffuses back through the membrane to repeat the process. Thus each of these ion-carrying ionophores catalyses ion transport by a shuttle to and fro across the membrane. This is a relatively slow process and is limited by the rate of diffusion of the ionophore in the membrane. This model is illustrated in Figure 1.14b. The ion-carrying ability therefore depends on strong complexation in the lipid membrane phase with decreasing stability of the complex in more polar media. Support for this hypothesis is found in a recent complexation study by Linderbaum and coworkers.¹²¹

Since the neutral carrier substances form a positive complex, it is necessary to provide a lipid-soluble anion in order for the carrier to extract cations into organic solvents. Electroneutrality is maintained in both the aqueous and organic phases by extracting equivalent amounts of the positively charged lipid soluble complex and lipid soluble anion. Whereas the electrically insensitive carriers (ie nigericin class) are able to extract cations directly into lipid solvents without the additional requirement of a lipid soluble anion. Nigericins, unlike valinomycins, however, cannot move across the membrane without a bound cation.

Generally the carriers form 1:1 complexes¹²²⁻¹²⁵ with their respective alkali metal cation, but in a few cases 2:1 complexes¹²⁶⁻¹²⁹ and 3:2 complexes were also observed. Structural studies using X-ray, NMR, Raman, IR techniques¹¹⁵ etc showed that in the complexes, the cation is surrounded by ligand sites containing electronegative atoms. The selective complex formation and biological activity are closely related to their conformational structure. Fig. 1.15 shows the selectivity series among alkali cations for the various ion-carrier

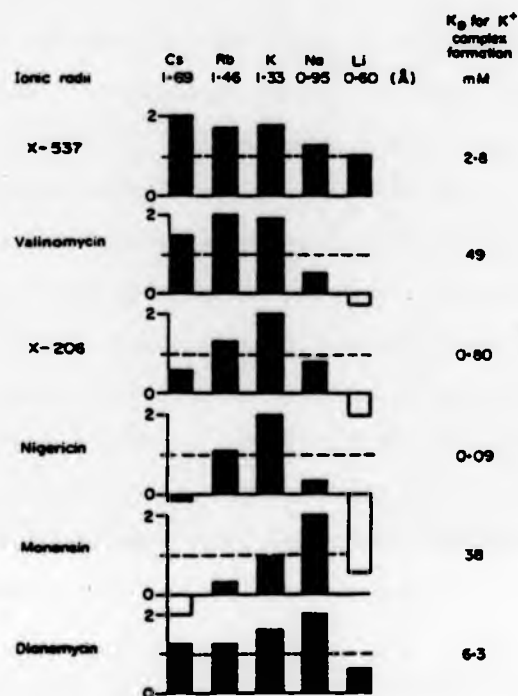


Fig 1.15

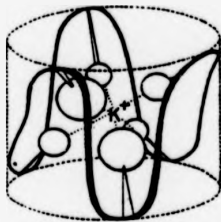
Ion selectivity pattern for valinomycin and various anionic (nigericin-like) ion carrier substances. The data were mainly derived from the ability of the ions to displace $^{86}\text{Rb}^+$ from complexes with the antibiotics in two phase extraction experiments. The relative affinities are plotted on a log scale, so that a difference of 1 indicates a 10-fold preference of the carrier substance of one ion over another. It can be seen that nigericin has a one hundred fold preference for K^+ over Na^+ and that monensin has a tenfold preference for Na^+ over K^+ .¹³⁰

substances. The 1:1 complexes show marked discrimination between closely-related ions. Valinomycin shows a 10000:1 preference for K^+ ions over Na^+ ions;^{108,110,130} (the diameter of K^+ being 0.27 and Na^+ 0.19 nm) which serves to emphasize the precision of fit on the ion into the critically orientated polar oxygen atoms in the cavity of the ionophore. With K^+ ion valinomycin has been found to coordinate with six oxygen atoms with an approximately octahedral distribution.¹¹³ K^+ ion coordinates with five oxygen atoms in nigericin (Fig 1.16). Monensin shows a high degree of specificity for Na^+ , while X537A and dianemycin are characterized by having a very broad range of cationic specificity. For ionophores with inflexible backbones the complexation energy is dependent on the ionic radius of the participating ions.^{110,130-132}

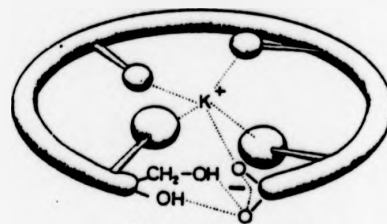
The properties of the 1:1 complexes of carrier antibiotics with monovalent cations studied may be summarized as follows:

1. The metal ion is coordinated to 5 to 8 oxygen atoms.
2. The external surface of the complexes is lipophilic, enhancing lipid solubility of these carrier complexes.
3. The alkali metal cation as such is not hydrated.
4. The alkali metal cation complexes of compounds of the valinomycin group are positively charged.
5. The alkali metal cation complexes of compounds of the nigericin group are electrically neutral.
6. The carrier molecules have sufficient flexibility to allow for a step-wise substitution of the solvent molecules resulting in a low activation barrier and fast complexation reaction rates.¹³³

The ion-selective properties of the naturally occurring ion-carriers are mimicked by the synthetic macrocyclic polyethers or "crown ethers"



Valinomycin-K⁺ complex:



Nigericin-K⁺ complex.

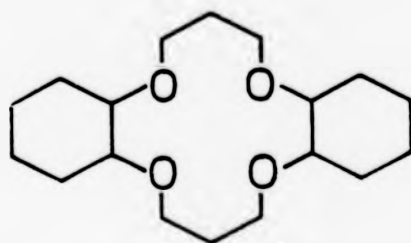
Fig 1.16

Schematic representation of ionophorecation crystalline complexes. (a) Valinomycin forms a complex in octahedral coordination with the potassium ion. (b) The potassium-nigericin complex shows no such symmetry. Hydrogen bonds hold the nigericin in a ring-like structure and the potassium is coordinated by the oxygen atoms projecting into the ring.⁶⁹

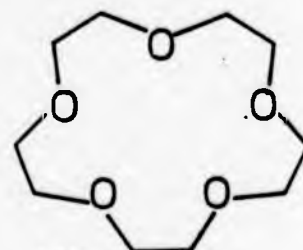
(Fig 1.17), first synthesized by Pedersen;¹³⁴ the macrobicyclic polyether diamines or "cryptands" (Fig 1.18), first synthesized by Lehn and coworkers;¹³⁵⁻¹³⁸ and the nonmacrocyclic synthetic ion-carriers (Fig 1.19), first synthesized by the group in Switzerland.^{139,140} These synthetic carriers also form stable 1:1 complexes with alkali and alkali earth cations^{137,141} and other metal cations.¹⁴²⁻¹⁴⁴ Some of them have been shown to display selective complexation and cation transport properties similar to those of the naturally occurring ligands.¹⁴⁵⁻¹⁵⁰

The selectivity of these synthetic ligands toward the metal cations is again primarily due to the geometry of the intramolecular cavity containing the cation. The order of selectivity is strongly dependent on the relative size of the cation and ligand cavity,^{136,145,151} e.g. the selectivity order of various crown ethers in methanol¹¹⁵ was found to change from $\text{Na}^+ > \text{K}^+$ for perhydrodibenzo[14]-crown-4, to $\text{K}^+ > \text{Na}^+$ for [18]-crown-6 and dibenzo[18]-crown-6 to $\text{K}^+ = \text{Cs}^+ \gg \text{Na}^+$ for dibenzo[21]-crown-7 to $\text{Cs}^+ > \text{K}^+$ for dibenzo[24]-crown-8. Cryptand ligands with their spheroidal cavities also show a strong size dependence in their selectivity. They form more stable complexes with metal cations than do the crown ethers.^{142,143}

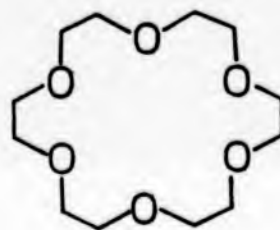
The stable complex formation and high selectivity for metal cations (especially alkali cations and alkali earth cations) displayed by synthetic ligands have aroused considerable interest in the field of cation transport across membranes. Kinetic studies between metal cations and macrocyclic ligands are of considerable interest, and are also relevant to many chemical and biological processes. Detailed kinetic results of some of the naturally-occurring¹¹⁵ and synthetic compounds¹⁵²⁻¹⁵⁴ have been reported and have increased the



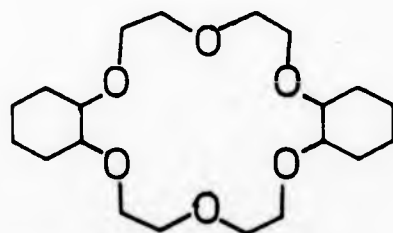
Dicyclohexano-[14]-Crown-4



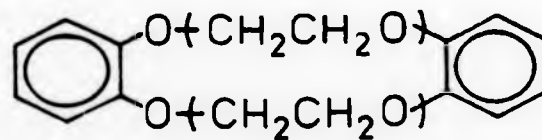
[15]-Crown-5



[18]-Crown-6

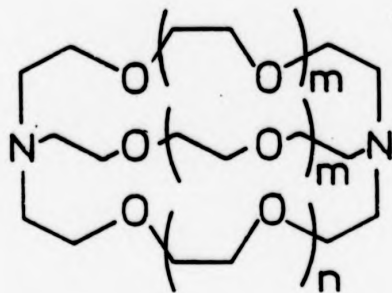


Dicyclohexano-[18]-Crown-6



Dibenzo-[18]-Crown-6, $n = 2$
 Dibenzo-[24]-Crown-8, $n = 3$
 Dibenzo-[30]-Crown-10, $n = 4$

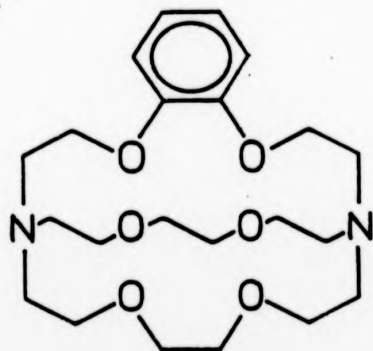
Fig 1.17 Structures of some Crown ethers.



$n=1$ $m=0$; (2,1,1) cryptand: 4,7,13,18-tetraoxa-1,10-diazabicyclo[8,5,5]-
eicosane

$n=0$ $m=1$; (2,2,1) cryptand: 4,7,13,16,21-pentaoxa-1,10-diazabicyclo-[8,8,5]-
tricosane

$n=m=1$; (2,2,2) cryptand: 4,7,13,16,21,24-hexaoxa-1,10-diazabicyclo-
[8,8,8]-hexacosane



(2,2,2) cryptand: 5,6-Benzo-
4,7,13,16,21,24-hexaoxa-1,10-
diazabicyclo-[8,8,8]-hexacosane

Fig 1.18 Structures of some cryptands.

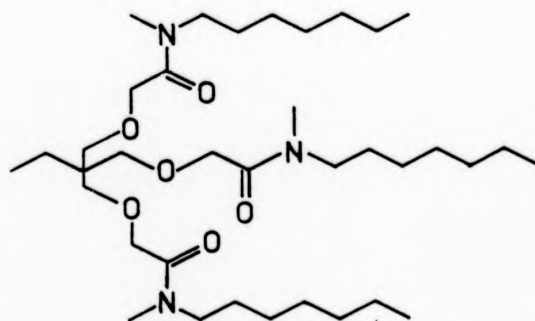
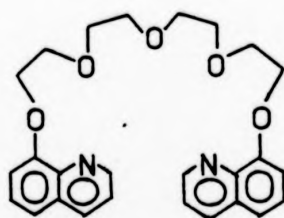
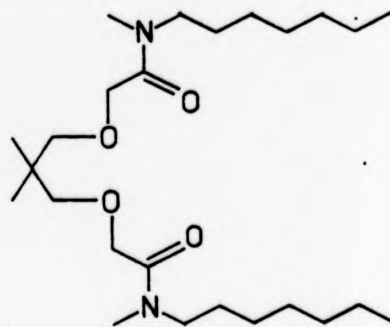
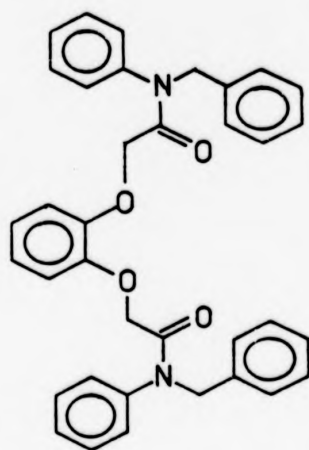


Fig 1.19 Structures of some non macrocyclic synthetic ion-carriers.

understanding of cation transport by the ligands. Preliminary investigations of cation transport properties of synthetic ligands have been recently reported.^{146,147,150}

Solvent effects on both the kinetics of complex formation and the stability of the complex have also been widely studied.¹⁵⁵⁻¹⁵⁷ The results show that the change of solvent dramatically alters the kinetic rate and the stability of metal complexation: eg on changing from water to methanol the complex stabilities are increased by a factor of about $10^2 - 10^5$.

Apart from the cited properties, naturally-occurring and synthetic compounds have been widely utilized in many fields of chemistry and biochemistry. The reader's attention is directed to a number of excellent reviews that treat various general aspects of synthetic and/or naturally-occurring ionophores,^{112,125,132,158-162} including the channel or pore formers (eg gramicidin A; amphotericin B; etc).

(c) Active Transport

Many of the transport processes that are essential to living cells are intimately linked to the cell's metabolism and are therefore referred to as active transport.^{163,164} Active transport is mediated by a specific transport protein, but, unlike facilitated diffusion, active transport operates against concentration gradient and requires energy. The distinguishing features of active transport are summarized in Table 1.4.⁹²

The energy required to transport one mole of substrate from compartment 1 to compartment 2 is given by the equation

$$\Delta G = -2.303 RT \log C_1/C_2 \quad \text{eq 2}$$

where ΔG is the free-energy change, R is the gas constant, T is the absolute temperature, C_1 and C_2 are the concentration in compartments

TABLE 1.4 Properties of transport processes⁹²

Diffusion	Facilitated diffusion	Active transport
Mediated by membrane lipid	Mediated by membrane proteins	Mediated by membrane proteins
Net flux ceases at electron chemical equilibrium	Net flux ceases at electrochemical equilibrium	Achieves transport against electrochemical gradient
No energy coupling	May be indirectly coupled to electrochemical energy	Directly coupled to energy supply
Low specificity	High specificity	High specificity
Non-saturating	Saturates at high substrate concentration	Saturates at high substrate concentration
No counter transport	Displays counter transport	Almost irreversible

1 and 2 respectively. If $C_1 > C_2$, then the log term is positive, ΔG is negative and transport is spontaneous from compartment 1 to compartment 2. If $C_1 < C_2$, then ΔG is positive, and energy must be supplied to "pump" the substrate "uphill" to the region of higher substrate concentration.

The pumping of ions, particularly K^+ and Na^+ into and out of cells against considerable concentration gradients is a feature of all plasma membranes. It is not at all apparent why most cells maintain high levels of K^+ and low level of Na^+ (Table 1.2), although it is clear that the maintenance of these ion concentrations has great physiological significance, since over one-third of the adenosine triphosphate (ATP) utilized by an average "resting" cell serves to maintain K^+ and Na^+ gradients. This massive expenditure of energy is necessary since in thermodynamic terms cells are open systems and so require a continual supply of energy for their survival. In contrast, isolated systems move to a state of maximum entropy or disorder as predicted by the second law of thermodynamics.

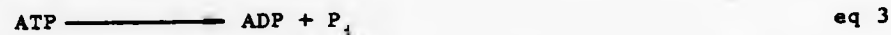
Active transport systems may be distinguished as primary and secondary. In the former, the energy required for transport is supplied directly by a chemical reaction involving the transport system. This energy comes from direct enzymatic splitting of covalent bonds, usually of ATP, or by coupling to certain redox reaction systems such as those occurring in the chloroplasts and mitochondria. In secondary transport, the uphill movement of one solute is coupled to and driven by the flow of a second solute down its gradient of electrochemical potential, this process being referred to a co-transport. In animals Na^+ is in most cases the driving ion. In bacteria and plants it is H^+ . The subject of secondary active transport has been thoroughly reviewed

recently.^{165,166}

In the following discussion an example of a primary active transport system will be examined, followed by examples of secondary active transport systems.

(Na^+/K^+) -ATPase though postulated earlier, was first described by Skou.¹⁶⁷ Although a lot of structural details are known for active transport proteins like $(\text{Na}^+ + \text{K}^+)$ -ATPase and (Ca^{2+}) -ATPase, little is known about their mechanism by which they catalyse transport. In the last year or two a degree of concensus has emerged and a model can now be discussed that satisfactorily incorporates a great deal of the detailed experimental information, though on many points an alternative interpretation is favoured by some workers.

$(\text{Na}^+ + \text{K}^+)$ -ATPase is related to the active transport of Na^+ and K^+ in red blood cells, nerves, brain membranes, electric tissues, and others. The overall reaction catalyzed by the ATPase involves the hydrolysis of the γ (terminal) phosphate of ATP to give adenosine diphosphate (ADP) and orthophosphate:



The reaction is exergonic with ΔG° values of approximately -7 kcal mol^{-1} .⁸³ Magnesium ions are always required for this activity, together with the synergistic effect of sodium and potassium. This hydrolysis in the inner surface of the membrane is coupled to the transport of 3 Na^+ ions from the inside toward the outside of the membrane and with the transport of 2 K^+ ions in the opposite direction.

The current view is that the $(\text{Na}^+ + \text{K}^+)$ -ATPase undergoes a series of conformational changes which bring about translocation of the ions. The changes in conformation are initiated by the phosphorylation-dephosphorylation process.¹⁶⁸⁻¹⁷⁰ In the

dephosphorylation conformation, sodium acceptor sites are available on the inner membrane surface. Binding of sodium to these sites permits ATP to phosphorylate the enzyme. This phosphorylation is known to occur at a glutamyl residue in the ATPase active site. The phosphorylation results in a change in conformation, such that potassium binding sites are exposed to the outer surface, and the bound Na^+ is carried to the outer surface also. The external facing Na^+ sites have a lower affinity, and thus Na^+ is lost to the exterior. Meanwhile, binding of K^+ stimulates dephosphorylation, and the enzyme reverts to its original conformation. The reversion carries K^+ to the inner membrane and lowers the affinity of the sites, thus releasing K^+ into the cell. Parallel with this the Na^+ sites regain their high affinity, Na^+ binds to the sites and the whole cycle of events is repeated. This transport process is illustrated in Fig 1.20.

In 1956, Cohen and Monad and their coworkers¹⁷¹ established that β -galactoside transport depends on a membrane protein. This protein was termed a permease and was shown to be controlled by the lac Y genes in the lactose operon of Escherichia coli.

The concepts embodied in the chemiosmotic hypothesis of oxidative phosphorylation proposed by Mitchell¹⁷²⁻¹⁷⁴ are generally applicable to all energy-coupled transport systems. Thus, the membrane's osmotic energy or proticity resulting from a transmembrane proton gradient can be applied to the carrier system. This potential energy of the membrane is termed by Mitchell the proton motive force and, in the chemiosmotic interpretation of the E. coli lactose transport system, it is this which is the driving force for lactose uptake.

Suppose that the lactose carrier, in addition to its binding site for lactose, has a further binding site for protons. The carrier then

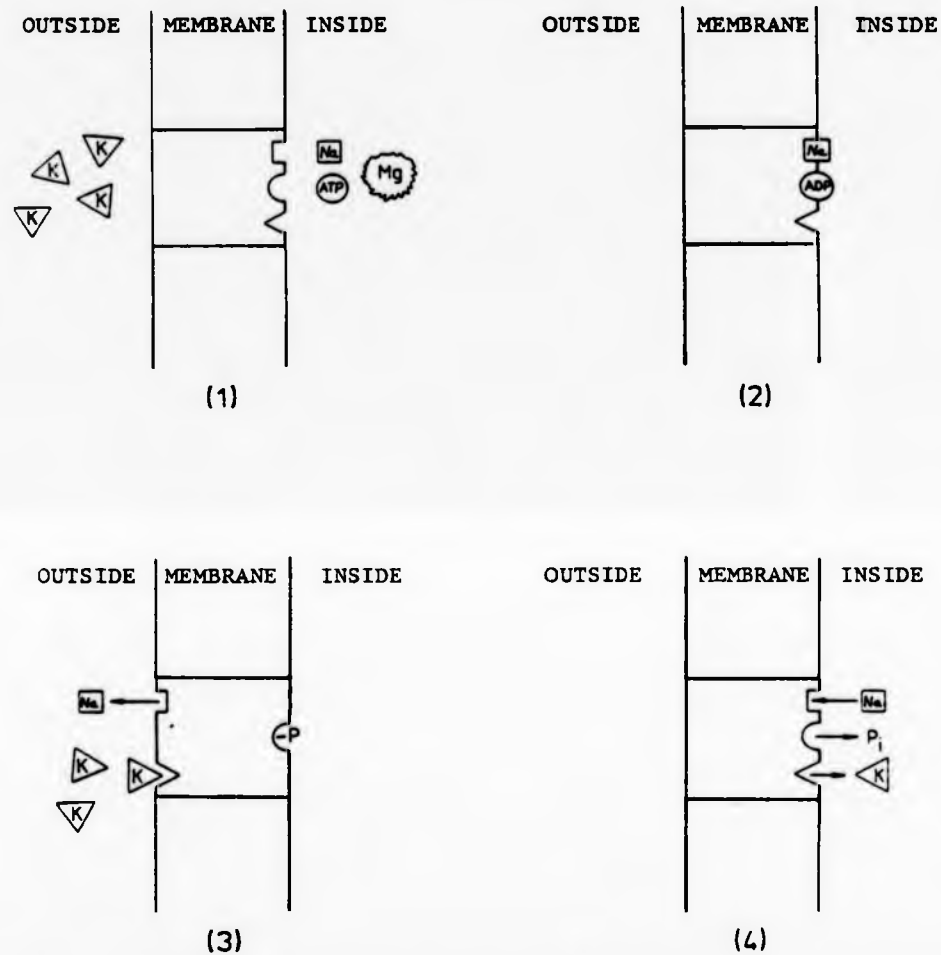


Fig 1.20 The $\text{Na}^+ \text{K}^+$ ATPase pump: In (1) Na^+ and ATP approach the inner face of the ATPase complex and bind to specific sites (2). In (3) phosphorylation of the ATPase results in a re-orientation of the binding sites for Na^+ and K^+ . In (4) dephosphorylation of the protein results in a reversion of the conformation to that of stage (1), and the whole process may then be repeated.⁶⁹

binds to lactose and to protons at the outer face of the membrane, and the movement of the protons down their concentration gradient. Thus proticity provides the energy for the active transport of lactose. In this system the permease is said to be acting as a proton symport. (Fig 1.21).

Supporting evidences for the proposed mechanism comes from work carried out with uncoupling agents, where levels of ATP and ATP dependent processes are not affected by uncoupling agents.¹⁷⁵ West and Mitchell^{176,177} found a stoichiometry of 1:1 for the proton:lactose ratio as predicted by the proton symport model of the permease. Furthermore, lactose uptake can be stimulated by inducing a pH gradient across the cells.^{177,178}

The transport of a number of amino acids and sugars has been observed to have a specific dependence on sodium ions, and it seems that this mode of transport may operate in an analogous manner to the proton symport model as discussed above.

There is as yet no clear idea of the molecular nature of the various symport systems. They are assumed to be membrane proteins with specific binding sites for both co-ion and the permeant. A diffusing carrier as depicted in figure 1.21 provides a schematic model for the symports but current thinking on transporters is more in favour of a relatively stationary protein with perhaps a series of binding sites spanning the membrane. As considered in the discussion of the $[Na^+ + K^+]$ -ATPase, it is possible that minor conformational changes in adjacent binding sites for permeant induced by Na^+ binding and by transfer along a series of Na^+ -dependent sites could result in a vectorial sequential binding of the permeant as depicted in figure 1.22.

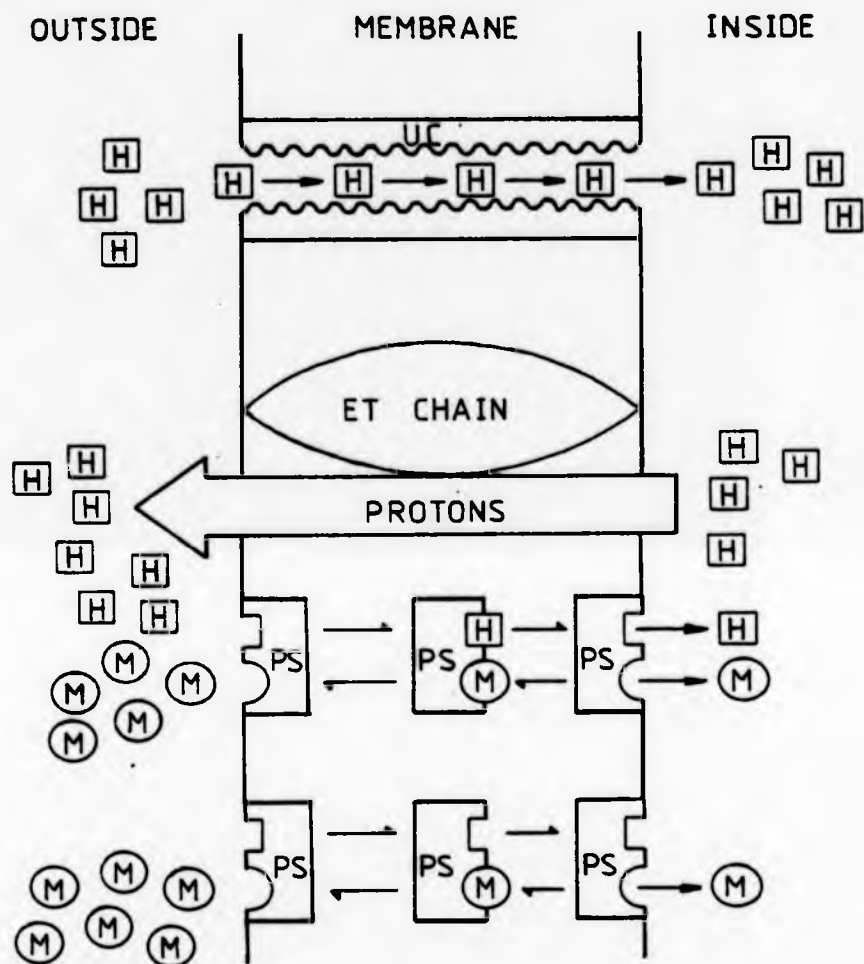


Fig 1.21

Active transport; the chemiosmotic model: The electron transport chain (ET chain) produces a transmembrane proton gradient. Proton symport (PS) combines with metabolite (M) and protons (H). Protons run down their concentration gradient and power the active uptake of M. Uncoupler (UC) short-circuits the proton return and diminishes the power source. Under these conditions PS can still function as a facilitated diffusion carrier as shown in the lower part of the diagram.⁶⁹

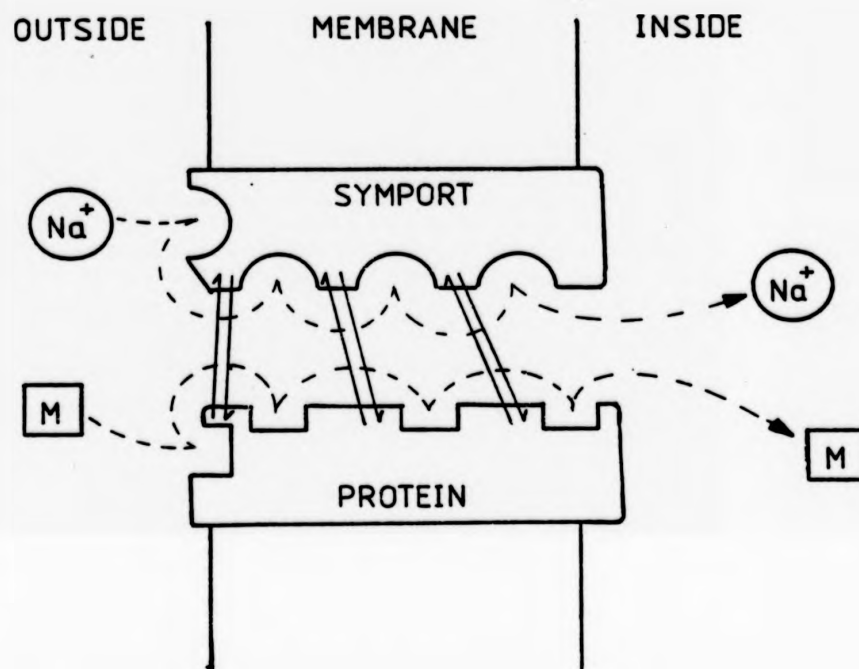


Fig 1.22

The sodium symport : binding of Na^+ to sites at the outside face of a channel formed by a trans-membrane protein induces a change in the affinity of a site for metabolite M. Sequential binding of Na^+ to sites along the protein induces changes in the metabolite binding sites such that a vectorial sequential binding occurs.⁶⁹

1.3 PARAMAGNETIC LANTHANIDE SHIFT REAGENTS IN NUCLEAR MAGNETIC RESONANCE SPECTROSCOPY

Traditional methods of analysis for cellular monovalent cations include atomic absorption (AA) spectroscopy, flame emission photometry, radioisotope tracer^{179,180} and cation selective microelectrode techniques.¹⁸¹⁻¹⁸³ The sensitivity of AA and radioisotopic methods is a distinct advantage. However, a serious drawback with these methods (except for that employing microelectrodes) is the necessity for the use of destructive methods to achieve physical separation of intracellular and extracellular compartments. Thus, these techniques can be both time consuming and often ineffectual because of two inherent problems: 1) the potential binding of cations to the outside cell surface and 2) cation fluxes occurring during the separation procedure. Hence, although these methods have provided a body of information concerning ion concentrations and fluxes, they are tedious. Ion selective microelectrodes can provide continuous, though not always rapid monitoring of intracellular ion activities and impalements by microelectrodes can be performed meaningfully only with reasonably large organelles.^{183,184} The impalement of the great bulk of the intracellular structures, such as the endoplasmic reticulum, Golgi apparatus, yolk platelets and a variety of other small membrane bound vesicles would be associated with appreciable membrane damage. Ion selective microelectrodes also only give a local ionic concentration not the total intracellular concentration.

Nuclear magnetic resonance (nmr), on the other hand, provides a noninvasive and non-destructive method for the study of intact cells and tissues.¹⁸⁶⁻¹⁹² The two cations present at highest concentration inside living cells, Na^+ and K^+ , are both observable by nmr spectroscopy through their isotopes ^{23}Na and ^{39}K .¹⁹³ There are,

however, some difficulties. Considerably more cellular material is necessary for the nmr analysis of Na^+ and K^+ than is necessary for analysis with ion-selective microelectrodes. Furthermore, a longstanding problem is that the intra- and extracellular ions in cell suspensions occur at the same frequency in the nmr spectrum¹⁹⁴ and also the chemical shifts of aqueous alkali metal cations are virtually anion independent. This lack of separation of spectral resonances has so far limited the applicability of the noninvasive nmr method in the study of the states of intracellular Na^+ and K^+ ions.

The recent development of aqueous shift reagents (SR) for cationic nmr¹⁹⁵⁻²⁰¹ has made it possible to resolve distinct signals from intracellular and extracellular compartments. The SR, negatively charged chelates of lanthanides, do not cross biological membranes readily, and when present in extracellular media, shift the extracellular cation nmr signal away from the intracellular signal without the requirement of physical separation. Since the method relies on the fact that the plasma membrane is impermeable to the shift reagent, the rates of transport of Na^+ or K^+ ions across membranes can now be estimated. This has already been reported with large unilamella vesicles²⁰²⁻²⁰⁴ and yeast cells²⁰⁴⁻²⁰⁵ using ²³Na nmr.

Knowledge of the relaxation times of biological nuclei can prove important in many investigations.²⁰⁶ For example, it is necessary to know those parameters for studies involving quantitation of metabolites and saturation transfer experiments. They may also provide information in their own right. The study of linewidths can indicate the environment of a metabolite of interest, for example, whether it is mobile and whether it is compartmentalized. Such information has been obtained by chemists from relatively simple systems in vitro, but in many

cases the interpretation has been controversial.²⁰⁷ Because of the complex nature of the intracellular environment it is likely that such controversy will extend to metabolic studies. However, it is in this very area of nmr application that the technique has unique advantages, since no other method has the potential for obtaining so much information non-invasively.

Thus, the nmr technique presents very real advantages. Different chemical forms of the nuclide under study can be identified and characterized functionally. Furthermore, the rates of exchange among the various forms of Na^+ or K^+ can be estimated.

The nuclei ^{23}Na and ^{39}K , constituting the naturally abundant isotopes of the respective elements, are characterized by a spin quantum number I of $3/2$. By far, most of the published data deal with ^{23}Na . Very few papers have presented studies of ^{39}K probably due to the fact that the relative sensitivity of ^{39}K at constant field is two orders of magnitude smaller than that for ^{23}Na . Thus, despite its relatively high concentration, intracellular K^+ presents a signal which is at least an order of magnitude smaller than that provided by intracellular Na^+ . The formidable technical problem of achieving a satisfactory signal-to-noise ratio can be largely resolved by the use of superconducting magnets providing fields three to four times greater than those routinely available. Both nuclides under discussion are however also subject to a nuclear quadrupolar interaction which, in aqueous solutions of biological preparations, is the major factor determining their spectroscopic properties.

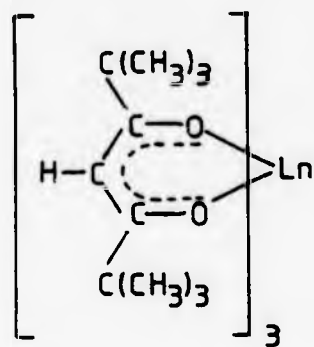
The large chemical shifts induced by lanthanide complexes in nmr spectroscopy have been known for sometime. Strictly, any reagent which induces chemical-shift changes in a dissolved substrate is a "shift

reagent". However, since the first reported use of a lanthanide shift reagent by Hinckley²⁰⁸ in 1969, interest in the field of shift reagents is overwhelmingly concerned with the lanthanide chelates, to the extent that the term "shift reagent" is widely used as an abbreviation for "lanthanide shift reagent".

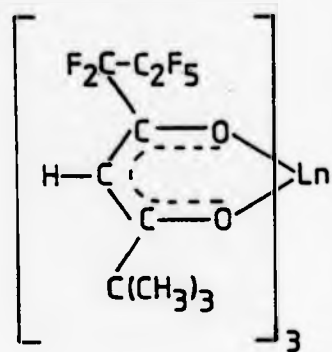
Lanthanide nmr shift reagents have become extremely valuable tools in a relatively short period of time. Several general reviews on shift reagents have been published.²⁰⁹⁻²²⁵ Some of the lanthanide tris- β -diketonates, eg the dipivaloyl methanates, $\text{Ln}(\text{dpm})_3$ (2)^{208,226,227} or the 1,11,2,2,3,3-heptafluoro-7,7-dimethyl-4,6-octanedionates, $\text{Ln}(\text{fod})_3$ (3)²²⁸ have been shown to produce substantial shifts (with little concomitant broadening) for protons removed as far as 20Å from the site of the coordination.

The lanthanides are the series of atoms between atomic numbers 58 and 71 in which the 4f electronic shell is progressively filled. Thus the tripositive ions provide us with a remarkable multitude of spectroscopic and magnetic properties. On the other hand the 4f electrons are effectively shielded by the outer 5s and 5p orbitals and as a result complex formation is largely due to electrostatic attraction accompanied by little covalency. The chemical properties of the lanthanides show only a gradual variation along the series, which results from the well known ionic radius contraction (Table 1.5). Although the lanthanides seem to be of little biological importance per se, their properties may render them as important probes for studying biological systems.

The main phenomena evident in the nmr spectra of paramagnetic complexes are chemical shifts, line broadenings and spin-decouplings. The purpose of this section is to summarize the principles governing



(2)



(3)

TABLE 1.5

The lanthanides and some properties of their trivalent ions²¹⁶

Atomic No	Name	Symbol	f shell of Ln ³⁺	Ground State	Ionic radius ^a [A]
57	Lanthanum	La	4f ⁰	1s ₀	1.061
58	Cerium	Ce	4f ¹	2F _{5/2}	1.034
59	Praseodymium	Pr	4f ²	3H ₄	1.013
60	Neodymium	Nd	4f ³	4I _{9/2}	0.995
61	Promethium	Pm	4f ⁴	has no stable isotopes	
62	Samarium	Sm	4f ⁵	6H _{5/2}	0.964
63	Europium	Eu	4f ⁶	7F ₈	0.950
64	Gadolinium	Gd	4f ⁷	8S _{7/2}	0.938
65	Terbium	Tb	4f ⁸	7F ₆	0.923
66	Dysprosium	Dy	4f ⁹	6H _{15/2}	0.908
67	Holmium	Ho	4f ¹⁰	5I ₈	0.894
68	Erbium	Er	4f ¹¹	4I _{15/2}	0.881
69	Thulium	Tm	4f ¹²	3H ₆	0.869
70	Ytterbium	Yb	4f ¹³	2F _{7/2}	0.858
71	Lutetium	Lu	4f ¹⁴	1s ₀	0.848

^a Reference (229)

^b The lowest excited state, 7F₁, is only 400 cm⁻¹ from the ground and therefore appreciably populated at room temperature.

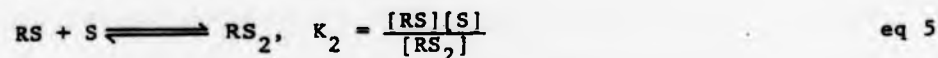
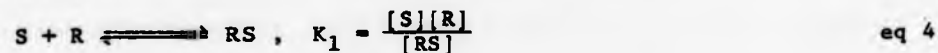
these phenomena and their reflection in the spectra of coordinated molecules as well as to present a comprehensive account of the hitherto accumulated information on the methodology and application of paramagnetic lanthanide complexes as shift reagents.

1.3.1 Induced Shifts and Complex Formation Equilibria

One of the first observations resulting from the presence of shift reagents is that the induced shifts increase with increasing the reagent to substrate ratio.²⁰⁸ This implies that conditions of fast exchange on the nmr time scale exist between the complexed substrate molecules, i.e. molecules in the first coordination sphere of the paramagnetic ion, and the free uncomplexed molecules. Regarding the induced shifts, the behaviour of such a system should be very similar to that in hydrogen-bonded systems²³⁰ or in weak charge transfer complexes,²³¹ which have been extensively studied. Thus, although not always realised, the approach of treating shift reagent data in terms of complex formation equilibria is also similar.

The interpretation of the observed shift depends upon several factors. Firstly, a knowledge of the stoichiometry and geometry of the interaction is required. Secondly, the position of the equilibrium between shift reagent and substrate must be known. Finally, one must be able to separate the contact and pseudocontact components of the observed shift (vide infra). The accurate study of the binding modes of substrates to lanthanide shift reagent is often not straightforward. Chemical exchange between free and complexed substrate is normally fast on the nmr time scale even at temperatures around -100°C . Early studies tended to support 1:1 adduct formation in most cases but it is now becoming evident that it is not uncommon for more than one binding

mode to occur. A two-step mechanism is now usually considered.



where R and S denote the shift reagent and substrate respectively and K_1 and K_2 are the two equilibrium constants involved.

Examples of procedures for characterizing stoichiometries and limiting shifts are to be found in papers by Reuben.^{211,222,232-235} Generally, both 1:1 and 1:2 complexes at least coexist in the solutions, the relative amounts being determined by the appropriate binding constants. Possibly the first really convincing evidence that 1:1 and 1:2 complexes exist together in shift reagent-substrate systems was presented by Shapiro and Johnston.²³⁵ Reuben²³² has discussed the effect that the simultaneous existence of such complexes would have on the shape of plots of observed shift versus the shift reagent-substrate ratio, and has made the point that the observation of linear plots does not allow any conclusion to be drawn with regard to the complex stoichiometry. These findings are of rather fundamental importance since if more than one complex is formed, or if a single 1:2 complex is formed, it becomes more difficult to extract chemical shifts appropriate to each complex and the validity of the application of the McConnell-Robertson equation²³⁶ to such complexes becomes suspect (vide infra).

1.3.2 Chemical Shifts in Paramagnetic Lanthanide Complexes

The mechanisms by which the unpaired spin(s) of the metal affect ligand resonances have been well reviewed,²⁰⁹⁻²²⁵ and will therefore be only briefly summarized here.

Paramagnetic ions exert their influence on nuclei in their vicinity via the so-called hyperfine interaction, which has two major pathways. The Fermi "contact" interaction takes place only if there is a finite probability of finding an unpaired electron spin on s orbital of the atom. For nuclei (protons in particular) in complexes of the lanthanide ions this interaction is likely to be very small except for those nuclei immediately adjacent to the lanthanide ion.²¹¹ Study of contact shifts therefore provides information about the nature of the metal-ligand bond, and often about the bonding within the ligand itself. The dipolar (pseudocontact) interaction or "through-space" interaction between the magnetic dipole due to the unpaired spin(s) and the nuclear magnetic dipole, which always results in enhanced nuclear relaxation (vide infra), will cause nuclear-resonance shift only when the magnetic susceptibility of the lanthanide ion is anisotropic. The trivalent lanthanides, except for Gd^{3+} , La^{3+} , and Lu^{3+} which are s-state ions (Table 1.5), have this property and therefore nuclei in their complexes experience large dipolar (pseudocontact) shifts. The pseudocontact term is also a function of the geometry of the complex and was first described in detail by McConnell and Robertson.²³⁷

The shift arising from these interactions may thus be expressed as a sum of the two terms: contact, $\Delta\delta_{i, \text{contact}}$, and pseudocontact,

$\Delta\delta_{i, \text{dipolar}}$, viz:

$$\Delta\delta_{i, \text{obs.}} = \Delta\delta_{i, \text{contact}} + \Delta\delta_{i, \text{dipolar}} \quad \text{eq 6}$$

$\Delta\delta_{i, \text{obs.}}$ is the shift of a given nucleus (ie i-th nucleus) in the complexed species relative to its diamagnetic (uncomplexed) position.

One quite serious objection with regard to the equation above, is the almost universal neglect of what might loosely be called the "diamagnetic term". Equation 6 should in fact be:

$$\Delta\delta_{i,\text{obs.}} = \Delta\delta_{i,\text{contact}} + \Delta\delta_{i,\text{dipolar}} + \Delta\delta_{i,\text{diamag.}} \quad \text{eq 7}$$

where $\Delta\delta_{i,\text{diamag.}}$ in practice encompasses all those factors which contribute to the shifts of the ligand nuclei other than those arising from the paramagnetism of the metal atom. The importance of this term has been stressed by Tori and Yoshimura.²³⁸ Nevertheless, since it is experimentally very simple to check that the $\Delta\delta_{i,\text{diamag.}}$ term is effectively zero in any given case, such a check should be carried out as a routine part of any shift reagent investigation.²³⁹

The magnitude and sign of the shift depends upon the situation of the nucleus with respect to the central ion and the magnetic axes (Fig 1.23). Hinckley²⁰⁸ believed that contributions to the observed shifts from the contact interaction would be negligible and the interest in the lanthanide shift reagents stems partly from this belief. If this is the case, the observed shift for complexes of axial symmetry treated in terms of the McConnell and Robertson equation for the dipolar term only is given by:

$$\Delta\delta_{i,\text{obs.}} = \Delta\delta_{i,\text{dipolar}} = \frac{K(3\cos^2\theta_i - 1)}{r_i^3} \quad \text{eq 8}$$

where θ_i is the angle between the principal magnetic axis and the vector of length r_i joining the i -th nucleus to the paramagnetic centre and K is a constant for the particular complex. The observed shift is therefore a function of the geometrical term $(3\cos^2\theta_i - 1)/r_i^3$ and thus the pseudocontact term is independent of the nucleus but is strongly dependent on its geometrical position with respect to the central ion and the principal axis of symmetry. There is the r_i^{-3} dependence predicting that the shift decreases rapidly with distance. The angular dependence predicts that within the same molecule there may

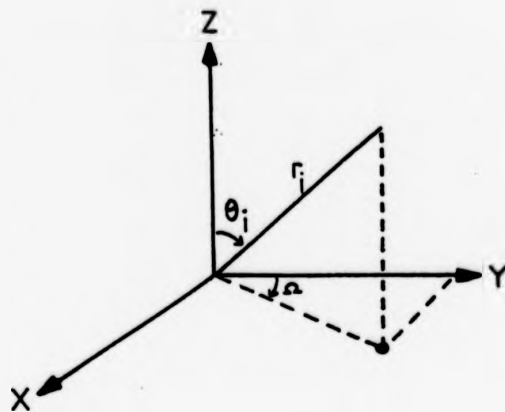


Fig 1.23 The coordinate system of the g-tensor and the position of a nucleus in it.

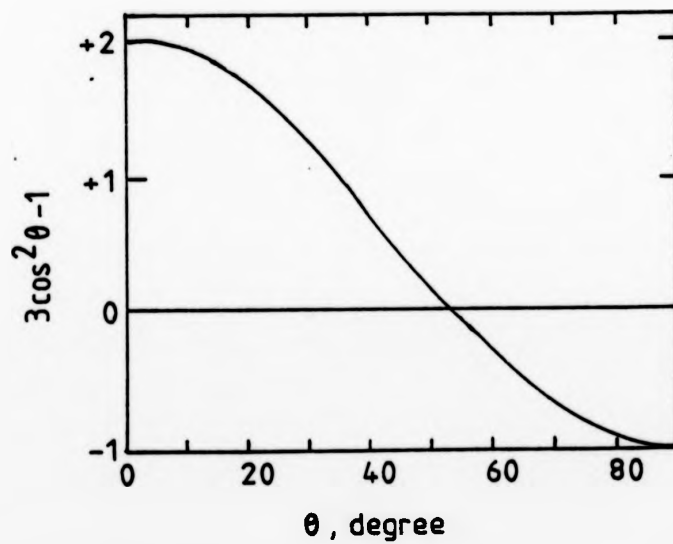


Fig 1.24 The angular function $(3\cos^2\theta - 1)$ plotted versus θ .²¹¹

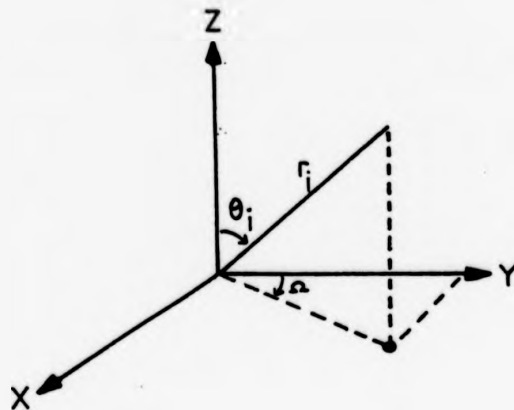


Fig 1.23 The coordinate system of the g-tensor and the position of a nucleus in it.

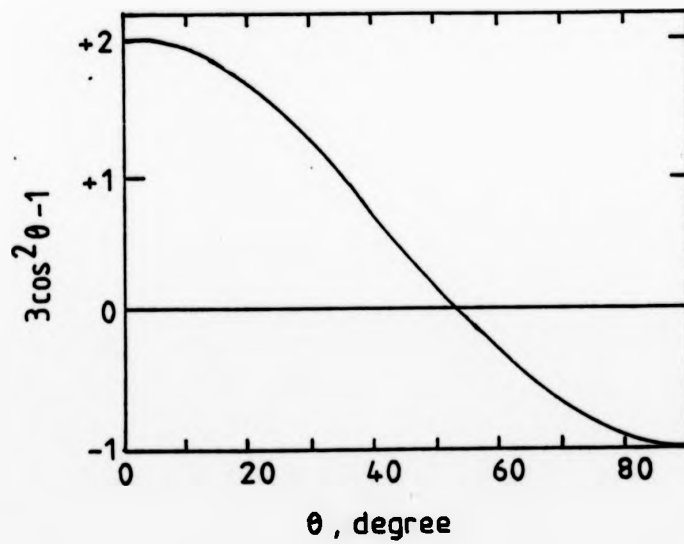


Fig 1.24 The angular function $(3\cos^2\theta - 1)$ plotted versus θ .²¹¹

be shifts of different signs since $(3 \cos^2 \theta_1 - 1)$ changes sign at $\theta_1 = 54^\circ 44'$. This function is plotted in Fig 1.24²¹¹. Positive values obtain for $0^\circ < \theta_1 < 54.7^\circ$ and for $125.3^\circ < \theta_1 < 180^\circ$, negative values arise for $54.7^\circ < \theta_1 < 125.3^\circ$.¹

Reuben²⁴⁰ has in fact reported calculations which suggest that, for the lanthanide reagents, the contact term is likely to become progressively more important along the series Yb < Tm < Dy < Er < Ho < Nd < Eu. Several authors have in fact stressed the usefulness of Yb^{III} shift reagents which, based on the experimental criteria discussed above, produce quite large shifts which do seem to be wholly dipolar in origin.²⁴⁰

Recent work by Golding and his group, however, shows that one cannot readily split such shifts into contact and pseudocontact terms.^{241,242} Slight residual covalent bonding (eg 1-2% covalent interaction) or interaction at distances 10\AA could lead to very different results from those predicted by the simple pseudocontact theory.

However, The frequently successful use of the McConnell-Robertson equation²³⁷ in shift reagent studies, despite the many, seemingly arbitrary, assumptions involved, has puzzled a number of workers in this field. For example, the assumption that the principal molecular axis is coincident with the principal magnetic susceptibility axis, and that both lie along the shift reagent-substrate bond direction, seems quite untenable on the basis of the crystallographic studies reviewed earlier.²⁴³ It has been proposed that the substrate may be incorporated into the complex in a number of different ways; rapid exchange between these systems would then give rise to an apparent complex with effectively axial symmetry.^{244,245}

The temperature dependence of lanthanide induced shifts (LIS) has

been discussed by three groups.²⁴⁶⁻²⁴⁸ Cheng and Gutowsky²⁴⁶ have presented an excellent and balanced summary of the relationships and differences between the theoretical treatments of LIS presented earlier this decade or so (see Ref. 249 and cited work therein). These authors have tackled the difficult task of separating the observed temperature dependence of the LIS into equilibrium and intrinsic components, using the system $\text{Pr}(\text{fod})_3$ -dimethylacetamide-tetrachloroethane. The intrinsic temperature dependence is then compared with the various theoretical predictions for the LIS. In the temperature range studied, the intrinsic LIS contributions could be fitted by either a T^{-1} or a T^{-2} dependence.

1.3.3 Nuclear Relaxation in Lanthanide Complexes

A requirement of major importance is that the shifts induced by shift reagent be much larger than the accompanying line broadening. The lanthanides form six-coordinate metal complexes which may behave as Lewis acids, so that basic substrates become weakly bound as labile ligands; for such "outer sphere" ligands exchange is again rapid on the nmr timescale.

For paramagnetic systems, short electron relaxation times tend to favour fairly narrow nmr linewidths, which would otherwise be broadened due to the large fluctuating magnetic fields associated with paramagnetic species in thermal motion.²⁵⁰ Of the paramagnetic trivalent lanthanides, Gd^{3+} is a s-state ion with isotropic g-tensor and no pseudocontact shifts are expected in its complexes. In addition, its electron spin relaxation time is relatively long, giving rise to enhanced nuclear relaxation and extensive broadening of nmr lines. In Sm^{3+} and Eu^{3+} the J states are closely spaced and there are substantial

been discussed by three groups.²⁴⁶⁻²⁴⁸ Cheng and Gutowsky²⁴⁶ have presented an excellent and balanced summary of the relationships and differences between the theoretical treatments of LIS presented earlier this decade or so (see Ref. 249 and cited work therein). These authors have tackled the difficult task of separating the observed temperature dependence of the LIS into equilibrium and intrinsic components, using the system $\text{Pr}(\text{fod})_3$ -dimethylacetamide-tetrachloroethane. The intrinsic temperature dependence is then compared with the various theoretical predictions for the LIS. In the temperature range studied, the intrinsic LIS contributions could be fitted by either a T^{-1} or a T^{-2} dependence.

1.3.3 Nuclear Relaxation in Lanthanide Complexes

A requirement of major importance is that the shifts induced by shift reagent be much larger than the accompanying line broadening. The lanthanides form six-coordinate metal complexes which may behave as Lewis acids, so that basic substrates become weakly bound as labile ligands; for such "outer sphere" ligands exchange is again rapid on the nmr timescale.

For paramagnetic systems, short electron relaxation times tend to favour fairly narrow nmr linewidths, which would otherwise be broadened due to the large fluctuating magnetic fields associated with paramagnetic species in thermal motion.²⁵⁰ Of the paramagnetic trivalent lanthanides, Gd^{3+} is a s-state ion with isotropic g-tensor and no pseudocontact shifts are expected in its complexes. In addition, its electron spin relaxation time is relatively long, giving rise to enhanced nuclear relaxation and extensive broadening of nmr lines. In Sm^{3+} and Eu^{3+} the J states are closely spaced and there are substantial

contributions from excited states. Usually Sm^{3+} gives very small shifts while trivalent europium (Eu^{3+}) owing to its diamagnetic 7F_0 ground state has its first excited 7F_1 state significantly populated at room temperature (ca 36 per cent) to give rise to substantial magnetic susceptibility.²⁵¹ As a result, chemical shifts of nuclei in molecules coordinated to europium are expected. The cations Pr^{3+} , Nd^{2+} , Tb^{3+} , Dy^{3+} , Ho^{3+} , Er^{3+} , Tm^{3+} and Yb^{3+} have relatively short electron spin relaxation times—shorter than molecular reorientation times - and should, therefore, produce only minimal broadening of the nmr spectral lines. Complexes of Eu^{III} and Pr^{III} are of especial interest in that the electronic relaxation times are generally sufficiently short that very narrow nmr lines are observed, the fine structure frequently persisting to quite high relative concentrations of shift reagent to substrate.

In addition to the effects described above, line-broadening may be caused by the inhomogeneity of the magnetic field at the sample. It is thus, important in all experiments to provide a homogeneous field over the sample volume. The convenient way of reducing residual inhomogeneity is to spin the sample and 'even out' the perceived field.

1.4 CONCLUSION

Accordingly, this study was undertaken with three principal objectives.

1. To develop a shift reagent for ${}^{39}\text{K}$ nmr and to investigate further the shift reagents, $\text{Ln}(\text{PPP}_1)_2$, introduced by Gupta and Gupta.¹⁹⁷
2. To employ the shift reagents developed for direct observation of resolved resonances and measurement of intracellular Na^+ or K^+

ion concentrations by ^{23}Na or ^{39}K nmr respectively, in studies of cellular systems.

3. To study the mechanism/s of metal cation transport by ionophores across prepared large unilamellar vesicles using nmr techniques:
Use of paramagnetic lanthanide shift reagent to resolve the $^{23}\text{Na}^+$ nmr peaks.

CHAPTER 2

Discussion

CHAPTER 22.1 SHIFT REAGENTS FOR ²³Na AND ³⁹K NMR2.1.1 Introduction

Aqueous shift reagents for Na^+ and K^+ consist of a paramagnetic lanthanide ion (Ln^{3+}) and a polyvalent ligand which complexes strongly with the Ln^{3+} and weakly with the Na^+ and K^+ ions. Springer et al.²⁰³ have shown that a useful feature of the 'strong' interaction is that the complex derived from the lanthanide and ligand should have large numbers of negatively charged oxygen atoms on its surface to which the alkali metal ions are attracted, thus bringing them close to the paramagnetic lanthanide ion.

It seems probable from the description of the mode of operation of the shift reagents that they operate largely via the so called pseudocontact (or through space dipolar) mechanism rather than by a contact (or through bond) mechanism. The theory of pseudocontact shifts shows that the magnitude and direction of the observed shifts depends heavily on the distance apart of the two magnetic centres and the geometry of the instantaneous complex.²⁵²

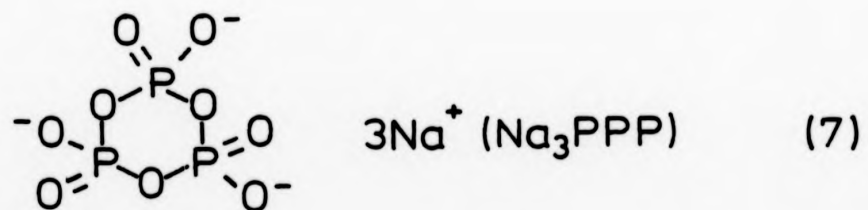
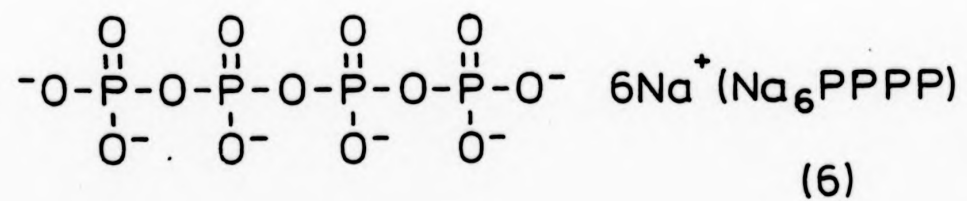
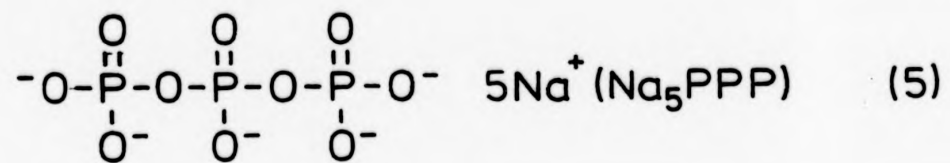
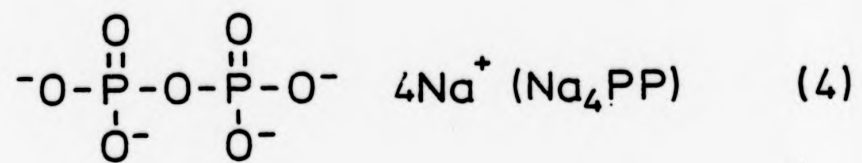
Moreover, the "pseudocontact theory" does not predict the absolute direction of hyperfine shift for a given Ln^{3+} complex. There are geometric factors relating to the structure of the adducts and has no means of knowing what the stoichiometries or geometries of the complexes are. There is no current method for predicting which shift reagents for sodium or potassium would be superior to others. Thus, the only resort available was to determine this experimentally.

2.1.2 Discussion of Results

The shifts of sodium ions in various polyvalent ligands (4-7) on addition of the lanthanide, Dysprosium chloride (DyCl_3) have been investigated. As expected, no shift phenomenon was observed on using the monophosphate, sodium hydrogen phosphate. The results for the diphosphate (hydrated tetrasodium pyrophosphate), tripolyphosphate (pentasodium tripolyphosphate) and tetrapolyphosphate (hydrated hexasodium tetrapolyphosphate) are presented in Figs 2.1-2.6.

The shape of the titration curve is independent of the concentration of the polyvalent ligand (4-7) used: the maximum shift obtained varies slightly with different concentrations of the ligand. With hydrated tetrasodium pyrophosphate ($\text{Na}_4\text{P}_2\text{O}_7 \cdot 10\text{H}_2\text{O}$) (Fig 2.1) and pentasodium tripolyphosphate ($\text{P}_3\text{O}_{10}^{5-}$ ie Na_5PPP) (Fig 2.2-2.5), the curves are initially linear with slopes varying inversely with the ligand concentration and directly with Dy^{3+} concentration, and the relative concentrations needed to obtain the maximum shift are identical. In these cases titration was stopped when the curve had gone through a maximum and the first signs of a precipitate appeared in the tube. With hydrated tetrasodium pyrophosphate (Fig 2.1) the maximum in the graph appears at about a 1:2.5 ratio, suggesting that this complex is $\text{Dy}^{3+} (\text{PP}^{4-})_{2.5}$.

In the four cases with Na_5PPP (Figs 2.2-2.5), line broadening is slight at first but becomes more important at molar ratios $[\text{Dy}^{3+}]/[\text{PPP}^{5-}] > 0.4$. Such behaviour is indicative of complex equilibria involving at least two different stoichiometries for the interaction between Dy^{3+} and PPP^{5-} . In the initial stages with a low molar $[\text{Dy}^{3+}]/[\text{PPP}^{5-}]$ ratio, only one species appears to be involved, and since the maximum in the graph appears at just below a 1:2 ratio it



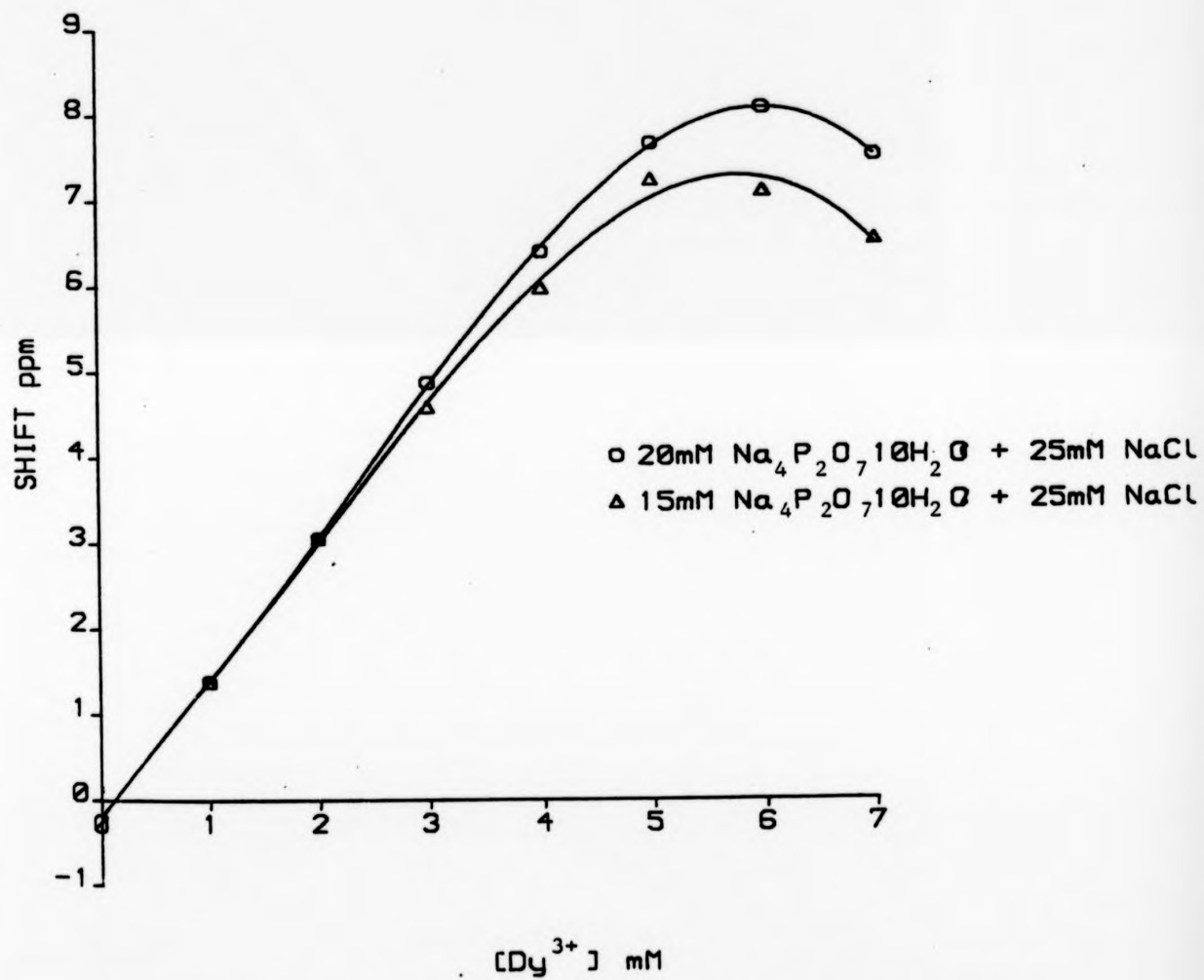


FIGURE 2.1 ^{23}Na shifts (21.19MHz) observed on titration of hydrated tetrasodium pyrophosphate with Dysprosium chloride.

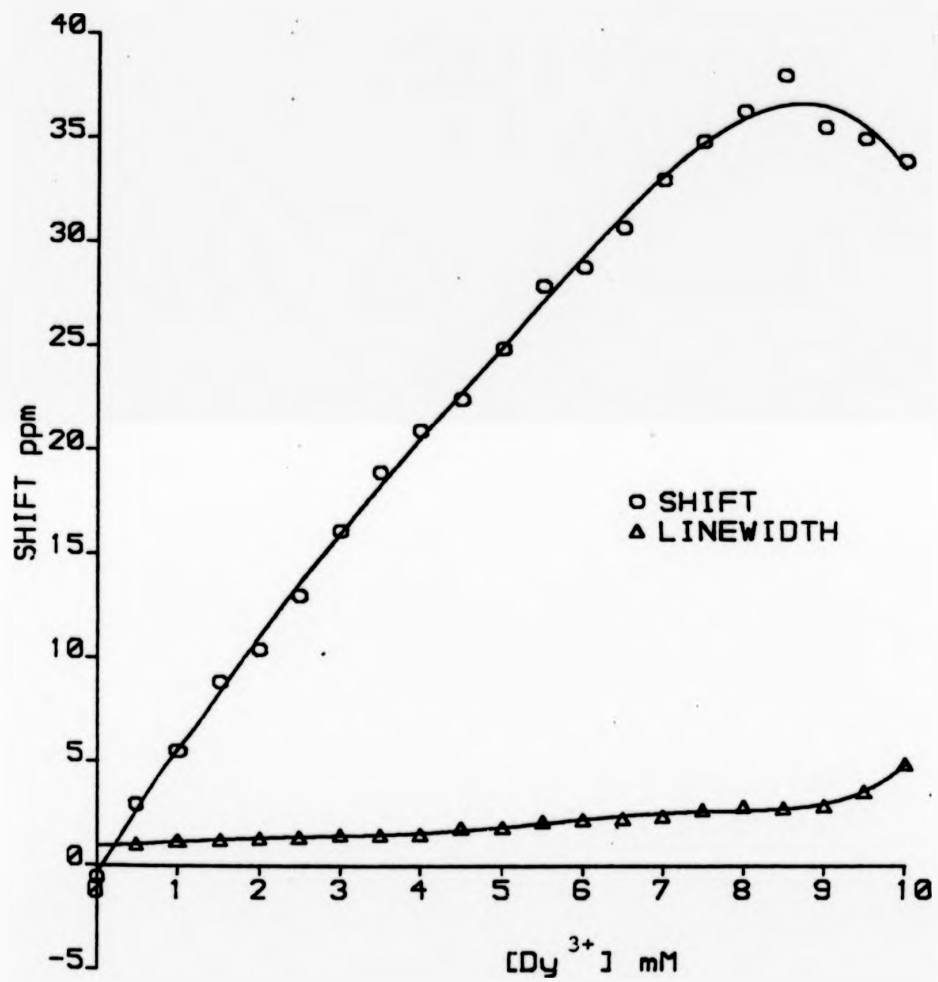


FIGURE 2.2 ²³Na shifts (21.19MHz) observed on titration of 20mM Na₅PPP with Dysprosium chloride.

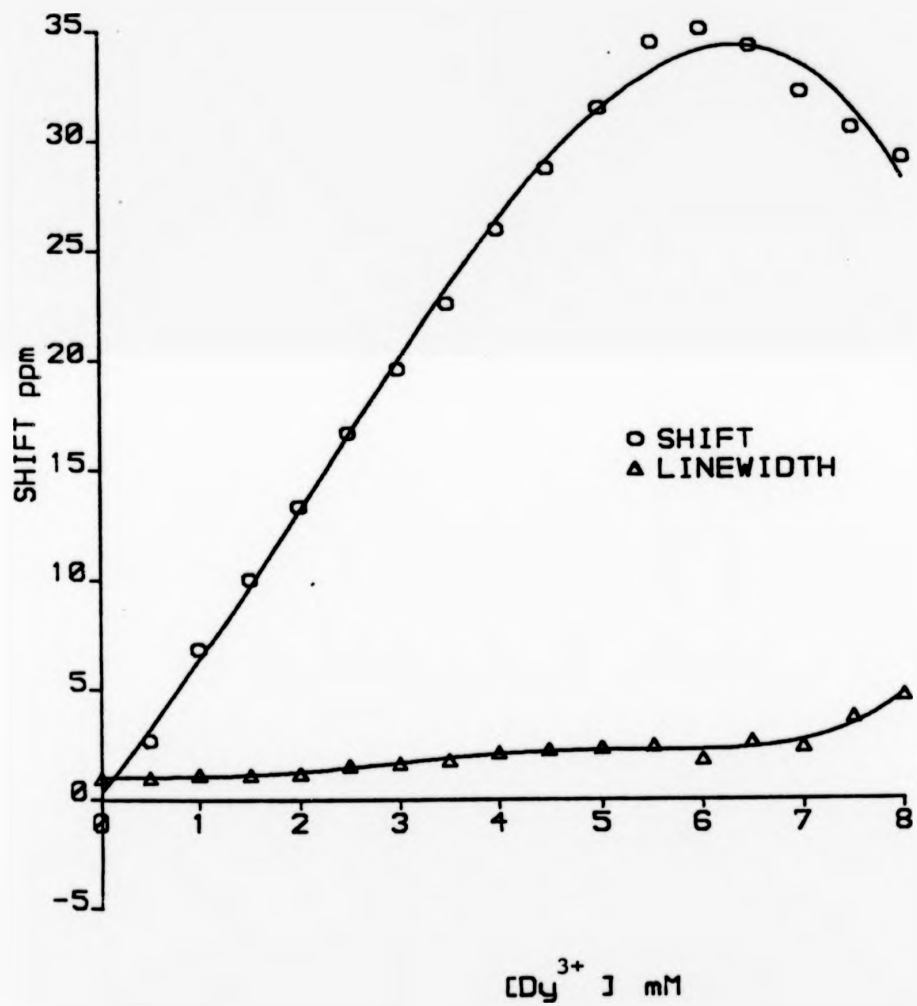


FIGURE 2.3 ²³Na shifts (21.19MHz) observed on titration of 15mM Na₅PPP with Dysprosium chloride.

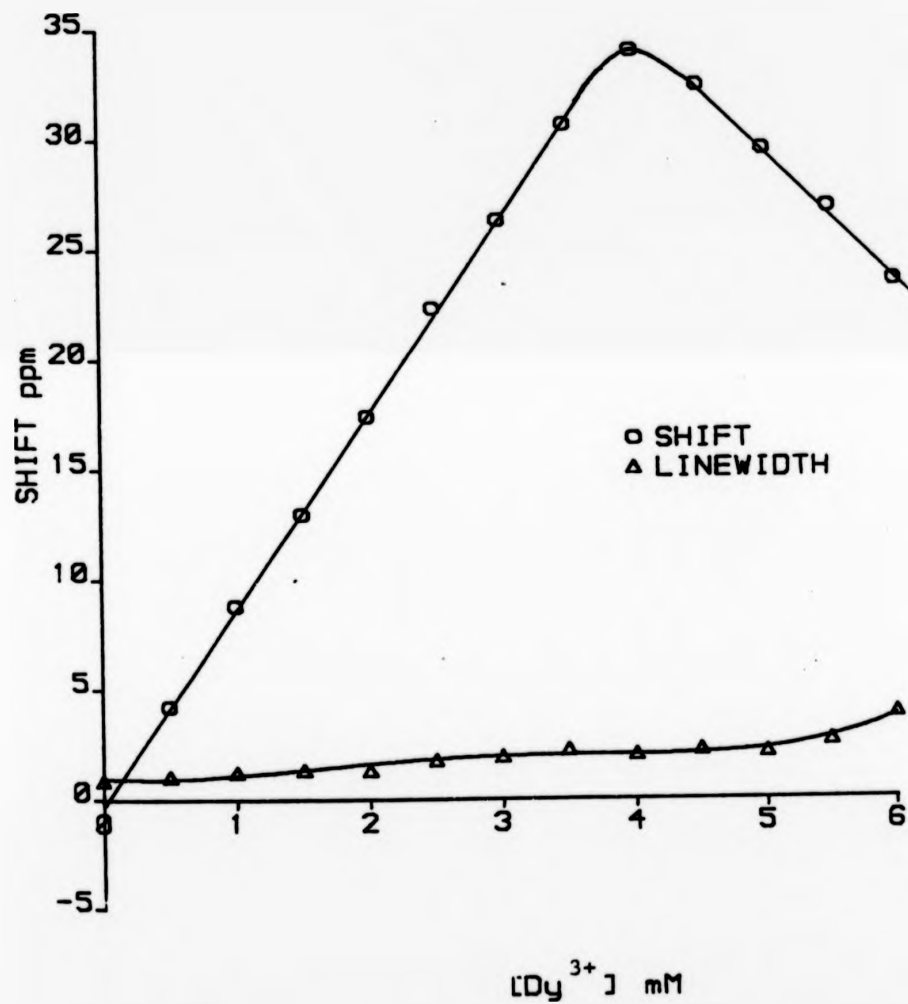


FIGURE 2.4 ²³Na shifts (21.19MHz) observed on titration of 10mM Na₅PPP with Dysprosium chloride.

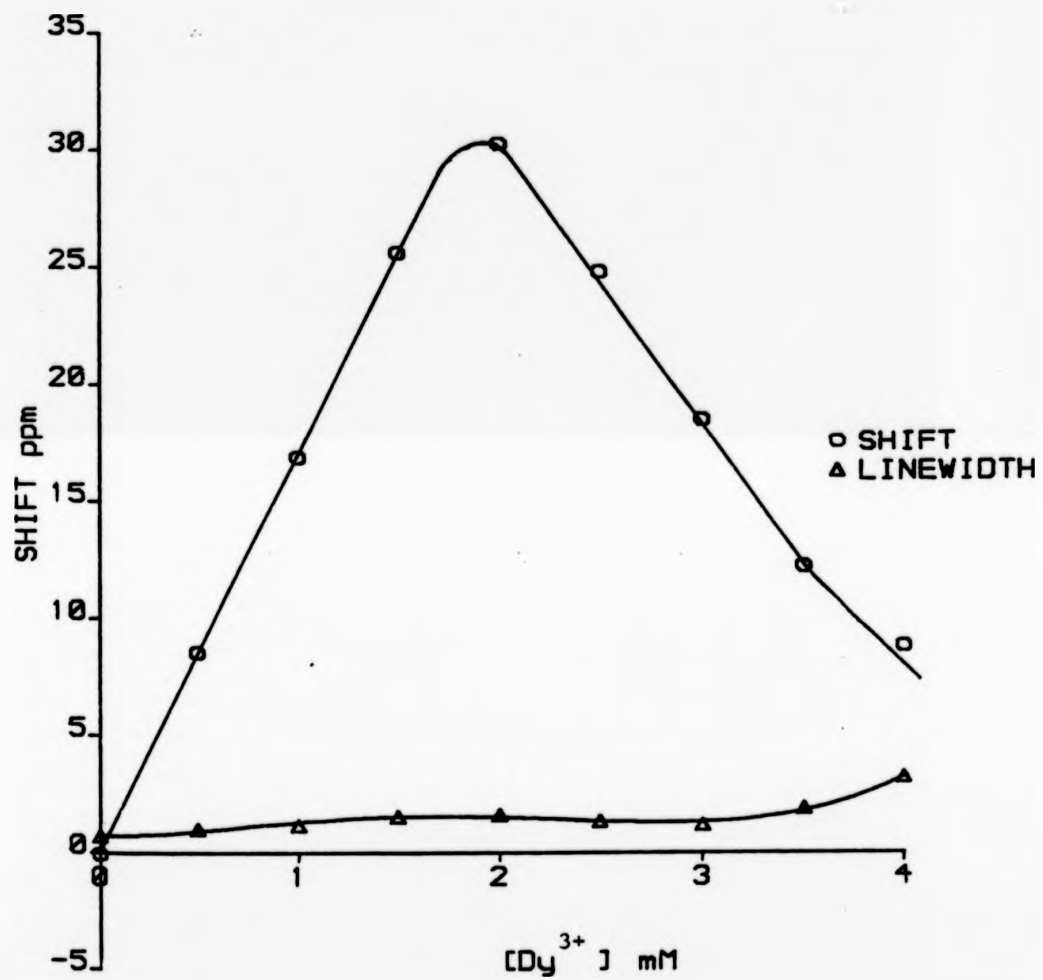
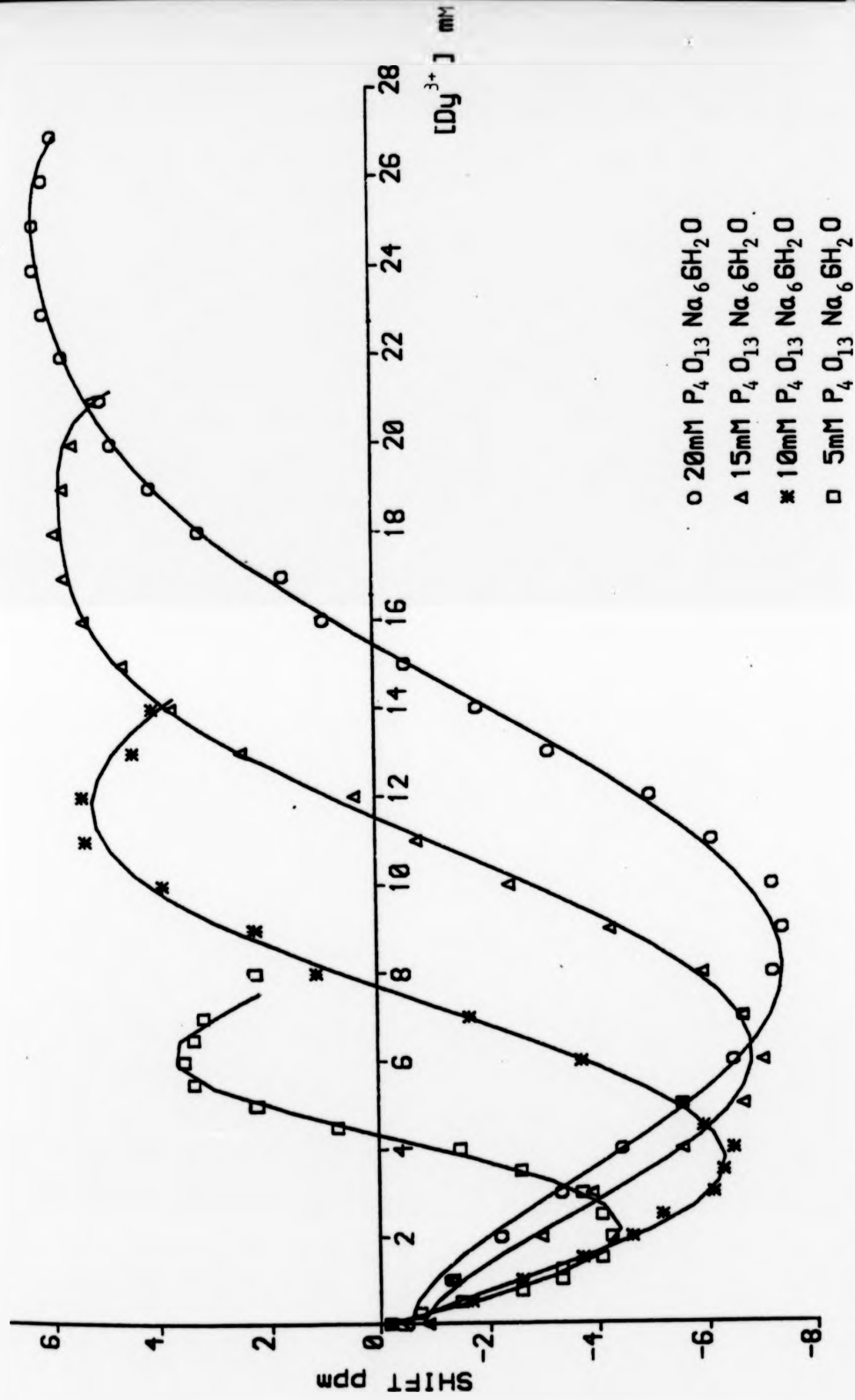


FIGURE 2.5 ^{23}Na shifts (21.19MHz) observed on titration of 5mM Na_5PPP with Dysprosium chloride.



23
 FIGURE 2.6 Na shifts (21.19MHz) observed on titration of hexasodium tetrapolyphosphate with Dysprosium chloride.

suggests that this complex is $[\text{Dy}^{3+}(\text{PPP}^{5-})_2]^{7-}$ as was suggested by Gupta and Gupta.¹⁹⁷ The fact that the shifts go through a maximum when $[\text{PPP}^{5-}]/[\text{Dy}^{3+}]$ is greater than 2.0 indicates that the reaction,

$$\text{Dy}^{3+} + \text{Dy}(\text{PPP})_2^{7-} \rightleftharpoons 2 \text{Dy}(\text{PPP})_2^{2-}$$

is reasonably probable and increasing $[\text{Dy}^{3+}]$ moves the equilibria to the right.

No attempt was made to control the pH during the titrations. However, the pH values were measured for all samples. In all four cases, the initial pH was ca 9.5 and decreased as a sigmoid curve to a final value of ca 7.7. The maximum shift observed corresponds to the point just before the pH curve begins to fall sharply (Fig 2.7).

Fig 2.8 illustrates the effect of doubling the concentration of sodium. The observed shift halves when the $[\text{Na}^+]$ doubles, ie shift is inversely proportional to the concentration of sodium ions present.

$$\text{shift} \sim \frac{1}{[\text{Na}^+]}$$

On substituting the 50mM NaCl used above with 50mM KCl solution, the observed shifts indicate that K^+ binds slightly better to the shift reagent $[\text{Dy}(\text{PPP})_2^{7-}]$ than Na^+ (Fig 2.9). In Table 2.1 are listed binding constant values for relevant metals under study. Sodium and potassium are noted to have a similar binding constant for $(\text{PPP})^{5-}$.

With the polyvalent ligand, hydrated hexasodium tetrapolyphosphate ($\text{P}_4\text{O}_{13}\text{Na}_6\text{H}_2\text{O}$) ie Na_6PPPP (Fig 2.6), the shift reagent was observed to be bidirectional. Each of the curves plotted for different concentrations of Na_6PPPP follows the same stoichiometric relationship as all the others. Slopes, intercepts, maxima and minima are all in the identical ratios for the relative amounts of reagent. Quite clearly,

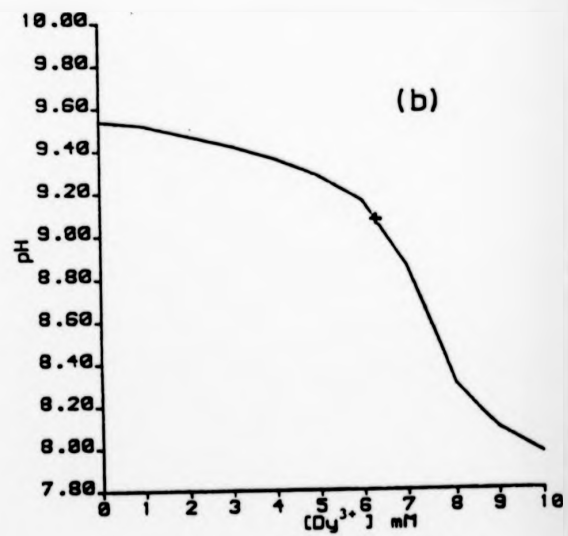
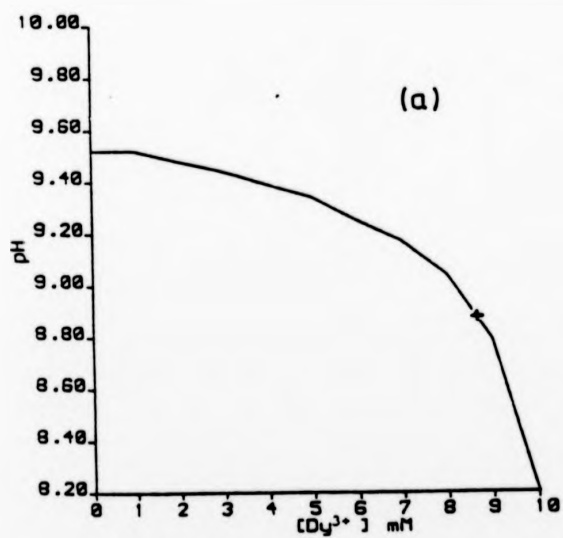
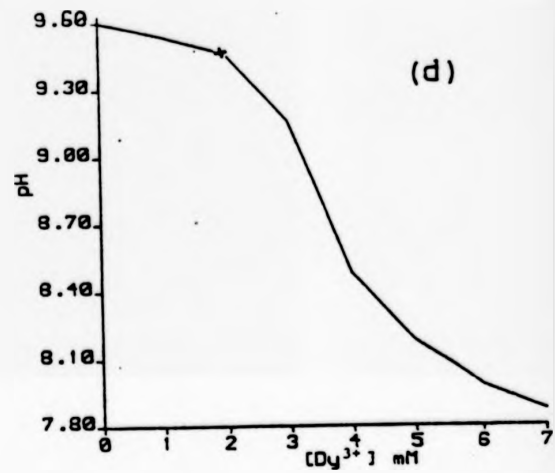
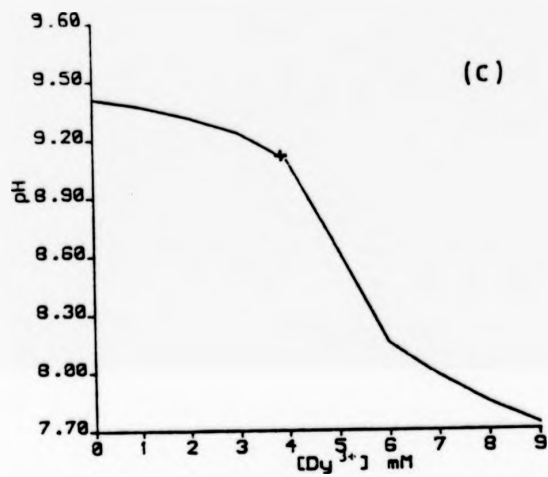


FIGURE 2.7 Change in pH of Na₃PPP solutions, (a) 20mM, (b) 15mM, (c) 10mM and (d) 5mM, on titration with DyCl₃. T=298K
* - pH of maximum shift

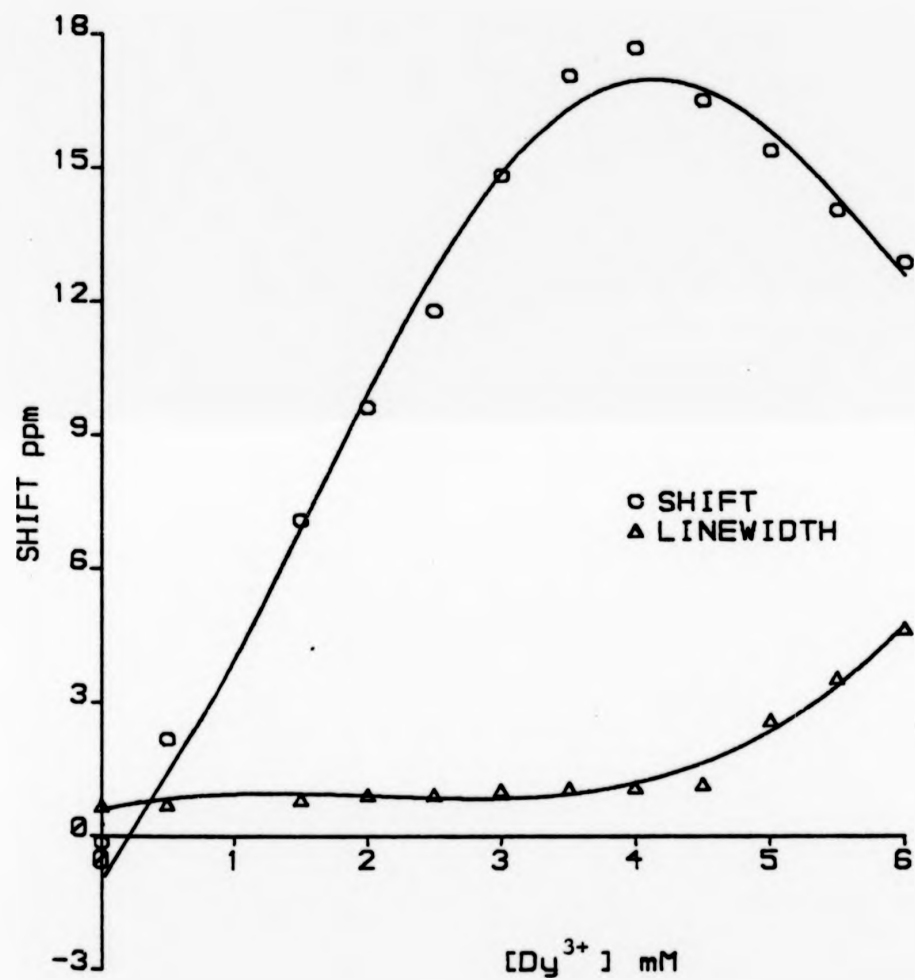


FIGURE 2.8 ²³Na shifts (21.19MHz) observed on titration of 10mM Na₅PPP + 50mM NaCl with Dysprosium chloride.

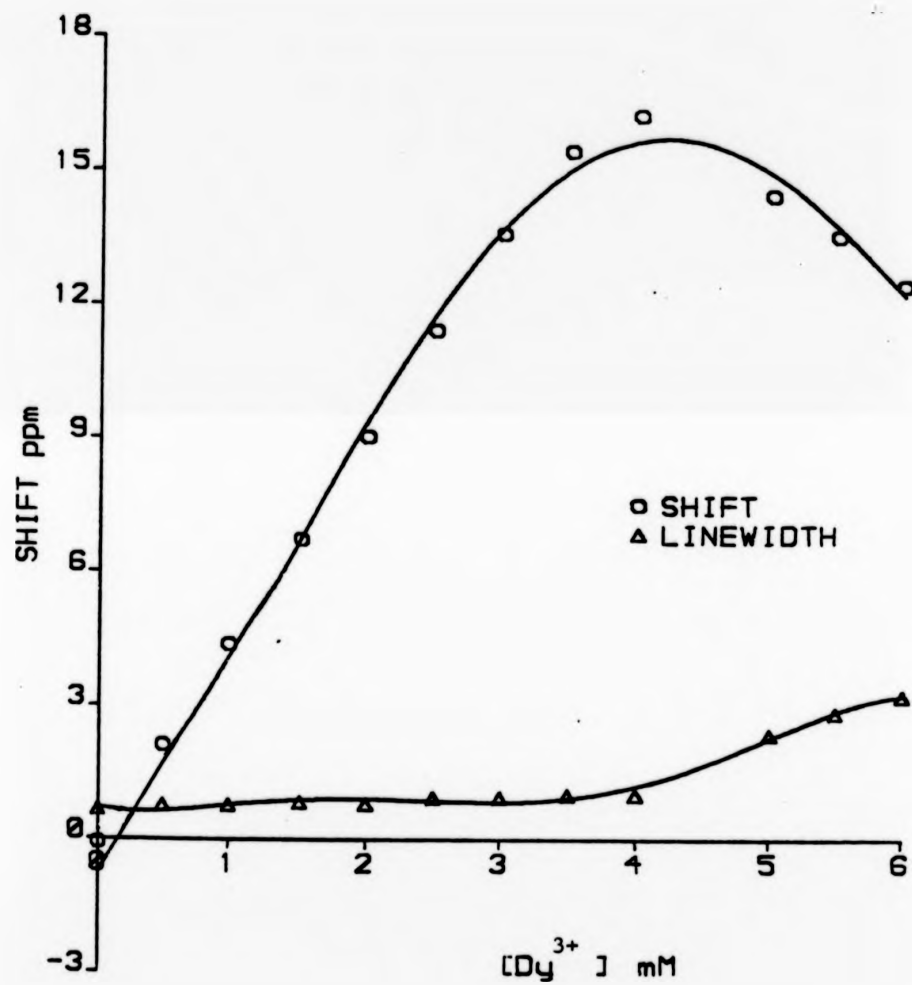


FIGURE 2.9 ²³Na shifts (21.19MHz) observed on titration of 10mM Na₃PPP + 50mM KCl with Dysprosium chloride.

TABLE 2.1

Binding constant data for $\text{P}_3\text{O}_{10}^{5-}$ (L^{5-})

Metal	Log K	T°C	Conditions	Ref (253)
Li^+	3.9(25°), 3.8(40°)	25-40	0 corr	a
Na^+	2.8(25°, 40°)	25-40	0 corr	a
K^+	2.8(25°, 40°)	25-40	0 corr	a
Dy^{3+}	6.9(25°)	25-45	$\mu = 0.1\text{M}(\text{KNO}_3)$ R: $\text{Dy}^{3+} + 2\text{HL}^{8-} =$ $\text{DyH}_2\text{L}_2^{5-}$	b
Tb^{3+}	6.8(25°)	25-45	$\mu = 0.1\text{M}(\text{KNO}_3)$ R: $\text{Tb}^{3+} + 2\text{HL}^{8-} =$ $\text{TbH}_2\text{L}_2^{5-}$	b
Yb^{3+}	6.7(25°)	25-45	$\mu = 0.1\text{M}(\text{KNO}_3)$ R: $\text{Yb}^{3+} + 2\text{HL}^{8-} =$ $\text{YbH}_2\text{L}_2^{5-}$	b
Pr^{3+}	6.3(25°)	25-45	$\mu = 0.1\text{M}(\text{KNO}_3)$ R: $\text{Pr}^{3+} + 2\text{HL}^{8-} =$ $\text{PrH}_2\text{L}_2^{5-}$	b

different complexes of Dy^{3+} with Na^+ and PPP^{6-} are involved, each having a differing geometric relationship between Dy^{3+} , the phosphate and the Na^+ ions. It is believed that the results indicate the presence of both $\text{Dy}(\text{PPPP})_2^{9-}$ and $\text{Dy}(\text{PPPP})_3^{3-}$ and that they produce opposite shifts of $^{23}\text{Na}^+$. Also, since the shifts go through a maximum when $[\text{PPPP}^{6-}]/[\text{Dy}^{3+}]$ is greater than 2.0, a reaction analogous to that for Dysprosium tripolyphosphate must exist.



This is the only bidirectional shift reagent known to our knowledge.

No hyperfine shift was observed with the cyclic trimetaphosphate trisodium (7). It is believed that the Dy^{3+} binds strongly with the three negatively charged oxygen atoms, leaving no free negatively charged oxygen for binding by the Na^+ ions, thus no ^{23}Na hyperfine shift is observed.

Of the above aqueous shift reagents investigated the largest ^{23}Na shifts have been obtained with the reagent $[\text{Dy}(\text{PPP})_2^{7-}]$ (30 to 35 ppm) introduced by Gupta and Gupta.¹⁹⁷ Gupta and Gupta used a 2:1 molar ratio of tripolyphosphate to Dy^{3+} to shift ^{23}Na . Our data show that a molar ratio 2.3:1 induces a greater shift with $^{23}\text{Na}^+$ and a molar ratio of 2.5:1 with $^{39}\text{K}^+$ (vide infra).

The shift reagent $[\text{Dy}(\text{PPP})_2^{7-}]$ was then employed in the measurement of intracellular Na^+ or K^+ concentration in cellular systems. The method relies on the fact that the plasma membrane is impermeable to the shift reagent.

The intracellular Na^+ of the following cellular system was investigated to check the practicability of using these shift reagents with living cells. Bakers' yeast (Saccharomyces cerevisiae), Escherichia coli and Tetrahymena pyriformis. They were respectively resuspended in

a medium containing 10mM Na_5PPP and 4mM DyCl_3 so as to shift the extracellular Na^+ signal away from the resonance arising from intracellular Na^+ . Calculation of the fractional space that was intracellular followed by comparison of the integrated area of the intracellular Na^+ peak with that of the reference spectrum gave values for the Na_{IN}^+ concentration of 12mM and 14mM for Saccharomyces cerevisiae and Escherichia coli respectively (Figs 3.2 and 3.3). These concentrations are biologically reasonable but were not checked by any other established technique. While investigation with Tetrahymena pyriformis failed to give a reasonable separation of Na_{IN}^+ and Na_{OUT}^+ resonances. This may be due to several factors:

(i) Tetrahymena pyriformis has a buccal cavity (mouth) near the anterior end and the variation in chemical shift with time that was observed for this organism and none of the others suggests ingestion of the shift reagent, (ii) the cilia (hairs) surrounding Tetrahymena with which it moves contain substantial amounts of phospholipids which may interact with the shift reagent.

The above results show that typical yeast and bacterial cells are amenable to our shift reagent but Tetrahymena pyriformis (a protozoan) is not.

In the measurement of K^+ concentration within erythrocytes, the ratio of Dy^{3+} to tripolyphosphate that resulted in the maximum chemical shift of the K^+ resonance at three different concentrations of K^+ was first determined in a resuspension medium designed to support the erythrocytes (Fig 2.10). The optimal concentration of DyCl_3 (6.5mM) was independent of the K^+ concentration, although the chemical shifts were greater with 20mM-KCl than with 40mM- or 60mM- KCl.

The intracellular K^+ concentrations of 81mM, 85mM and 81mM that

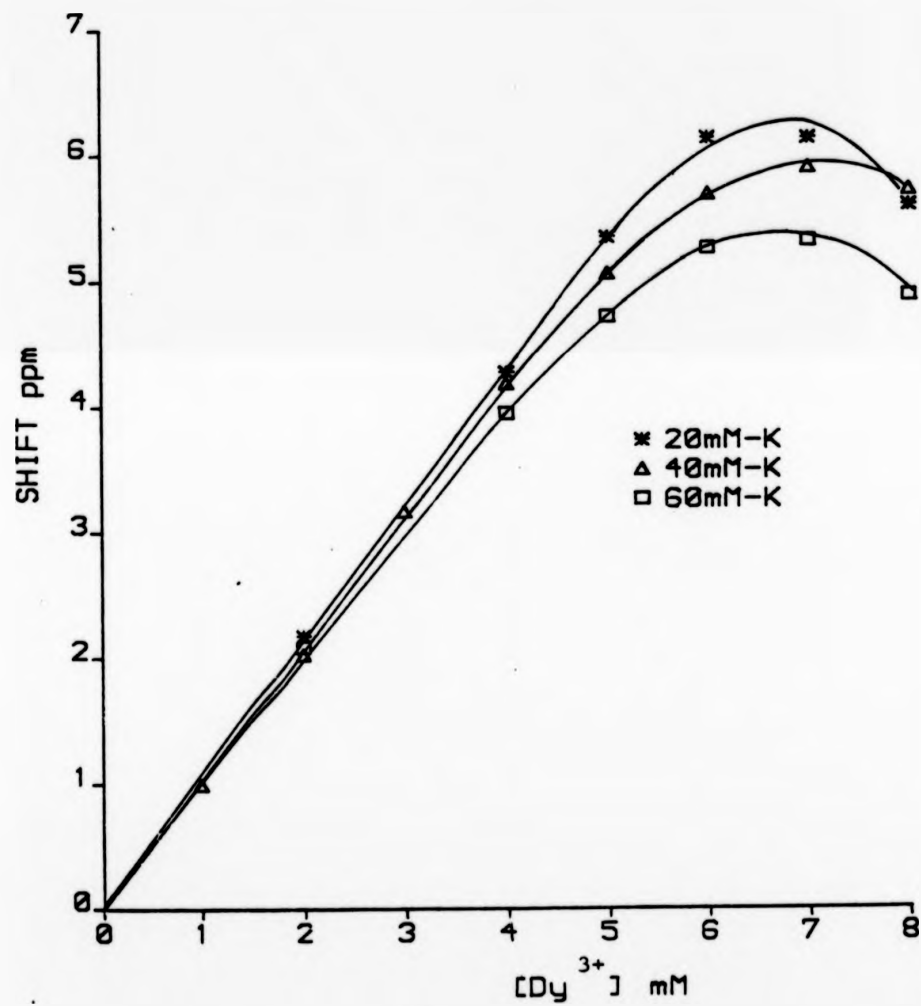


FIGURE 2.10 ³⁹K shifts (16.8MHz), observed at three different concentrations of K in resuspension medium containing 15mM Na₅PPP with Dysprosium chloride.

were calculated (see Experimental) when the erythrocytes were resuspended in media containing 20mM-, 40mM- and 60mM-KCl respectively, agree well with the value of 88mM that was measured by classical flame photometry on the same sample.

Since Na^+ and K^+ ions compete for the binding sites on the shift reagent, Dysprosium tripolyphosphate, the observed shift of K^+ is correspondingly reduced. In order to investigate the shifts of potassium ions in the absence of sodium ions, potassium tripolyphosphate (K_5PPP) was prepared from Na_5PPP by passing the latter down an ion exchange column loaded with the K^+ form. The shifts of potassium ions in K_5PPP on addition of Dysprosium chloride are presented in Figs 2.11-2.13 and display similarities to those obtained for Na^+ . The shape of the titration curve is independent of the concentration of the K_5PPP used: the maximum shift is obtained at the same $[\text{PPP}^{5-}]/[\text{Dy}^{3+}]$, the curves are initially linear with slopes varying inversely with the tripolyphosphate concentration, and the relative concentrations needed to obtain the maximum shift are identical. In all three cases titration was stopped when the curve had gone through a maximum and the first signs of a precipitate appeared in the tube. In all three cases line broadening is slight at first but becomes more important at molar ratios $[\text{Dy}^{3+}]/[\text{PPP}^{5-}] > 0.3$. Such behaviour is indicative of complex equilibria involving at least two different stoichiometries for the interaction between Dy^{3+} and PPP^{5-} and a reaction analogous to that of Na^+ ions with Dysprosium tripolyphosphate must exist (see above). Again, no attempt was made to control the pH during titrations. In all cases the initial pH was ca 9.0 and decreased as a sigmoid curve to a final value of ca 7.7. The maximum shift observed corresponds to the point where the pH curve begins to level off

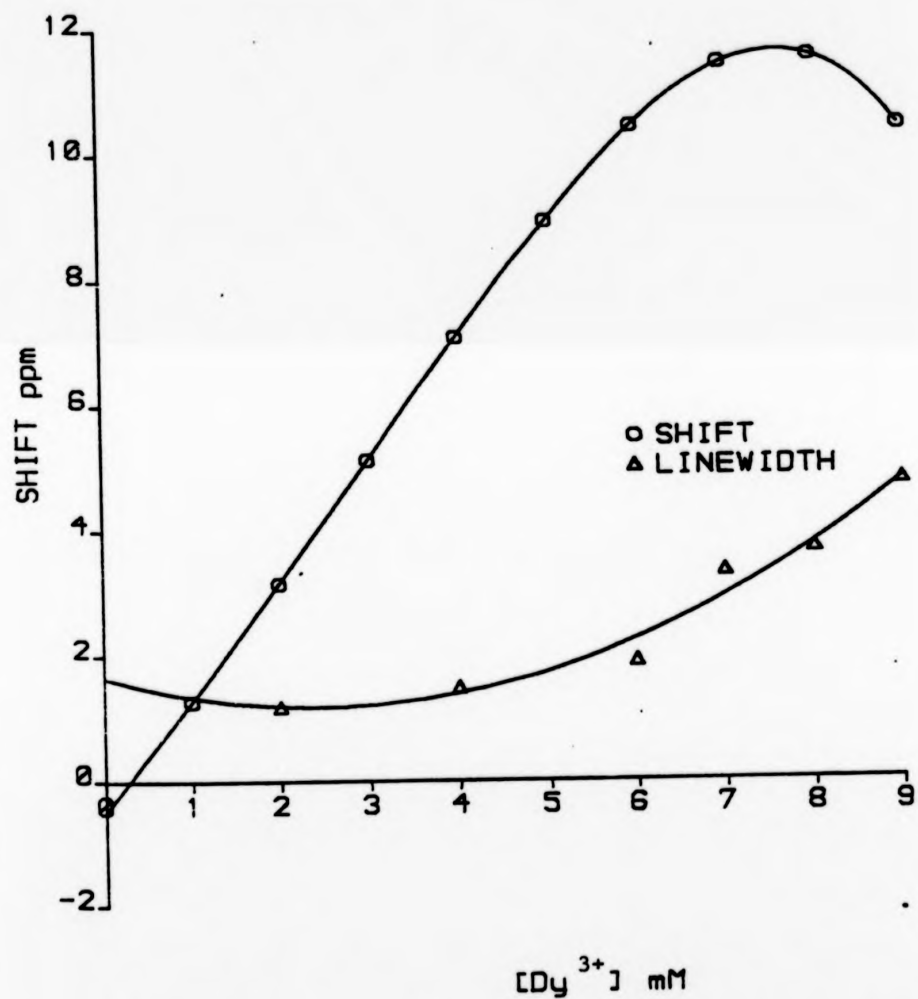


FIGURE 2.11 ³⁹K shifts (16.8MHz) observed on titration of 20mM K₅PPP with Dysprosium chloride.

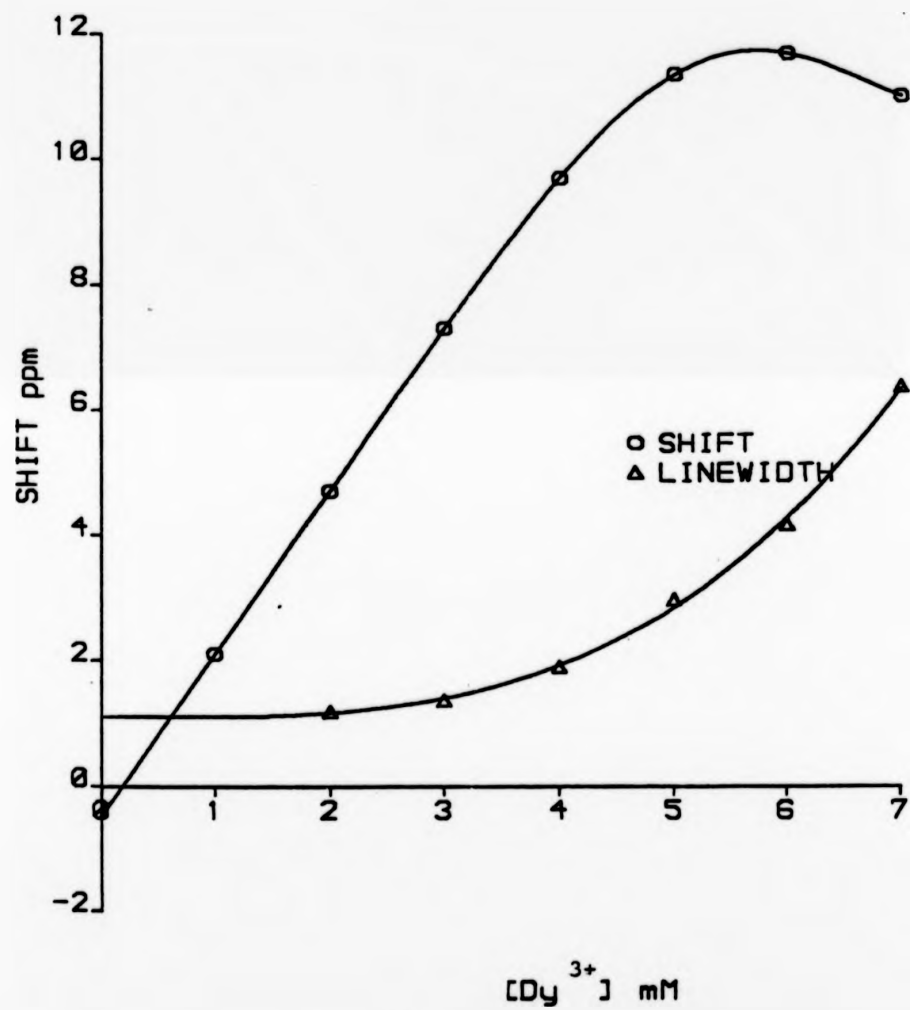


FIGURE 2.12 ³⁹K shifts (16.8MHz) observed on titration of 15mM K₅PPP with Dysprosium chloride.

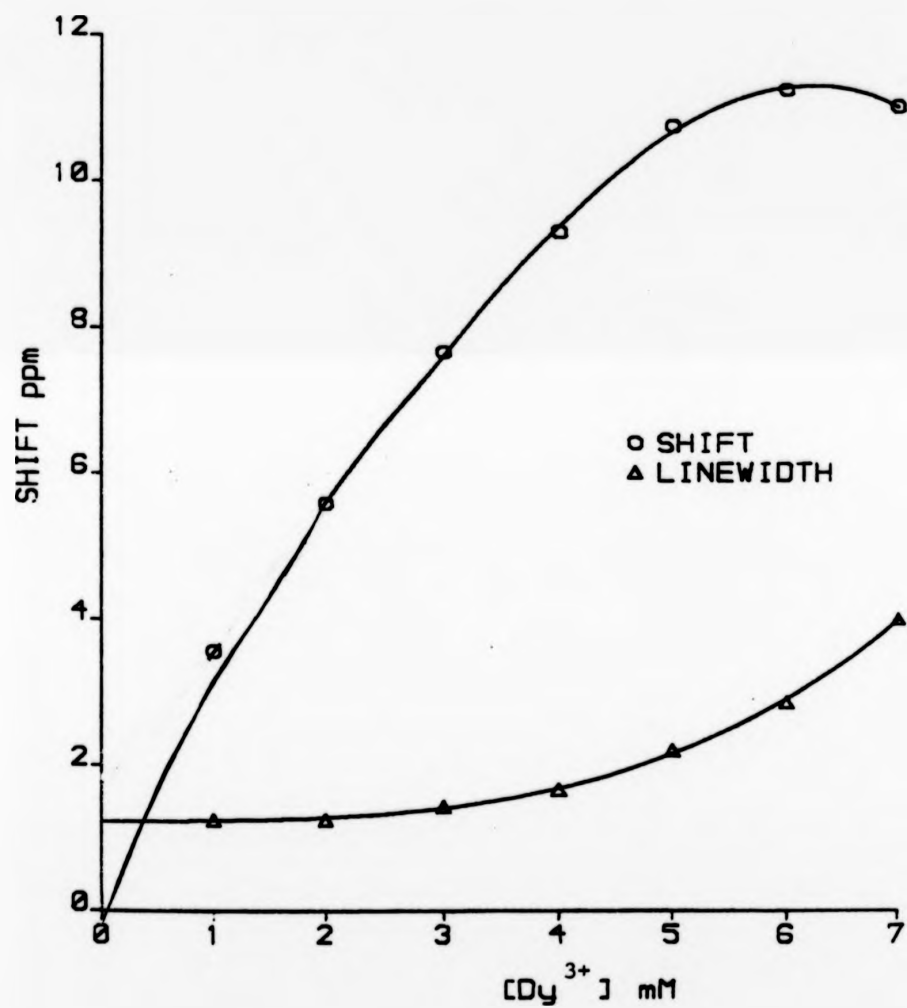


FIGURE 2.13 ^{39}K shifts (16.8MHz) observed on titration of 10mM K_5PPP with Dysprosium chloride.

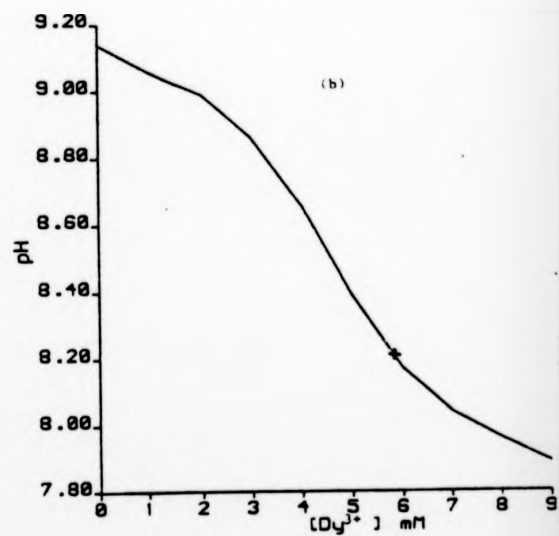
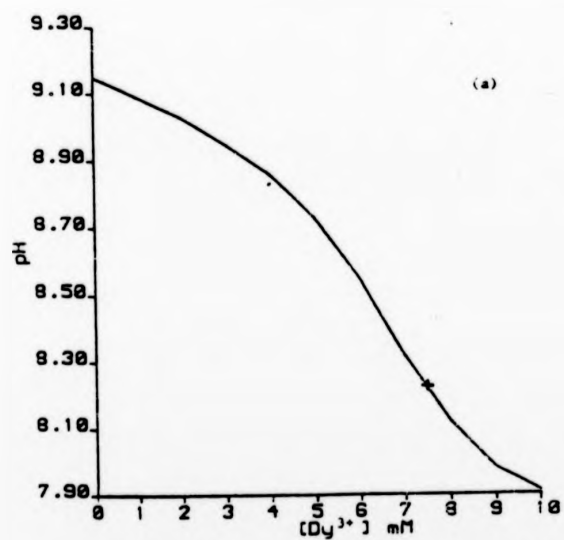
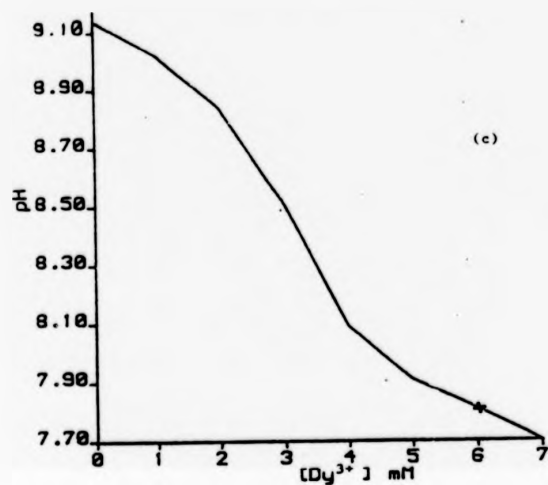


FIGURE 2.14 Change in pH of K_3PPP solutions, (a) 20mM, (b) 15mM and (c) 10mM, on titration with $DyCl_3$. $T=298K$
 * - pH of maximum shift

(Fig 2.14).

In a separate experiment, Na^+ shifts were investigated in an equimolar solution of Na_5PPP and K_5PPP on addition of Dysprosium chloride. The result is presented in Fig 2.15. The maximum shift observed is slightly less than that obtained with equivalent total concentration of Na_5PPP (Fig 2.4).

In an attempt to investigate the effect on ^{23}Na and ^{39}K shifts by other counter cations, Li_5PPP was prepared by ion exchange of Na_5PPP . On addition of DyCl_3 (2mM) to a solution of Li_5PPP (5mM) failed to cause a shift of the Li^+ ions (^7Li nmr, 31.14 MHz). Literature value for the binding constant (Table 2.1) suggest that lithium ions bind strongly to the tripolyphosphate. This was further supported in another experiment where the ^{23}Na isotropic hyperfine shift, in a solution of 15mM Na_5PPP and 3mM DyCl_3 was observed to decrease as increasing quantities of crystalline $\text{LiCl}\cdot\text{H}_2\text{O}$ were added.

Preliminary investigation of ^{23}Na shifts in the presence of choline chloride $[\text{CH}_2(\text{OH})\text{CH}_2\text{N}^+(\text{CH}_3)_3]\text{Cl}^-$, indicated that it might be a suitable counter cation. However, repeated attempts to ion exchange Na_5PPP to $(\text{choline})_5\text{PPP}$ failed to obtain complete exchange. In the first attempt, the product obtained was presumed to be a mixture of $(\text{Na})_x(\text{choline})_y\text{PPP}$ and H_5PPP since the strong-acid ion-exchange column used was only partly loaded with choline $^+$. The product was then converted to $(\text{Na})_x(\text{choline})_y\text{PPP} + \text{Na}_5\text{PPP}$ and $(\text{Na})_x(\text{choline})_y\text{PPP} + \text{K}_5\text{PPP}$ by titration with NaOH and KOH respectively to pH 6.5. Each solution made was ca 26mM in tripolyphosphate (^{31}P nmr, 32.44 MHz). The results of the titrations with DyCl_3 are presented in Figs 2.16 and 2.17. The ^{23}Na maximum shift observed is ca 10% less to that obtained for 20mM Na_5PPP (Fig

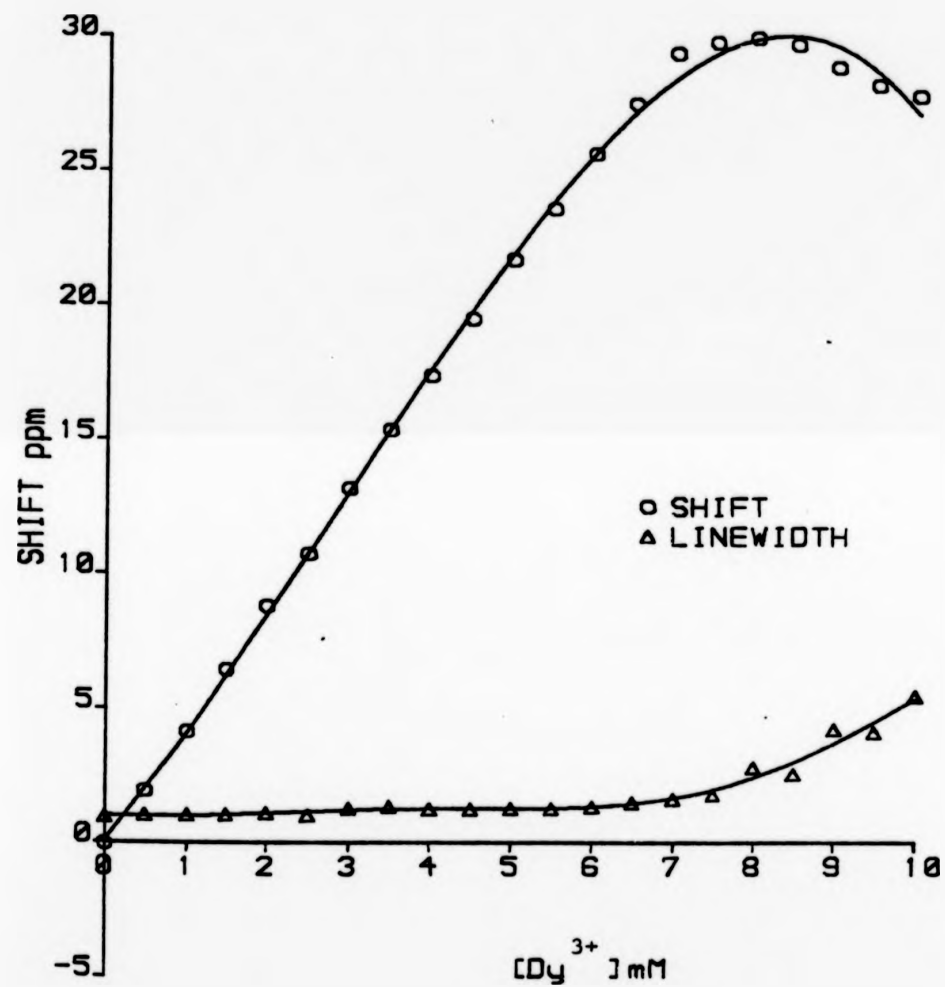


FIGURE 2.15 ²³Na shifts (21.19MHz) observed on titration of 10mM Na₅PPP + 10mM K₅PPP with Dysprosium chloride.

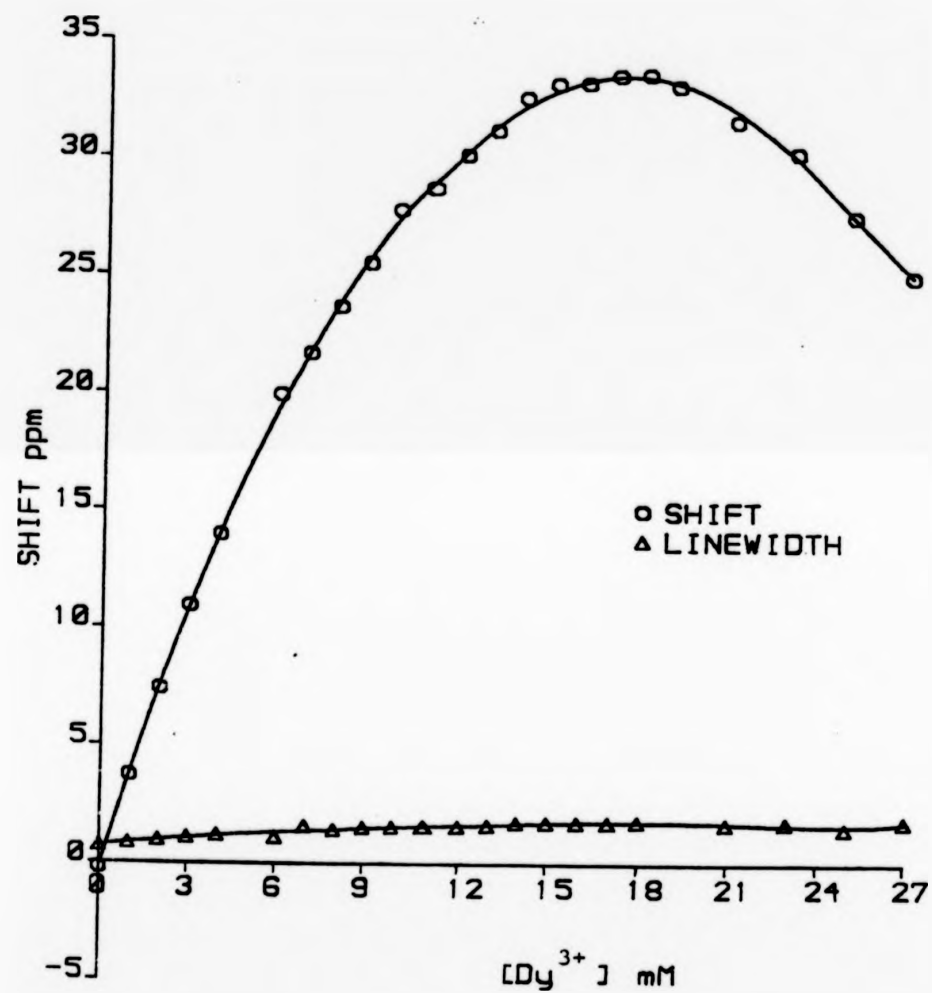


FIGURE 2.16 ²³Na shifts (21.19MHz) observed on titration of Na₅PPP + (Na)_x(Choline)_yPPP with Dysprosium chloride. [PPP⁵⁻] ~ 26mM

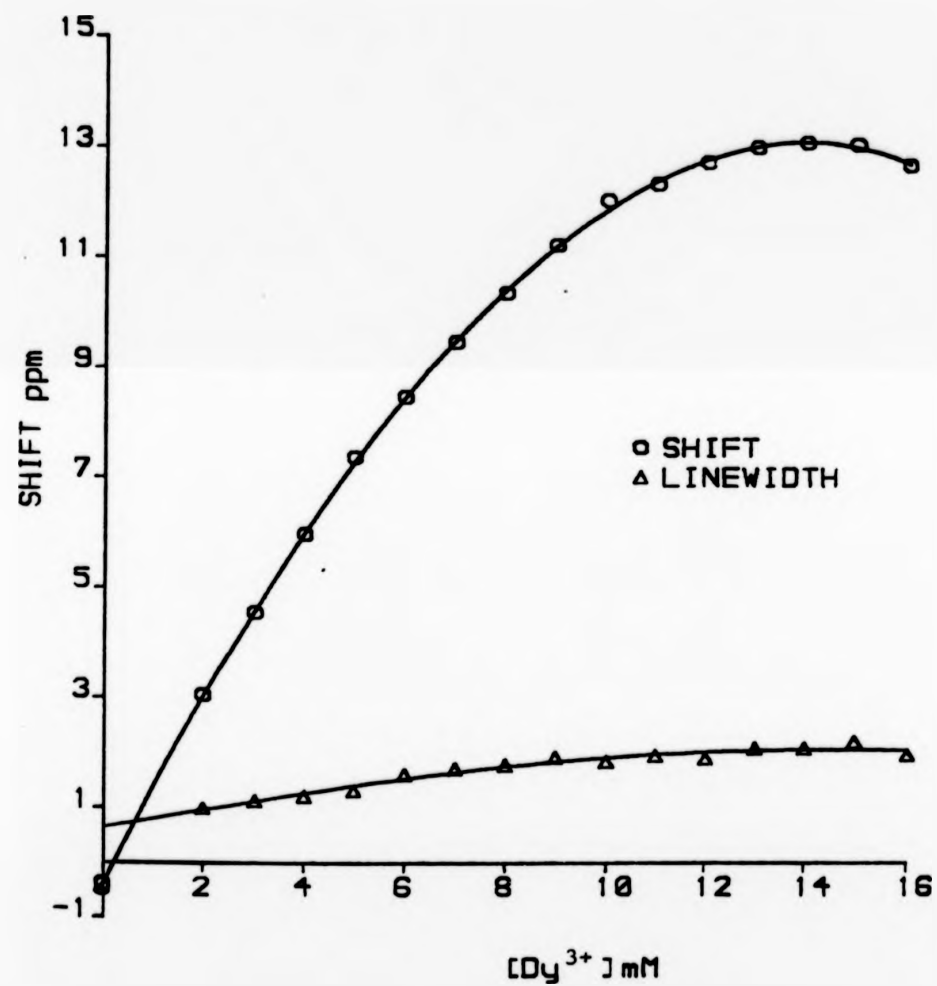


FIGURE 2.17 ³⁹K shifts (16.8MHz) observed on titration of K₃PPP + (Na)₂(Choline)_y PPP with Dysprosium chloride. [PPP³⁻] ~ 26mM

2.2) and the ^{39}K maximum shift observed is ca 10% better to that observed for 20mM K_5PPP (Fig 2.11). In both cases, however, the line broadening has reduced approximately by a factor of 0.5 at the observed maximum shift. These results are of interest as they suggest that other non-metallic supporting cations may produce larger shifts and lower line broadenings. This area needs further investigation.

The shifts of sodium and potassium ions in Na_5PPP and K_5PPP respectively on addition of the lanthanides, Terbium, Ytterbium and Praseodymium were then investigated. The dipolar hyperfine shift theory suggests that Terbium should give substantial shifts to low frequency similar to Dysprosium whilst Ytterbium should give much smaller shifts in the opposite direction of the same substrate.^{252,254} The results are presented in Figs 2.18-2.24.

With Terbium nitrate pentahydrate, the maximum ^{23}Na and ^{39}K shifts observed were slightly less (32.5 ppm vs ca 36.5 ppm) and a slightly greater (12.4 ppm vs ca 11.5 ppm) respectively than the corresponding shifts observed with Dysprosium chloride and the line broadenings were slightly smaller (Figs 2.18-2.22). The shape of the curve is similar to that obtained for Dysprosium and the stoichiometries suggested by the titration curve are also similar to those for Dysprosium. Terbium would thus seem to be marginally inferior to Dysprosium as the lanthanide in a ^{23}Na shift reagent and marginally preferable to Dysprosium as the lanthanide in a ^{39}K shift reagent.

Again no attempt was made to control the pH during titrations of respective PPP^{5-} solutions with $\text{TbCl}_3 \cdot 5\text{H}_2\text{O}$. In a separate experiment, in all cases the initial pH was ca 9.5 and decreased as a sigmoid curve to a final value of ca 7.8 (Figs 2.25 and 2.26). As for DyCl_3 , the ^{23}Na maximum shifts observed correspond to the point just

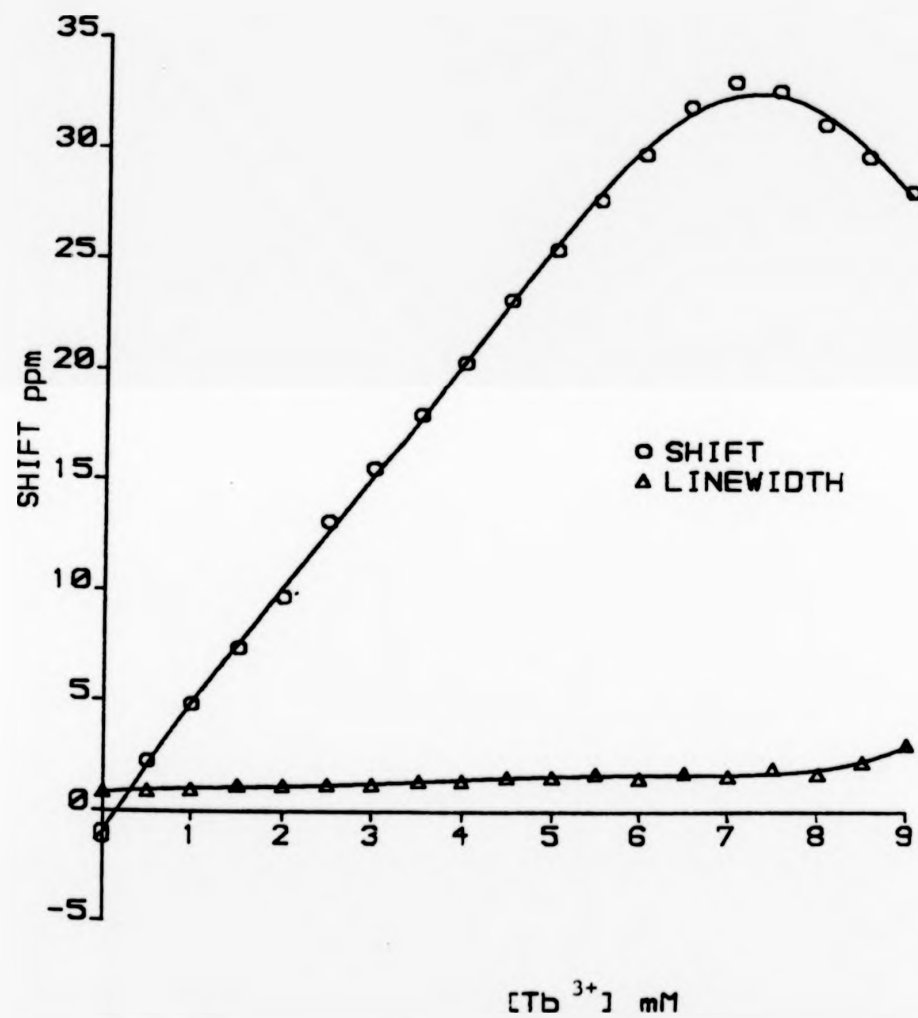


FIGURE 2.18 ²³Na shifts (21.19MHz) observed on titration of 20mM Na₅PPP with Terbiium nitrate pentahydrate.

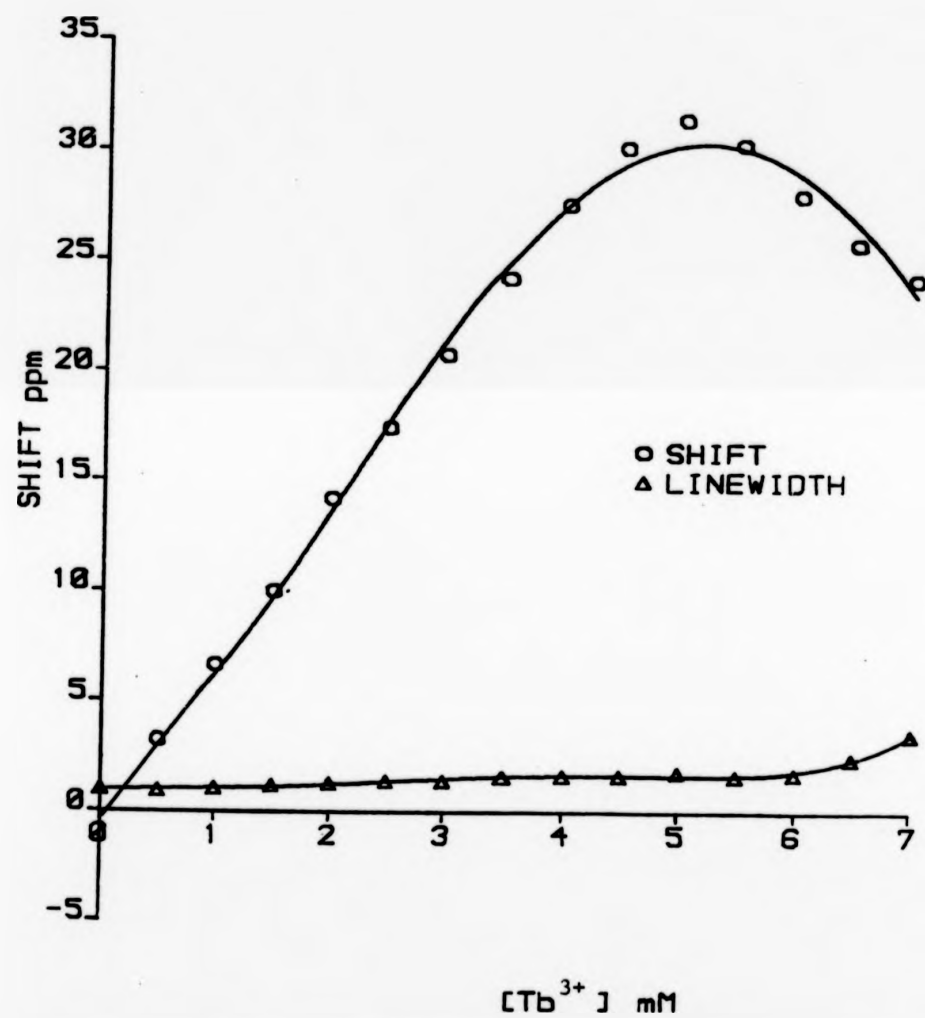


FIGURE 2.19 ²³Na shifts (21.19MHz) observed on titration of 15mM Na₅PPP with Terbium nitrate pentahydrate.

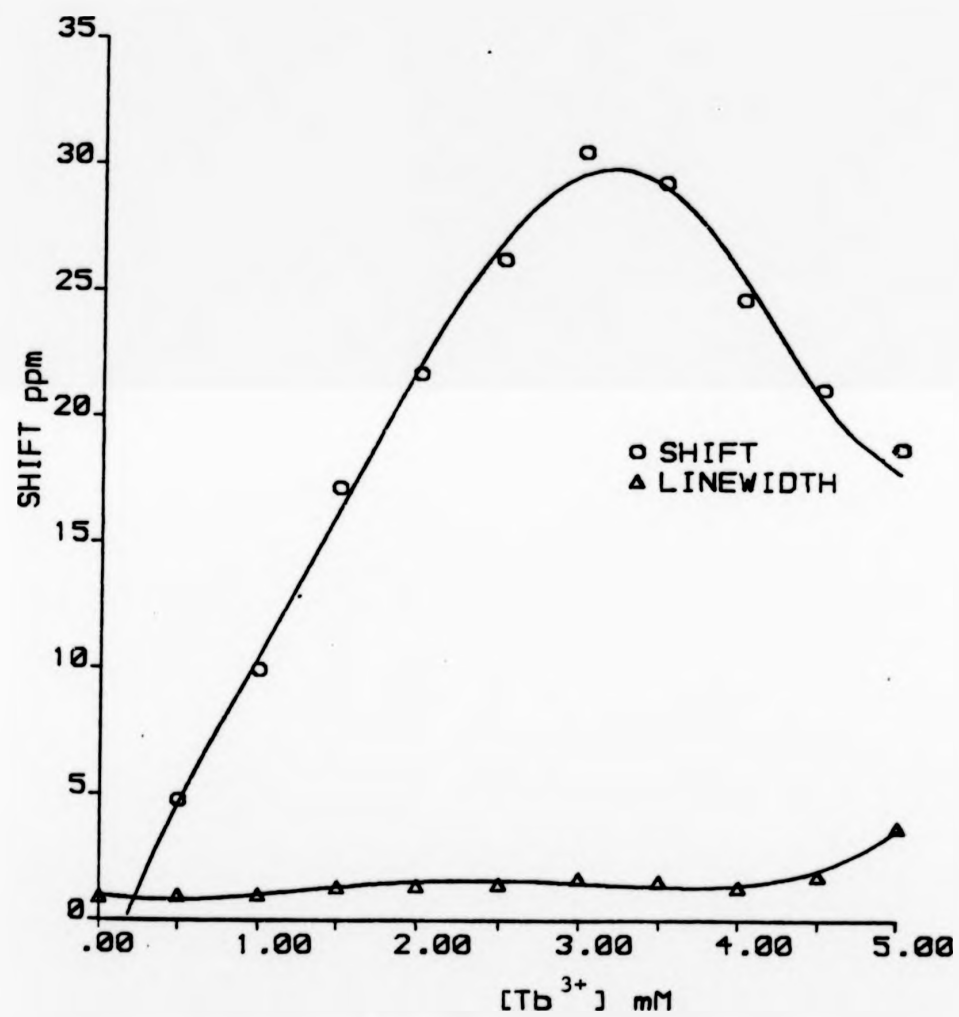


FIGURE 2.20 ²³Na shifts (21.19MHz) observed on titration of 10mM Na₅PPP with Terbium nitrate pentahydrate.

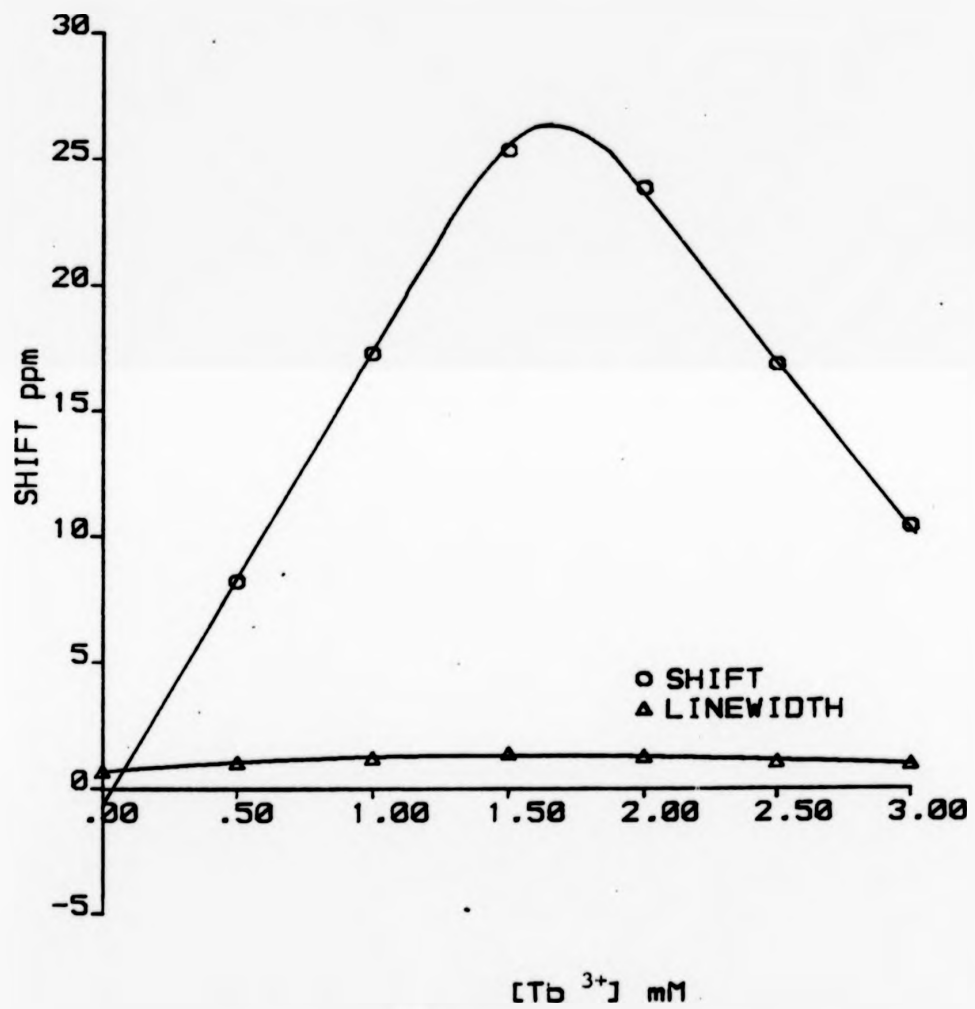


FIGURE 2.21 ²³Na shifts (21.19MHz) observed on titration of 5mM Na₅PPP with Terbium nitrate pentahydrate.

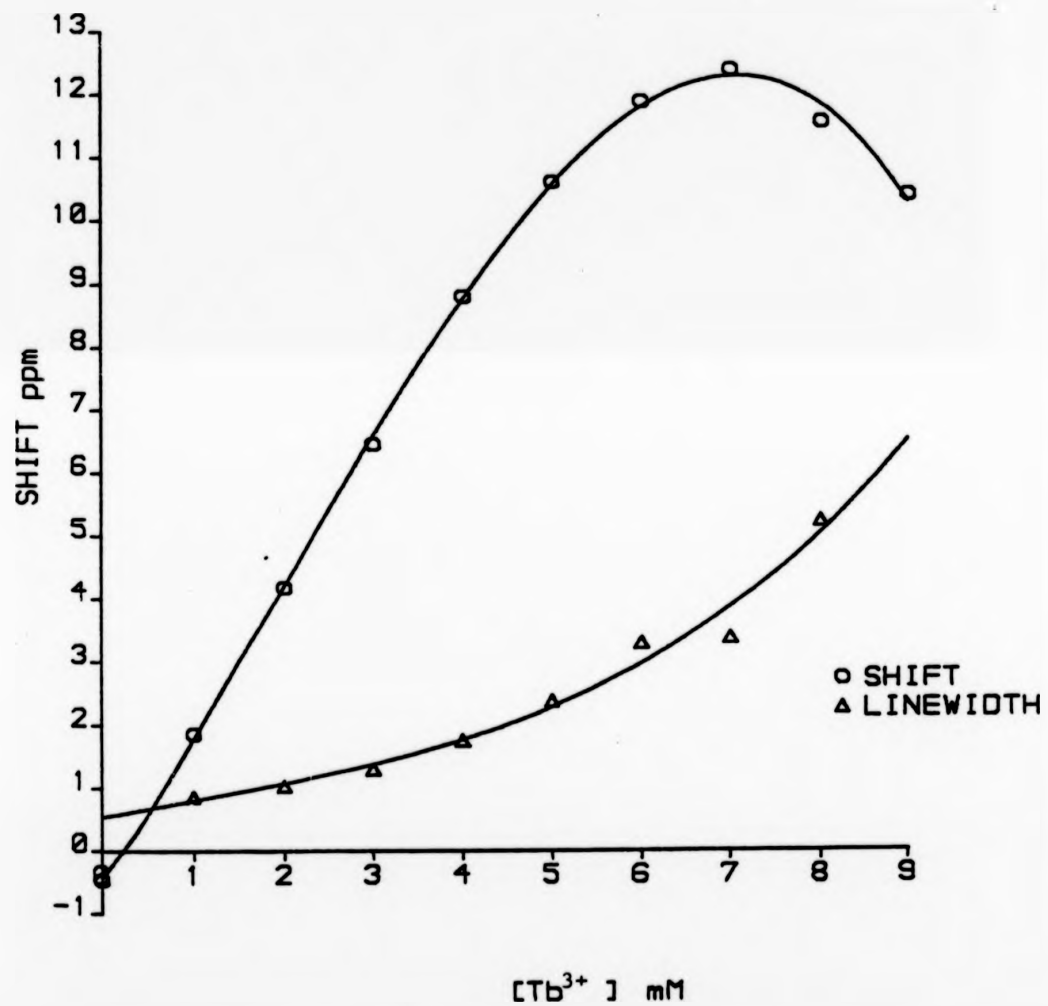


FIGURE 2.22 ³⁹K shifts (16.8MHz) observed on titration of 20mM K₅PPP with Terbium nitrate pentahydrate.

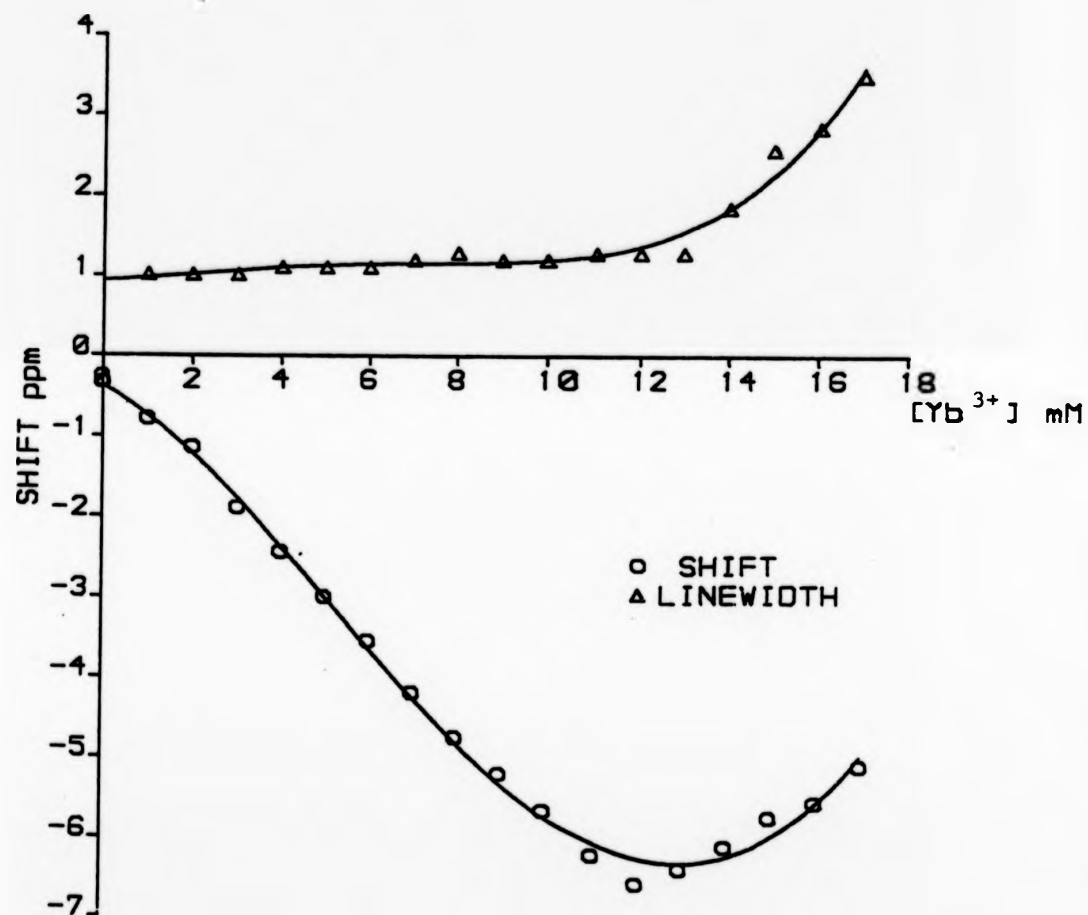


FIGURE 2.23 ^{23}Na shifts (21.19MHz) observed on titration of 20mM Na_5PPP with Ytterbium trichloride.

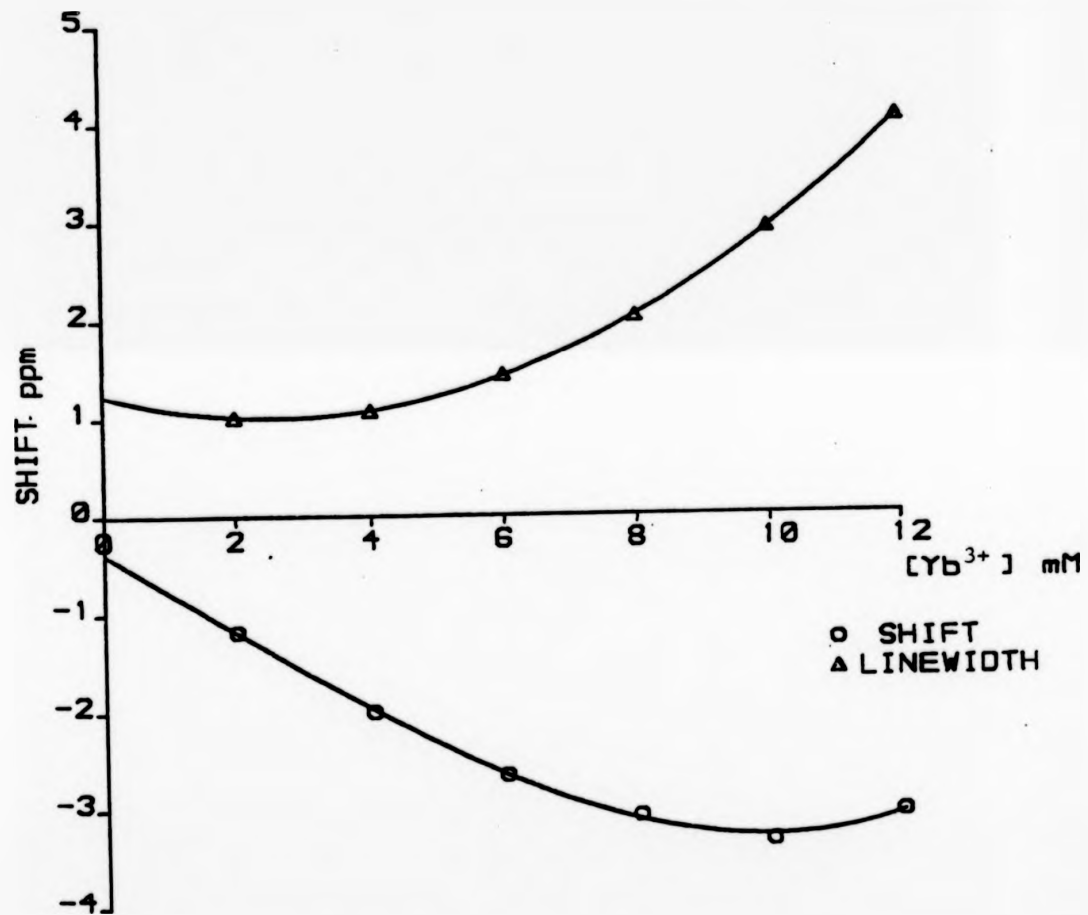


FIGURE 2.24 ³⁹K shifts (16.8MHz) observed on titration of 20mM K₅PPP with Ytterbium trichloride.

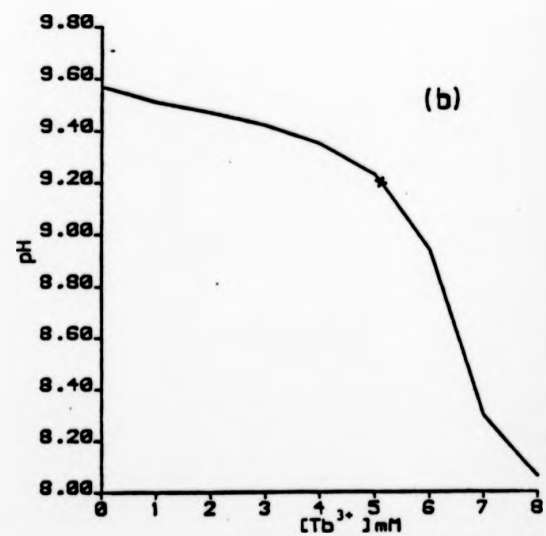
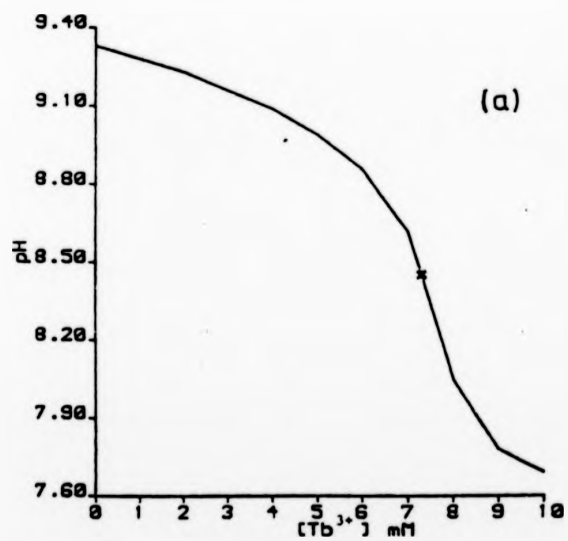
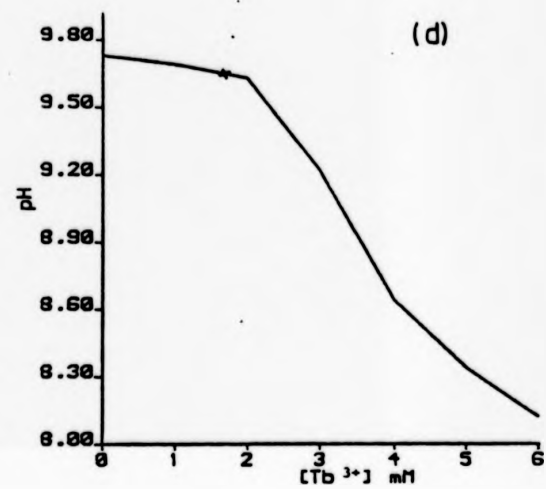
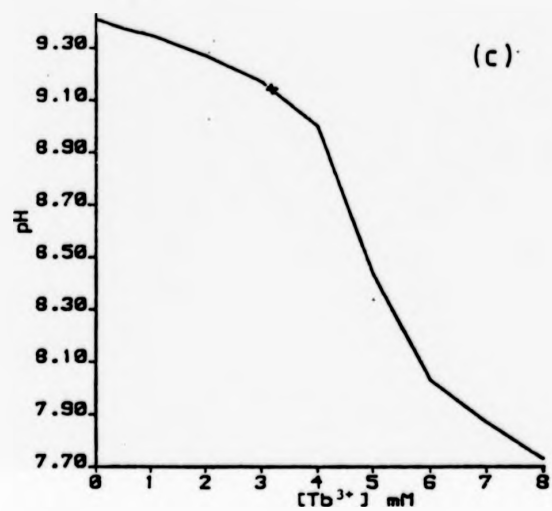


FIGURE 2.25 Change in pH of Na₃PPP solutions, (a) 20mM, (b) 15mM, (c) 10mM and (d) 5mM, on titration with TbCl₃·5H₂O. T=298K
 * - pH of maximum shift

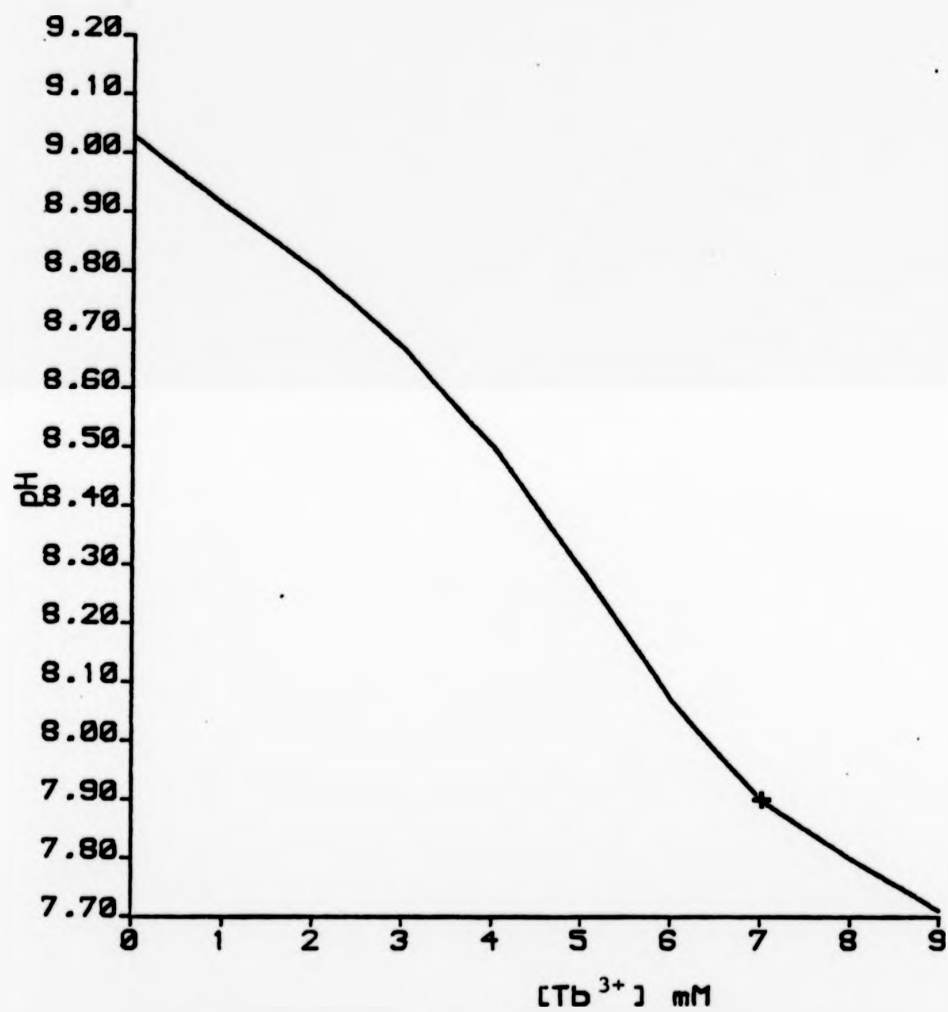


FIGURE 2.26 pH change observed on titration of 20mM K_5PPP with Terbium nitrate pentahydrate.

* - pH of maximum shift

before the pH curve begins to fall sharply. While the ^{39}K maximum shift observed corresponds to the point where the pH curve begins to level off.

Ytterbium, as predicted by theory, gave inferior shifts in the opposite direction to Dysprosium and Terbium (Figs 2.23 and 2.24). The change in pH observed on titration of 20mM Na_5PPP and 20mM K_5PPP with Ytterbium trichloride are illustrated in Figs 2.27 and 2.28 respectively. The maximum shift observed in Figs 2.23 and 2.24 correspond to the point where the pH curves begin to level off. In the case of K_5PPP with YbCl_3 , it is extremely interesting to compare the shifts obtained to the line broadenings (Fig 2.24). At the maximum shift (ca 3.5 ppm) the line broadening is comparable (ca 3 ppm) to the shift difference.

With the lanthanide Praseodymium, a maximum shift of 2.6ppm with 10mM Na_5PPP solution was observed and the line broadening was ca 1 ppm.

In a separate experiment with Lanthanum as the lanthanide, no shift phenomenon was observed on addition of aliquots of Lanthanum to the tripolyphosphate. This result indicating that there is no diamagnetic contribution to the hyperfine shifts observed above.

Bulk susceptibility experiments with substrates sodium chloride and potassium chloride gave a 0.35 ppm ^{23}Na shift to lower frequency and a 1.014 ppm ^{39}K shift to higher frequency respectively. The results indicate a very small bulk susceptibility effect on the shifts investigated above.

2.1.3 Conclusion

The usefulness of various paramagnetic lanthanide ions for shifting and/or relaxing nuclear magnetic resonances in aqueous solutions has been

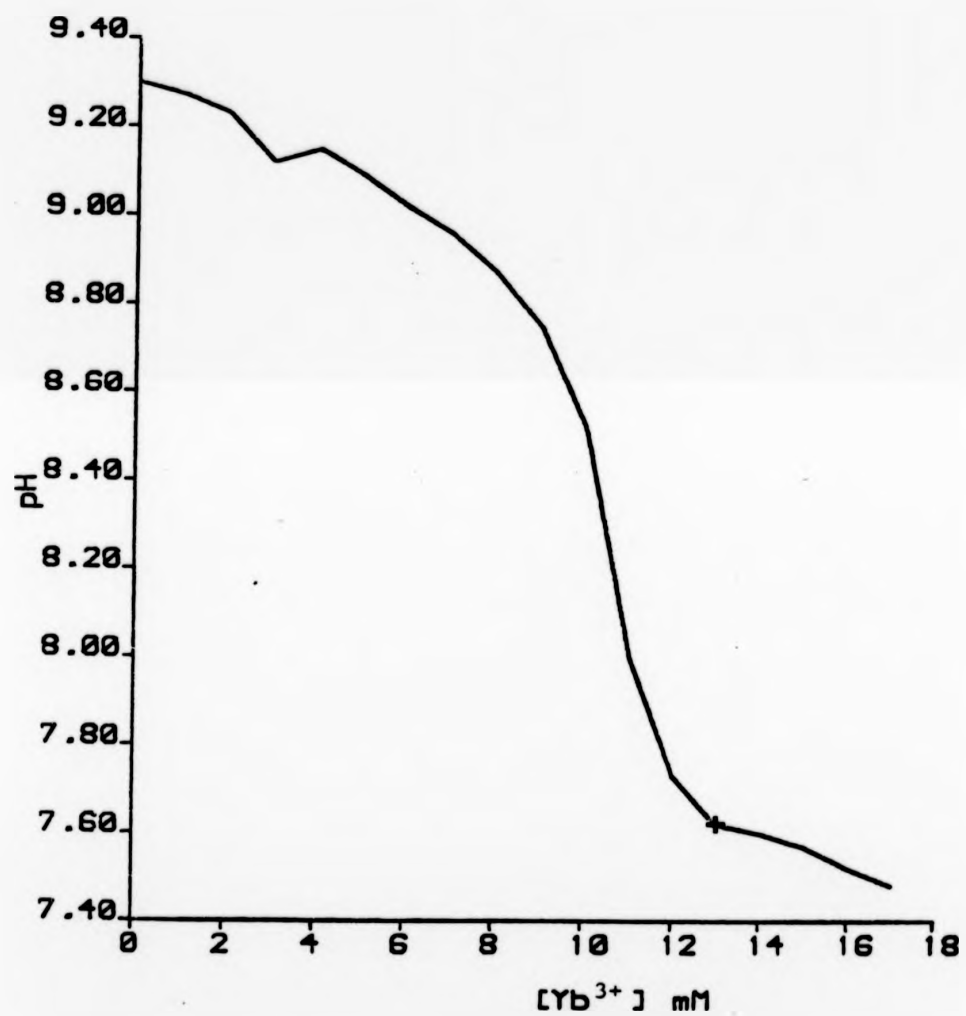


FIGURE 2.27 pH change observed on titration
of 20mM Na₅PPP with Ytterbium trichloride.
* - pH of maximum shift

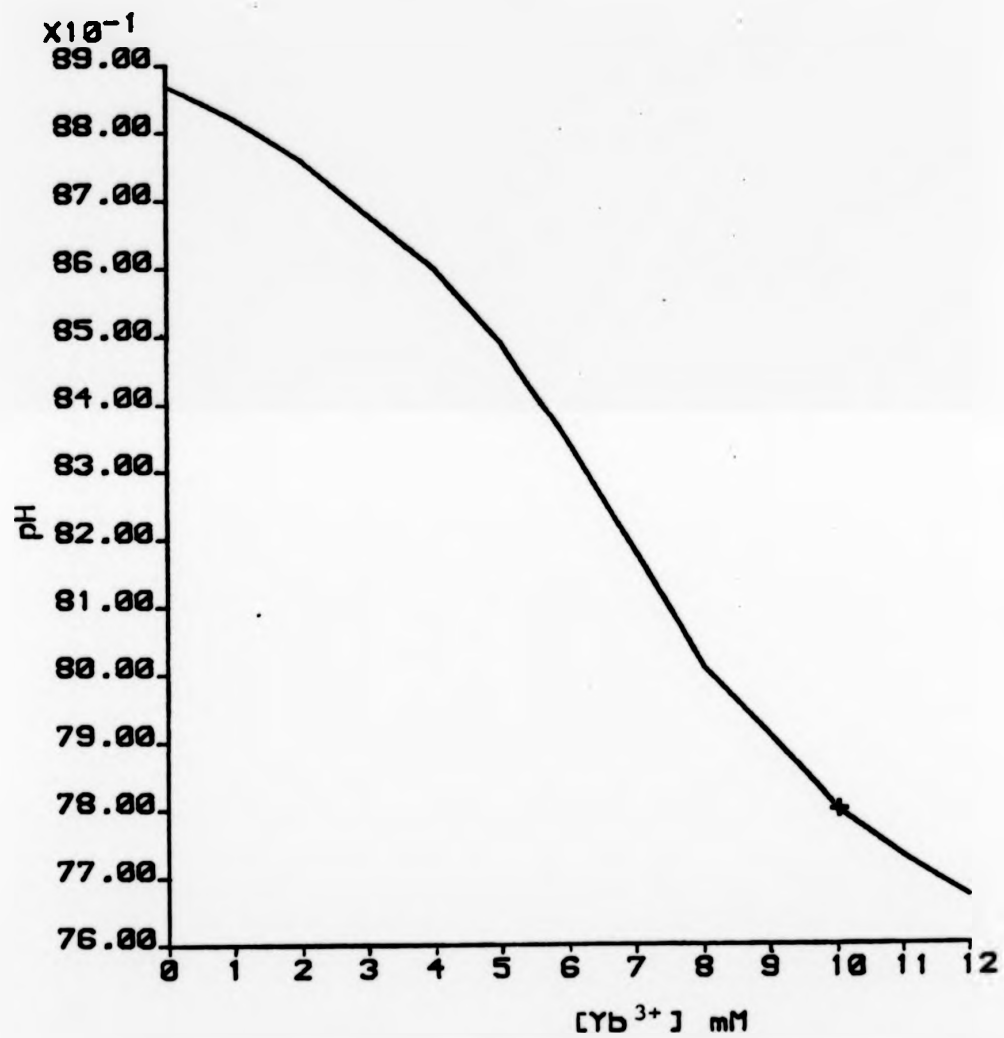


FIGURE 2.28 pH change observed on titration
of 20mM K₅PPP with Ytterbium trichloride.
* - pH of maximum shift

known for more than a decade.²⁵⁵ Most subsequent studies have employed various lanthanide coordination complexes as aqueous hyperfine shift^{222,233,254,256-258} or relaxation^{256,259-264} reagents and as aqueous susceptibility shift²⁶⁵ or relaxation²⁶⁶ reagents. Of the resonances of the physiological alkali-metal or alkali-earth-metal ions, only that of ^{23}Na has been the subject of specific hyperfine relaxation^{267,268} or shifting^{197,199,204,254} and susceptibility shifting²⁶⁵ experiments and these have employed paramagnetic lanthanide complexes.

Our results (ref. 269 and in this thesis) and those of others^{201,254} indicate that increased charge on the anionic shift reagent is not the only factor required to produce an efficient shift reagent. Springer et al have found that the anions $\text{Dy}(\text{TTHA})^{3-}$ and $\text{Tm}(\text{TTHA})^{3-}$ (TTHA^{6-} is triethylenetetraminehexaacetate) induce shifts of the $^{23}\text{Na}^+$ resonance comparable to those induced by the $\text{Dy}(\text{CA})_3^{6-}$ and $\text{Tm}(\text{CA})_3^{6-}$ complexes²⁰¹ (CA^{3-} is chelidamate). Bryden et al²⁵⁴ have reported that the neutral $\text{Dy}(\text{NOTA})$ complex (NOTA^{3-} is 1,4,7-triazacyclononane- $\text{N},\text{N}',\text{N}''$ -triacetate) induces larger shifts of the $^{23}\text{Na}^+$ resonance than any of the anionic complexes tested by them, although the (unclear) concentration ratios in their various experiments are not strictly comparable.

Assuming that the hyperfine shift is totally dipolar (pseudocontact) in nature, there are at least three factors that determine the magnitude and sign of the limiting shift, Δ^0 . These are the particular lanthanide ion chosen, the asymmetry of the magnetic susceptibility tensor of the lanthanide ion (determined by the molecular structure of the shift reagent anion), and the geometrical coordinates of the cation binding site (its distance from the lanthanide ion and the angular

relationships to the principal axes of the magnetic susceptibility tensor.^{252,254} Springer et al^{199,201} have demonstrated that various combinations of these factors are important. Thus, in these kind of experiments, there are three essential components: a) the Ln³⁺ ion, b) the metal cation observed, and c) the chelate ligand.

In general lanthanides such as Praseodymium, Europium and Ytterbium are used in shift reagents for ¹H and ¹³C applications in preference to Dysprosium and Terbium because the latter lanthanides produce much larger line broadenings which outweigh their advantages in terms of larger shifts.²⁵² With ²³Na and ³⁹K the reverse is true, and the larger shifts obtained with Dysprosium and Terbium are not at the expense of unacceptable line broadenings.

Typical polyvalent ligands that have been used for ²³Na and/or ³⁹K so far include diphosphate (PP⁴⁻), tripolyphosphate (PPP⁵⁻), tetrapolyphosphate (PPPP⁶⁻), nitrotriacetate (NTA³⁻), ethylenediaminetetraacetate (EDTA⁴⁻) triethylenetetraminehexaacetate (TTHA⁶⁻), 1,4,7,10-tetraazacyclododecane-N,N',N'',N'''-tetraacetate (DOTA⁴⁻) and chelidamate (CA³⁻).^{197-201, 203, 269.}

Of these by far the largest ²³Na shifts have been obtained with tripolyphosphate. The Dy(PPP)₂⁷⁻ complex of Gupta and Gupta,¹⁹⁷ the Tm (PPP)₂⁷⁻ complex of Springer et al²⁰¹ and the Tb(PPP)₂⁷⁻ complex introduced here are each capable of inducing very large shifts in the ²³Na⁺ resonance. The high charge of the complex ion certainly must serve to increase the fraction of Na⁺ ions bound, compared with the other shift reagents.²⁰⁰ Wall and Doremus²⁷⁰ found that, even for the free PPP⁵⁻ ligand, the fraction of the Na⁺ ions bound in a 33mM solution of Na₅PPP was 37%. However, under equivalent conditions, the shift induced by Dy(PPP)₂⁷⁻ is so much greater than

that induced by $\text{Dy}(\text{CA})_3^{6-}$ ²⁰⁰ (by a factor of ca four), that a more specific interaction is indicated. Inspecting the molecular structure of the PPP^{5-} ion as determined from X-ray crystallography of Na_5PPP ²⁷¹ and the way the Na^+ ions are coordinated in the crystal, Springer et al hypothesized a structure related to that shown in Fig 2.29 for the transient interaction of Na^+ with $\text{Ln}(\text{PPP})_2^{7-}$. This structure features a specific Na^+ binding site close to the Ln^{3+} ion. The limiting dipolar hyperfine shift is inversely proportional to the cube of the distance of the binding site from the paramagnetic centre. If the stoichiometry of the $\text{Na}^+.\text{Ln}(\text{PPP})_2^{6-}$ complex is greater than 1:1,²⁷² the additional Na^+ ions could not occupy the same binding site as that shown in Fig. 2.29, except on a time-averaged basis.

The largest ^{39}K shifts (ca 18ppm, 14.0 MHz) have been obtained with the ligand, chelidamate and lanthanide, Dysprosium.²⁰⁰ The chelidamate method, however, suffers from the disadvantage that large concentrations of lithium ions (or other counter cations) are needed to support the reagent meaning that very high ionic strengths are required to obtain appreciable ^{39}K shifts. For example, the maximum shift for 10mM K^+ would require 90mM Li^+ . Repeated attempts to prepare the hexasodium chelidamate complex of Dysprosium $\text{Na}_6\text{Dy}(\text{CA})_3.3\text{NaCl}$, failed. The chelate ligand K_5PPP introduced in this work gave reasonable shifts of the ^{39}K resonance (maximum shift of ca 12 ppm) when titrated against the lanthanides, DyCl_3 and TbCl_3 (Figs 2.11 and 2.22). In the presence of counter-cations, Na^+ and choline⁺ (Fig 2.17) the maximum shift observed is comparable to those obtained above.

Our results also show that the shift reagent developed by Gupta and Gupta¹⁹⁷ can be used to measure the concentrations of K^+ within

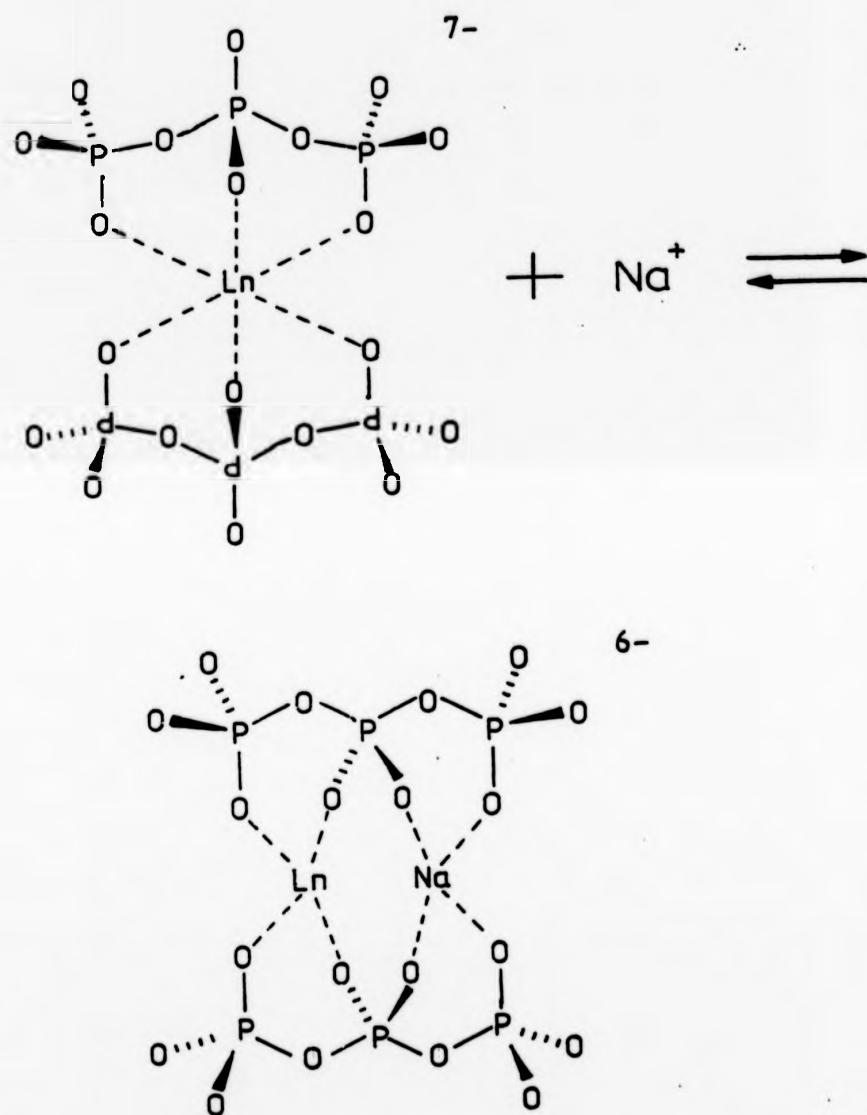


Fig 2.29 Hypothetical structures for $\text{Ln}(\text{PPP})_2^{7-}$ and $\text{Na}^+ \cdot \text{Ln}(\text{PPP})_2^{6-}$. 201

erythrocytes²⁷³ and Na^+ within the cellular systems, Saccharomyces cerivisiae and Escherica coli. The detection of resolved resonances from intra- and extracellular ions in cell suspensions depends on the fact that the anionic paramagnetic shift reagent is present only on the outside of the cell and does not penetrate the cell membrane within the time scale of nmr measurements. Anionic shift reagents are preferred for physiological experiments because the vast majority of polyelectrolytes in nature are anionic. Therefore anionic shift reagents will have little tendency to bind to macromolecules or to cross biological membranes.

Downfield shift reagents (eg $\text{Tm}(\text{CA})_3^{6-}$ ²⁰⁰; $\text{Yb}(\text{PPP})_2^{7-}$, in this thesis) may prove particularly useful in studies of compartmented samples (eg tissue) in vertical superconducting magnets. For a cylindrical sample coaxial with the static magnetic field, the bulk susceptibility shift, due to a paramagnetic substance, is downfield.^{265,274} Thus, the isotropic hyperfine shift induced by a downfield shift reagent will add to the susceptibility shift in such a case. Finally, it is interesting to note that the shifts observed with Dysprosium tetrapolyphosphate are bidirectional (Fig 2.6). Thus by adjusting $[\text{PPPP}^{6-}]/[\text{Dy}^{3+}]$ one can choose the direction of desired shift.

2.2 ²³Na NMR STUDIES OF ION TRANSPORT ACROSS THE MEMBRANE OF PHOSPHATIDYLCHOLINE VESICLES

2.2.1 Introduction

A membrane is a layer which separates two solutions, differs in chemical composition from both of them, forms a sharp boundary towards both these solutions and exhibits different permeability for individual

erythrocytes²⁷³ and Na^+ within the cellular systems, Saccharomyces cerevisiae and Escherichia coli. The detection of resolved resonances from intra- and extracellular ions in cell suspensions depends on the fact that the anionic paramagnetic shift reagent is present only on the outside of the cell and does not penetrate the cell membrane within the time scale of nmr measurements. Anionic shift reagents are preferred for physiological experiments because the vast majority of polyelectrolytes in nature are anionic. Therefore anionic shift reagents will have little tendency to bind to macromolecules or to cross biological membranes.

Downfield shift reagents (eg $\text{Tm}(\text{CA})_3^{6-}$ ²⁰⁰; $\text{Yb}(\text{PPP})_2^{7-}$, in this thesis) may prove particularly useful in studies of compartmented samples (eg tissue) in vertical superconducting magnets. For a cylindrical sample coaxial with the static magnetic field, the bulk susceptibility shift, due to a paramagnetic substance, is downfield.^{265,274} Thus, the isotropic hyperfine shift induced by a downfield shift reagent will add to the susceptibility shift in such a case. Finally, it is interesting to note that the shifts observed with Dysprosium tetrapolyphosphate are bidirectional (Fig 2.6). Thus by adjusting $[\text{PPPP}^{6-}]/[\text{Dy}^{3+}]$ one can choose the direction of desired shift.

2.2 ²³Na NMR STUDIES OF ION TRANSPORT ACROSS THE MEMBRANE OF PHOSPHATIDYLCHOLINE VESICLES

2.2.1 Introduction

A membrane is a layer which separates two solutions, differs in chemical composition from both of them, forms a sharp boundary towards both these solutions and exhibits different permeability for individual

components of the solutions.²⁷⁵ This control of ion movement is clearly of fundamental importance since it will directly affect such factors as cellular pH and various osmotic and metabolic functions.

In order to understand at least some of the phenomena occurring at biological membranes very simple models which are seemingly quite distant from living nature, must be used. This is a difficult task when the extreme complexity of the biological membrane is considered. However, if we gave up we would lose the hope of elucidating basic processes in organisms. Our present-day understanding of the structure and dynamics of natural biomembrane systems owes a considerable amount to the development and study of model systems. The model biomembrane systems are based on the present consensus view of biomembrane structures: biomembranes are built on a liquid bilayer matrix.

Single bilayered phospholipid vesicles and multi-layered liposomes have proven to be useful for studying some permeability mechanism, as well as for gaining better information on the mode of interaction between membrane proteins and lipids.²⁷⁶ These systems may have important applications in Biology and Medicine.²⁷⁷ Their usefulness is enhanced by the fact that the aqueous interior is composed of whatever solution was used to disperse the lipid. This solution is cut off from the surrounding solvent by the wall of lipid. The validity and power of model structures as tools in the investigation of the architecture and function of biological membranes have been well demonstrated in a number of review articles²⁷⁸⁻²⁸³ and books^{84,88,284-286} devoted to the subject.

Phospholipids and glycolipids that contain some unsaturated fatty acids spontaneously form lipid bilayers (given the right experimental conditions) in which the polar head groups are exposed to the aqueous

phase and the hydrocarbon tails are buried in the van der Waals contact with one another. The hydrophobic effect⁵⁸ provides the driving force for the formation of lipid bilayer and biological membranes. These lipid bilayers form closed vesicles (Fig 2.30) that are similar in many respects to biological membranes. The absence of strong attractive forces in the interior of the bilayer makes it fluid and deformable and the hydrocarbon tails have considerable mobility.

The phospholipids are distributed asymmetrically between the inner and outer halves of the bilayer. This asymmetry results partly from steric considerations and partly from electrostatic effects. Since the bilayer (or membrane) is highly curved in small vesicles (Fig 2.30) there is less room in the inner half than in the outer half. The ionic heads therefore repel one another more on the inner surface of the membrane than on the outer surface, and the tails are more tightly packed in the inner half of the bilayer.

Large unilamellar vesicles (LUV) can be prepared by the removal of the detergent, n-octyl- β -D-glucopyranoside, from micelles of egg yolk phosphatidylcholine (egg PC).²⁸⁸ This method leads to the formation of LUV with external diameters in the range 200-600nm. Fig 2.31 is representative of the distribution of sizes of LUV formed in this work.

Using these preparations it is possible to study the permeability, electrical characteristics of lipid bilayers and to follow transport kinetics in situations where no electrochemical gradients exist (ie by equating the chemistry of the internal and external aqueous solutions). Artificial bilayers possess a high resistivity and a lower ion permeability than natural membranes and do not show selectivity for the passage of various ions.²⁸⁹ Several recent studies of hydrogen ion movements across unilamellar phospholipid vesicle membranes show that

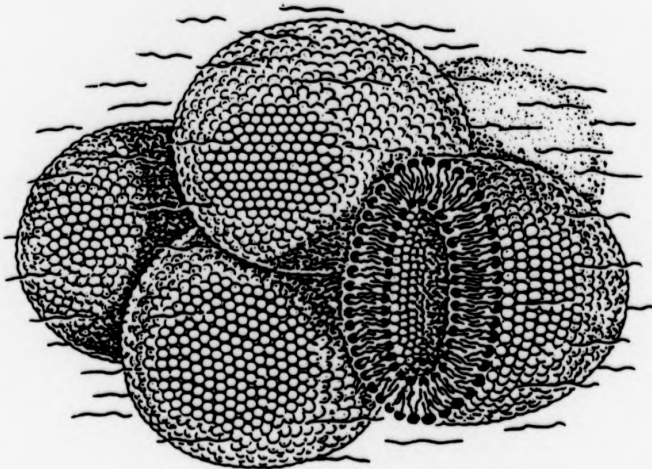


Fig 2.30 A representation of single-walled bilayer vesicles. Each vesicle contains a volume of water which is separated from the extracellular water.²⁸⁷



Fig 2.31 Electron microscopy of egg phosphatidylcholine vesicles prepared by using a molar detergent/lipid ratio 15:1, examined by negative staining. The electron micrograph shows an average area of the total field (x 50 000).

— ca 200nm



Fig 2.31 Electron microscopy of egg phosphatidylcholine vesicles prepared by using a molar detergent/lipid ratio 15:1, examined by negative staining. The electron micrograph shows an average area of the total field ($\times 50\ 000$).

— ca 200nm

these membranes are several orders of magnitude more permeable to protons and/or hydroxyl ions than to other small, monovalent ions,²⁹⁰⁻²⁹³ with a net H^+/OH^- permeability of $\sim 10^{-4} \text{ cm s}^{-1}$, compared with permeabilities of $10^{-10} - 10^{-14} \text{ cm s}^{-1}$ for other monovalent cations. However, the incorporation of certain ionophores and/or proteins may alter the properties of these membranes considerably. With the addition of these molecules, the membrane may acquire selectivity, electrical excitability, and even chemical receptor properties.^{80,294}

The recent development of aqueous shift reagents for metal cationic nmr^{197-200,204,273} have been used in bioinorganic chemistry, particularly in the study of transport of alkali-metal ions (Na^+ and Li^+) across model²⁰³ and real²⁰⁵ biological membranes.

In this work, the transport process is directly monitored using the nmr of the transported species. The method of employing a shift reagent to separate the resonances of the intra- and extracellular resonances of species under study is extended here. Specifically, the transport of sodium metal ions through phospholipid membranes of vesicles using ^{23}Na nmr and employing $Dy(PPP)_2^{7-}$ as the shift reagent is considered. The method is non-destructive and can be applied for both very slow kinetics (halflives longer than several minutes) as well as very fast rates (halflives shorter than 10^{-3} s). For the fast rates, where transport is dynamic on the nmr timescale, the concentration of sodium ions is kept the same in the bulk aqueous solutions on either side of the LUVs and the pH is assumed to be equal because of rapid influx and efflux of H^+/OH^- ions.²⁹⁰⁻²⁹³

In these preparations, about 2.5% of the sodium ions are intravesicular while the rest is dissolved in the bulk solvent. The single line observed in the spectrum (Fig 3.5b) thus consists of a

superimposition of both the signals of the inner and outer sodium ions. In order to monitor the transport between the inner and outer compartments we must be able to record both of the signals separately. A discrimination between the two signals can be achieved by using the paramagnetic shift reagent, $\text{Dy}(\text{PPP})_2^{7-}$. The shift reagent anion was found to be impermeable to the large unilamellar vesicles.

The central topic of this section is the consideration of substances which are able to induce ionic permeability in inert model membranes. The model membrane system has been treated with naturally occurring (monensin) and synthetic (crown-ethers) ionophores. Interpretations of their effects is then based upon a knowledge of their chemical structure.

2.2.1 Discussion of Monensin Mediated Transport

The monocarboxylic polyether antibiotics which are isolated from Streptomyces form a well defined class of carriers for alkaline and alkaline earth cations. The carrier provides a polar interior for binding the cation and a hydrophobic exterior for solvating in the hydrocarbon phase. This generally reduces the energy for transferring the ion across the membrane. Among these cation-carriers, monensin shows the greatest selectivity towards sodium ions.^{295,296} The selectivity of ion-transport mechanisms may be explained in general terms by the difference between the energies of binding and solvation for different ions. Furthermore, these cation-carriers do not affect the electrical properties of lipid bilayers.²⁹⁷

Although antibiotic ionophores have been widely used in biochemical research in the investigation of the effect of ions on cell metabolism, there is no evidence that they serve any transport function in vivo or that ionophores associated with transport enzymes behave in a similar

manner.

To study monensin mediated transport of sodium ions across the vesicular membrane, the line broadening of the inner signal can be monitored as the monensin concentration is altered. An example of spectra obtained using this procedure is shown in Fig 3.6. There is a conspicuous increase in linewidth upon increasing the ionophore concentration which we attribute to enhancement of the transport rate across the membrane. Using the equation,²⁹⁸

$$k_{\text{obs}} = \pi (W_{1/2}^1 - W_{1/2}^0)$$

the ionophore-mediated permeabilities could be determined. The results of LUV containing 250, 200, 175, 150, 120, 100, 75, 50 and 25 mM NaCl and equivalent extracellular cation concentration are presented in Figs 2.32 - 2.40 respectively.

In a separate experiment, the linewidth of the inner signal was observed to remain unchanged with time in the absence of monensin.

The above results (Figs 2.32 - 2.40) indicate that monensin accelerates the transport of Na^+ through vesicle; the sodium transport rate increases linearly with the ionophore concentration, indicating that the transport process is first order in monensin and therefore that the dominant transporting species is a 1:1 complex of sodium with the ionophore. The actual transport mechanism by an anionic ion-carrier can be discussed in terms of the following steps (Fig. 2.41).

1. Formation of a carrier-ion complex (MI) at the interface of the membrane;
2. Diffusion of the complex through the bilayer;
3. Dissociation of the ion from the carrier at the other interface of the membrane;
4. Complexation with another positive species N^+ (H^+ or M^+) followed by back diffusion.

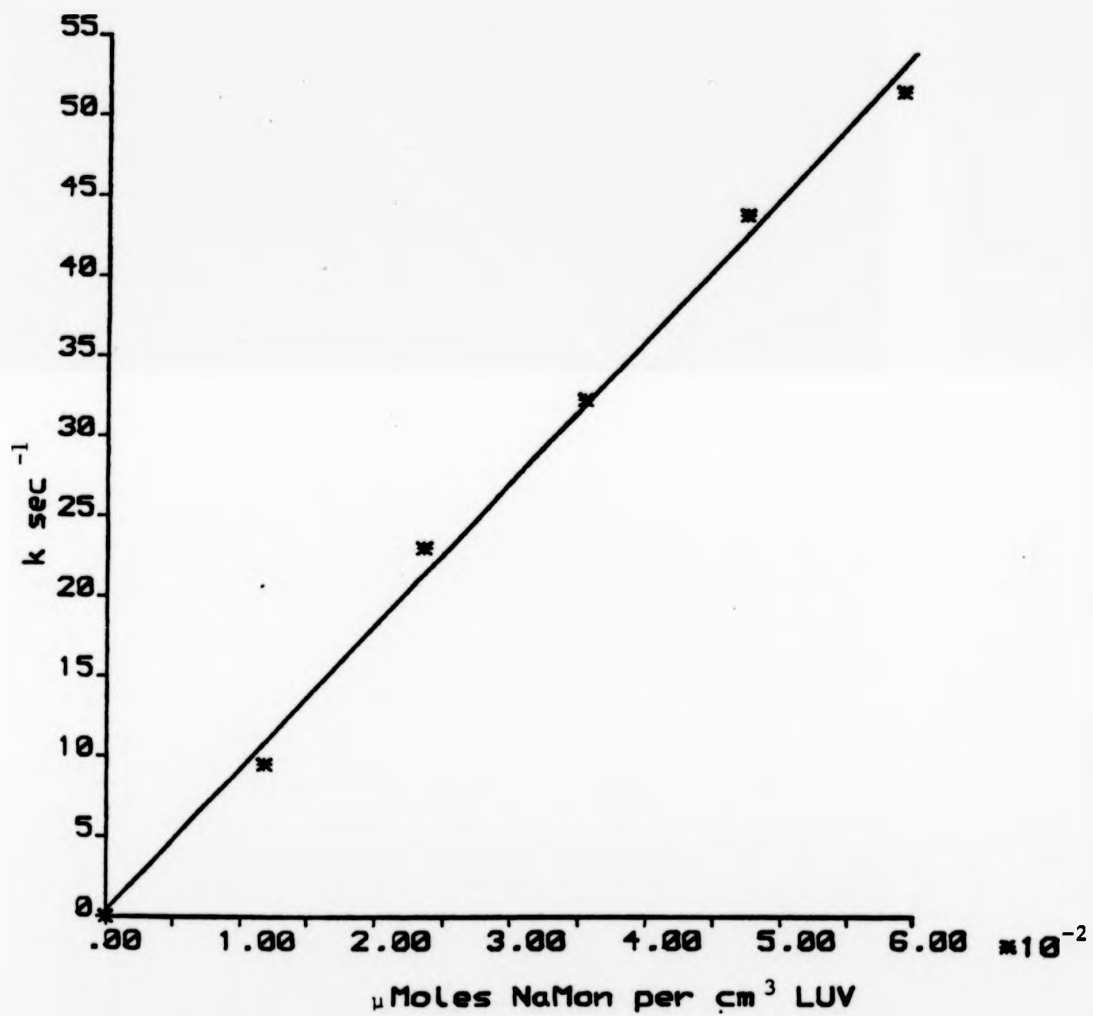


FIGURE 2.32 Monensin mediated Na⁺_{IN} transport in large unilamellar vesicles trapped with 250mM NaCl (21.19MHz).

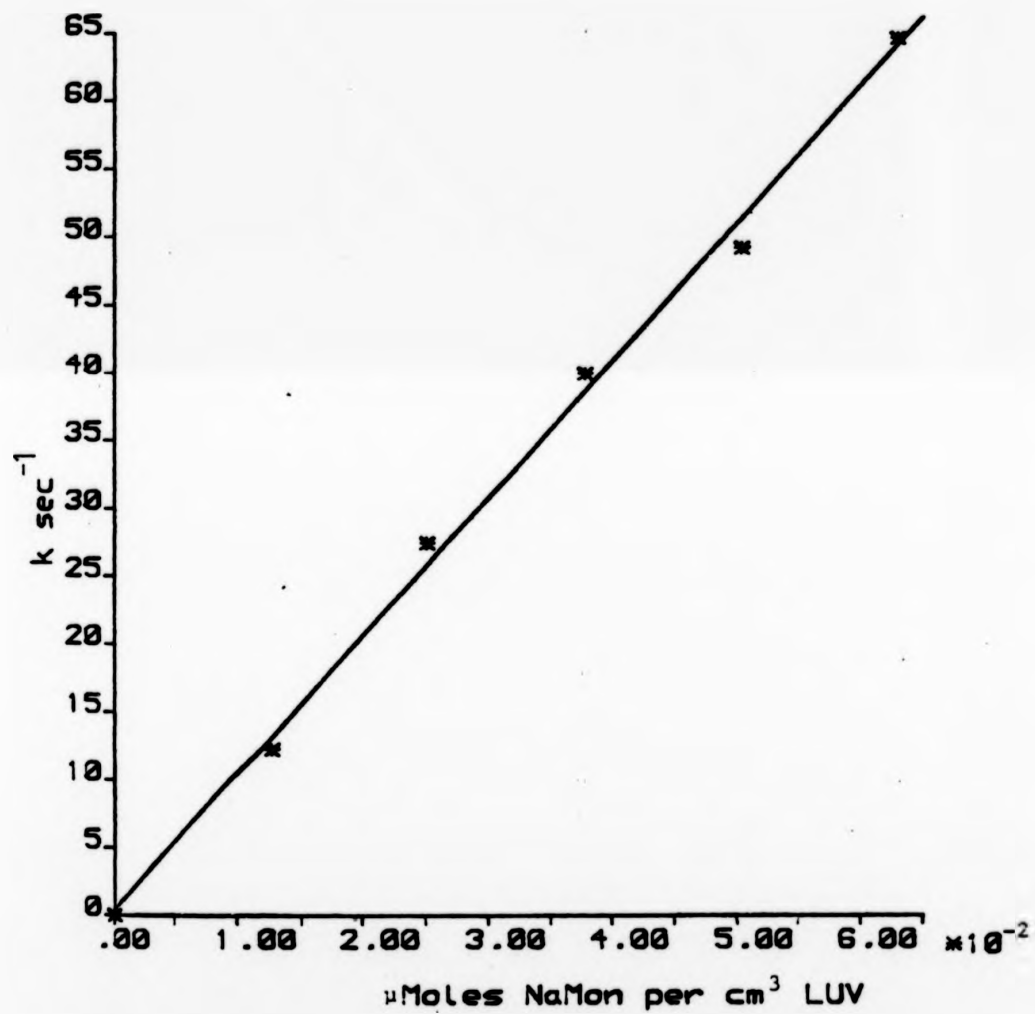


FIGURE 2.33 Monensin mediated Na_{IN}^+ transport in large unilamellar vesicles trapped with 200mM NaCl (21.19MHz).

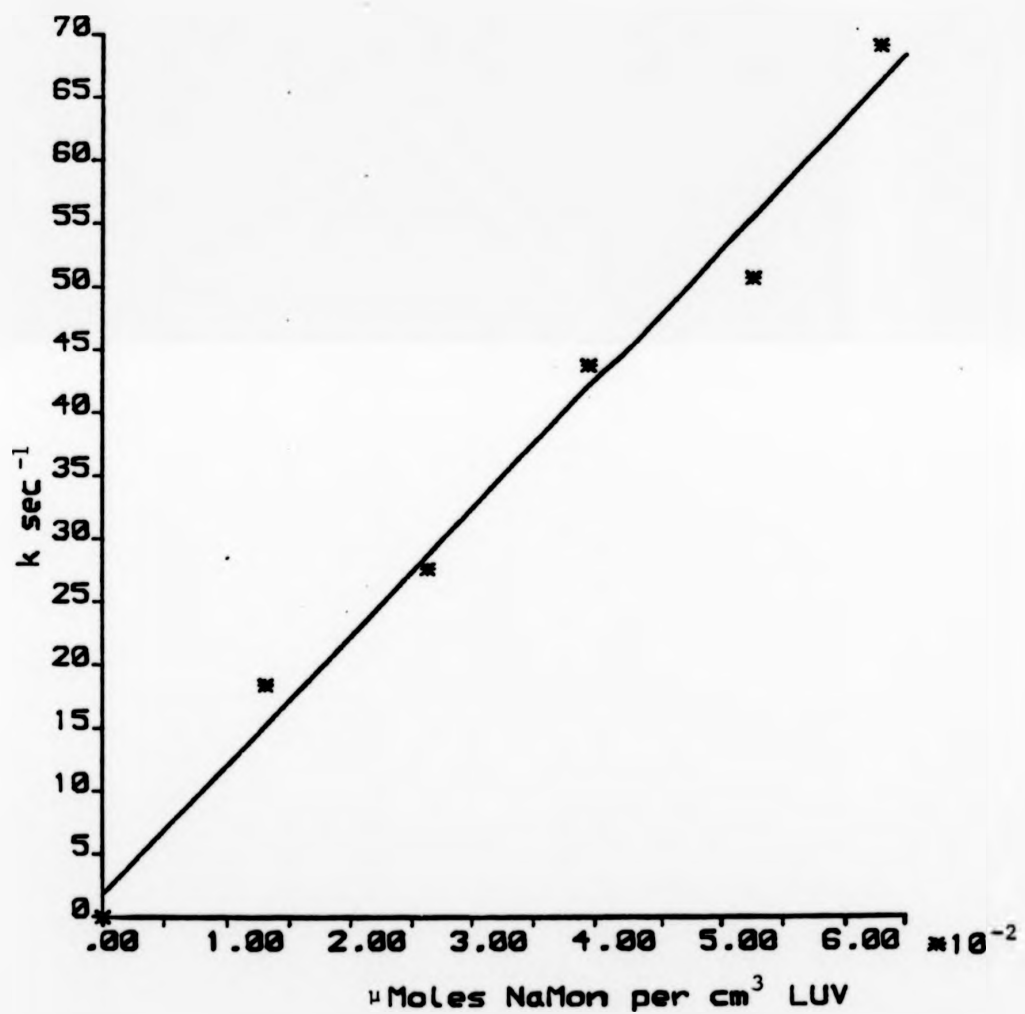


FIGURE 2.34 Monensin mediated Na^+ transport in large unilamellar vesicles trapped with 175mM NaCl (21.19MHz).

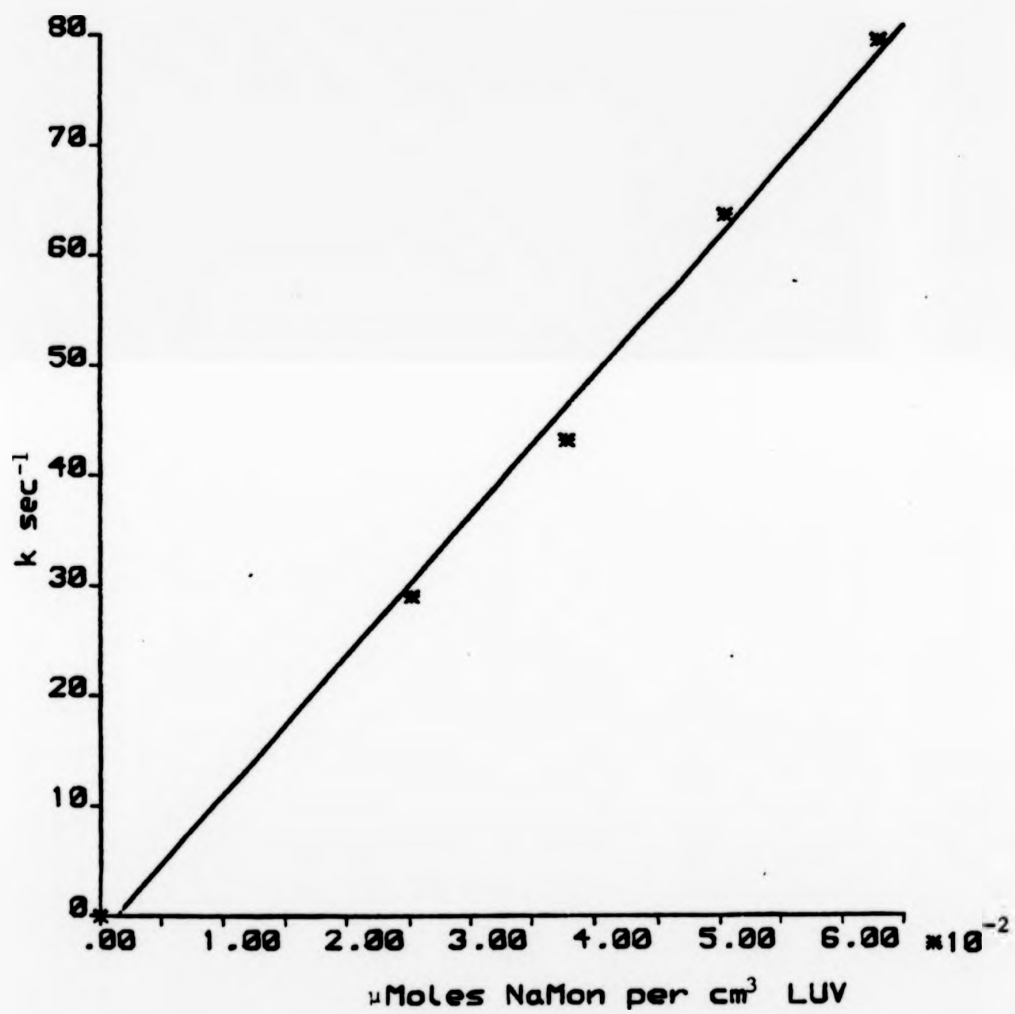


FIGURE 2.35 Monensin mediated Na^+_{IN} transport in large unilamellar vesicles trapped with 150mM NaCl (21.19MHz).

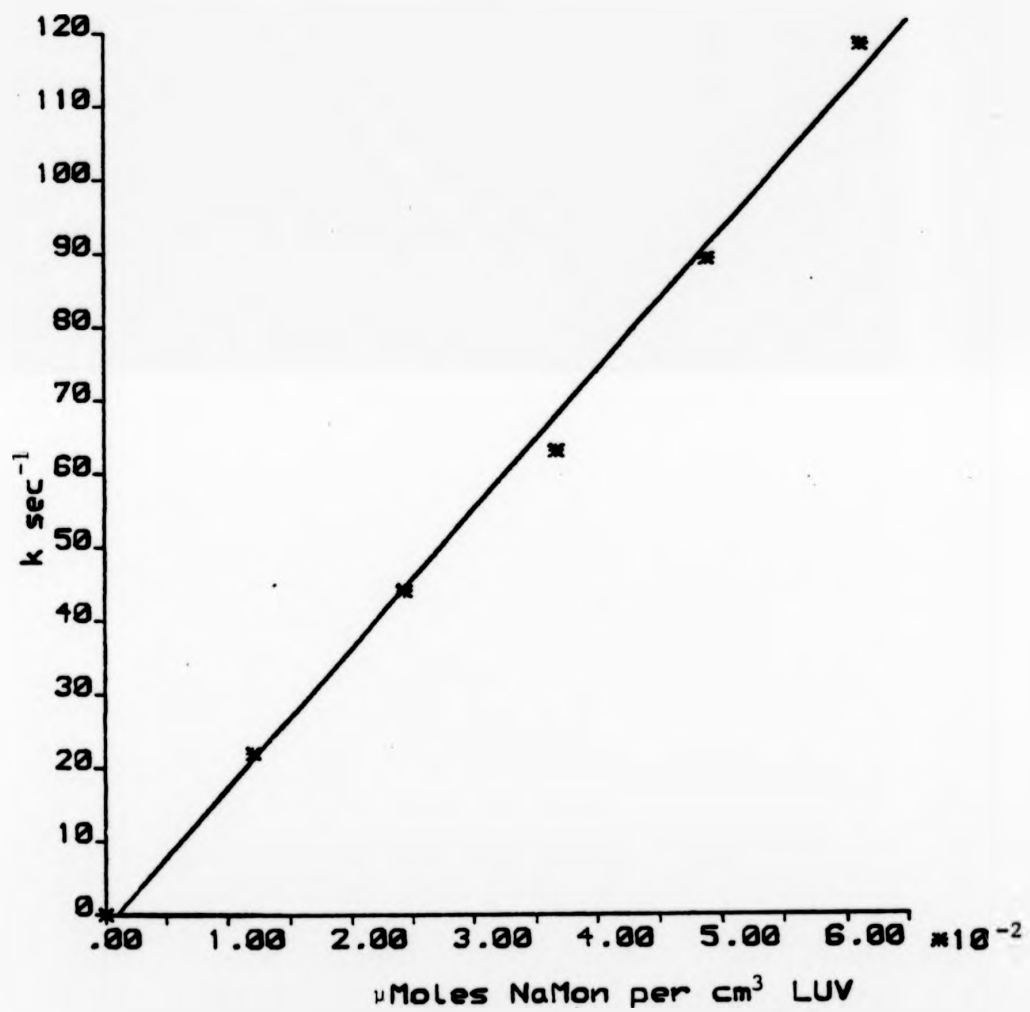


FIGURE 2.36 Monensin mediated Na⁺_{IN} transport in large unilamellar vesicles trapped with 120mM NaCl (21.19MHz).

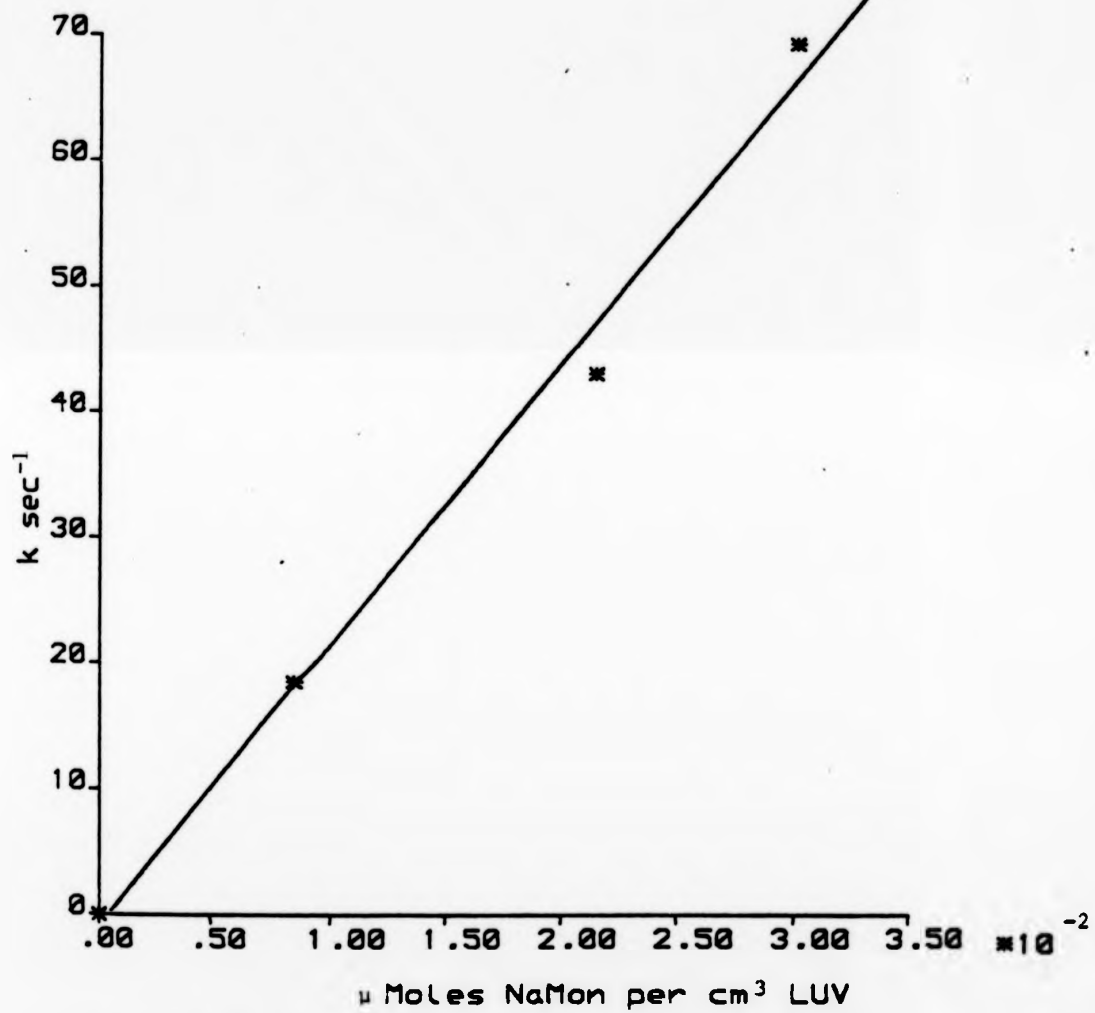


FIGURE 2.37 Monensin mediated Na^+ transport
in large unilamellar vesicles trapped with
100mM NaCl (21.19MHz).

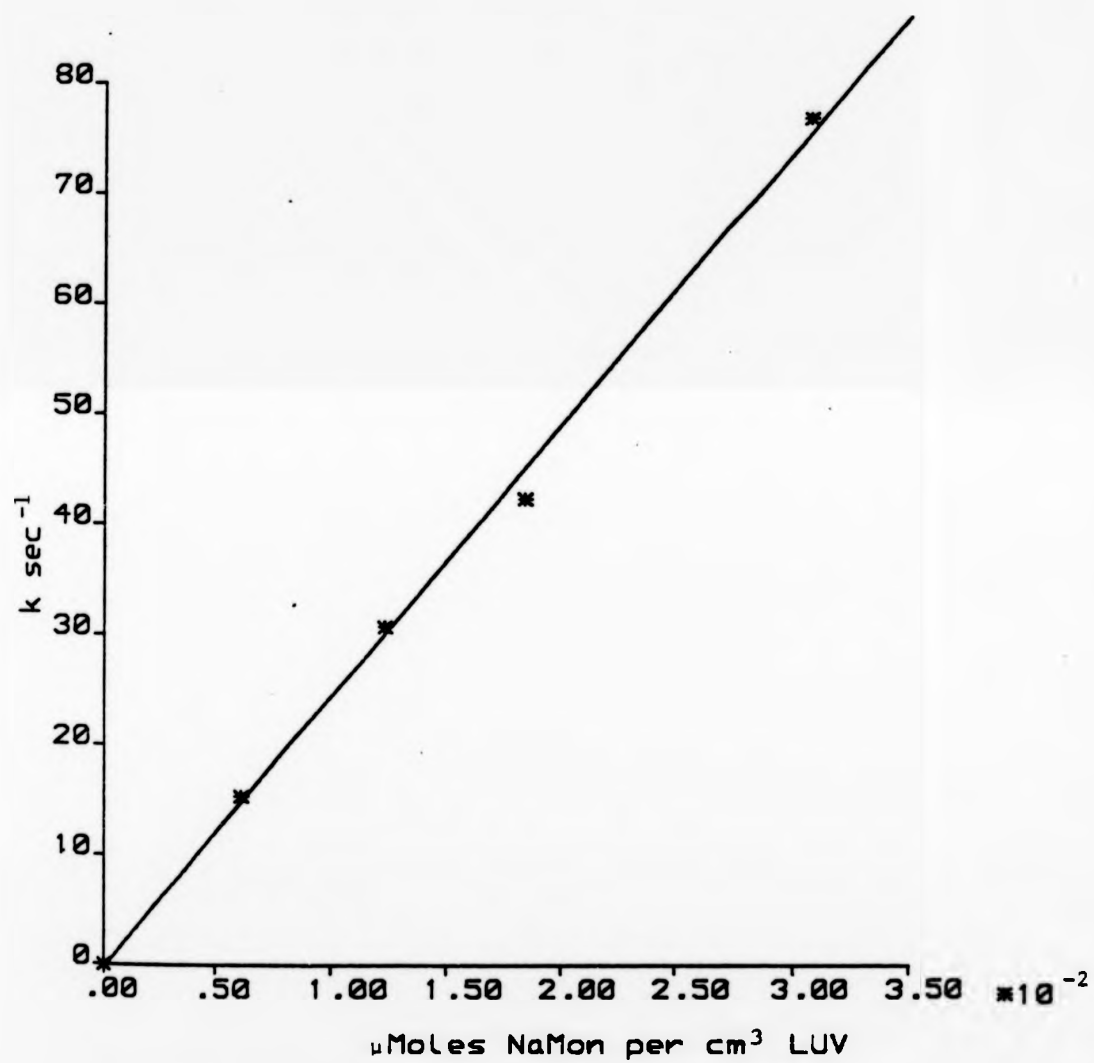


FIGURE 2.38 Monensin mediated Na_{IN}^+ transport in large unilamellar vesicles trapped with 75mM NaCl (21.19MHz).

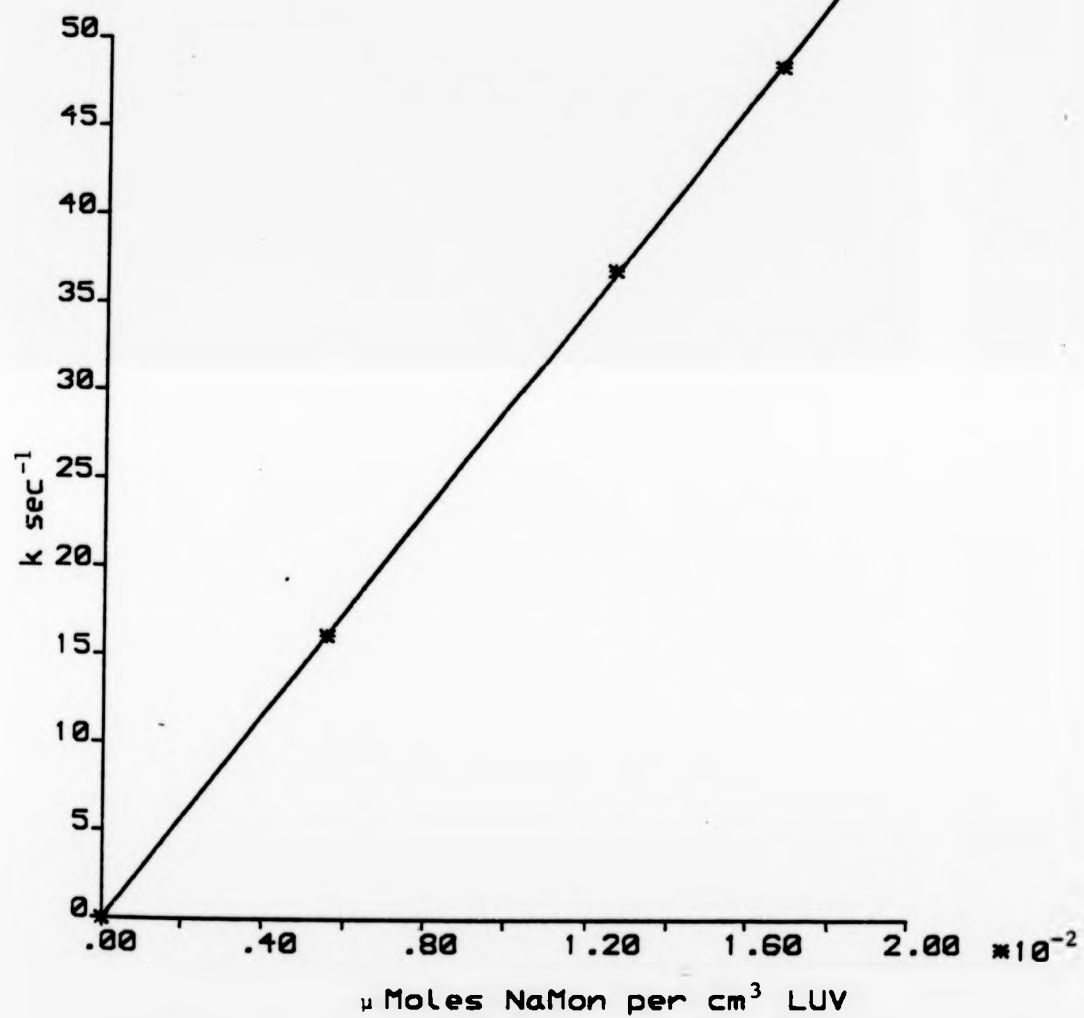


FIGURE 2.39 Monensin mediated Na_{NI}^+ transport in large unilamellar vesicles trapped with 50mM NaCl (21.19MHz).

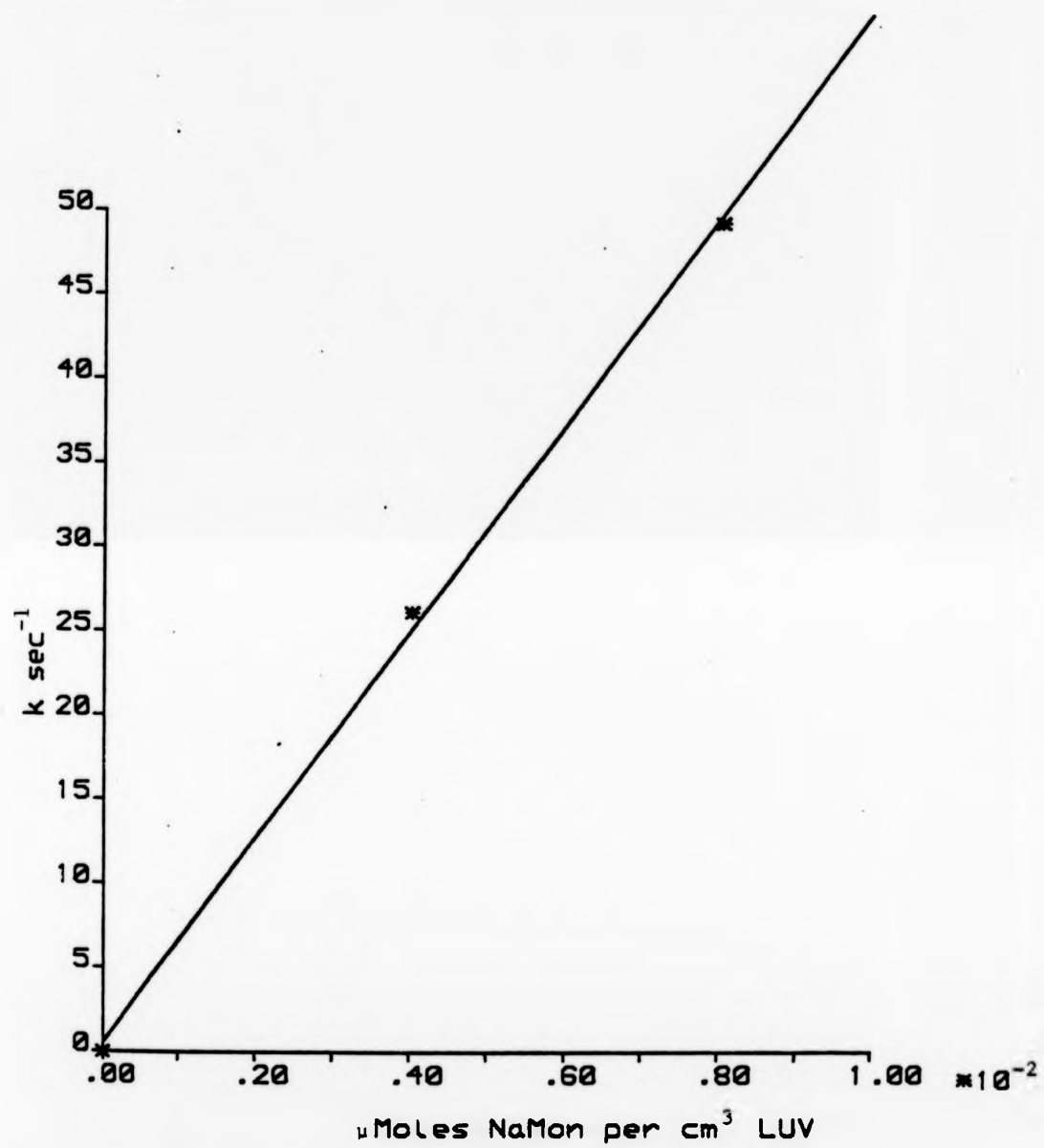


FIGURE 2.40 Monensin mediated Na_{NI}^+ transport in large unilamellar vesicles trapped with 25mM NaCl (21.19MHz).

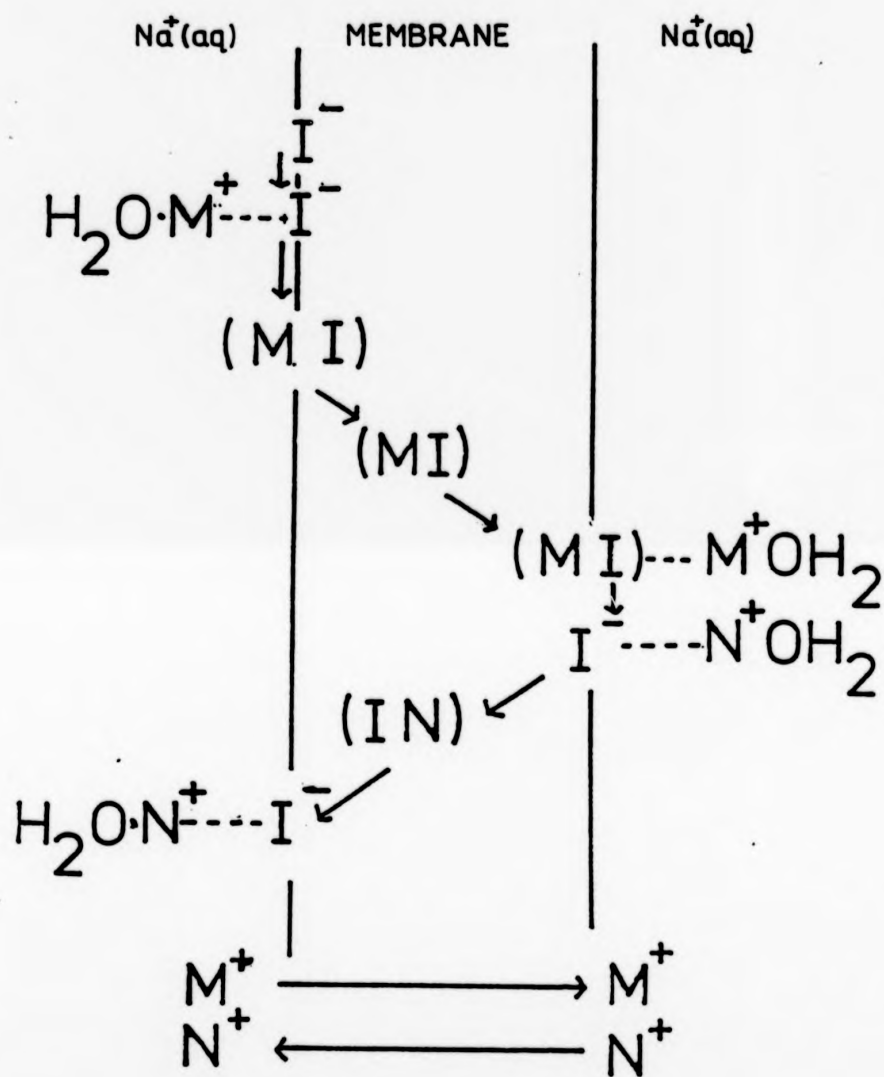


Fig 2.41

Schematic mechanism for an anionic ionophore mediated transfer of cations.

In the membrane the carboxylic carrier can exist in three different forms: the anionic I^- , protonated IH , and a complex with a cation M^+ , IM form. All three forms are located at the two interfaces between the membrane and the solutions. Heterogeneous reactions of proton exchange and cation complexation and decomplexation occur at each interface between the ionophore in the membrane and the ions H^+ or M^+ in the planes of closest approach of the adjoining aqueous solutions. In principle, each of these forms I^- , IH and IM can undergo a translocation reaction between the two sides of the membrane but the neutral species IH and IM will penetrate the interior of the bilayer far more readily than I^- .

Degani and Elgavish²⁹⁹ have proposed that the complex association-dissociation processes (step 1 and 3) determine the overall rate of transport. B G Cox³⁰⁰ has suggested that release of the cation following transport will be slower than capture of the cation under normal sodium concentration.

On plotting the ionophoric activity of monensin on Na^+ as a function of the NaCl concentration (Fig 2.42; Table 2.2), the result appears to indicate that increasing concentrations of Na^+ are converting monensin from an ionophore into an inhibitor. The transport is inhibited by the substrate itself, in a concentration dependent manner. A similar result was observed by Hamilton and coworkers in the study of Na^+ uptake by SV3T3 (Simian Virus 40) membrane vesicles.³⁰¹ They noted that at greater than 20mM Na^+ , monensin inhibits uptake by the vesicles.

Interaction between inorganic ions and biological membranes plays an important role in cell function and numerous studies have been performed on the interaction between ions and phospholipid membranes.^{302,303}

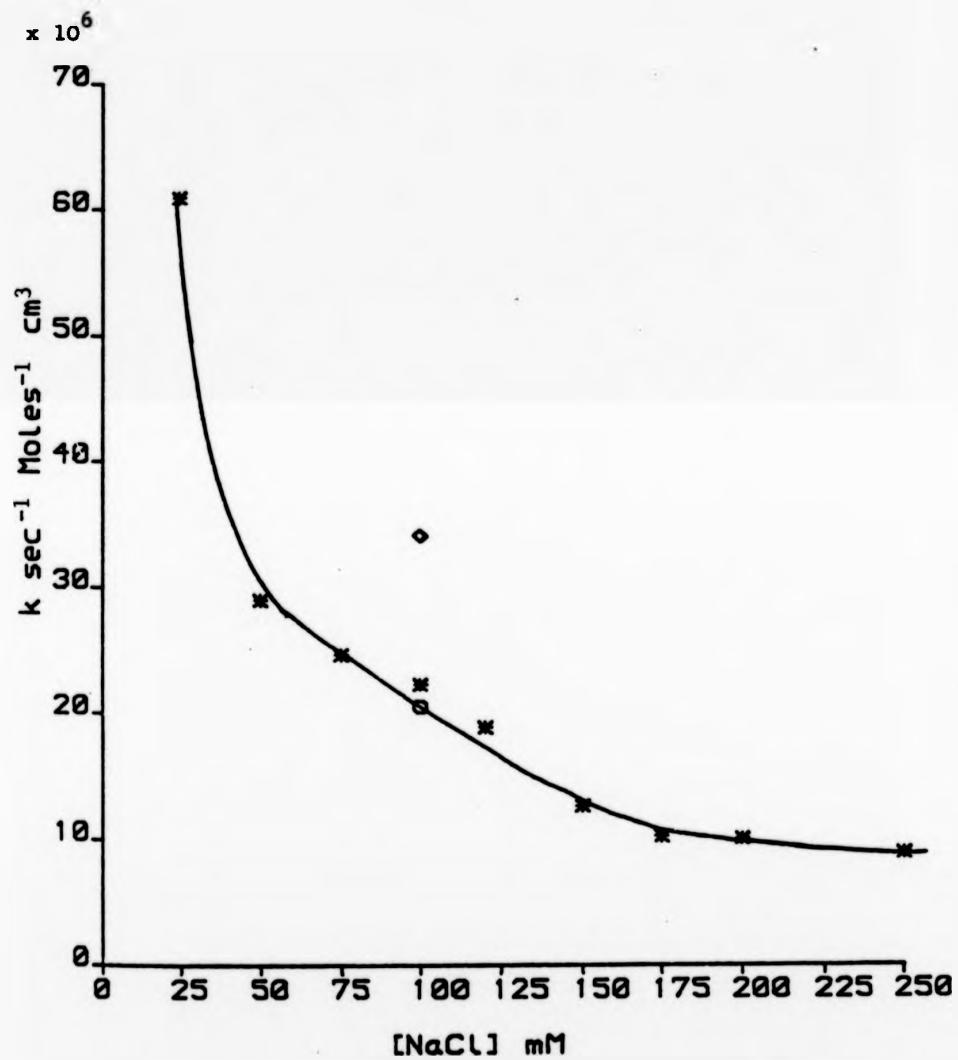


FIGURE 2.42 Monensin mediated Na_{IN}^+ transport in large unilamellar vesicles as a function of NaCl concentration.

○ - LUV trapped with 100mM NaCl + 100mM KCl
 ◊ - LUV trapped with 100mM NaCl and pH of final dialysis altered by 1.5 pH units.

TABLE 2.2 Monensin mediated Na_{IN}^+ transport in large unilamellar vesicles trapped with sodium chloride.

mM NaCl trapped in LUV	k $\times 10^6 \text{s}^{-1} \text{ moles}^{-1} \text{ cm}^3$	Correlation coefficient
250	8.93 ± 0.3	0.998
200	10.10 ± 0.3	0.998
175	10.25 ± 0.6	0.992
150	12.67 ± 0.5	0.998
120	18.91 ± 0.6	0.998
100	22.32 ± 1.5	0.995
75	24.66 ± 0.8	0.998
50	29.00 ± 0.2	1.000
25	60.92 ± 0.2	0.999

Information about ion binding in membrane systems was obtained by direct monitoring of the ions interacting with the bilayer through the quadruple splittings, as measured by nmr. Söderman et al³⁰³ concluded that at high salt concentration the phosphocholine head groups tend to be orientated perpendicular to the lipid bilayer surface. Hamilton et al³⁰¹ have suggested that Na^+ ions bind to the vesicles and that monensin inhibits this binding; thus accounting for the reduced accumulation of Na^+ with monensin present at greater than 20mM Na^+ . In order to determine whether some structural feature of the ionophore could be correlated with its ability to inhibit Na^+ uptake rates, they tested the effects of a number of ionophores of diverse structures on Na^+ uptake. The specificity for cation and ionophore from their results indicated that a precise interaction between the cation, ionophore, and membrane was required to inhibit Na^+ transport.

The possibility that differences in ionic strength are causing the variation in rate was ruled out by the preparation of LUV containing 100mM Na^+ and 100mM K^+ , inside and outside. The rate observed (Fig 2.43) is similar within experimental error to that observed using LUV trapped with 100mM Na^+ (Fig 2.42). The result indicates that the rate changes in Fig 2.42 are not due to changes in ionic strength.

However, on reducing the pH of the surrounding medium by ca 1.5pH units by the addition of concentrated hydrochloric acid (Fig 2.44) the rate of monensin mediated transport was observed to be ca 1.6 times faster compared with LUV trapped with 100mM NaCl (Fig 2.42) and a pH of ca 8.0 of the surrounding medium.

The second technique used to study monensin mediated cation transport was, selective inversion. Selective inversion first proposed by Forsen and Hoffmann,³⁰⁴⁻³⁰⁷ is important in the study of chemical

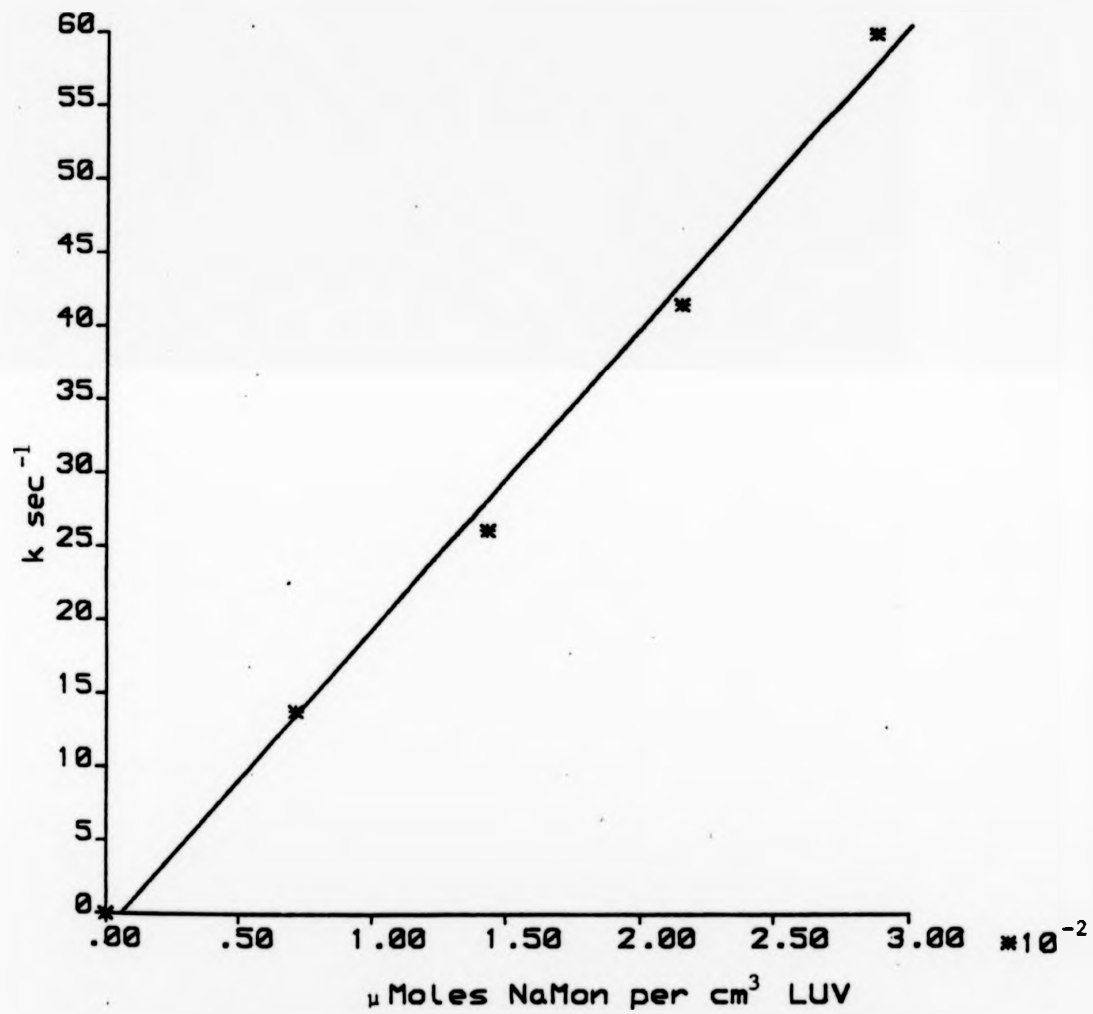


FIGURE 2.43 Monensin mediated Na^+ transport in large unilamellar vesicles trapped with 100mM NaCl + 100mM KCl (21.19MHz).

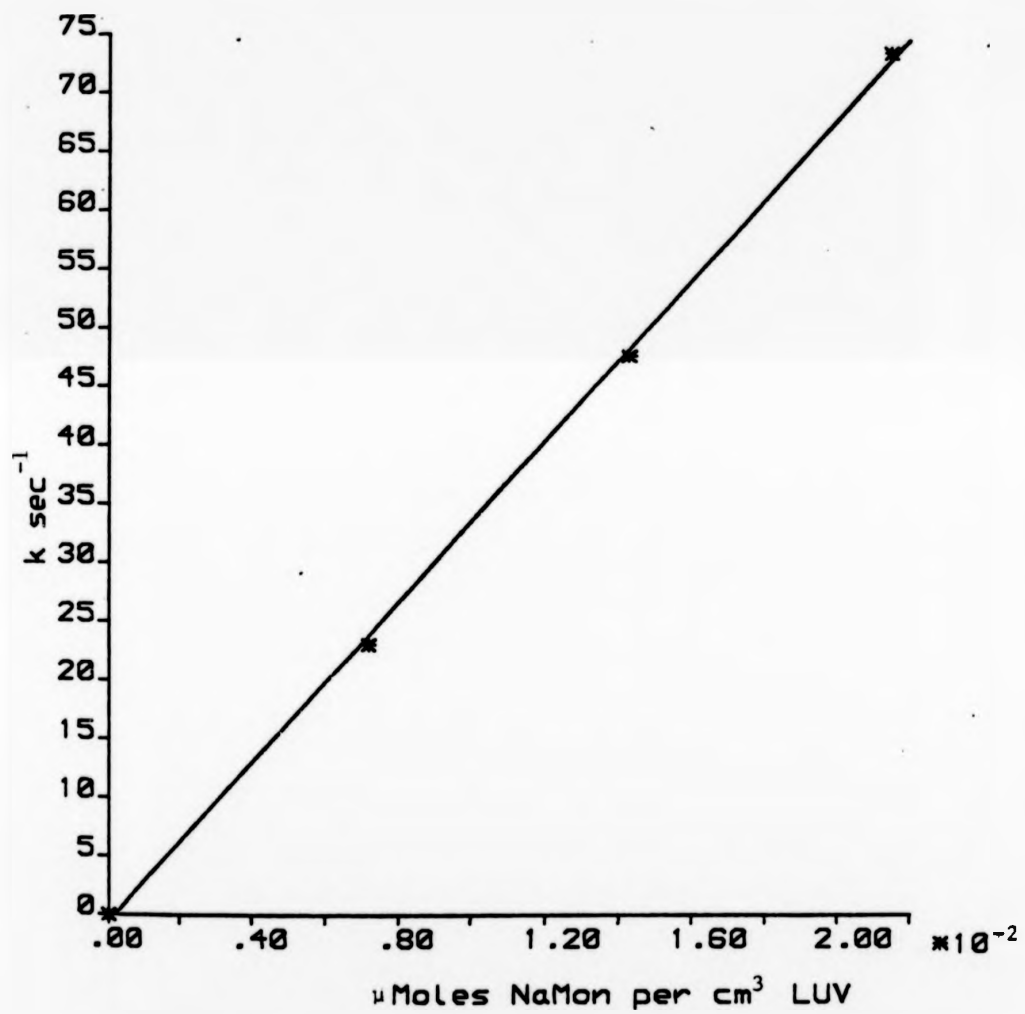


FIGURE 2.44 Monensin mediated Na_{IN}^+ transport in large unilamellar vesicles trapped with 100mM NaCl (21.19MHz). pH Final dialysis = 8.1

exchange processes by following the transfer of magnetization. In this technique the longitudinal magnetization of a resonance is measured as a function of time after the perturbation of another resonance with which it is exchanging. This perturbation may be the imposition of a saturating field, or a 180° pulse, or various other possibilities. The largest effects are seen when the longitudinal magnetizations of the exchanging sites are monitored after one resonance is selectively inverted, and this is the experiment we chose.

The experiments were performed using the pulse sequence as summarised in Fig 3.9. The expressions for magnetization at sites A (Na_{IN}^+) and B (Na_{OUT}^+) as a function of the delay τ between inversion and sampling are:³⁰⁸

$$\begin{aligned} M_Z^A/M_O^A &= 1 - (2k_A/\beta) \exp[-\frac{1}{2}(\alpha - \beta)\tau] - \exp[-\frac{1}{2}(\alpha + \beta)\tau] \\ M_Z^B/M_O^B &= 1 - (1/\beta) \{ \beta + R_B - R_A \} \exp[-\frac{1}{2}(\alpha + \beta)\tau] \\ &\quad + (\beta + R_A - R_B) \exp[-\frac{1}{2}(\alpha - \beta)\tau] \end{aligned}$$

where

$$\alpha = R_A + R_B, \quad \beta = [(R_A - R_B)^2 + 4k_A k_B]^{\frac{1}{2}}$$

and

$$R_A = k_A + (1/T_{1A}), \quad R_B = k_B + (1/T_{1B})$$

Thus by monitoring the recovery curves of sites A and B it is possible in favourable cases to extract both the exchange rate constants, k_A and k_B and the longitudinal relaxation times T_{1A} and T_{1B} , of the two sites.

The non-selective pulse sequence $180^\circ - \tau - 90^\circ$ was first used to

measure the longitudinal relaxation time of the sodium ions in the bulk solution, T_{1B} , and in the intravesicular bulk solution, T_{1A} , in the absence of ionophore monensin. Analysis of respective results yield the values $T_{1B} = 19.96$ and $T_{1A} = 55.6$ msec.

The experimental and calculated recovery curves of site A obtained in the presence of 1.72×10^{-2} μ Moles and 3.44×10^{-2} μ Moles monensin per cm^3 of LUV suspension are presented in Figs 2.45 and 2.46 respectively.

An attempt at a least squares analysis of the results was attempted by use of a computer program for a BBC model B microcomputer written in BASIC. The program accepted a range of values of T_{1A} , T_{1B} , k_A and k_B . However, T_{1B} was kept constant (20 msec) and since k_A is $k_B \times P_B/P_A$, where P_B (ca 0.975) and P_A (ca 0.025) are the respective populations of Na^+ ions inside and outside, only one rate constant was specified. Calculated points were compared with experimental points and the sum of the squares of the errors printed. A minimum which gave a reasonable fit was found for each of the two monensin concentrations examined.

The calculated curve that fits the results obtained with 1.72×10^{-2} μ Moles monensin per cm^3 of LUV was obtained using the values $T_{1A} = 48 \pm 2$ msec, $T_{1B} = 20$ msec, $k_A = 15 \pm 3 \text{ s}^{-1}$ and $k_B = 0.375 \text{ s}^{-1}$ (Table 2.3). While the calculated curve that fits the results obtained with 3.44×10^{-2} μ Moles monensin per cm^3 of LUV was obtained using the following values, $T_{1A} = 33 \pm 2$ msec, $T_{1B} = 20$ msec, $k_A = 30 \pm 3 \text{ s}^{-1}$ and $k_B = 0.75 \text{ s}^{-1}$ (Table 2.3). The results obtained here are similar within experimental error to those obtained in the study of monensin mediated Na^+ transport by line shape analysis: LUV trapped with 200mM NaCl, Fig 2.33, at 1.72×10^{-2} and 3.44×10^{-2} μ Moles

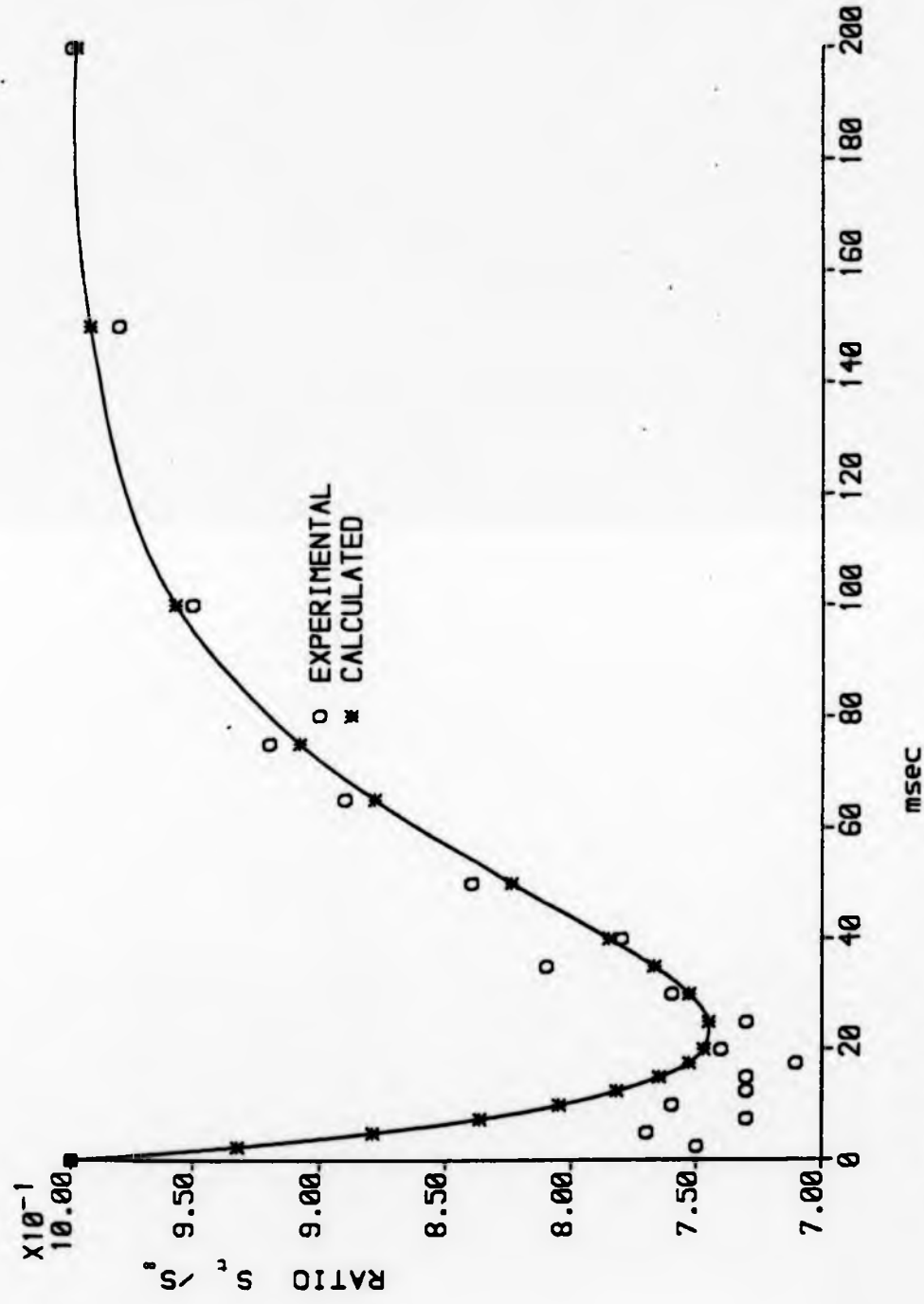


FIGURE 2.45 Ratio of S_t/S_∞ of Na^+ (95.23MHz) as a function of time, τ in the presence of 1.72×10^{-2} μ Moles monensin per cm^3 of LUV.

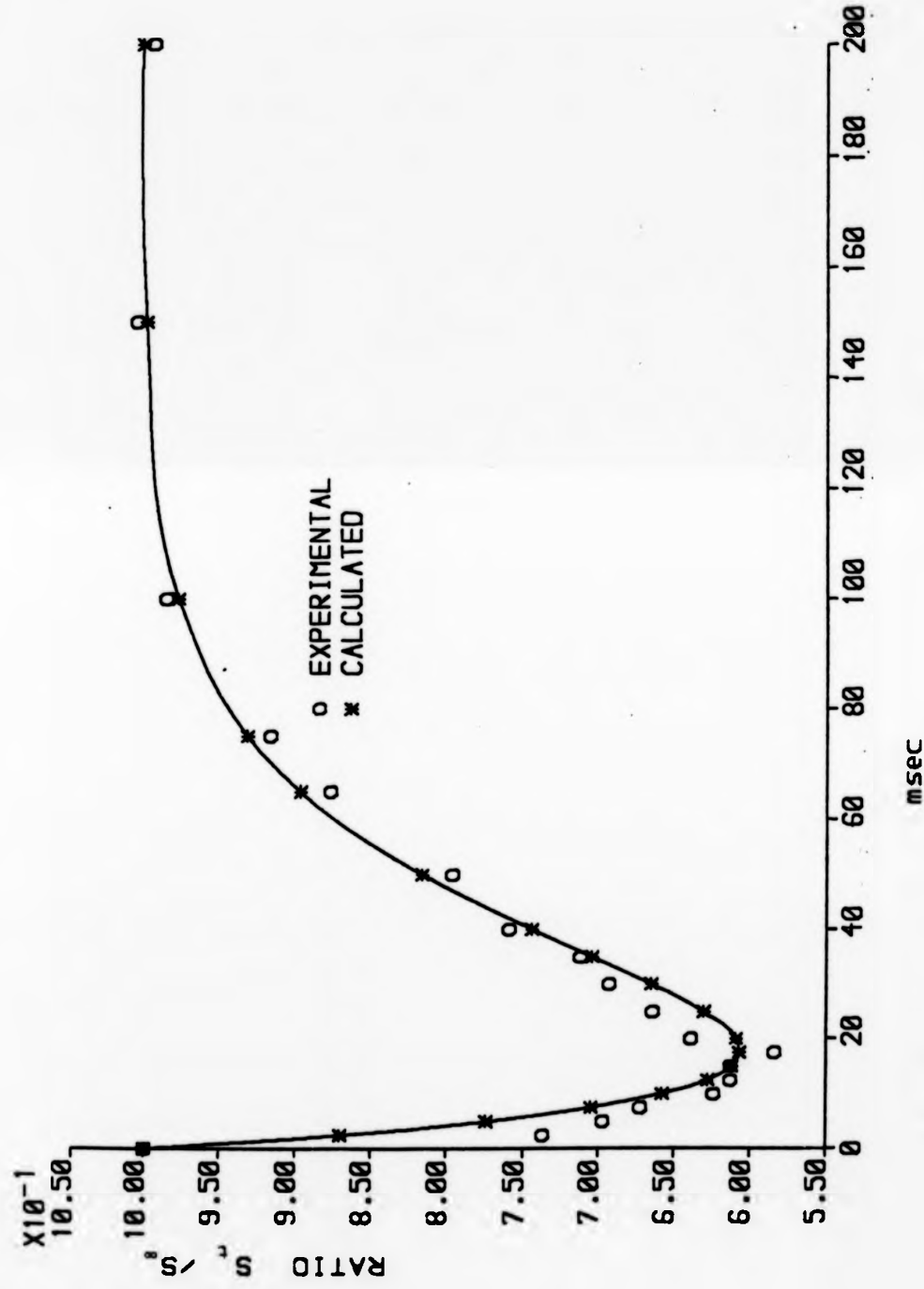


FIGURE 2.46 Ratio of S_t/S_∞ of Na^+ (95.23MHz) as a function of time, τ in the presence of 3.44×10^{-2} $\mu\text{Moles monensin per cm}^3$ of LUV.

TABLE 2.3

The calculated magnetization at site A(Na_{IN}^+), as a function of the delay τ .

$\mu\text{Moles monensin per cm}^3$ of LUV		
<hr/>		
	1.72×10^{-2}	3.44×10^{-2}
	<hr/>	
	$T_{1A} = 0.048$	$T_1 = 0.032$
	$T_{1B} = 0.02$	$T_{1B} = 0.02$
	$k_A = 15$	$k_A = 30$
	$k_B = 0.375$	$k_B = 0.75$
	<hr/>	
sec	Ratio S_t/S_∞	Ratio S_t/S_∞
<hr/>		
0.0025	0.933	0.870
0.0050	0.879	0.774
0.0075	0.837	0.705
0.010	0.805	0.658
0.0125	0.782	0.628
0.0150	0.765	0.612
0.0175	0.753	0.607
0.020	0.747	0.609
0.025	0.745	0.631
0.030	0.753	0.665
0.035	0.767	0.704
0.040	0.785	0.744
0.050	0.824	0.816
0.065	0.878	0.896
0.075	0.908	0.931
0.100	0.957	0.977
0.150	0.992	0.998
0.200	0.998	1.000
<hr/>		

monensin per cm^3 LUV yield k_A values of 12.2 s^{-1} and 35.1 s^{-1} respectively.

2.2.2 Discussion of Crown Ether Mediated Transport

Macrocyclic polyethers have been known for a long time and gained much attention when it was found that many such "crown" compounds form stable complexes with alkali cations and alkali earth cations.

[18]-Crown-6 (8) and [15]-crown-5 (9) are examples of synthetic macrocyclic polyethers and have been well characterised as carriers of monovalent cations.^{136,145,151}

In this work, the Na^+ ion mediated transport across large unilamellar vesicles using [15]-crown-5 derivatives (10 and 11) was investigated. The compounds [18]-crown-6 (8), [15]-crown-5 (9) and 2-(hydroxymethyl)-[15]-crown-5(10) form positive complexes while the acid derivative of [15]-crown-5 (11) forms a neutral complex with monovalent cations. Analogous to monensin, the crown ethers should become incorporated in the hydrophobic membrane phase by virtue of their lipophilic nature and effect a shuttle service between the interior and exterior environments.

To demonstrate sodium transport, a concentration gradient in sodium was established by preparing vesicles containing only aqueous sodium chloride on the inside, but having an equimolar concentration of Na^+ + K^+ outside the vesicles. Sodium transport would thus be mediated by a counter transport system involving the potassium ions or hydrogen ions which would maintain the electric potential across the membrane.

The [15]-crown-5 derivatives are selective for the inclusion of sodium cations in a 1:1 complex. The actual stability constants for the 5-oxygen crown complexes (benzo-[15]-crown-5) with sodium and potassium

monensin per cm^3 LUV yield k_A values of 12.2 s^{-1} and 35.1 s^{-1} respectively.

2.2.2 Discussion of Crown Ether Mediated Transport

Macrocyclic polyethers have been known for a long time and gained much attention when it was found that many such "crown" compounds form stable complexes with alkali cations and alkali earth cations.

[18]-Crown-6 (8) and [15]-crown-5 (9) are examples of synthetic macrocyclic polyethers and have been well characterised as carriers of monovalent cations.^{136,145,151}

In this work, the Na^+ ion mediated transport across large unilamellar vesicles using [15]-crown-5 derivatives (10 and 11) was investigated. The compounds [18]-crown-6 (8), [15]-crown-5 (9) and 2-(hydroxymethyl)-[15]-crown-5(10) form positive complexes while the acid derivative of [15]-crown-5 (11) forms a neutral complex with monovalent cations. Analogous to monensin, the crown ethers should become incorporated in the hydrophobic membrane phase by virtue of their lipophilic nature and effect a shuttle service between the interior and exterior environments.

To demonstrate sodium transport, a concentration gradient in sodium was established by preparing vesicles containing only aqueous sodium chloride on the inside, but having an equimolar concentration of $\text{Na}^+ + \text{K}^+$ outside the vesicles. Sodium transport would thus be mediated by a counter transport system involving the potassium ions or hydrogen ions which would maintain the electric potential across the membrane.

The [15]-crown-5 derivatives are selective for the inclusion of sodium cations in a 1:1 complex. The actual stability constants for the 5-oxygen crown complexes (benzo-[15]-crown-5) with sodium and potassium

have been found¹³⁶ to be similar (ca 3.7 l mol^{-1} in methanol at 25°C) due to the stability of a 2:1 complex between crown and potassium it was therefore predicted that the transport of both ions could occur via a 1:1 complex (Na^+) or a 2:1 complex (K^+).

A schematic representation of the counter transport system existing is given in Fig 2.47. The crown ether carries the respective ions down their concentration gradients. The net result is the transport of Na^+ ion from inside to outside at the expense of a K^+ ion from outside to inside.

The height (intensity) of the Na_{IN}^+ resonance was recorded for each of the spectra as a function of time. Assuming the linewidth to be unchanged, the height is proportional to the peak area.

For a first order transport process, the rate equation is,

$$dA/dt = -kA$$

where k is the rate constant and A is the concentration, in our case, of sodium ions in intravesicular bulk solution. The equation is solved by dividing both sides by A and integrating,

$$\int (dA/A) = - \int k dt$$

$$\ln A = -kt + C$$

when time $t=0$, $A=A_0$ and $C = \ln A_0$

so that

$$\ln A_t = -kt + \ln A_0$$

If the amount of sodium inside the vesicles at infinite time is A_∞ , the

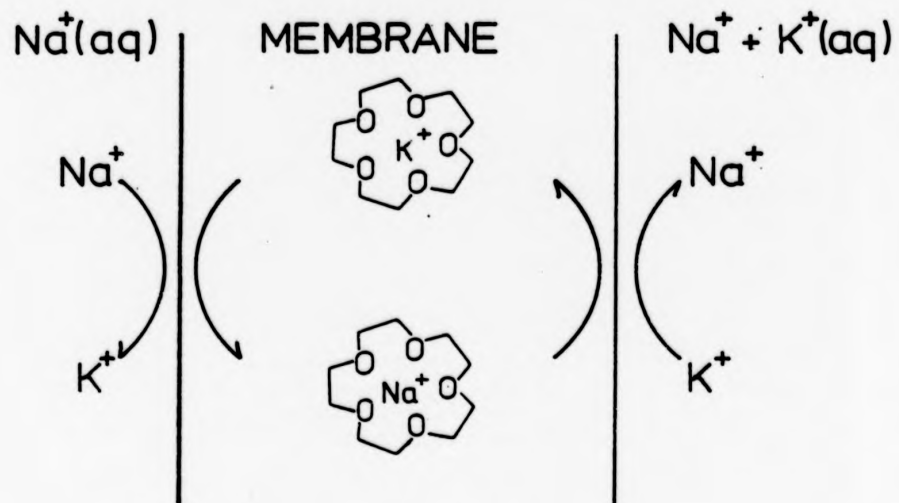


Fig 2.47

Schematic mechanism for carrier mediated counter-transport of sodium and potassium. (For simplicity the probable involvement of a 2:1 crown:potassium complex has been ignored since it is only the sodium transport which is of interest in this case.)

rate constant, k , can be found from the gradient of a graph of $\ln(A_t - A_\infty)$ vs t .

Figs 2.48 and 2.49 (a)-(c) present the results obtained with 4.0mM 2-(hydroxymethyl)-[15]-crown-5 (10) and 3.0mM [15]-crown-5 acid derivative (11) respectively.

An interesting result is observed with 3.0mM [15]-crown-5 acid derivative (11). It appears as if two distinct rate processes are being detected (Fig 2.49a): the first with a very fast reaction rate followed by a very slow reaction rate. In Tables 3.35 and 3.36 the values of S_t are listed as the height of the internal peak at the various times as this is proportional to the amount of sodium ions inside the vesicles. It follows that it should not fall below half its original value. However, in both experiments it did. A probable explanation for the lower than half values recorded after ca 3hr (Table 3.36) is that the vesicles are disintegrating. It is thus assumed that under the experimental conditions existing here, where we have an approximately 1:1 ratio of crown ether to egg PC, the vesicles are disintegrating at a slow rate. This slow rate is signified by the slow rate process observed in Fig 2.49a, while the initial fast rate process observed is probably due to transport by the [15]-crown-5 acid derivative (11).

If this is the case, then the slow rate should show an almost linear plot against time over the initial few hours (Fig 2.49a). A least square analysis of the last nine points gave a line of correlation coefficient 0.994 and the intercept on the Y-axis as 5.02. To correct the first five S_t values to take into account the disintegration rate of vesicles, the extrapolated values from Fig 2.49a were subtracted from the S_t values giving $S_{t(\text{corr})}$ (Table 2.4a). The rate constant is then obtained from the gradient of a graph of $\ln(S_{t(\text{corr})})$ vs t (Fig

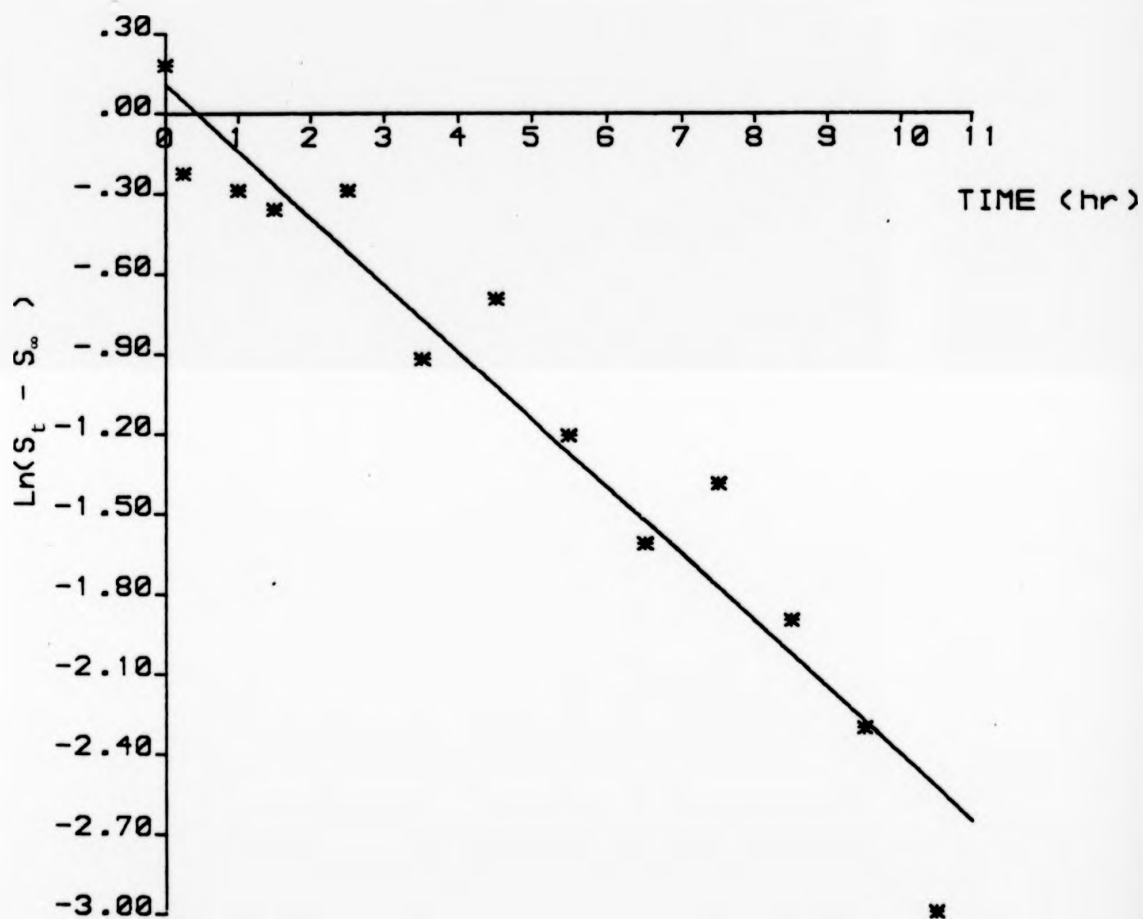


FIGURE 2.48 $\ln(S_t - S_\infty)$ of Na^+ resonance (21.19MHz) as a function of time in the presence of 4.0mM 2-(hydroxymethyl)-15-crown-5 in LUV trapped with 200mM NaCl. Surrounding medium contains 20mM Na_5PPP + 100mM KCl + 5.3mM DyCl_3

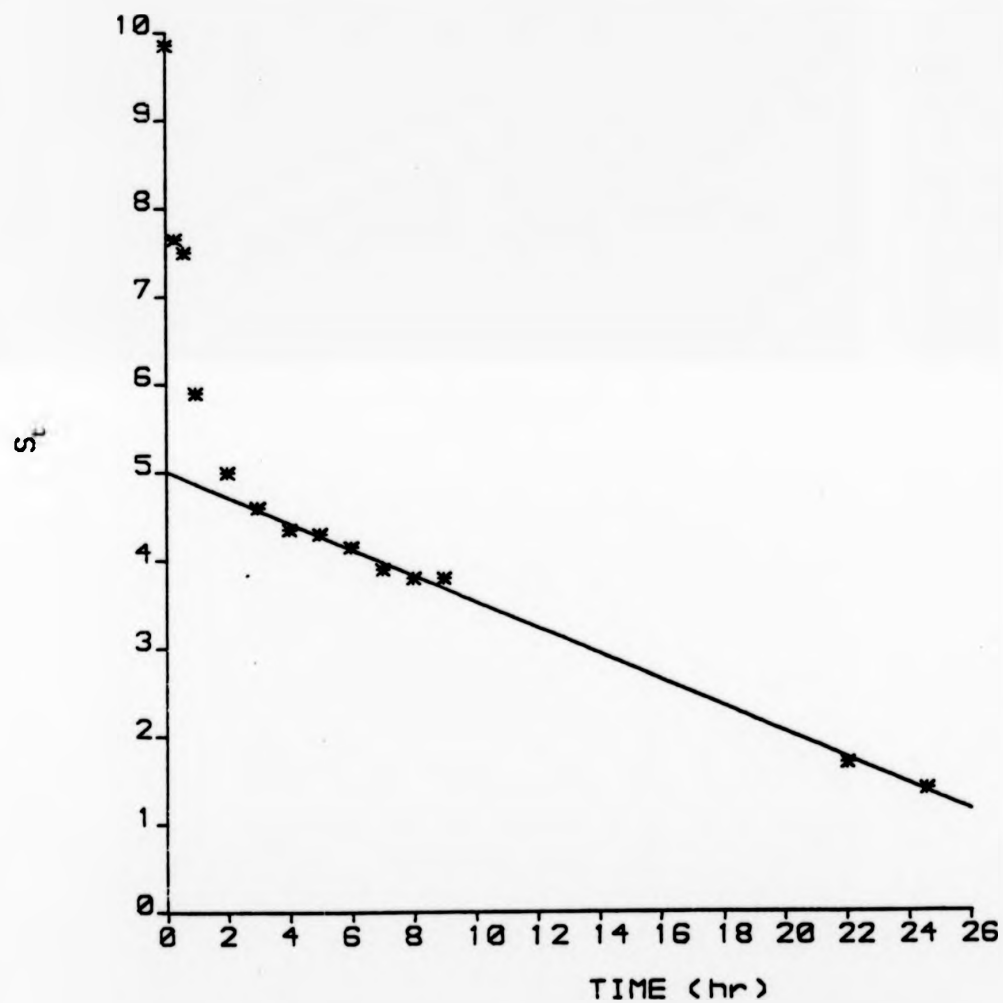


FIGURE 2.49a S_t of Na_{IN}^+ resonance (21.19MHz) as a function of time in the presence of 3.0mM 15-crown-5 derivative (11) in LUV trapped with 200mM NaCl. Surrounding medium contains 20mM Na_5PPP + 100mM KCl + 7.1mM DyCl_3

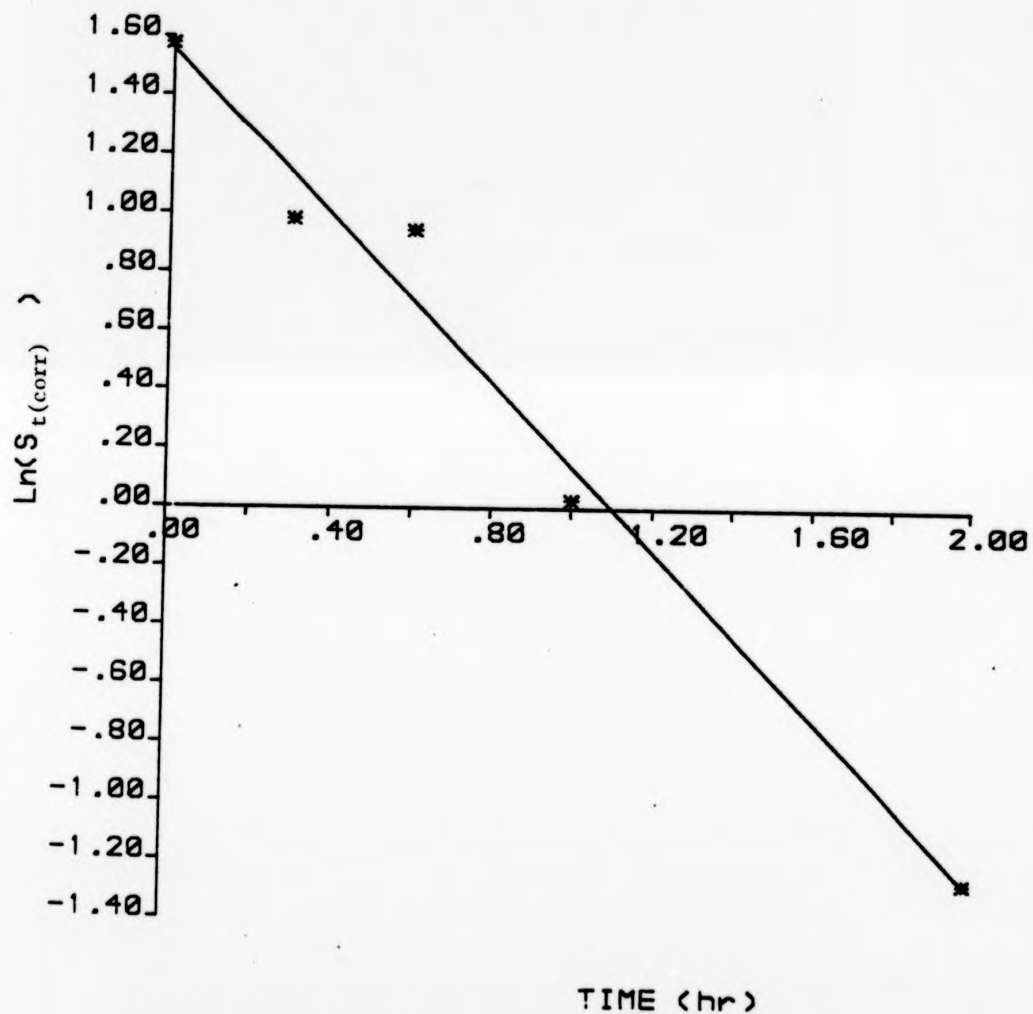


FIGURE 2.49b $\text{Ln}(S_{t(\text{corr})})$ of Na^+ resonance (21.19MHz) as a function of time in the presence of 3.0mM 15-crown-5 derivative(11) in LUV trapped with 200mM NaCl. Surrounding medium contains 20mM Na_5PPP + 100mM KCl + 7.1mM DyCl_3

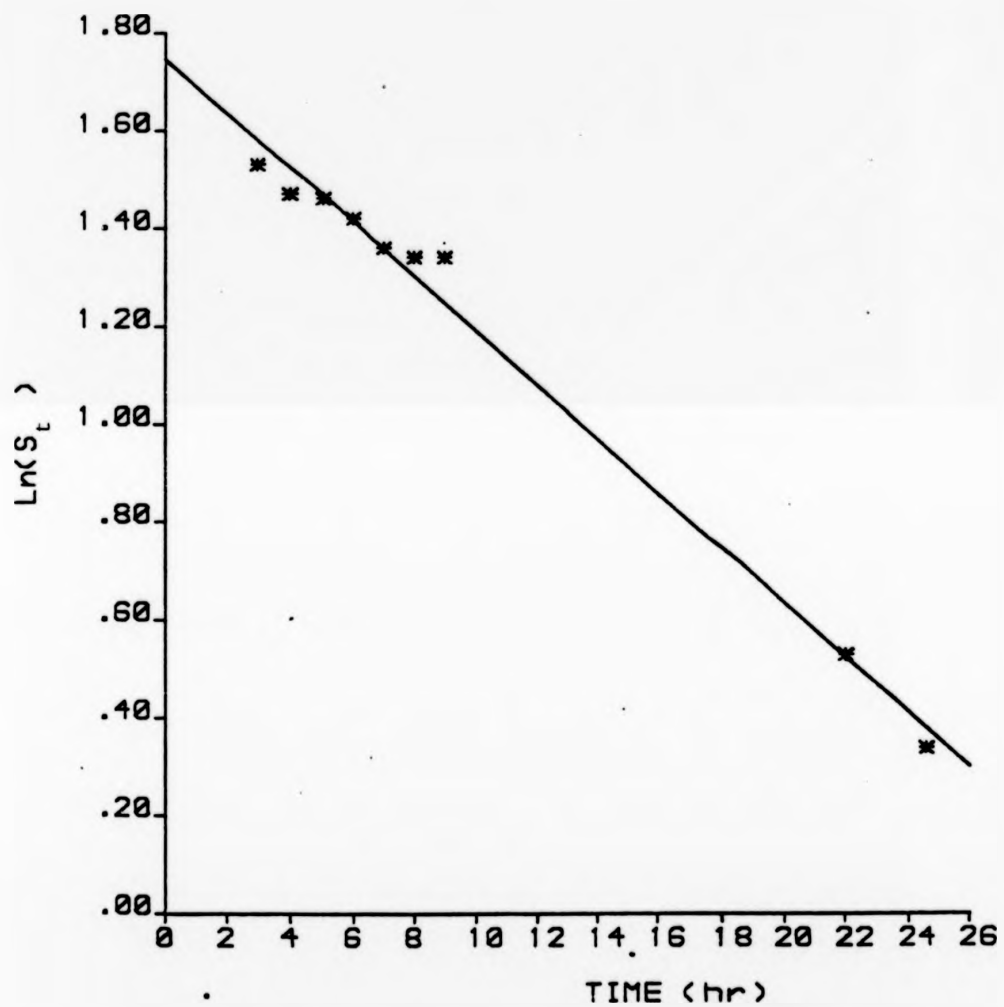


FIGURE 2.49c $\text{Ln}(S_t)$ of Na_{NI}^+ resonance (21.19MHz) as a function of time in the presence of 3.0mM 15-crown-5 derivative(11) in LUV trapped with 200mM NaCl. Surrounding medium contains 20mM Na_5PPP + 100mM KCl + 7.1mM DyCl_3

TABLE 2.4

[15]-Crown-5 acid derivative (3mM) mediated Na^+
transport in large unilamellar (LUV) trapped with 200mM
NaCl; surrounding medium contains 20mM Na_5PPP , 100mM
KCl and 7.1mM DyCl_3 . $T = 303^\circ\text{K}$.

(a)

Time (hr)	S_t	$(S_{t(\text{corr})})$	$\text{Ln}(S_{t(\text{corr})})$
0.0	9.85	4.83	1.58
0.3	7.65	2.67	0.98
0.6	7.50	2.57	0.94
1.0	5.90	1.03	0.03
2.0	5.00	0.28	-1.27

(b)

Time (hr)	S_t	$\text{Ln}(S_t)$
3.0	4.6	1.53
4.0	4.35	1.47
5.0	4.3	1.46
6.0	4.15	1.42
7.0	3.9	1.36
8.0	3.8	1.34
9.0	3.8	1.34
22.0	1.7	0.53
24.6	1.4	0.34

2.49b). The rate constant of the [15]-crown-5 acid derivative (11) mediated transport process was found to be ca $4.0 \times 10^{-4} \text{ s}^{-1}$. While the rate constant of the reaction of vesicles disintegrating is ca $1.5 \times 10^{-5} \text{ s}^{-1}$ (Fig 2.49c; Table 2.4b). The transport rate process is ca 27 times faster than the rate of disintegration of the vesicles.

In Fig 2.48, for the 2-(hydroxymethyl)-[15]-crown-5 mediated transport, the value of S_∞ has been taken as 1.70 and the plot of $\ln(S_t - S_\infty)$ vs t (Table 3.35) gives the gradient of the slope, of the best fit, as 1.42 ± 0.11 (Fig 2.48). The rate constant is ca $7.0 \times 10^{-5} \text{ s}^{-1}$. No two distinct rate processes are observed. The rate process monitored is probably the rate of disintegration of the vesicles.

Independent experiments carried out in the absence of an ionophore to check on leakage and bursting rates showed that the half-life of the Na_{IN}^+ peak was 10-20hr with rate constants in the range $2-4 \times 10^{-5} \text{ s}^{-1}$. Thus only rates faster than $5 \times 10^{-5} \text{ s}^{-1}$ are capable of being observed by this technique.

2.2.4 Conclusion

In the monensin mediated transport study, there are two obvious explanations of the origins of the line broadening observed for the Na_{IN}^+ resonance. The first is that exchange between Na_{IN}^+ and Na_{OUT}^+ is dynamic on the nmr time scale. The second arises from the much larger linewidth of NaMon (sodium monensin) than $\text{Na}(\text{aq})$. Thus if the exchange is between Na_{IN}^+ and NaMon inside the phospholipid bilayer, the linewidth of Na_{IN}^+ will increase. Even if the latter explanation holds such exchange must be dynamic on the nmr timescale, and such exchange is one half of the overall transport process.

The line broadening observed will arise from both sources. The

contribution to the line broadening from the NaMon is difficult to estimate because the linewidth of this species in a phospholipid medium is not known and the signal is so broad and weak under our conditions as to be unobservable. From observation on NaMon in methanol a line width of 1000Hz could be suggested as not unreasonable. For a typical experiment (200mM Na⁺) the ratio of NaMon to Na_{IN}⁺ is ca 1:10⁵. Thus we might expect a negligible contribution to the line broadening. It should, however, be noted that at lower Na⁺ concentration, the effect of this source of line broadening will increase and may account in part, for the shape of Fig 2.42. It was not possible to pursue this idea and further work is clearly needed.

The magnetisation transfer experiments were performed to try to resolve this dilemma. Selective inversion of the Na_{OUT}⁺ peak should not perturb the Na⁺ complexed as NaMon. The clear observation of transfer of magnetization points to the effects arising from a transport process and not an exchange involving NaMon. These experiments were however performed at high [Na⁺]. Magnetization transfer experiments using lower [Na⁺] could point to the relative contributions from transport and from exchange.

The comparison of the results for the crown ether alcohol (10) and its related acid (11) are extremely interesting. It had been hoped that by chemical modification of the alcoholic crown ether (10) an anionic side chain could be assembled which might confer increased transport activity. This being due to the formation of a neutral complex with increased encapsulation of the ion by the side arm arching over the macro-ring in a manner illustrated in Fig 2.50. The result is reinforced by data collected by Dishong, Diamond, Cinoman and Gokel³⁰⁹ who studied the extraction of sodium by various [15]-crown-5

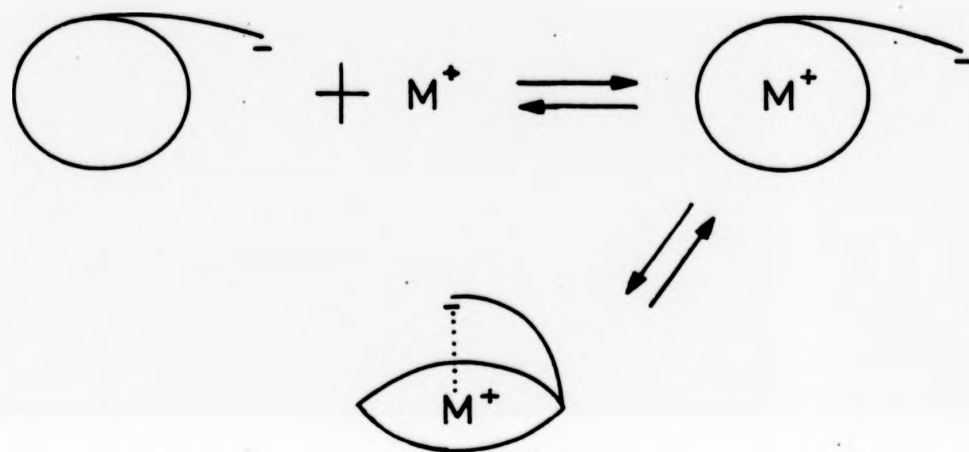


Fig 2.50 Generalized equation to illustrate macro-ring-bound cation complex formation.

derivatives. In general, the more efficient the side arm, for coordination to the metal ion, the higher the extraction constant.

Much research is still needed to achieve full understanding of membrane function. The lifetime of the vesicles under varying conditions needs to be determined and any unassisted diffusion across the artificial membranes needs to be found so that corrections may be made to the results.

Our present knowledge provides, at best some indication of the problems still to be resolved and perhaps a glimpse of the possibilities which exist. The nmr technique could open the way to some far reaching studies into the activity of all manner of compounds in the field of metal ion transport. Some advantages of the nmr approach which may prove of benefit include the following: (a) the use of stable isotopes, (b) the simultaneous determination of inside and outside concentrations, (c) the continuous, nondestructive monitoring of the approach to transport equilibrium (or steady state), (d) the study of transport kinetics at equilibrium (or steady state) by the use of magnetization transfer or exchange broadening,²⁰³ (e) the possibility of stable isotope labelling, and (f) the possibility of observing clear spectral distinctions of transport mechanism.^{202,203}

I end this work by quoting Sir Isaac Newton:

To me, we have been children, playing on the shore,

Picking up pretty pebbles from the beach...

While there beside us lay an Ocean,

Wide with undiscovered Truth.

CHAPTER 3

Experimental

CHAPTER 33.1 GENERAL NOTES

The ^{23}Na , ^7Li and ^{31}P nuclear magnetic resonance (nmr) spectra were obtained on a Bruker WP-80 Fourier transform spectrometer at 21.2, 31.14 and 32.44 MHz respectively unless otherwise stated. The ^{39}K nmr spectra were obtained on a Bruker WP-360 Fourier transform spectrometer at 16.8 MHz unless otherwise stated. These were always field frequency locked on the ^2H resonance of $^2\text{H}_2\text{O}$ present either in the inner compartment of a coaxial tube (5mm internal and 10mm external diameter) or in the bulk aqueous solvent. The isotropic hyperfine shift was measured as the difference of the observed resonance position from the resonance position of 100mM NaCl or 100mM KCl solutions. Shifts to lower frequency are defined as positive. Typically free induction decays were collected into 512 data points with a sweep width of 2000-3000 Hz and were zero filled and Fourier transformed in 4K or 8K data points. This process of zero-filling improves the digitalization of the spectrum, giving it a smoother and more realistic appearance and enabling peak maxima to be located more accurately. The spectra were obtained at ca 298K and normally an artificial line broadening of 2 Hz was used to improve the spectral signal-to-noise ratio unless otherwise stated.

The pH measurements were monitored on standard pH meters: PHM82 or PHM64 (Radiometer Copenhagen). The Sorvall RC-5B Refrigerated Superspeed Centrifugation and the MSE Centrifuge were used for high and low speed centrifugations respectively. The thermogravimetric analyses were done using a Perkin-Elmer TGS-2 Thermogravimetric system.

3.2 LANTHANIDE INDUCED SHIFTS

3.2.1 Dysprosium as the Lanthanide

Dysprosium trichloride (DyCl_3) supplied by Alfa Inorganics, was used after drying under vacuum overnight at 50°C . A one molar (0.538g) DyCl_3 solution was made in a 2 cm^3 standard volumetric flask with deionised water. The respective solutions of the substrates (made in deionised water) were normally added to the outer compartment of the coaxial nmr tube and to the inner tube was added a 100mM solution of a standard solution depending on the resonance under study, for example, when observing ^{23}Na nmr resonance, the standard solution in the inner tube is 100mM sodium chloride solution. The induced shift of monovalent ions of the respective chelate solutions was then monitored by titration with microlitre amounts of the DyCl_3 solution (micro syringe).

Substrate: Hydrated Trisodium Orthophosphate

The monophosphate used was hydrated trisodium orthophosphate, $\text{Na}_3\text{PO}_4 \cdot 12\text{H}_2\text{O}$ (Aldrich). A 20mM solution of the phosphate was placed in the outer compartment of the coaxial nmr tube and subsequent additions of DyCl_3 to the monophosphate solution by increments of 1mM up to 10mM failed to separate the ^{23}Na resonances of the outer tube from the inner tube sodium resonance.

Substrate: Hydrated Tetrasodium Pyrophosphate

The hydrated tetrasodium pyrophosphate, $\text{Na}_4\text{P}_2\text{O}_7 \cdot 10\text{H}_2\text{O}$ (Sigma), was used as the diphosphate chelate. No attempt was made to control the pH during titrations. The results of the two concentrations investigated are listed in Table 3.1.

Substrate: Pentasodium Tripolyphosphate

Pentasodium tripolyphosphate $\text{P}_3\text{O}_{10}\text{Na}_5$ ($\text{Na}_5\text{ PPP}$), supplied by Sigma, was used after drying under vacuum overnight at 50°C .

TABLE 3.1

^{23}Na Shifts observed using the substrate, hydrated tetrasodium pyrophosphate with the lanthanide, dysprosium chloride.
T = 298K.

Outer Tube = 25mM NaCl		
DyCl ₃ mM	+ 20mM Na ₄ P ₂ O ₄ 10H ₂ O	+ 15mM Na ₄ P ₂ O ₄ 10H ₂ O
	Shift ppm	Shift ppm
1	1.388	1.388
2	3.053	3.053
3	4.857	4.580
4	6.384	5.967
5	7.633	7.216
6	8.049	7.077
7	7.494	6.522

Phosphorus - 31 nmr (32.44 MHz) shows that it contains ca 20% of the diphosphate. No attempt was made to control the pH during titrations. In all cases the initial pH was ca 9.5 and decreased to a final value of ca 7.7 (Table 3.2). The results of the concentrations investigated are listed in Tables 3.3 and 3.4.

Substrate: Pentapotassium Tripolyphosphate

The pentapotassium tripolyphosphate (K_5PPP) was prepared from Na_5PPP by passing the latter down an ion exchange column loaded with the K^+ form of Dowex 50W-XB (200-400 BSS mesh size). The method of preparation is as follows: About 85g of the resin was soaked in deionised water for one hour (the volume of wet resin was 85 cm^3) before being transferred to a chromatographic column and washed with ca 700 cm^3 of 1M solution of hydrochloric acid to make sure that the resin is loaded with H^+ . The resin was then washed with an equal volume of deionised water. Approximately 600 cm^3 of 1M KCl was added slowly down the column at a rate of ca 10 cm^3 eluent collected per minute. The pH of eluent was monitored until acid evolution ceased, to make sure all H^+ had been replaced by K^+ . The column was then washed with a further 700 cm^3 deionised water. A solution of pentasodium tripolyphosphate (3.679g, 0.012 mols) in deionised water (25 cm^3) was allowed to run down the column at a rate of ca 5 cm^3 eluent collected per minute, followed by more deionized water. The first 100 cm^3 of eluent collected was evaporated to dryness on a rotary evaporator. The white crystalline product obtained was found to contain less than 1% Na_5PPP (^{23}Na nmr) and ca 20% potassium diphosphate (^{31}P nmr). The K_5PPP prepared was then dried under vacuum at 50°C for two days before being used.

Four different concentrations of the above prepared K_5PPP was

TABLE 3.2 Change in pH of pentasodium tripolyphosphate solutions on titration with Dysprosium chloride. T = 298K.

mM DyCl ₃	Na ₅ PPP : pH values			
	20mM	15mM	10mM	5mM
0	9.52	9.54	9.41	9.60
1	9.52	9.52	9.37	9.54
2	9.48	9.47	9.31	9.46
3	9.44	9.42	9.23	9.16
4	9.39	9.36	9.09	8.48
5	9.34	9.28	8.63	8.18
6	9.25	9.16	8.15	7.98 ^a
7	9.17	8.86	7.98 ^a	7.87
8	9.04	8.30	7.84	-
9	8.79	8.09 ^a	7.73	-
10	8.20 ^a	7.97	-	-

a - first signs of precipitation.

TABLE 3.3 ²³Na shifts observed using the substrate, pentasodium triphosphate and lanthanide, Dysprosium chloride. T = 303K.

mM DyCl ₃	20mM Na ₅ PPP		15mM Na ₅ PPP		10mM Na ₅ PPP		5mM Na ₅ PPP	
	Shift ppm	W _{1/2} ppm	Shift ppm	W _{1/2} ppm	Shift ppm	W _{1/2} ppm	Shift ppm	W _{1/2} ppm
0	-0.555	-	-	0.971	-	0.867	-0.069	0.694
0.5	2.949	1.041	2.671	1.006	4.233	1.041	8.535	1.006
1.0	5.516	1.214	6.835	1.145	8.777	1.249	16.826	1.145
1.5	8.849	1.284	10.026	1.145	12.941	1.353	25.534	1.527
2.0	10.373	1.318	13.322	1.180	17.381	1.318	30.148	1.596
2.5	12.975	1.388	16.653	1.527	22.273	1.769	24.736	1.318
3.0	16.063	1.492	19.567	1.631	26.263	1.943	18.457	1.180
3.5	18.875	1.492	22.551	1.769	30.565	2.220	12.212	1.874
4.0	20.887	1.527	25.916	2.116	33.897	2.012	8.812	3.192
4.5	22.412	1.839	28.657	2.255	32.334	2.220		
5.0	24.848	1.874	31.363	2.324	29.454	2.116		
5.5	27.826	2.151	34.346	2.429	26.820	2.637		
6.0	28.726	2.220	34.936	1.839	23.487	3.861		
6.5	30.599	2.290	34.173	2.637				
7.0	32.924	2.386	32.091	2.394				
7.5	34.728	2.706	30.461	3.712				
8.0	36.185	2.880	29.108	4.718				
8.5	37.887	2.783	-	-				
9.0	35.422	2.914	-	-				
9.5	34.867	3.573	-	-				
10.0	33.791	4.891	-	-				

TABLE 3.4

^{23}Na shifts observed using the substrate, pentasodium tripolyphosphate, and lanthanide, Dysprosium chloride.
T = 303K

DyCl ₃	10mM Na ₅ PPP+50mM NaCl		10mM Na ₅ PPP+50mM KCl	
	Shift ppm	W _{1/2} ppm	Shift ppm	W _{1/2} ppm
0	-0.1388	0.694	-0.069	0.659
0.5	2.186	0.729	2.116	0.763
1.0	-	-	4.371	0.763
1.5	7.077	0.833	6.731	0.833
2.0	9.610	0.937	9.020	0.797
2.5	11.761	0.937	11.141	0.937
3.0	14.779	1.041	13.505	0.937
3.5	17.000	1.076	15.404	1.006
4.0	17.624	1.110	16.202	1.006
4.5	16.445	1.180	-	-
5.0	15.334	2.602	14.432	2.359
5.5	14.016	3.553	13.530	2.845
6.0	12.836	4.649	12.420	3.226

titrated against the lanthanide, DyCl_3 . No attempt was made to control the pH during the titrations. In all cases the initial pH was ca 9.0 and decreased to a final value of ca 7.7 (Table 3.5). The results of the concentrations investigated are listed in Table 3.6.

Substrate: Equimolar Pentasodium Tripolyphosphate and Pentapotassium Tripolyphosphate

A solution containing 10mM Na_5PPP and 10mM K_5PPP was placed in the outer compartment of the coaxial nmr tube and a 100mM NaCl solution in the inner tube. No attempt was made to control the pH during titration. The result of the titration is listed in Table 3.7.

Substrate: Pentalithium Tripolyphosphate

The pentalithium tripolyphosphate (Li_5PPP) was prepared from Na_5PPP by passing the latter down an ion exchange column loaded with the Li^+ form of Dowex 50W-XB (200-400 BSS mesh size). The procedure adopted was similar to that for the preparation of K_5PPP (see above).

Li_5PPP , obtained as a white crystalline product, was identified by ^7Li nmr (at 31.14 MHz) and with ^{23}Na nmr no sodium resonance was observed indicating complete exchange. The ^{31}P nmr showed very broad peaks for the two environments of the tripolyphosphate group. The Li_5PPP prepared was dried under vacuum at 50°C overnight.

A 5mM Li_5PPP solution was added to the outer compartment of a coaxial nmr tube and to the inner tube was added a solution of 10mM Li_5PPP in $^2\text{H}_2\text{O}$. No isotropic hyperfine shift was observed when the outer tube was made 2mM in DyCl_3 .

In a second experiment, a 15mM Na_5PPP solution was added to the outer compartment of a coaxial nmr tube and a 100mM NaCl solution to the inner tube. The isotropic hyperfine shift in this instance was followed by ^{23}Na nmr. Addition of 3mM DyCl_3 to the pentasodium

TABLE 3.5

Change in pH of pentapotassium tripolyphosphate solution on titration with Dysprosium chloride. T = 298K.

mM DyCl ₃	K ₅ PPP : pH values		
	20mM	15mM	10mM
0	9.15	9.14	9.14
1	9.09	9.06	9.02
2	9.03	8.99	8.84
3	8.95	8.86	8.51
4	8.86	8.66	8.09
5	8.73	8.39	7.91
6	8.55	8.17	7.81 ^a
7	8.32	8.04 ^a	7.70
8	8.12	7.96	-
9	7.98 ^a	7.89	-
10	7.91	-	-

a - first signs of precipitation.

TABLE 3.6 ^{39}K shifts observed using the substrate, pentapotassium tripolyphosphate, and lanthanide, Dysprosium chloride. $T = 298\text{K}$.

■M DyCl ₃	20mM K ₅ PPP		15mM K ₅ PPP		10mM K ₅ PPP	
	Shift ppm	W _{1/2} ppm	Shift ppm	W _{1/2} ppm	Shift ppm	W _{1/2} ppm
1	1.28	-	2.11	-	3.56	1.25
2	3.15	-	4.70	1.190	5.58	1.25
3	5.11	-	7.30	1.369	7.65	1.429
4	7.06	1.488	9.68	1.905	9.29	1.667
5	8.90	-	11.33	2.976	10.72	2.202
6	10.40	1.905	11.66	4.167	11.22	2.85
7	11.40	3.333	10.99	6.319	10.99	3.988
8	11.51	3.690	-	-	-	-
9	10.40	4.762	-	-	-	-

TABLE 3.7

^{23}Na shifts observed using an equimolar solution of Na_5PPP and K_5PPP with the Lanthanide, Dysprosium chloride. $T = 298\text{K}$.

10mM Na_5PPP + 10mM K_5PPP		
mM DyCl_3	Shift ppm	$W_{1/2}$ ppm
0	-0.0347	0.971
0.5	1.943	1.041
1.0	4.129	1.041
1.5	6.418	1.041
2.0	8.777	1.110
2.5	10.720	1.006
3.0	13.149	1.284
3.5	15.334	1.353
4.0	17.347	1.249
4.5	19.463	1.214
5.0	21.649	1.284
5.5	23.522	1.284
6.0	25.569	1.353
6.5	27.408	1.492
7.0	29.281	1.631
7.5	29.697	1.804
8.0	29.871	2.810
8.5	29.628	2.567
9.0	28.795	4.233
9.5	28.136	4.129
10.0	27.755	5.447

tripolyphosphate gave ca 14 ppm shift. As increasing amounts of $\text{LiCl}\cdot\text{H}_2\text{O}$ was added to the outer tube the shift was observed to decrease and finally the two ^{23}Na resonances collapsed to a single resonance position equivalent to unshifted resonance position.

Substrate: (i) $(\text{Na})_x(\text{Choline})_y\text{PPP}$ and Na_5PPP .

(ii) $(\text{Na})_x(\text{Choline})_y\text{PPP}$ and K_5PPP

The sodium/choline tripolyphosphate, $(\text{Na})_x(\text{choline})_y\text{PPP}$, was prepared from Na_5PPP by passing the latter down an ion exchange column loaded with the choline⁺, $[\text{CH}_2(\text{OH})\text{CH}_2\overset{+}{\text{N}}(\text{CH}_3)_3]$ form of Dowex 50W-XB (200-400 BSS mesh size). After regenerating the resin to its original H^+ form (see above), 30g of choline chloride (Sigma) dissolved in deionized water (300 cm^3) was put down the column. The eluent was collected at a rate of ca 50 cm^3 per hour. The column was then washed down with deionised water until the eluent was noted to be neutral. A solution of Na_5PPP (2.0g, 5.6×10^{-3} mol) in deionised water (25 cm^3) was then allowed to run down the column at the same rate as above. 2.5g of a very viscous colourless product was obtained. ^1H nmr (Perkin-Elmer R-32) and ^{13}C nmr (Bruker WP80) confirmed the presence of choline. The pH of the product was noted to be ca 2.4. ^{23}Na nmr showed presence of an appreciable residue of sodium. These results suggest that the product is probably a mixture of $(\text{Na})_x(\text{choline})_y\text{PPP}$ and H_5PPP .

The product (2.5g) was made up to 25 cm^3 with deionised water. This was then split into two equal portions, one-half of which was titrated with 1M NaOH solution and the other half with 1M KOH solution to raise the pH of the respective solutions to near neutrality (pH 6.0). The titrations required 7.8mM of NaOH and KOH respectively. It can thus be assumed that there was ca 7.8mM H_5PPP in each of the 12.5 cm^3

portions of the ion-exchange product. The respective neutralised solutions were made up to 25 cm³. The concentration of tripolyphosphate in these solutions was measured as ca 132mM by ³¹P nmr (32.44 MHz). Hence, dilution by a factor of 4 would result in solutions of ca 26mM PPP. The results of the titrations with lanthanide, DyCl₃, are listed in Tables 3.8 and 3.9.

Substrate: Hydrated Hexasodium Tetrapolyphosphate

The hydrated hexasodium tetrapolyphosphate, P₄O₁₃Na₆·6H₂O (Na₆PPPP·6H₂O), was prepared from hydrated hexaammonium tetrapolyphosphate, (NH₄)₆PPPP·6H₂O (Sigma), by passing the latter down an ion exchange column loaded with the Na⁺ form of Dowex 50W-XB (200-400 BSS mesh size). The procedure adopted was similar to that for the preparation of K₅PPP and Li₅PPP (see above). 46mg (1.05 × 10⁻⁴ mol) of (NH₄)₆PPPP·6H₂O dissolved in ca 2 cm³ deionised water was added to the resin column loaded with Na⁺. The eluent collected was evaporated to dryness on a rotary evaporator and dried under vacuum at room temperature overnight. Yield - 46mg.

The product was dissolved in 2 cm³ of deionised water. On calibrating with respect to a 100mM NaCl solution (²³Na nmr) the sodium ion concentration in the tetrapolyphosphate solution was estimated as ca 250mM. This suggests that the product prepared was the hydrated hexasodium tetrapolyphosphate, Na₆PPPP·6H₂O.

The Na₆PPPP·6H₂O solution was added to the inner compartment of the coaxial nmr tube and to the outer tube was added ²H₂O. The spectrometer was field-frequency locked on the ²H resonance of the ²H₂O in the outer tube. No attempt was made to control the pH during titrations with DyCl₃. The results of the titrations are listed in Tables 3.10 and 3.11.

TABLE 3.8 ^{23}Na shifts observed using the mixture of substrates,
 $(\text{Na})_x(\text{Choline})_y$ PPP and Na_5PPP , with the lanthanide,
Dysprosium chloride. $T = 303\text{K}$.

ca 26mM PPP from Na_5PPP and $(\text{Na})_x(\text{choline})_y$ PPP

mM DyCl_3	Shift ppm	$W_{1/2}$ ppm
0	-0.2304	0.737
1	3.732	0.852
2	7.418	0.967
3	10.919	1.106
4	13.960	1/198
6	19.909	1.104
7	21.654	1.566
8	23.635	1.425
9	25.478	1.521
10	27.736	1.546
11	28.657	1.568
12	30.039	1.566
13	31.099	1.613
14	32.481	1.751
15	33.080	1.751
16	33.126	1.751
17	33.449	1.751
18	33.495	1.797
19	33.034	-
21	31.560	1.705
23	30.224	1.751
25	27.551	1.520
27 ^a	25.017	1.797

^a - first signs of precipitation

TABLE 3.9

^{39}K shifts observed using the mixture of substrates,
(Na) $_x$ (Choline) $_y$ PPP and Na_5PPP , with the
lanthanide, Dysprosium chloride. $T = 303\text{K}$.

ca 26mM PPP from Na_5PPP and (Na) $_x$ (choline) $_y$ PPP

mM DyCl_3	Shift ppm	$W_{1/2}$ ppm
0	-0.39	-
2	3.05	1.0
3	4.55	1.13
4	5.97	1.22
5	7.35	1.32
6	8.43	1.61
7	9.45	1.72
8	10.34	1.78
9	11.20	1.92
10	12.00	1.85
11	12.30	1.95
12	12.70	1.90
13	12.97	2.08
14	13.06	2.08
15	13.03	2.20
16	12.65	1.96

TABLE 3.10

^{23}Na shifts observed using the substrate, hydrated hexasodium tetrapolyphosphate, with the lanthanide, Dysprosium chloride. $T = 303\text{K}$.

mM DyCl_3	Shift ppm	Shift ppm
0	-0.184	-0.187
1	-1.290	-1.336
2	-2.212	-2.949
3	-3.317	-3.870
4	-4.423	-5.529
5	-5.529	-6.634
6	-6.450	-7.003
7	-6.634	-6.634
8	-7.187	-5.897
9	-7.372	-4.239
10	-7.187	-2.396
11	-6.082	-0.737
12	-4.976	0.369
13	-3.133	2.396
14	-1.843	3.686
15	-0.553	4.607 ($W_{1/2}=1.84$)
16	0.921 ($W_{1/2}=2.5$)	5.344
17	1.659 ($W_{1/2}=2.7$)	5.713
18	3.133	5.897 ($W_{1/2}=1.29$)
19	4.054 ($W_{1/2}=2.03$)	5.713
20	4.792	5.529
21	4.976	5.160
22	5.713	-
23	6.082	-
24	6.266	-
25	6.266 ($W_{1/2}=1.66$)	-
26	6.082 ($W_{1/2}=2.21$)	-
27	5.897	-

TABLE 3.11

²³Na shifts observed using the substrate, hydrated hexasodium tetrapolyphosphate, with the lanthanide, Dysprosium chloride. T = 303K

DyCl ₃ mM	ca 10mM Na ₆ PPPP.6H ₂ O		ca 5mM Na ₆ PPPP 6H ₂ O
	Shift ppm	W _{1/2} ppm	Shift ppm
0	-0.184	-	-0.184
0.25	-	-	-0.737
0.5	-1.659	-	-1.474
0.75	-	-	-2.580
1.00	-2.580	1.29	-3.317
1.25	-	-	-3.317
1.5	-3.686	-	-4.054
2.0	-4.607	-	-4.23
2.5	-5.160	2.03	-4.054
3.0	-6.082	-	-3.686
3.5	-6.266	-	-2.580
4.0	-6.450	-	-1.474
4.5	5.897	-	0.737
5.0	-5.529	-	2.212
5.5	-	-	3.317
6.0	-3.686	-	3.502
6.5	-	-	3.317
7.0	-1.659	-	3.133
8.0	1.106	2.21	2.212
9.0	2.212	2.03	-
10.0	3.878	-	-
11.0	5.344	0.90	-
12.0	5.400	-	-
13.0	4.423	1.10	-
14.0	4.050	-	-

Substrate: Trimetaphosphate Trisodium

Trimetaphosphate trisodium, $\text{Na}_3\text{P}_3\text{O}_9$, supplied by Aldrich, was used after drying under vacuum overnight at 50°C . A 20mM solution of the cyclic phosphate was placed in the outer compartment of the coaxial nmr tube and subsequent addition of aliquots of Dysprosium chloride to the phosphate solution by increments of 1mM up to 20mM failed to separate the ^{23}Na resonances.

Substrate: Sodium Chloride

A 100mM NaCl solution and 5mM DyCl_3 was added to the outer compartment of the coaxial nmr tube and to the inner tube was added a solution of 100mM NaCl in $^2\text{H}_2\text{O}$. A 0.35 ppm ^{13}Na shift to lower frequency was observed. The half widths of the ^{23}Na peaks in the absence and presence of the lanthanide were observed to be 0.34 and 0.35 ppm respectively.

Substrate: Potassium Chloride

A 100mM KCl solution and 5mM DyCl_3 was added to the outer compartment of the coaxial nmr tube and to the inner tube was added a solution of 100mM KCl in $^2\text{H}_2\text{O}$. The ^{39}K nmr spectra was obtained on a Bruker WP-200 Fourier-transform spectrometer at 9.34 MHz. 1000 free induction decays were collected into 512 data points and zero-filled and Fourier-transformed in 8K data points without any line broadening. A 1.014 ppm isotropic hyperfine shift of the ^{39}K nmr resonance to higher frequency was observed. The half-width of the ^{39}K peaks in the absence and presence of the lanthanide was observed to be 7.0 and 7.2 Hz respectively.

3.2.2 Lanthanum as the Lanthanide

Hydrated lanthanum nitrate, $\text{La}(\text{NO}_3)_3 \cdot 6\text{H}_2\text{O}$, supplied by BDH Chemocals Ltd, was used after drying overnight under vacuum at 50°C . Thermogravimetric analysis showed that the six water molecules are bound as water of crystallization. A one molar lanthanum nitrate solution was made in a 2 cm^3 (0.866g) standard volumetric flask with deionised water.

Substrate: Pentasodium Tripolyphosphate

Solution of Na_5PPP (10mM) was added to the outer compartment of the coaxial nmr tube and to the inner tube was added a solution of 100mM NaCl in $^2\text{H}_2\text{O}$. Addition of aliquots of lanthanide to the tripolyphosphate taking $[\text{La}^{3+}]$ from 1mM to 10mM showed no shift changes for the ^{23}Na resonance.

3.2.3 Praseodymium as the Lanthanide

Praseodymium trichloride, PrCl_3 , supplied by Alfa Inorganics, was used after drying overnight under vacuum at 50°C .

Substrate: Pentasodium Tripolyphosphate

A 10mM solution of Na_5PPP was added to the outer compartment of the coaxial nmr tube and to the inner tube was added a solution of 100mM NaCl in $^2\text{H}_2\text{O}$. After addition of 5mM PrCl_3 to the phosphate, a shift of 2.64 ppm to lower frequency of the ^{23}Na nmr resonance was observed with a half-width of ca 1 ppm.

3.2.4 Terbium as the Lanthanide

Terbium was used as its nitrate pentahydrate, $\text{Tb}(\text{NO}_3)_5 \cdot 5\text{H}_2\text{O}$, supplied by Aldrich, because of the limited solubility of the chloride. 0.87g of $\text{Tb}(\text{NO}_3)_3 \cdot 5\text{H}_2\text{O}$ was transferred to a 2 cm^3 standard volumetric flask, from the container in which it was received, under an atmosphere of dry nitrogen. This gives a one molar solution in

deionised water.

A solution of the substrate was added to the outer compartment of the coaxial nmr tube and to the inner tube was added either a solution of NaCl (100mM) or KCl (100mM) in $^2\text{H}_2\text{O}$.

Substrate: Pentasodium Tripolyphosphate

No attempt was made to control the pH during titrations. In all cases the initial pH was ca 9.5 and decreased to a final value of ca 7.9 (Table 3.12). The results of the four different concentrations of Na_5PPP investigated are listed in Table 3.13.

Substrate: Pentapotassium Tripolyphosphate

Again no attempt was made to control the pH during titration. The initial pH was ca 9.0 and decreased to a value of ca 7.7 (Table 3.14). The result of the titration of K_5PPP with terbium is listed in Table 3.14.

3.2.5 Ytterbium as the Lanthanide

Ytterbium trichloride, YbCl_3 , supplied by Alfa Inorganics, was used after drying under vacuum overnight at 50°C . A one molar YbCl_3 (0.538g) solution was made in a 2cm^3 standard volumetric flask with deionised water.

As above, solution of the substrate was added to the outer compartment of the coaxial nmr tube and to the inner tube was added either a solution of NaCl (100mM) or KCl (100mM) in $^2\text{H}_2\text{O}$.

Substrate: Pentasodium Tripolyphosphate

No attempt was made to control the pH during the titration of 20mM Na_5PPP with YbCl_3 . The initial pH was ca 9.3 and decreased to ca 7.5. The values of the pH and observed ^{39}K shifts are listed in Table 3.15.

TABLE 3.12

Change in pH of pentasodium tripolyphosphate solutions on titration with Terbium nitrate pentahydrate. T = 298K.

Tb(NO ₃) ₃ · 5H ₂ O mM	Na ₅ PPP : pH values			
	20mM	15mM	10mM	5mM
0	9.33	9.57	9.40	9.73
1	9.28	9.51	9.35	9.69
2	9.23	9.47	9.27	9.63
3	9.16	9.42	9.17	9.22
4	9.09	9.35	9.00	8.64
5	8.99	9.23	8.44	8.34 ^a
6	8.86	8.94	8.03	8.12
7	8.62	8.30 ^a	7.87 ^a	-
8	8.05	8.06	7.73	-
9	7.78 ^a	-	-	-
10	7.69	-	-	-

a- first signs of precipitation

TABLE 3.13 ^{23}Na shifts observed using the substrate, pentasodium tripolyphosphate, with the lanthanide, Terbium nitrate pentahydrate. $T = 303^\circ\text{K}$.

$\text{Tb}(\text{NO}_3)_3 \cdot 5\text{H}_2\text{O}$ mM	20mM Na_5PPP Shift ppm	$W_{1/2}$ ppm	15mM Na_5PPP Shift ppm	$W_{1/2}$ ppm	10mM Na_5PPP Shift ppm	$W_{1/2}$ ppm	5mM Na_5PPP Shift ppm	$W_{1/2}$ ppm
0	-	0.864	-	0.979	-	0.921	-	0.691
0.5	2.246	0.922	3.225	0.922	4.780	0.979	8.235	1.037
1.0	4.838	0.979	6.623	1.037	9.963	1.037	17.277	1.209
1.5	7.372	1.152	9.963	1.152	17.162	1.325	25.340	1.382
2.0	9.675	1.152	14.167	1.267	21.712	1.382	23.843	1.267
2.5	13.073	1.209	17.393	1.382	26.261	1.440	16.874	1.094
3.0	15.492	1.209	20.733	1.382	30.523	1.670	10.424	0.979
3.5	17.911	1.382	24.188	1.555	29.314	1.555	-	-
4.0	20.272	1.382	27.528	1.613	24.706	1.325	-	-
4.5	23.094	1.555	30.120	1.613	21.136	1.785	-	-
5.0	25.397	1.555	31.387	1.785	18.775	3.743	-	-
5.5	27.643	1.728	30.293	1.613	-	-	-	-
6.0	29.717	1.497	27.989	1.728	-	-	-	-
6.5	31.848	1.785	25.801	2.419	-	-	-	-
7.0	32.999	1.613	24.188	3.513	-	-	-	-
7.5	32.596	1.958	-	-	-	-	-	-
8.0	31.099	1.728	-	-	-	-	-	-
8.5	29.659	2.246	-	-	-	-	-	-
9.0	28.104	3.052	-	-	-	-	-	-

TABLE 3.14 Change in pH and ^{39}K shifts observed using the substrate, pentapotassium tripolyphosphate, with the lanthanide, Terbium nitrate pentahydrate.

$\text{Tb}(\text{NO}_3)_3 \cdot 5\text{H}_2\text{O}$ mM	20mM K_5PPP T = 298K pH values	SF = 16.8 MHz T = 303K Inner Tube = 100mM KCl in D_2O 20mM K_5PPP Shift ppm	$W_{1/2}$ ppm
0	9.03	-0.47	-
1	8.91	1.86	0.86
2	8.80	4.18	1.03
3	8.67	6.46	1.30
4	8.50	8.80	1.75
5	8.29	10.61	2.38
6	8.07	11.89	3.30
7	7.90	12.40	3.39
8	7.80 ^a	11.58 ^a	5.24
9	7.71	10.42	-

a - First signs of precipitation

TABLE 3.15 Change in pH and ^{23}Na shifts observed using the substrate, pentasodium tripolyphosphate, with the lanthanide, Ytterbium trichloride.

mM YbCl_3	20mM Na_5PPP T = 298 ^o K pH values	SF = 21.196 MHz, T = 303K Inner Tube = 100mM NaCl in D_2O 20mM Na_5PPP	
		Shift ppm	$W_{1/2}$ ppm
0	9.30	-0.323	-
1	9.27	-0.780	1.014
2	9.23	-1.134	1.014
3	9.12	-1.889	1.014
4	9.15	-2.442	1.106
5	9.09	-2.995	1.106
6	9.02	-3.548	1.106
7	8.96	-4.193	1.198
8	8.87	-4.746	1.290
9	8.75	-5.206	1.198
10	8.52	-5.667	1.198
11	8.00	-6.220	1.290
12	7.73 ^a	-6.588	1.290
13	7.62	-6.404 ^a	1.290
14	7.60	-6.128	1.850
15	7.57	-5.759	2.580
16	7.52	-5.575	2.857
17	7.48	-5.114	3.502

a - first signs of precipitation

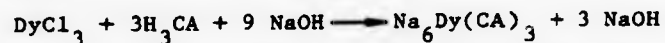
Substrate: Pentapotassium Tripolyphosphate

Again no attempt was made to control the pH during the titration of 20mM K_5PPP with $YbCl_3$. The initial pH was ca 8.9 and decreased to ca 7.7. In Table 3.16 are listed the pH values and the observed ^{39}K shifts.

3.3 ATTEMPTED SYNTHESIS OF THE HEXASODIUM CHELIDAMATE COMPLEX OFDYSPROSIUM: $Na_6Dy(CA)_3 \cdot 3NaCl$ ²⁰⁰

Chelidamic acid, H_3CA (Aldrich), was recrystallized according to the method of Bag et al.³¹⁰ The crystalline product obtained was colourless, mp 245-246°C; lit mp 248°C.³¹¹

The complex $[Na_6Dy(CA)_3]$ was prepared in situ by adding up to 9 equivalents of NaOH (1.5×10^{-2} mol, ie 7.5 cm³ of 2M NaOH solution) slowly (burette), with stirring, to an aqueous dispersion of $DyCl_3$ (0.448g, 1.67×10^{-3} mol) and the insoluble H_3CA (5.0×10^{-3} mol, ie 1g in 50 cm³ deionized water). The synthesis is described by the reaction:



The pH was monitored continuously and never allowed to rise above 6 or 7 (even transiently) during the early stages. Precipitation was observed to form and remained even on warming. Repeated attempts gave a similar result. The "complex" formed was observed to give only 2 ppm shift to lower frequency of the ^{23}Na resonance with respect to unshifted ^{23}Na resonance of a 100mM NaCl solution.

3.4 MEASUREMENT OF INTRACELLULAR CONCENTRATIONS: CELLULAR SYSTEMS

The ^{23}Na nmr spectra were obtained on a Bruker WP-80 Fourier-transform spectrometer at 21.2 MHz and ^{39}K nmr spectra were

TABLE 3.16

Change in pH and ^{39}K shifts observed using the substrate, pentapotassium tripolyphosphate, with the lanthanide, Ytterbium trichloride.

mM Yb Cl ₃	20mM K ₅ PPP T = 298K pH values	SF = 16.8 MHz; T = 303K Inner Tube = 100mM KCl in D ₂ O 20mM K ₅ PPP	
		Shift ppm	W _{1/2} ppm
0	8.87	-	-
1	8.82	-	-
2	8.76	-1.18	1.012
3	8.68	-	-
4	8.60	-2.00	1.071
5	8.49	-	-
6	8.34	-2.66	1.429
7	8.18	-	-
8	8.01	-3.09	2.024
9	7.91 ^a	-	-
10	7.80	-3.35 ^a	2.917
11	7.73	-	-
12	7.67	-3.07	4.048

a - first signs of precipitation

obtained on a Bruker WP-360 Fourier-transform spectrometer at 16.8 MHz. These were always field-frequency locked on the ^2H resonance of $^2\text{H}_2\text{O}$ [25% (v/v)] present in the resuspension medium which thus served as an internal reference. The spectra were obtained at 298K.

For quantitative comparisons Fourier transforms were performed under the same absolute intensity conditions. Therefore, the integrated areas of the resonances arising from intra- and extra-cellular K^+ or Na^+ could be compared directly with a reference spectrum of shifted K^+ or Na^+ in resuspension medium alone. By subtracting the spectrum derived from K^+ or Na^+ in the resuspension medium from the spectrum obtained from the cellular system suspension, the fractional space occupied by the extracellular fluid and therefore that occupied by the cellular system could be determined. The concentration of the intracellular K^+ or Na^+ was measured by comparing the integrated intensity of the subtracted spectrum with the integrated intensity of the spectrum obtained from a known concentration of K^+ or Na^+ in resuspension medium. A correction was then made for the fractional space occupied by the cellular system.

Typically with ^{23}Na nmr spectra, 4000 free induction decays were collected (ca 20 mins) into 512 data points with a sweep width of 2000 Hz in order to achieve a rapid pulse rate, but they were zero filled and Fourier transformed in 4K data points without any line broadening.

3.4.1 Human Erythrocytes

Blood was drawn from a healthy donor (Dr P J Brophy, Biological Sciences Department, Stirling University) into heparinized tubes. The erythrocytes were washed three times by centrifugation at 1000g for 10 min in 140mM NaCl/10mM glucose/5mM potassium phosphate buffer, pH 7.4,

and the buffy coat was removed by aspiration. Immediately before the nmr measurements were made erythrocytes were transferred to an nmr tube (10mm outside diameter) and washed twice in a resuspension medium containing (final concentrations) 10mM glucose, 5mM sodium hydrogen phosphate, 6mM DyCl_3^* , 15mM sodium tripolyphosphate, 55mM NaCl and 20mM KCl in 25% (v/v) $^2\text{H}_2\text{O}$ adjusted to pH 7.4. The total concentration was 120mM. When the erythrocytes were suspended in media of higher KCl concentrations (40mM or 60mM KCl), the amount of NaCl was decreased proportionately in order to maintain the same ionic strength. The erythrocytes were packed gently in the nmr tube by centrifugation at 1000g for 10 min.

^{39}K nmr spectra were obtained at 25°C with a Bruker WP-360 Fourier-transform spectrometer at 16.8MHz. Preliminary experiments showed that the spin-lattice relaxation times for both shifted and unshifted resonances were approximately 5ms. A 90° pulse was used with a repetition rate of 64 ms (more than 12 spin-lattice relaxation times). 20000 free induction decays were collected (ca 20 min) into 256 data points with a sweep width of 2000Hz in order to achieve a rapid pulse rate, but they were zero filled and Fourier transformed in 4K data points without any line broadening. The spectra is presented in Fig 3.1.

Calculation of the fractional space that was intracellular followed by comparison of the integrated area of the intracellular K^+ peak with that of the reference spectrum gave values for the intracellular K^+ concentrations of 81mM, 85mM and 81mM when the erythrocytes were

*In a separate experimental set up the ratio of Dy^{3+} to tripolyphosphate that resulted in the maximum chemical shift of the K^+ resonance in this resuspension medium was studied. Resuspension medium that contained 15mM Na_5PPP but no Dy^{3+} was added to the inner and outer tubes of a coaxial nmr tube. Addition of DyCl_3 to the outer tube caused the K^+ signal to shift to a maximum at about 6.5mM DyCl_3 . The values of the titrations are listed in Table 3.17.

TABLE 3.17 ^{39}K shifts observed at three different concentrations of K^+ in resuspension medium containing 15mM pentasodium tripolyphosphate with the lanthanide, Dysprosium chloride. $T = 298\text{K}$.

mM DyCl_3	+ 20mM KCl		+ 40mM KCl		+ 60mM KCl	
	Shift ppm	$W_{1/2}$ ppm	Shift ppm	$W_{1/2}$ ppm	Shift ppm	$W_{1/2}$ ppm
1	-	-	1.00	-	-	-
2	2.18	1.07	2.03	-	2.09	1.07
3	-	-	3.17	-	-	-
4	4.27	1.43	4.18	-	3.95	1.31
5	5.35	1.37	5.06	1.61	4.72	1.37
6	6.13	1.79	5.69	1.90	5.26	1.67
7	6.13	2.08	5.90	2.14	5.32	1.96
8	5.60	2.74	5.72	2.38	4.88	2.38

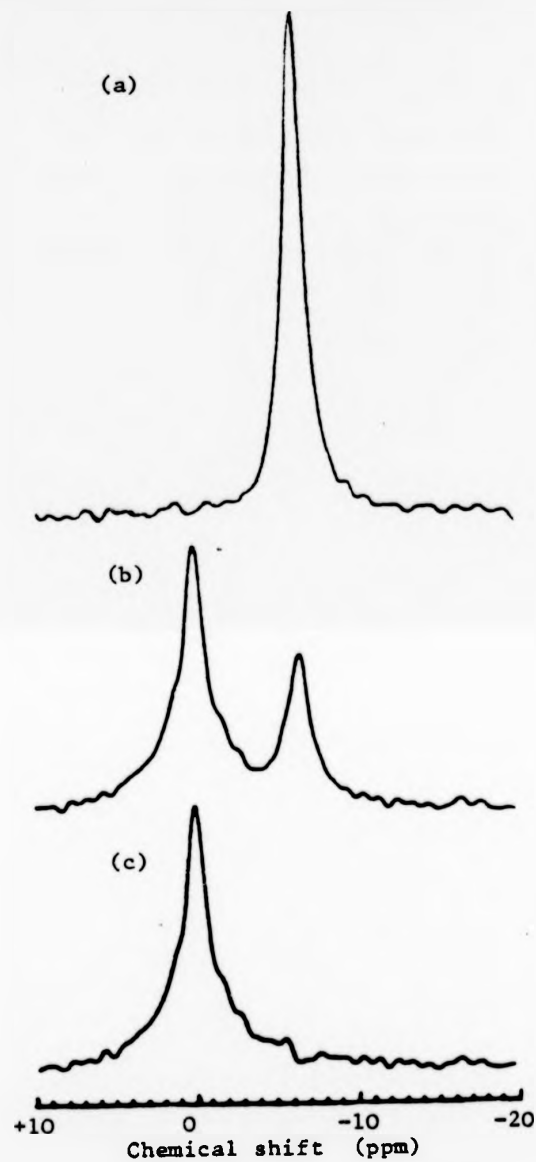


Fig 3.1 ³⁹K nmr spectra of (a) resuspension medium containing 60mM-K⁺, 6mM-Dy³⁺ and 15mM tripolyphosphate; (b) human erythrocytes in the same medium and (c) difference spectra after the subtraction of 0.3 of the integrated intensity of spectrum (a) from spectrum (b). For each spectrum 20,000 free induction decays were collected in approximately 20 min.

resuspended in media containing 20mM KCl, 40mM KCl and 60mM KCl respectively. The error in the spectral subtraction is estimated to be about $\pm 10\%$.

Intracellular K^+ concentration measured with a EEL model 150 clinical flame photometer after haemolysis of the erythrocytes gave a result of 88mM.

3.4.2 Baker's Yeast (*Saccharomyces cerevisiae*)

The yeast cells were cultured by smearing sterile agar plates with sporulating yeast from a stock culture of the fungus, using sterile technique throughout. The cultures were left for ca 1 week at ca 25°C . The yeast were then recultured by inoculating flasks containing sterile growth media (Malt Extract Medium). A third and final culture was performed by inoculating conical flasks containing sterile liquid Malt Extract Medium with yeast from the second culture. The cultures were then left to grow for 10 days at 298K on an agitator.

On completion, the yeast cells were centrifuged at 2500g for 10 mins. Most of the nutrient medium was poured away and the cells centrifuged at 2500g for 20 mins. The nutrient was removed by aspiration and the yeast cells were washed three times by centrifugation at 2200g for 10 mins in acetate buffer,³¹² pH 6.6 and the buffy coat was removed by aspiration. The yeast cells were transferred to an nmr tube (10mm outside diameter) and washed twice in a resuspension medium containing (final concentrations) 10mM Na_3PPP and 4mM DyCl_3 in 25% (v/v) $^2\text{H}_2\text{O}$. The yeast cells were packed gently in the nmr tube by centrifugation at 1000g for 10 min. The spectra shown in Fig 3.2 represents 4000 free induction decays collected in about 15 min.

Calculation of the fractional space that was intracellular followed by comparison of the integrated area of the intracellular Na^+ peak with

resuspended in media containing 20mM KCl, 40mM KCl and 60mM KCl respectively. The error in the spectral subtraction is estimated to be about +10%.

Intracellular K^+ concentration measured with a EEL model 150 clinical flame photometer after haemolysis of the erythrocytes gave a result of 88mM.

3.4.2 Baker's Yeast (*Saccharomyces cerevisiae*)

The yeast cells were cultured by smearing sterile agar plates with sporulating yeast from a stock culture of the fungus, using sterile technique throughout. The cultures were left for ca 1 week at ca 25°C. The yeast were then recultured by inoculating flasks containing sterile growth media (Malt Extract Medium). A third and final culture was performed by inoculating conical flasks containing sterile liquid Malt Extract Medium with yeast from the second culture. The cultures were then left to grow for 10 days at 298K on an agitator.

On completion, the yeast cells were centrifuged at 2500g for 10 mins. Most of the nutrient medium was poured away and the cells centrifuged at 2500g for 20 mins. The nutrient was removed by aspiration and the yeast cells were washed three times by centrifugation at 2200g for 10 mins in acetate buffer, ³¹² pH 6.6 and the buffy coat was removed by aspiration. The yeast cells were transferred to an nmr tube (10mm outside diameter) and washed twice in a resuspension medium containing (final concentrations) 10mM Na_5PPP and 4mM $DyCl_3$ in 25% (v/v) 2H_2O . The yeast cells were packed gently in the nmr tube by centrifugation at 1000g for 10 min. The spectra shown in Fig 3.2 represents 4000 free induction decays collected in about 15 min.

Calculation of the fractional space that was intracellular followed by comparison of the integrated area of the intracellular Na^+ peak with

that of the reference spectrum gave a value for the intracellular Na^+ concentration of 12mM.

3.4.2 Escherichia coli

The Escherichia coli* was centrifuged at 10000g for 5 min and most of the nutrient medium was poured away. The E. coli pellet formed was broken up on a whirly mixer and washed two times by centrifugation at 10000g for 5 mins in 10mM tris buffer [Tris(hydroxymethyl)aminomethane], pH 7.0 and the buffy coat decanted. The pellet formed was again broken up gently on a whirly mixer and washed by centrifugation at 2400g for 15 mins in tris buffer, pH 7.0. The tris buffer was removed by aspiration from the gently packed cells. The E. coli cells were then transferred to an nmr tube (10mm outside diameter) and washed three times in a resuspension medium containing (final concentrations) 10mM Na_5PPP and 4mM DyCl_3 in 25% (v/v) $^2\text{H}_2\text{O}$. The cells were packed gently in the nmr tube by centrifugation at 2400g for 15 mins at each washing. The spectra shown in Fig 3.3 represents 4000 free induction decays collected was resuspended in a medium containing (final concentrations) 10mM in about 15 min.

Calculation of the fractional space that was intracellular followed by comparison of the integrated area of the intracellular Na^+ peak with that of the reference spectrum gave a value for the intracellular Na^+ concentration of 14.3mM.

3.4.4 Tetrahymena pyriformis

The Tetrahymena pyriformis culture* was centrifuged at 10000g for 5 mins and most of the nutrient medium was decanted. The pellet formed

*Culture prepared by Dr M North, Biological Sciences Department, Stirling University.

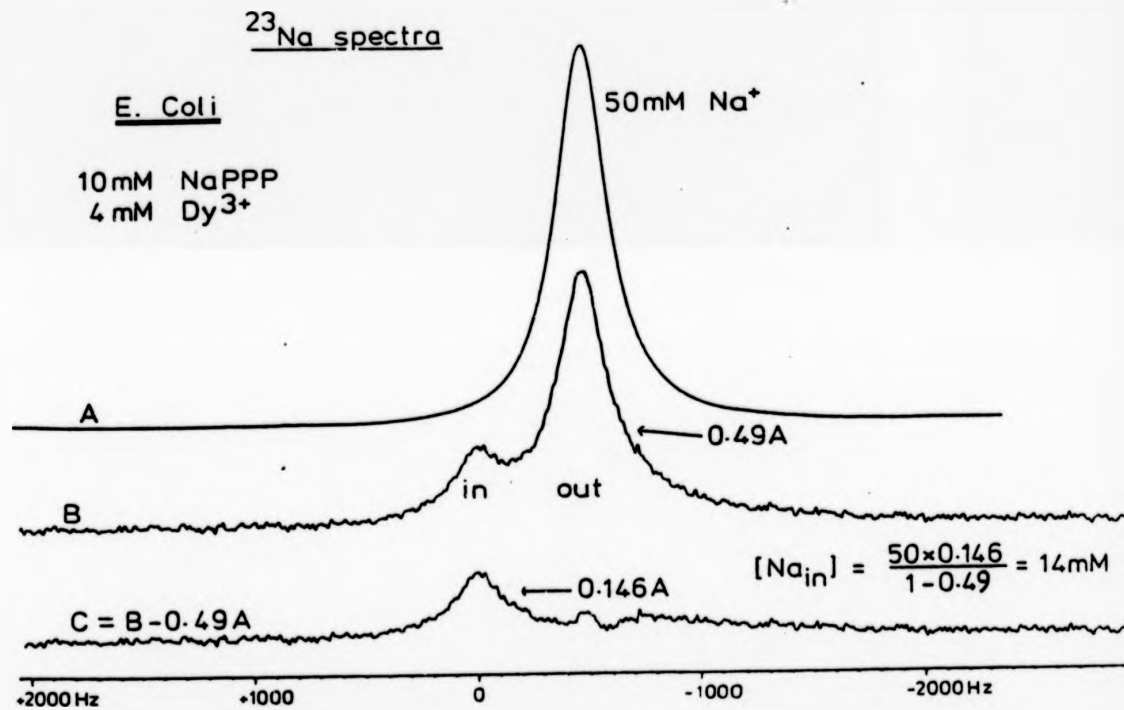


Fig 3.3 ²³Na nmr spectrum of (A) resuspension medium containing 10mM Na₂PPP and 4mM DyCl₃, (B) Escherichia coli in the same medium and (C) difference spectra after subtraction of 0.49 of the integrated intensity of spectrum (A) from spectrum (B).

Na_5PPP and 4mM DyCl_3 in 25% (v/v) $^2\text{H}_2\text{O}$ and centrifuged at $10000g$ for 5 mins and the buffy coat was removed by aspiration. The cells were then transferred to an nmr tube (10mm outside diameter) and washed once in the resuspension medium as above. The Tetrahymena pyriformis were packed gently in the nmr tube by centrifugation at $2400g$ for 10 mins.

The ^{23}Na nmr spectrum of the cells was followed for several hours. The spectra shown in Fig 3.4 represents 4000 free induction decays collected in about 15 mins.

3.5 MEASUREMENT OF IONOPHORE MEDIATED SODIUM ION TRANSPORT IN LARGE UNILAMELLAR PHOSPHOLIPID VESICLES

Large unilamellar phospholipid vesicles (LUV) are prepared using the method adopted by Reynolds et al²⁸⁸ where the molar ratio of detergent/lipid in the final solution is of the order of 15:1. A typical procedure is illustrated by the preparation of 3cm^3 of LUV suspension trapped with 200mM NaCl solution and the surrounding medium containing an equivalent Na^+ ion concentration.

The standard solution of egg phosphatidylcholine (egg PC), supplied by Dr P Brophy (Biological Sciences Department, Stirling University), contained $400\ \mu\text{Moles}$ of egg PC per cm^3 of benzene. $20\ \mu\text{Moles}$ of egg PC are required for the preparation of $1\ \text{cm}^3$ of LUV suspension. For 3cm^3 of LUV suspension, $60\ \mu\text{Moles}$ of egg PC in benzene (ie $150\ \mu\text{l}$ of stock solution) were taken and dried under vacuum at room temperature for 4-5 hours.

15 equivalents ($0.9\ \text{mMoles}$) of detergent (262mg, n-octyl- β -glucopyranoside, molecular weight 292.38g; supplied by Sigma) were dissolved in 3cm^3 200mM NaCl solution; the solution being achieved by

^{23}Na Spectrum

Tetrahymena

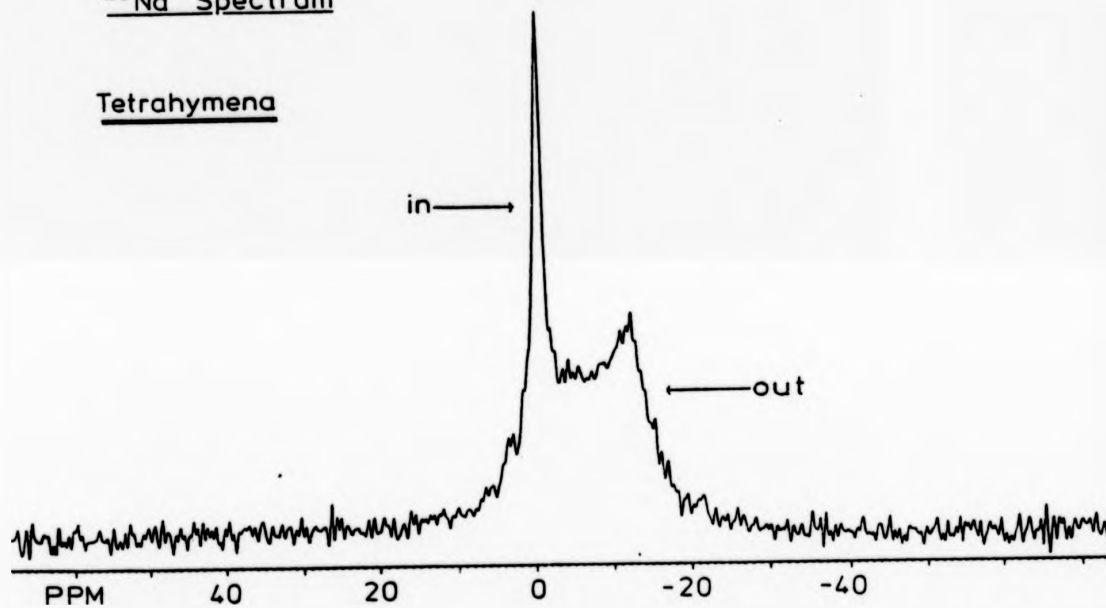


Fig 3.4 ^{23}Na nmr spectra of Tetrahymena pyriformis resuspended in a medium containing 10mM Na_5PP and 4mM DyCl_3 .

continual stirring for a period of 1/2 - 1 hour. The lipid film was redissolved in the NaCl/detergent solution; stirred for about one hour until all the egg PC had been solvated by the detergent micelles. The NaCl/detergent/egg PC solution was then transferred by pipette into the previously softened (soaked overnight in distilled water at ca 277K) dialysis tubing (Visking, size 1-8/32") and sealed.

The tubing was placed in 5 litres of 200mM solution of NaCl in a cold room (ca 277K). The external solution was changed twice at 10-12 hours intervals. This affects the slow dialytic removal of the detergent from the tubing leaving the egg PC 'unshielded' from the ionic medium. As a result the egg PC spontaneously forms phospholipid bilayers which arrange themselves into vesicles giving a turbid suspension. The large unilamellar vesicles so formed have 200mM NaCl (aq) solution both inside and outside.

A final dialysis at ca 4°C against 5 litres (20mM Na₅PPP and 100mM NaCl) results in the incorporation of Na₅PPP in the surrounding medium with the total sodium ion concentration remaining at 200mM. The vesicles prepared thus had 200mM NaCl inside and a solution of 20mM PPP⁵⁻, 200mM Na⁺ and 100mM Cl⁻ outside. All experiments were performed within 24hr after the preparation of the vesicles.

The transport studies were carried out on a Bruker WP80 FT nmr spectrometer by recording the changes in the ²³Na nmr spectrum of the sodium ions inside the vesicles at 21.19 MHz. The spectrometer was always field frequency locked on the ²H resonance of ²H₂O present in the inner compartment of a coaxial tube which served as an internal reference. The spectra were obtained either at 298K or 303K and normally an artificial line broadening of 2Hz was used to improve the spectral signal-to-noise ratio.

The ^{23}Na nmr spectrum of the LUV obtained gave a peak of slightly greater width than that obtained for pure NaCl solution due to the very slight environmental distinctions between the sodium inside and outside the vesicles. (Fig 3.5).

Sufficient Dysprosium chloride was added to give a chemical shift separation of at least 8ppm between the Na^+ resonances inside and outside the vesicles. The internal sodium peak was set to zero chemical shift.

3.5.1 Monensin Mediated Sodium Ion Transport

The monensin (sodium salt), supplied by Sigma, was recrystallized before being made into a standard solution in methanol (MeOH). Microlitre amounts of this solution were added to the LUV preparations.

(a) Lineshape Analysis

In the study of monensin mediated sodium ion transport by lineshape analysis, LUV trapped with varying concentrations of NaCl were prepared as described above and are tabulated in Table 3.18. The average concentration of egg PC per cm^3 of LUV prepared was 18.8 ± 2.0 μMoles .

Typically 4000 free induction decays were collected into 512 data points with a sweep width of 1500-2000 Hz, zero filled and transformed in 4K data points. For LUV containing less than 100mM NaCl, 10000-30000 free induction decays were collected to improve the spectral signal-to-noise ratio.

An average 2.5% of the total sodium ion concentration was noted to be present within the LUV (Table 3.18).

The spectral data collected for LUV trapped with 120mM NaCl (as an illustration) is included in Fig 3.6. The change in linewidth is directly related to the exchange rate by the equation:²⁹⁸

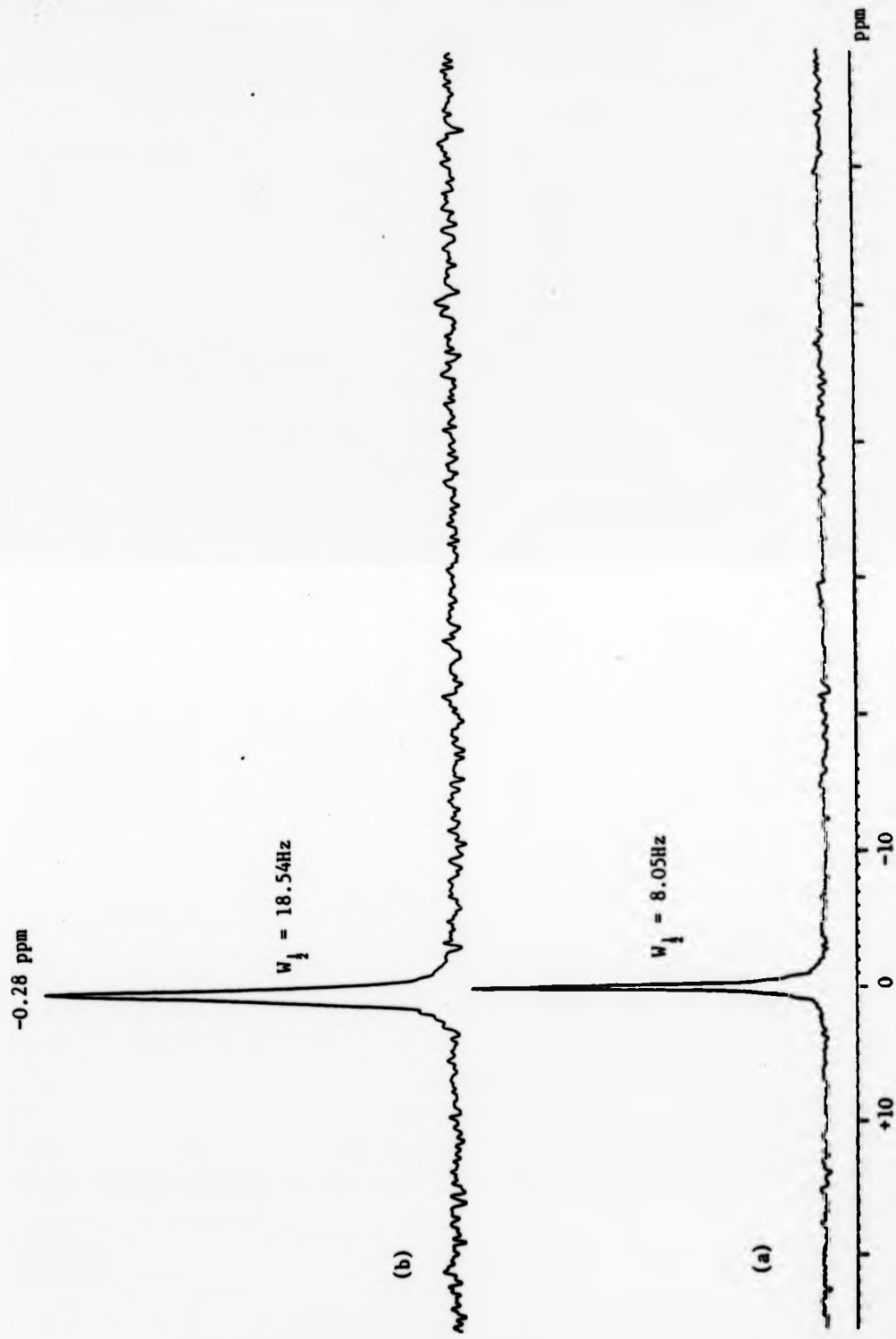


Fig 3.5 (a) ^{23}Na spectrum of a 100mM NaCl solution.

(b) ^{23}Na spectrum of LUV containing 150mM NaCl and surrounding medium contains 15mM Na_5PPP and 75mM NaCl.

TABLE 3.18 Preparation of large unilamellar vesicles (LUV) using the dialysis method²⁸⁸ where the molar ratio of n-octyl- β -glucopyranoside to egg phosphatidylcholine is about 15:1 and the set-up ^{23}Na nmr experiment conditions for monensin mediated Na^+ transport in LUV. $T = 303\text{K}$.

LUV	First Three Dialysis (T=277K) mM NaCl	Final Dialysis (T=277K)	$\mu\text{Moles egg PC}$ per cm^3 LUV	^{23}Na nmr set-up Experiment cm^3 LUV	mM DyCl_3	Na^+ Shift ppm	Na^+ +0.37 -0.37
250mM NaCl	250	20mM Na_5PPP 150mM NaCl	18.8	1.6	6.3	8.4	-
200mM NaCl	200	20mM Na_5PPP 100mM NaCl	18.8	1.5	5.3	10.6	2.6
175mM NaCl	175	20mM Na_5PPP 75mM NaCl	20.8	1.44	5.6	10.9	-
150mM NaCl	150	15mM Na_5PPP 75mM NaCl	19.0	1.5	4.0	10.5	2.5
120mM NaCl	120	10mM Na_5PPP 70mM NaCl	18.4	2.0	4.0	11.8	-
100mM NaCl	100	10mM Na_5PPP 50mM NaCl	17.6	1.5	3.3	13.5	2.5
75mM NaCl	75	10mM Na_5PPP 25mM NaCl	19.5	1.54	3.3	16.3	2.3
50mM NaCl	50	10mM Na_5PPP	17.6	1.7	2.4	18.6	2.2
25mM NaCl	25	5mM Na_5PPP	18.75	1.6	1.25	15.2	-
100mM NaCl +100mM KCl	100 +100mM KCl	20mM Na_5PPP 100mM KCl	16.7	1.8	6.7	9.3	2.6

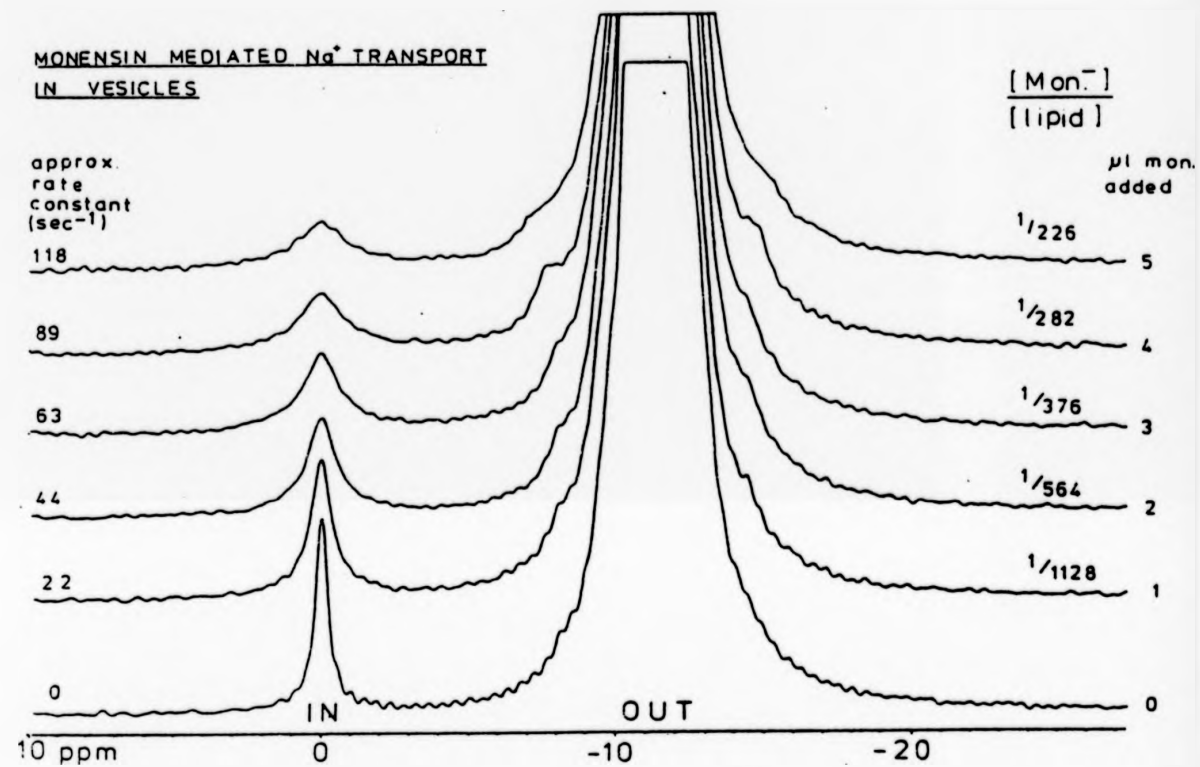


Fig 3.6

²³Na nmr of LUV, trapped with 120mM NaCl and surrounding medium contains 10mM Na₂PPP, 70mM NaCl and 4.0mM DyCl₃, on addition of increasing micro litre amounts of 2.446×10^{-2} M sodium monensin (in MeOH) solution. T = 303K.

$$k_{\text{obs}} = \pi(W_{\frac{1}{2}}^1 - W_{\frac{1}{2}}^0)$$

where $W_{\frac{1}{2}}^0$ is the linewidth in the absence of the ionophore. The linewidths recorded at various concentrations are presented in Table 3.23.

The results of the study of monensin mediated Na^+ transport in LUV trapped with varying concentrations of NaCl are listed in Tables 3.19 to 3.27. Table 3.28 shows the monensin mediated Na^+ transport in LUV trapped with 100mM NaCl and 100mM KCl. The surrounding media accordingly contained 100mM Na^+ and 100mM K^+ (Table 3.18). The rate constant observed is very similar to that observed in LUV trapped with just 100mM NaCl (Table 3.24).

In a separate experiment, 6 μl of methanol was added to the external medium in the absence of monensin (using LUV trapped with 120mM NaCl). No effect was observed on the shift or the linewidth of the Na_{IN}^+ resonance.

In all the above experiments, no attempt was made to control the pH during the dialyses and the titrations. Table 3.29 presents the results obtained from LUV trapped with 100mM NaCl, where the solution of the final dialysis (10mM Na_5PPP + 50mM NaCl) was adjusted from pH 9.0 to pH 8.1 with concentrated hydrochloric acid, while Table 3.30 includes the pH values measured at ca 298K of a selection of substrates.

(b) Magnetization Transfer

Preliminary indications on the Bruker WP80 FT spectrometer showed that monensin mediated sodium ion transport could be studied by magnetization transfer (vide infra), but more satisfactory results could be obtained on the Bruker WP360 FT spectrometer, operating at 95.23 MHz for ^{23}Na , and these are reported in the thesis.

LUV trapped with 200mM NaCl were prepared as described above. The

TABLE 3.19 Monensin mediated Na^+ transport in large unilamella vesicles (LUV) trapped with 250mM NaCl. T = 303K.

μL of $1.89 \times 10^{-2}\text{M}$ NaMon (in MeOH)	μMoles NaMon	μMoles NaMon per cm^3 of LUV	$W_{1/2}$ Hz	$k \text{ s}^{-1}$
0	0.0	0.0	10.26	0.0
1	0.0189	0.0118	13.30	9.550
2	0.0378	0.0236	17.59	23.028
3	0.0567	0.0354	20.53	32.264
4	0.0756	0.0473	20.21	43.825
5	0.0945	0.0591	26.66	51.52

TABLE 3.20 Monensin mediated Na^+ transport in large unilamella vesicles (LUV) trapped with 200mM NaCl. T = 303K.

μL of $1.89 \times 10^{-2}\text{M}$ NaMon (in MeOH)	μMoles NaMon	μMoles NaMon per cm^3 of LUV	$W_{1/2}$ Hz	$k \text{ s}^{-1}$
0	0.0	0.0	9.77	0.0
1	0.0189	0.0126	13.67	12.25
2	0.0378	0.0252	18.50	27.43
3	0.0567	0.0378	22.46	39.87
4	0.0756	0.0504	25.40	49.10
5	0.0945	0.0630	30.30	64.50

TABLE 3.21 Monensin mediated Na^+ transport in large unilamella vesicles (LUV) trapped with 175mM NaCl. T = 303K.

μL of $1.89 \times 10^{-2}\text{M}$ NaMon (in MeOH)	μMoles NaMon	μMoles NaMon per cm^3 of LUV	$W_{1/2}$ Hz	k s^{-1}
0	0.0	0.0	10.26	0.00
1	0.0189	0.0131	16.13	18.44
2	0.0378	0.0263	18.33	27.65
3	0.0567	0.0394	24.19	43.76
4	0.0756	0.0525	26.40	50.71
5	0.0945	0.0630	36.25	69.11

TABLE 3.22 Monensin mediated Na^+ transport in large unilamella vesicles (LUV) trapped with 150mM NaCl. T = 303K.

μL of $1.89 \times 10^{-2}\text{M}$ NaMon (in MeOH)	μMoles NaMon	μMoles NaMon per cm^3 of LUV	$W_{1/2}$ Hz	k s^{-1}
0	0.0	0.0	9.76	0.0
2	0.0379	0.0253	19.00	29.03
3	0.0567	0.0378	23.50	43.17
4	0.0756	0.0504	30.00	63.59
5	0.0945	0.0630	35.00	79.29

TABLE 3.23 Monensin mediated Na^+ transport in large unilamella vesicles (LUV) trapped with 120mM NaCl. T = 303K.

μL of $2.446 \times 10^{-2} \text{M}$ NaMon (in MeOH)	μMoles NaMon	$\mu\text{Moles NaMon per}$ cm^3 of LUV	$W_{1/2}$ Hz	$k \text{ s}^{-1}$
0	0.0	0.0	10.6	0.0
1	0.0245	0.01223	17.60	21.99
2	0.0489	0.0245	24.61	44.01
3	0.0734	0.0367	30.65	62.99
4	0.0978	0.0489	38.93	87.00
5	0.1223	0.0612	48.16	118.00

TABLE 3.24 Monensin mediated Na^+ transport in large unilamella vesicles (LUV) trapped with 100mM NaCl. T = 303K.

μL of $1.29 \times 10^{-2} \text{M}$ NaMon (in MeOH)	μMoles NaMon	$\mu\text{Moles NaMon per}$ cm^3 of LUV	$W_{1/2}$ Hz	$k \text{ s}^{-1}$
0	0.0	0.0	12.2	0.0
1	0.0129	0.0086	25.87	18.54
2.5	0.0323	0.0215	25.87	42.95
3.5	0.0451	0.0301	34.18	69.05

TABLE 3.25 Monensin mediated Na^+ transport in large unilamella vesicles (LUV) trapped with 75mM NaCl. $T = 303\text{K}$.

μL of $1.89 \times 10^{-2}\text{M}$ NaMon (in MeOH)	μMoles NaMon	μMoles NaMon per cm^3 of LUV	$W_{1/2}$ Hz	$k \text{ s}^{-1}$
0.0	0.0	0.0	10.98	0.0
0.5	0.0095	0.00614	15.68	15.33
1.0	0.0189	0.0123	20.75	30.69
1.5	0.0284	0.0184	24.42	42.22
2.5	0.0473	0.0307	35.40	76.72

TABLE 3.26 Monensin mediated Na^+ transport in large unilamella vesicles (LUV) trapped with 50mM NaCl. $T = 303\text{K}$.

μL of $1.89 \times 10^{-2}\text{M}$ NaMon (in MeOH)	μMoles NaMon	μMoles NaMon per cm^3 of LUV	$W_{1/2}$ Hz	$k \text{ s}^{-1}$
0	0.0	0.0	10.27	0.0
0.5	0.009451	0.00556	15.39	16.09
1.0	0.0189	0.0126	21.99	36.82
1.5	0.0284	0.0167	25.66	48.35

TABLE 3.27 Monensin mediated Na^+ transport in large unilamella vesicles (LUV) trapped with 25mM NaCl. T = 303K.

μL of $1.29 \times 10^{-2}\text{M}$ NaMon (in MeOH)	μMoles NaMon	μMoles NaMon per cm^3 of LUV	$W_{1/2}$ Hz	$k \text{ s}^{-1}$
0	0.0	0.0	9.28	0.0
0.5	0.00645	0.00403	17.58	26.07
1.0	0.0129	0.00806	24.90	49.10

TABLE 3.28 Monensin mediated Na^+ transport in large unilamella vesicles (LUV) trapped with 100mM NaCl and 100mM KCl. T = 303K.

μL of $1.29 \times 10^{-2}\text{M}$ NaMon (in MeOH)	μMoles NaMon	μMoles NaMon per cm^3 of LUV	$W_{1/2}$ Hz	$k \text{ s}^{-1}$
0	0.0	0.0	9.28	0.0
1	0.0129	0.00717	13.67	13.79
2	0.0258	0.0143	17.58	26.08
3	0.0387	0.0215	22.47	41.44
4	0.0516	0.0287	28.32	59.82

TABLE 3.29 Monensin mediated Na^+ transport in large unilamella vesicles (LUV) trapped with 100mM NaCl. $T = 303\text{K}$. pH of final dialysis solution was adjusted to ca 8.1 with concentrated hydrochloric acid.

μL of $1.29 \times 10^{-2}\text{M}$ NaMon (in MeOH)	μMoles NaMon	μMoles NaMon per cm^3 of LUV	$W_{1/2}$ Hz	$k \text{ s}^{-1}$
0	0.0	0.0	8.30	0.0
1	0.0124	0.00717	15.64	23.06
2	0.0258	0.0143	23.44	47.56
3	0.0381	0.0215	31.60	73.20

TABLE 3.30 pH values measured at ca 298K of substrates used in the study of Monensin mediated sodium ion transport in LUV.

Substrate	Ionic Strength	pH
20mM Na ₅ PPP 100mM NaCl 5.3mM Dy Cl ₃	0.43	8.61
100mM NaCl	0.10	5.8
10mM Na ₅ PPP 50mM NaCl xHCl	-	8.07
10mM Na ₅ PPP 50mM NaCl xHCl 6.7mM DyCl ₃	-	5.87
10mM Na ₅ PPP 2.4mM DyCl ₃	0.164	9.27
100mM NaCl 100mM KCL	-	6.40
20mM Na ₅ PPP 100mM KCl 6.7mM DyCl ₃	0.44	8.36

surrounding media containing 20mM PPP^{5-} , 100mM Cl^- , 200mM Na^+ and sufficient DyCl_3 to give a reasonable shift difference between the Na_{IN}^+ and Na_{OUT}^+ resonances.

The spectrometer was always field frequency locked on the ^2H resonance of $^2\text{H}_2\text{O}$ present in the inner compartment of a coaxial nmr tube which served as an internal reference. The spectra were obtained at 303K and an artificial line broadening of 10Hz was used to improve the spectral signal-to-noise ratio.

The spin-lattice relaxation (T_1) measurements of the Na_{IN}^+ and Na_{OUT}^+ resonances, in the absence of ionophore, were performed by a non-selective inversion recovery method (180° -wait τ - 90°), in which a 180° pulse was applied to invert the magnetization to the $-z$ axis. The changes in the height of the population inverted ^{23}Na resonance as the magnetization relaxes was recorded. The spectral data collected for the spin-lattice relaxation measurements of Na_{IN}^+ and Na_{OUT}^+ resonances in the absence of monensin are included in Figs 3.7 and 3.8 respectively. While in Tables 3.31 and 3.32 are listed the changes in spectral height. Plots of $\ln(S_\infty - S_t)$ against t should give straight lines, allowing us to extract values for T_1 with respect to the Na_{IN}^+ (T_{1A}) and Na_{OUT}^+ (T_{1B}) resonances.

In the magnetization transfer technique the longitudinal magnetization of a resonance is measured as a function of time after the perturbation of another resonance with which it is exchanging.³⁰⁸ The largest effects are seen when the longitudinal magnetizations of the exchanging sites are monitored after one resonance is selectively inverted. Fig 3.9 presents a schematic diagram of the pulse sequence. Tables 3.33 and 3.34 show the results obtained on monitoring the recovery of Na_{IN}^+ resonance (Na_{OUT}^+ selectively inverted) in the presence

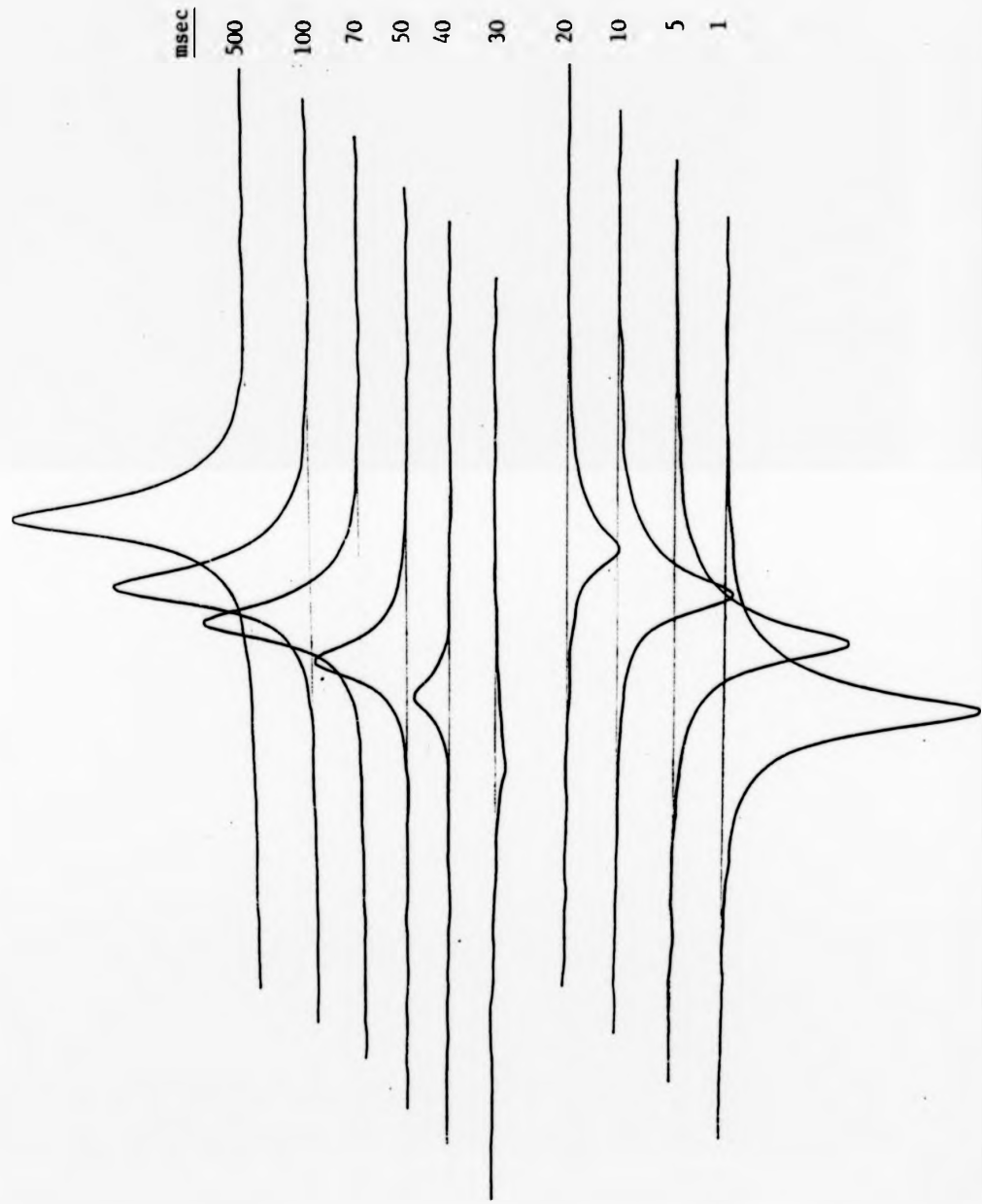


Fig 3.7 The spectral data of LUV collected for the spin-lattice relaxation measurement of Na⁺ resonance by a non-selective inversion recovery method, in the absence of sodium monensin, as a function of the delay τ .

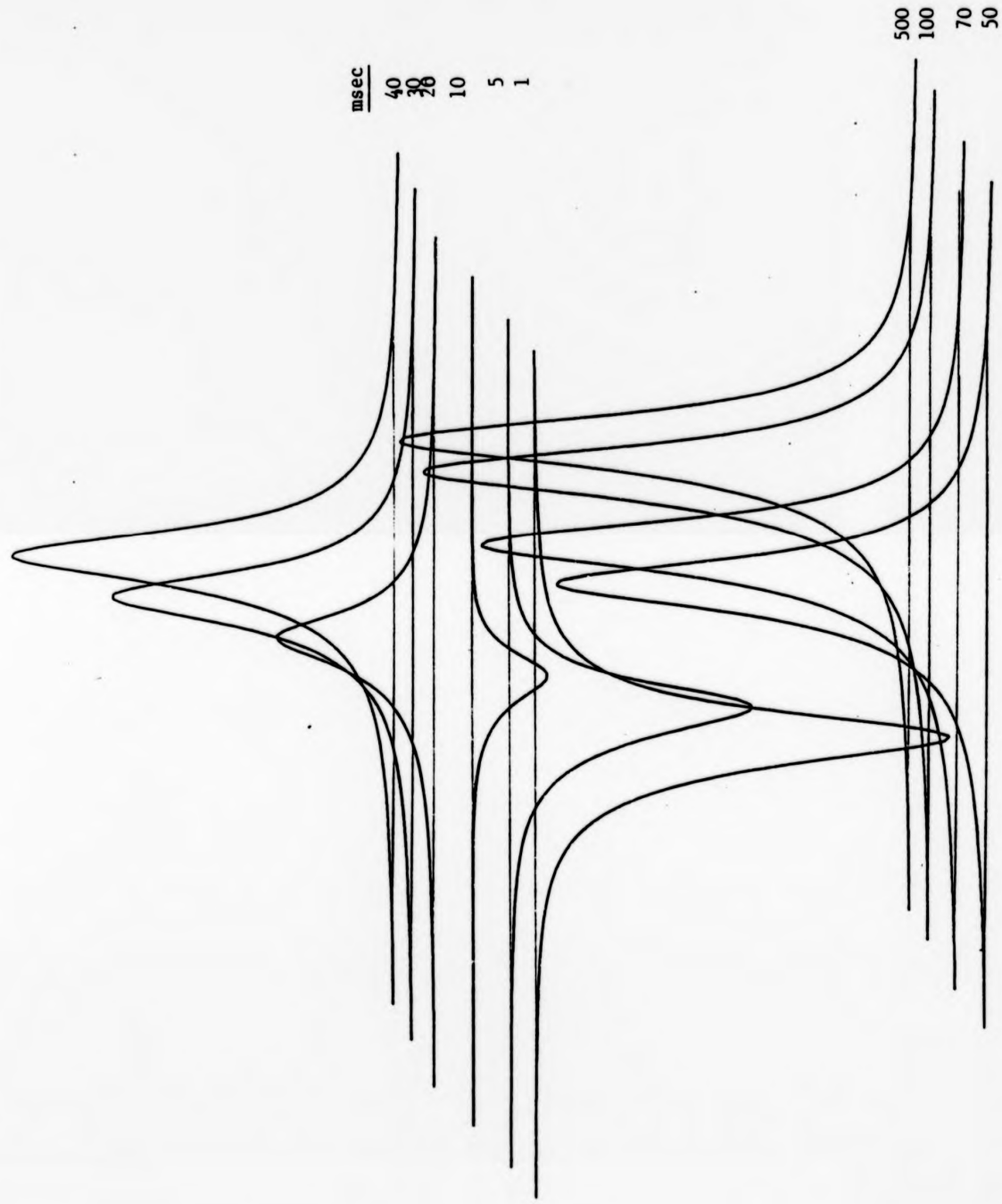


Fig 3.8 The spectral data of LUV collected for the spin-lattice relaxation measurement of NaQT resonance by a non-selective inversion recovery method, in the absence of sodium monensin, as a function of the delay τ .

TABLE 3.31 Change in spectral height (S_t) of Na_{IN}^+ resonance as a function of delay τ (95.23 MHz) $T = 303\text{K}$.

msec	S_t	$(S_\infty - S_t)$	$\text{Ln}(S_\infty - S_t)$
500	58.5 (S_∞)	0.0	-
100	40.0	18.5	2.918
70	26.0	32.5	3.481
50	12.5	46.0	3.829
40	2.5	56.0	4.025
30	-8.0	66.5	4.197
20	-12.0	79.5	4.376
10	-36.0	94.5	4.549
5	-45.5	104.0	4.644
1	-54.5	113.0	4.727

TABLE 3.32 Change in spectral height (S_t) of Na_{OUT}^+ resonance as a function of delay τ (95.23 MHz) $T = 303\text{K}$.

msec	S_t	$(S_\infty - S_t)$	$\text{Ln}(S_\infty - S_t)$
500	129.5 (S_∞)	0.0	-
100	128.5	1.0	-
70	114.5	15.0	2.708
50	109.5	20.0	2.996
40	96.0	33.5	3.512
30	75.0	54.5	3.998
20	39.0	90.5	4.505
10	-19.0	148.5	5.001
5	-61.0	190.5	5.250
1	-105.5	235.0	5.460

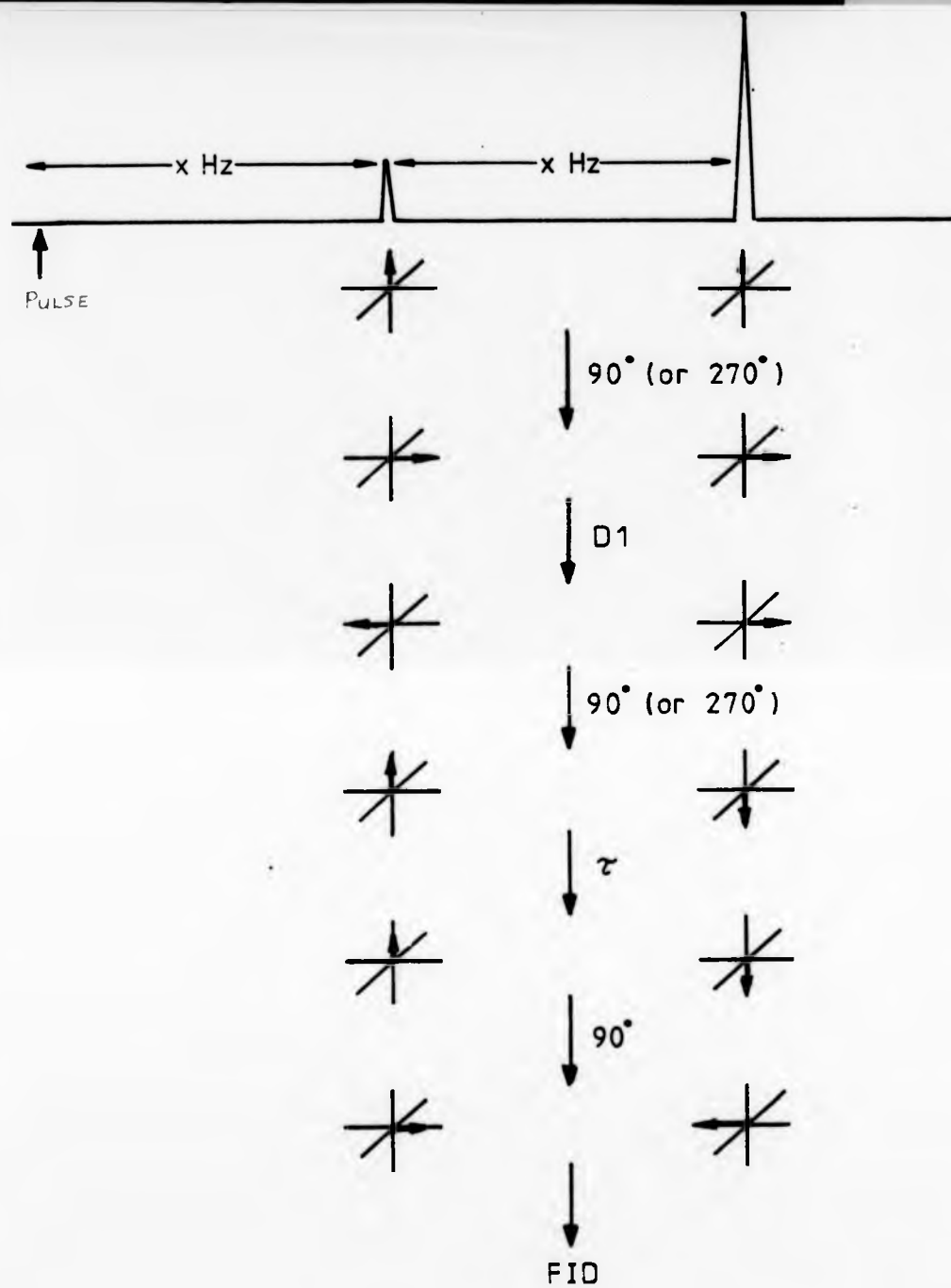


Fig 3.9 The pulse sequence for magnetization transfer (ie selective inversion recovery) experiment.

TABLE 3.33

The magnetization at site A (Na_{IN}^+), as a function of the delay τ between inversion and sampling in the presence of 1.72×10^{-2} $\mu\text{Moles monensin per cm}^3$ of LUV.

sec	S_t	S_t/S_∞
0.0025	7.00*	0.75
0.0050	7.70	0.77
0.0075	6.75*	0.73
0.010	7.60	0.76
0.0125	6.75*	0.73
0.0150	7.25	0.73
0.0175	6.60*	0.71
0.020	7.40	0.74
0.025	6.75*	0.73
0.030	7.60	0.76
0.035	7.40*	0.81
0.040	7.80	0.78
0.050	8.35	0.84
0.065	7.85 [#]	0.89
0.075	8.60*	0.92
0.100	9.50	0.95
0.150	9.70	0.98
0.200	9.95 (S_∞)	1.00

* $S_\infty = 9.3$

$S_\infty = 8.85$

TABLE 3.34

The magnetization at site A (Na_{IN}^+), as a function of the delay τ between inversion and sampling in the presence of 3.44×10^{-2} $\mu\text{Moles monensin per cm}^3$ of LUV.

sec	S_t	S_t/S_∞
0.0025	10.10	0.737
0.0050	9.55	0.697
0.0075	9.20	0.672
0.0100	8.55	0.624
0.0125	8.40	0.613
0.0150	8.40	0.613
0.0175	8.00	0.584
0.0200	8.75	0.639
0.0250	9.10	0.664
0.0300	9.50	0.693
0.0350	9.75	0.712
0.0400	10.40	0.759
0.0500	10.90	0.796
0.0650	12.00	0.876
0.0750	12.55	0.916
0.1000	13.50	0.985
0.1500	13.75	1.004
0.2000	13.60	0.993
0.5000	13.7 (S_∞)	1.000

of 1.72×10^{-2} μ Moles and 3.44×10^{-2} μ Moles monensin per cm^3 of LUV (Figs 3.10 and 3.11 include the spectral data) respectively.

3.5.2 [15]-Crown-5 Derivatives Mediated Sodium Ion Transport

The [15]-Crown-5 derivatives were prepared by Chemistry Honours' student, N C Howarth.

The LUV were prepared as described above, trapped with 200mM NaCl and the external media contained 20mM Na_5PPP , 100mM KCl and sufficient DyCl_3 to give a reasonable shift difference between Na_{IN}^+ and Na_{OUT}^+ resonances. The exchange monitored involved K_{OUT}^+ exchanging with Na_{IN}^+ .

4000 free induction decays were collected into 512 data points with a sweep width of 1000 Hz in order to achieve a rapid pulse rate, and were zero filled and Fourier transformed in 4K data points with a 2Hz line broadening. All Fourier-transforms were performed under the same absolute intensity conditions. The spectra were obtained at 303K.

In the experiment using 2-(hydroxymethyl)-[15]-crown-5 (10), a sufficient quantity of the compound was added to the vesicles to give a 4 mMolar concentration. While in another experiment 3 mMolar of the [15]-crown-5 acid derivative (11) was used. An example of the ^{23}Na nmr spectra recorded at various times over the 26hr period is included in Fig 3.12. The height of the peak due to the internal sodium at zerotime was taken as 100% Na^+ and the decrease in the height of that signal was taken as indicative of the transport of sodium out of the vesicles and of potassium in. The heights recorded at the various times are presented in Tables 3.35 and 3.36.

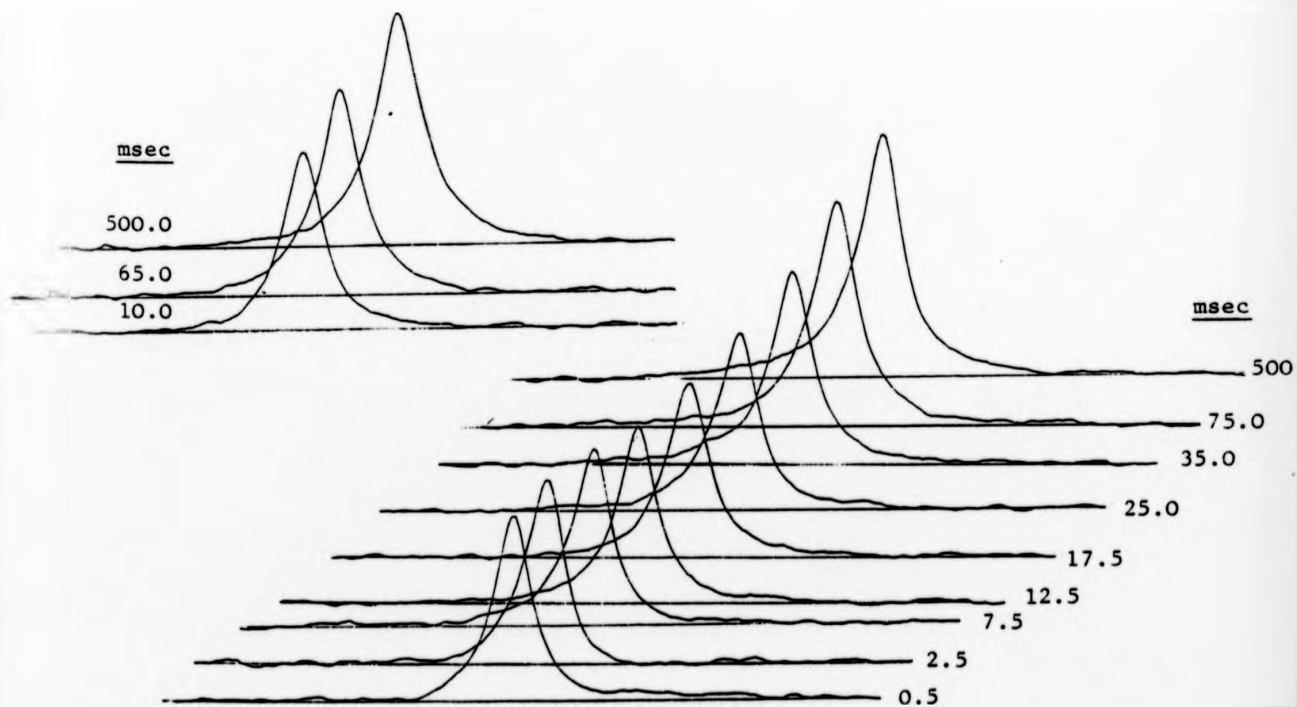
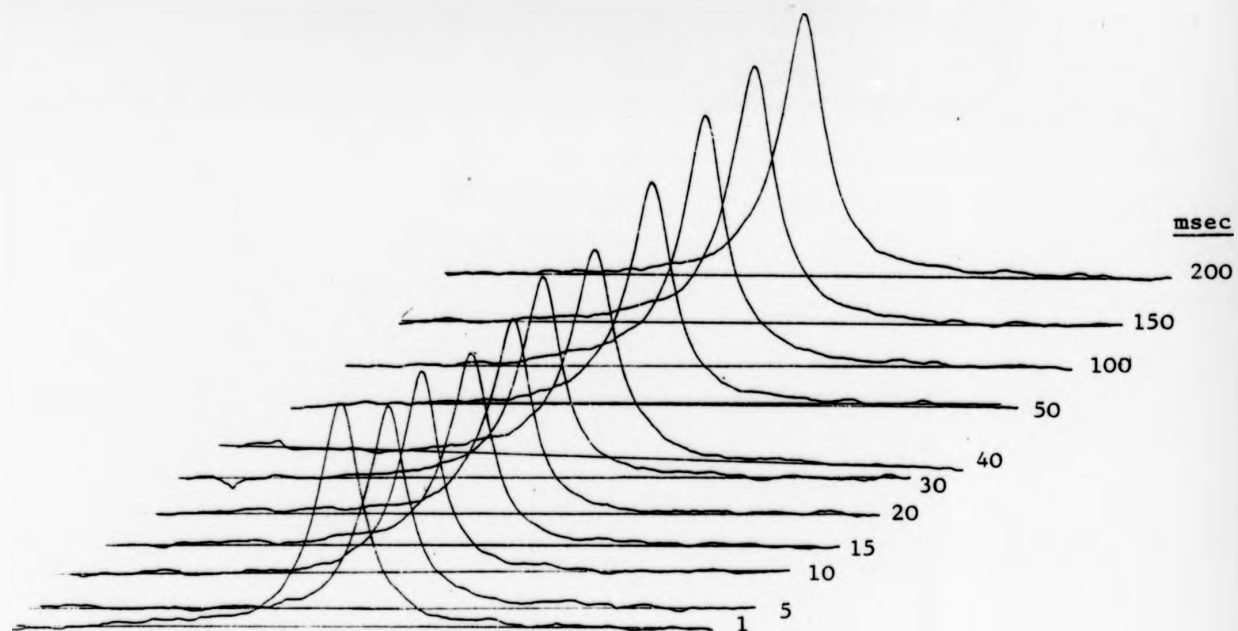


Fig 3.10 The recovery of Na^+ resonance monitored in the presence of 1.72×10^{-2} $\mu\text{Moles}_{\text{IN}}$ monensin per cm^3 of LUV by the Magnetization Transfer technique.

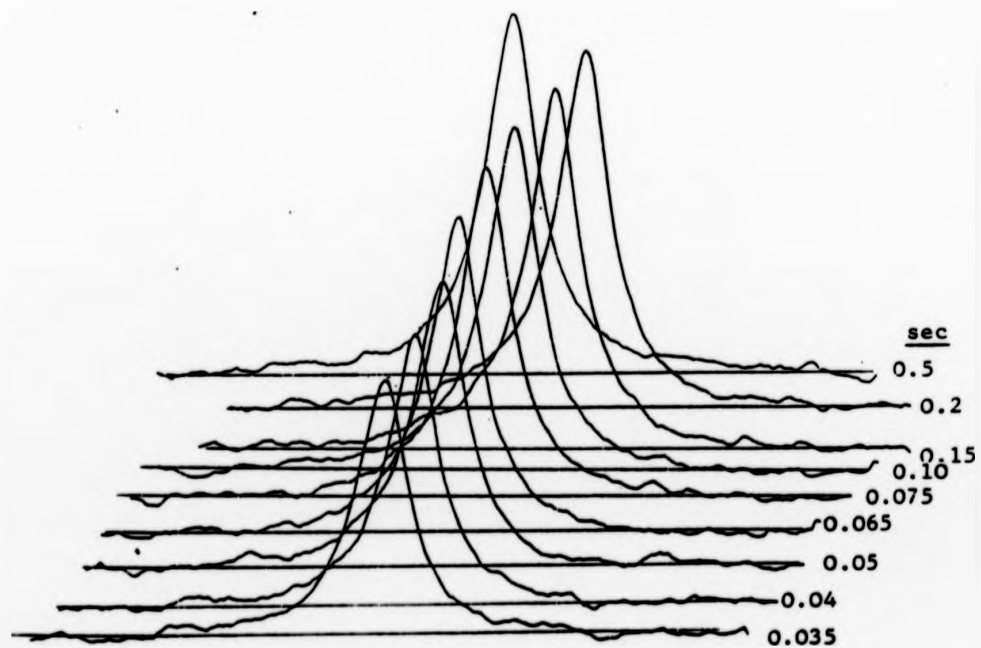
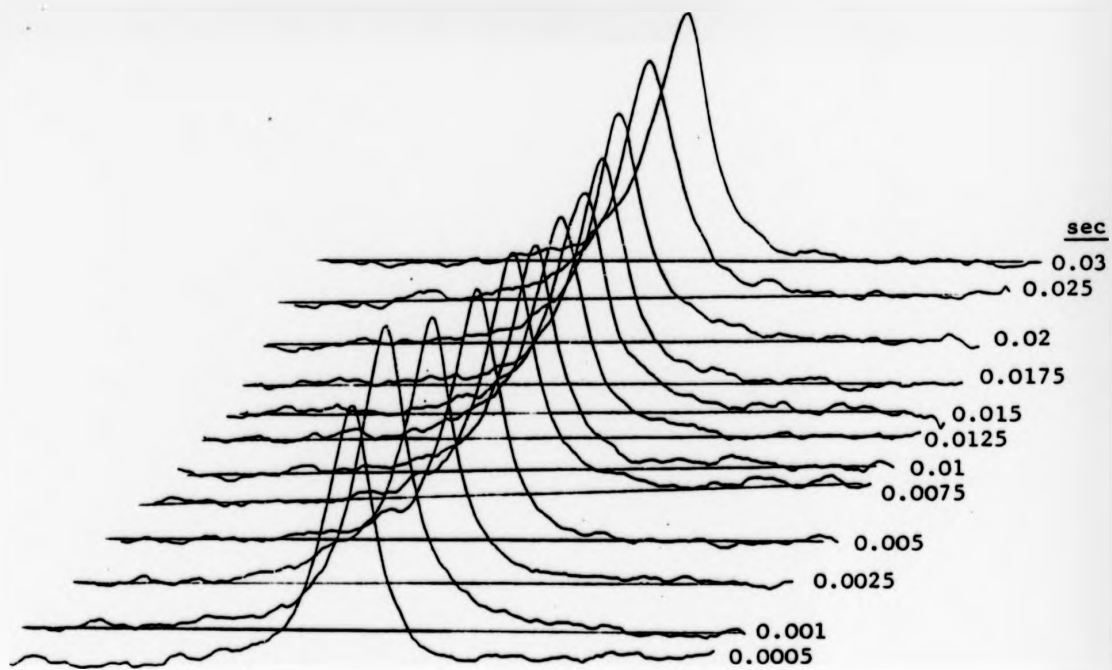


Fig 3.11 The recovery of Na^+ resonance monitored in the presence of 3.44×10^{-2} $\mu\text{Moles monensin per cm}^3$ of LUV by the Magnetization Transfer technique.

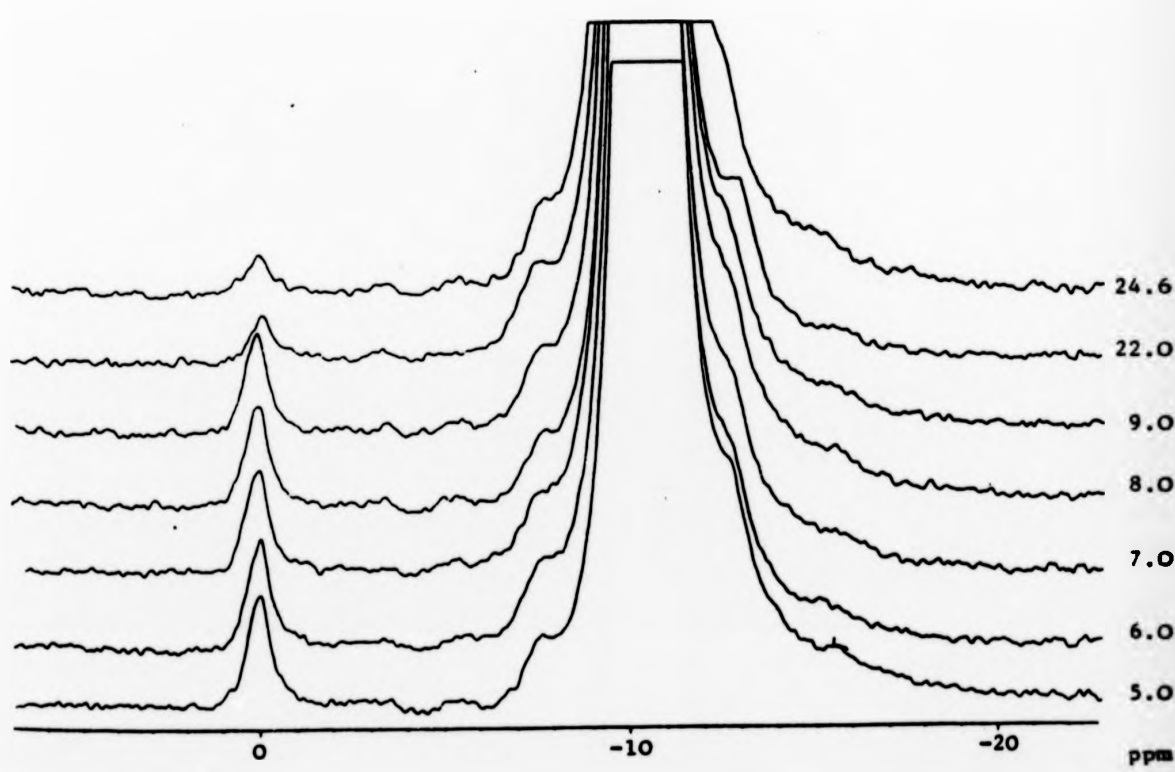
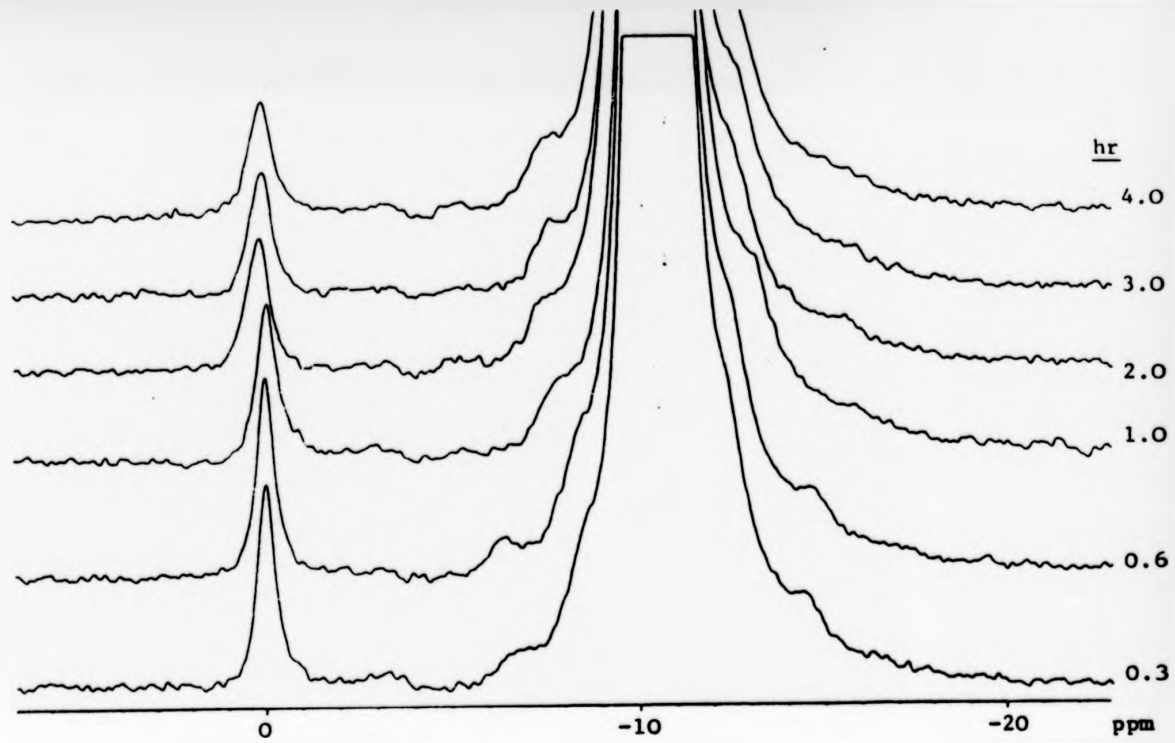


Fig 3.12 Na^+ resonance monitored as a function of time in LUV, trapped with 200mM NaCl and surrounding medium contains 20mM $Na_2P_2O_7$, 100mM KCl and 7.1mM $DyCl_3$, in the presence of [15]-crown-5 acid derivative (3mM).

TABLE 3.35 2-(hydroxymethyl)-15-crown-5 (4mM) mediated Na^+ transport in large unilamellar vesicles (LUV) trapped with 200mM NaCl; surrounding medium contains 20mM Na_3PPP , 100mM KCl and 5.3mM DyCl_3 . $T = 303^\circ\text{K}$.

Times (hr)	Height of Na^+ IN (S_t)	($S_t - S_\infty$)	$\text{Ln}(S_t - S_\infty)$
0	2.90	1.20	0.182
0.25	2.50	0.80	-0.223
1.0	2.45	0.75	-0.288
1.5	2.40	0.70	-0.357
2.5	2.45	0.75	-0.288
3.5	2.10	0.40	-0.916
4.5	2.20	0.50	-0.693
5.5	2.00	0.30	-1.204
6.5	1.90	0.20	-1.609
7.5	1.95	0.25	-1.386
8.5	1.85	0.15	-1.897
9.5	1.80	0.10	-2.303
10.5	1.75	0.05	-2.996
11.5	1.70	0.00	-
12.5	1.70 (S_∞)	0.00	-

TABLE 3.36 [15]-Crown-5 acid derivative (3mM) mediated Na_{IN}^+ transport in large unilamellar vesicles (LUV) trapped with 200mM NaCl; surrounding medium contains 20mM Na_5PPP , 100mM KCl and 7.1mM DyCl_3 . $T = 303\text{K}$.

Time (hr)	Height of Na_{IN}^+ (S_t)
0.0	9.85
0.3	7.65
0.6	7.50
1.0	5.9
2.0	5.0
3.0	4.6
4.0	4.35
5.0	4.3
6.0	4.15
7.0	3.9
8.0	3.8
9.0	3.8
22.0	1.7
24.6	1.4

3.6 ELECTRON MICROSCOPY

For negative staining,^{313,314} the LUV suspension (100mM Na⁺ in and out vesicles) was diluted 10 times with deionised water just before being applied to the carbon-coated grid. Most of the excess solvent was blotted carefully with filter paper and the remainder dried off using a hot air blower very gently. The grid was then stained with ca 2% uranyl acetate in water and excess stain blotted with filter paper and dried as above. The heavy-metal salt forms a dense amorphous mass around the membrane showing up the outlines of the membrane vesicles.

A Jeol 100C electron microscope was used, with a sheet-film camera. Grid was scanned at low magnification to select regions having a good distribution of vesicles and an even deposit of stain. These areas were imaged randomly.

REFERENCES

REFERENCES

1. R J P Williams (1970) Quart.Rev., 24, 331.
2. M H Hughes and N J Birch (1982) Chem. in Britain, 18, 196.
3. S W Kuffler and J G Nicholls (1976) "From Neuron to Brain", Sinauer Assoc.Inc., Sunderland M A, 88-104 and 237-247.
4. K C Koch and H L Leffert (1979) Cell, 18, 153.
5. I L Cameron, N K R Smith, T B Pool and R L Sparks (1980) Cancer Res., 40, 1493.
6. C D Cone (1980) Ann. N.Y.Acad.Sci., 339, 115.
7. E Rozengurt and S Mendoza (1980) Ann.N.Y. Acad.Sci., 339, 175.
8. S Ebashi and M Endo (1968) Progr.Biophys.Mol.Biol., 18, 123.
9. R P Rubin (1970) Pharmacol.Rev., 22, 389.
10. A Kleinzeller (1972) "Metabolic Pathways. Metabolic Transport", 3rd ed., Vol.VI, Academic Press, New York, 91.
11. H Rasmusser, D B P Goodman and A Tenenhouse (1972) CRC Crit.Rev.Biochem., 1, 95.
12. C H Suelter (1970) Science, 168, 789.
13. M Lezzi and L I Gilbert (1970) J.Cell Sci., 6, 615.
14. M Lubin (1967) Nature (London), 213, 451.
15. J T Tupper (1973) Dev.Biol., 32, 140.
16. B M Bremer and R W Berliner (1973) in "Handbook of Physiology", American Physiological Society, Washington D.C., 497.
17. M R Quastel and J G Kaplan (1970) Exp.Cell Res., 62, 407.
18. W G Negendank and C R Collier (1976) Exp. Cell Res., 101, 31.
19. A D C Macknight, M M Civan and A Leaf (1975) J.Membr.Biol., 20, 365.
20. V G Allfrey, R Meudt, J W Hopkins and A E Mirsky (1961) Proc.Natl.Acad.Sci. USA, 47, 907.

21. S G Schultz and P F Curran (1970) *Physiol.Rev.*, 60, 637.
22. E F Grollman (1982) "Hormone Receptors", John Wiley, New York.
23. M Ernst and G Adam (1981) *J.Membr.Biol.*, 61, 155.
24. M Canessa, N Adragna, H S Solomon, T M Connolly and D C Tosteson (1980) *New Engl.J.Med.*, 302, 772.
25. R P Garay, D Dagher, M G Pernollet, M A Devynck and P Meyer (1980) *Nature*, 284, 281.
26. R P Garay, J L Elghozi, G Dagher and P Meyer (1980) *New Engl.J.Med.*, 302, 769.
27. N Chr Hemmingsen and D Nelson (1981) *Acta.Med.Scand.*, 210, 85.
28. R Levy, R Zimlichman, A Keynan and A Livne (1982) *Biochim.Biophys.Acta.*, 685, 214.
29. B E Ehrlich and J M Diamond (1980) *J.Membr.Biol.*, 52, 187.
30. D C Tosteson (1981) *Sci.Amer.*, 244, 164.
31. K R Hull and A D Roses (1976) *J.Physiol.*, 254, 169.
32. S H Appel and A D Roses (1976) "Membranes and Disease", Raven Press, New York.
33. B Festoff (1977) "Pathogenesis in Human Dystrophies", *Excepta Medica*, Amsterdam.
34. H W Smith (1962) *Circulation*, 26, 987.
35. E Overton (1895) *Vierteljahrsschrift Naturforsch Ges. Zurich*, 40, 159.
36. E Overton (1899) in "Papers on Biological Membrane Structure", eds. D Branton and R B Park, Little, Brown & Co., Boston (1968).
37. I Langmuir (1927) *J.Physical Chem.*, 31, 1719.
38. E Gorter and F J Grendel (1925) *J.Exp.Med.*, 41, 439.
39. K S Cole (1932) *J.Cell.Comp.Physiol.*, 1, 1.
40. E N Harvey and H Shapiro (1934) *J.Cell Comp.Physiol.*, 5, 255.
41. J F Danielli and H Davson (1935) *J.Cell Comp.Physiol.*, 5, 495.

42. J F Danielli and E N Harvey (1935) *J.Cell Comp. Physiol.*, 5, 483.
43. H Davson and J F Danielli (1943) "The Permeability of Natural Cell Membranes", Cambridge University Press.
44. H Davson (1962) *Circulation*, 26, 1022.
- 45a. J D Robertson (1959) in "The Structure and Function of Subcellular Components", ed, E M Crook, *Biochem.Soc. Symposium No 16*, Cambridge University Press.
 - b J D Robertson (1966) *Ann.N.Y.Acad.Sci.*, 137, 421.
46. J D Robertson (1960) *Prog.Biophys.*, 10, 343.
47. J D Robertson (1964) in "Cellular Membranes in Development", ed. M Locke, Academic Press, London and New York.
48. J D Robertson (1967) in "Molecular Organisation and Biological Function", ed. J M Allen, Harper and Row, New York.
49. J D Robertson (1966) in "Nerve as a Tissue", eds. K Rodahl and B Issekulz Jr., Harper and Row, New York.
50. J D Robertson (1967) *Protoplasm*, 63, 218.
51. F S Sjöstranol (1963) *J.Ultrastructure Res.*, 9, 340.
52. F S Sjöstranol (1963) *J.Ultrastructure Res.*, 9, 561.
53. D Branton (1967) *Exp.Cell Res.*, 45, 703.
54. D Branton and R B Park (1967) *J.Ultrastructure Res.*, 19, 283.
55. D Branton and R B Park (1968) "Papers on Biological Membrane Structure", Little, Brown and Co., Boston.
- 56a. S J Singer and G L Nicolson (1972) *Science*, 175, 720.
 - b. B Tagawa (1975) in "Cell Membranes; Biochemistry, Cell Biology and Pathology", eds, G Weismann and R Claiborne , H P Publishing Co. Inc., New York, 38.
57. D Chapman, P Byrne and G G Shipley (1966) *Proc.R.Soc. London, Series A*, 290, 115.

58. C Tanford (1980) in "The Hydrophobic Effect: Formation of Micelles and Biological Membranes", John Wiley and Sons, New York.
59. J D Rawn (1983) "Biochemistry", Harper & Row, New York, 449.
60. E P Kennedy (1967) in "The Neurosciences - A Study Program" eds, G C Quarton, T Melnechuk and F O Schmitt, Rockefeller Press, New York, 271.
61. F A Vandenhauvel (1966) J.Am.Oil Chem.Soc., 43, 258.
62. S A Rosenberg and G Guidotti (1969) J.Biol.Chem., 244, 5118.
63. M J Osborn, J E Gander, E Parisi and J Carson (1972) J.Biol.Chem., 247, 3961.
64. G Guidotti (1972) Ann.Rev.Biochem., 41, 731.
65. M K Jain and R C Wagner (1980) "Introduction to Biological Membranes", John Wiley, New York.
66. A H Maddy (1969) in "The Molecular Basis of Membrane Functions" ed, D C Tosteson, Prentice-Hall Inc., Englewood Cliffs, N J.
67. R Fettiplace, D M Andrews and D A Haydon (1971) J.Membr.Biol., 5, 277.
68. D Chapman (1969) "Introduction of Lipids", McGraw-Hill Publishing Company, London.
69. R Harrison and G L Lunt (1980) "Biological Membranes - Their Structure and Function", Second Edition, Blackie, Glasgow.
70. W De Witt (1977) "Biology of the Cell - An Evolutionary Approach", W B Saunders Co., Toronto.
71. R A Capaldi (1977) in "Membrane Proteins and Their Interactions with Lipids", Vol 1, ed, R A Capaldi, Marcel Dekker, New York, 1.
72. I Silman (1970) Trends Biochem.Sci., 1, 225.
73. H Davson and J F Danielli (1952) "The Permeability of Natural Membranes", Cambridge; University Press.

74. E J Harris (1956) "Transport and Accumulation in Biological System", Butterworth & Co Ltd., London.
75. H N Cristensen (1962) "Biological Transport", W A Benjamin, New York.
76. J F Hoffman (ed) (1964) in "The Cellular Functions of Membrane Transport", Prentice-Hall Inc., Englewood Cliffs, N J.
77. A S Troshin (1966) "Problems of Cell Permeability" Pergamon Press, Oxford.
78. E Schgoffeniels (1967) "Cellular Aspects of Membrane Permeability", Pergamon Press, Oxford.
79. D C Tosteson (ed) (1969) in "The Molecular Basis of Membrane Function", Prentice-Hall Inc., Englewood Cliffs, N J.
80. D S Parsons (ed) (1975) "Biological Membranes", Clarendon Press, Oxford.
81. P J Garrahan and R P Garay (1976) in "Current Topics in Membranes and Transport", Vol 8, ed, F Bronner and A Kleinzeller, Academic Press, New York, 29.
82. F Bronner and A Kleinzeller (eds) (1976) in "Current Topics in Membranes and Transport", Academic Press, New York.
83. J L Hall and D A Baker (1977) "Cell Membranes and Ion Transport", Longman Group Limited, New York.
84. B Gomperts (1977) "The Plasma Membrane: Models for Structure and Function", Academic Press, London.
85. S L Bonting and J J H H M de Pont (eds) (1981) in "Membrane Transport", New Comprehensive Biochemistry Vol 2, General eds, A Neuberger and L L M van Deenen, Elsevier, Amsterdam.
86. I C West (1983) "The Biochemistry of Membrane Transport", Outline Studies in Biology, Chapman and Hall, London.
87. G Eisenman (ed) (1973) "Membranes - Vol 2 - Lipid Bilayers and Antibiotics", Marcel Dekker, New York.

88. W D Stein (1967) "The Movement of Molecules across Cell Membranes", Academic Press, New York and London.
89. R D Dyson (1979) "Cell Biology - A Molecular Approach" Second Edition, Allyn and Bacon Inc., U S A.
90. D F Wilson (1980) in "Membrane Structure and Function" Vol 1, ed, E E Bittar, John Wiley & Sons, Chichester.
91. M E Starzak (1984) "The Physical Chemistry of Membranes", Academic Press, London.
92. M D Houslay and K K Stanley (1982) "Dynamics of Biological Membranes - Influence on Synthesis, Structure and Function", John Wiley & Sons, New York.
93. R Collander (1949) *Physiol. Plantarum.*, 2, 300.
94. J F Danielli (1954) *Symp.Soc.Exp.Biol.*, 8, 502.
95. J M DiRienzo, K Nakamura and M Inouye (1978) *Ann.Rev.Biochem.*, 47, 481.
96. Z I Cabantchik, P A Knauf and A Rothstein (1978) *Biochim.Biophys. Acta.*, 515, 239.
97. P A Knauf (1979) *Curr.Top.Membr.Transp.*, 12, 249.
98. S A Baldwin and G E Lienhard (1981) *Trends.Biochem.Sci.*, 6, 208.
99. B Lugtenberg (1981) *Trends.Biochem.Sci.*, 6, 262.
100. E R Batt, R E Abbot and D Schachter (1976) *J.Biol.Chem.*, 251, 7184.
101. M Kasahara and P C Hinkle (1976) *Proc.Natl.Acad.Sci. USA*, 73, 396.
102. M Kasahara and P C Hinkle (1977) *J.Biol.Chem.*, 252, 7384.
103. T Ferenci, J Brass and W Boos (1980) *Biochem.Soc.Trans.*, 8, 680.
104. J K Nickson and M N Jones (1982) *Biochim.Biophys.Acta*, 690, 31.
105. F R Gorga and G E Lienhard (1982) *Biochemistry*, 21, 1905.
106. B C Pressman, E J Harris, W S Jagger and J H Johnson (1967) *Proc.Natl.Acad.Sci.*, 58, 1949.

107. B C Pressman (1963) in "Energy-Linked Functions of Mitochondria", ed, B Chance, Academic Press, New York, 181.
108. C Moore and B C Pressman (1964) Biochem.Biophys.Res.Comm., 15, 562.
109. B C Pressman (1965) Fed.Proc., 24, 425.
110. B C Pressman (1965) Proc.Natl.Acad.Sci.USA, 53, 1076.
111. P J F Henderson, J D McGivan and J B Chappell (1969) Biochem.J., 111, 521.
112. W Simon, W E Morf and P C H Meier (1973) in "Structure and Bonding 16 - Alkali Metal Complexes with Organic Ligands", eds, J D Dunitz, P Hemmerich, J A Ibers, C K Jorgensen, J B Neilands, D Reinen and R J P Williams, Springer-Verlag, Berlin and New York, 113.
113. W Simon and W E Morf (1963) in "Membranes", A Series of Advances, Vol 2, ed, G Eisenman, Marcel Dekker Inc., New York, 329.
114. G Szabo, G Eisenman, R Laprade, S M Ciani and S Krasne (1973) in "Membranes", A Series of Advances, Vol 2, ed. G Eisenman, Marcel Dekker Inc., New York, 179.
115. W Burgermeister, R Winkler-Oswatitsch (1977) "Topics in Current Chemistry", 69, 91.
116. A Finkelstein and A Cass (1968) J.Gen.Physiol. 52, 145, supplement.
117. G Eisenman, S M Ciani and G Szabo (1968) Fed.Proc., 27, 6.
118. D W Urry (1971) Proc.Natl.Acad.Sci., 68, 672.
119. D H Haynes, A Kowalsky and B C Pressman (1969) J.Biol.Chem., 244, 502.
120. B C Pressman (1973) in "Inorganic Biochemistry", ed, G L Eichhorn, Elsevier, Amsterdam.
121. S Linderbaum, L Sternson and S Rippel (1977) J.Chem.Soc.Chem. Commun., 268.
122. Z Štefanac and W Simon (1966) Chimia(Switz.), 20, 436.

123. Z Štefanac and W Simon (1967) *Microchem.J.*, 12, 125.
124. L A R Pioda, H A Wachter, R E Dohner and W Simon (1967) *Helv.Chim.Acta.*, 50, 1373.
125. H K Wipf, W Pache, P Jordan, H Zahner, W Keller-Schierlein and W Simon (1969) *Biochem.Biophys.Res.Comm.*, 36, (3), 387.
126. S M Johnson, J Herrin, S J Liu and I C Paul (1970) *J.Amer.Chem.Soc.*, 92, 4428.
127. D J Patel and C Shen (1976) *Proc.Natl.Acad.Sci.*, 73, 1786.
128. C Shen and D J Patel (1976) *Proc.Natl.Acad.Sci.*, 73, 4277.
129. M J O Anteunis (1977) *Bioorg.Chem.*, 6, 1.
130. B C Pressman (1968) *Fed.Proc., Fed.Am.Soc.Exp.Biol.*, 27, 1283.
131. W McMurry and R W Begy (1959) *Arch.Biochem.Biophys.*, 84, 546.
132. Yu A Ovchinnikov, V T Ivanov and A M Shkrob (1974) in "Membrane Active Complexones", Vol 12, ed, B B A Library, Elsevier, New York.
133. H Diebler, M Eigen, G Ilgenfritz, G Maass and R Winkler (1968), *ICCC*, 11; (1969) *Pure Appl. Chemistry*, 20, 93.
134. C J Pedersen (1967) *J.Amer.Chem.Soc.*, 89, 2495; (1967) *ib.* 89, 7017; (1970), *ib.*, 92, 386; (1970) *ib.* 92, 391.
135. J M Lehn and J P Sauvage (1971) *J.Chem.Soc.Chem.Comm.*, 440.
136. J M Lehn (1973) in "Structure and Bonding 16" eds, J D Dunitz, P Henmerich, J A Ibers, C K Jorgensen, J B Neilands, D Reinan and R J P Williams, Springer-Verlag, Berlin and New York, 1.
137. J M Lehn and J P Sauvage (1975) *J.Amer.Chem.Soc.*, 97, 6700.
138. J M Lehn and J Simon (1977) *Helv.Chim.Acta*, 141.
139. D Ammann, R Bissig, Z Cimerman, U Fiedler, M Guggi, W E Morf, M Oehme, H Osswald, E Pretsch and W Simon (1976) in "Ion and Enzyme Electrodes in Biology and Medicine", eds, M Kessler, L C Clark Jr, D W Lubbers, I A Silver and W Simon, Urban & Schwarzenberg, Munich, Berlin, Vienna, 22.

140. W Simon, E Pretsch, D Ammann, W E Morf, M Guggi, R Bissig and M Kessler (1975) *Pure Appl.Chem.*, 44, 613.
141. C J Pedersen and H K Frensdorff (1972) *Agnew Chem.Internal.Ed. (English)*, 11, 16.
142. E L Lee, O A Gansow and M J Weaver (1980) *J.Amer.Chem.Soc.*, 102, 2278.
143. G Anderegg (1981) *Helv.Chim.Acta.*, 64(6), 1790.
144. F Arnaud-Neu, B Spiess and M J Schwing-Weil (1982) *J.Amer.Chem.Soc.*, 104, 5641.
145. H K Frensdorff (1971) *J.Amer.Chem.Soc.*, 93, 600, 4684.
146. M Kirch and J M Lehn (1975) *Angew.Chem.Internal.Ed. (English)*, 14, 555.
147. J M Lehn (1977) *Pure and Appl.Chem.*, 49, 857.
148. J M Lehn (1978) *Pure and Appl.Chem.*, 50, 871.
149. J M Lehn (1979) *Pure and Appl.Chem.*, 51, 979.
150. J D Lamb, T J Christensen, J L Oscarson, B L Nielsen, B W Asay and R M Izatt (1980) *J.Amer.Chem.Soc.*, 102, 6820.
151. J J Christensen, J O Hill and R M Izatt (1971) *Science*, 174, 459.
152. G W Liesegang, M M Farrow, F A Vazquez, N Purdie and E M Eyring (1977) *J.Amer.Chem.Soc.*, 99, 3240.
153. B G Cox, H Schneider and J Stroka (1978) *J.Amer.Chem.Soc.*, 100, 4746.
154. V M Loyola, R Pizer and R G Wilkins (1977) *J.Amer.Chem.Soc.*, 99, 7185.
155. B G Cox, J Garcia-Rosas and H Schneider (1981) *J.Amer.Chem.Soc.*, 103, 1384.
156. B G Cox, J Garcia-Rosas and H Schneider (1981) *J.Amer.Chem.Soc.*, 103, 1054.
157. I M Kolthoff and M K Chantooni (1980) *Anal.Chem.*, 52, 1039.

158. S McLaughlin and M Eisenberg (1975) *Ann.Rev.Biophys.Bioeng.*, 4, 335.
159. B C Pressman (1976) *Ann.Rev.Biochem.*, 45, 501.
160. S Masamune, G S Bates and J W Corcoran (1977) *Angew Chem.Int.Ed.*
(English), 16, 585.
161. J W Westley (1977) in "Advances in Applied Microbiology", Vol 22,
ed, D Perlman, Academic Press, London.
162. R M Izatt and J J Christensen (eds) (1979) "Progress in Macrocyclic
Chemistry" Vol 1, John Wiley & Sons, New York.
163. H H Ussing (1949) *Acta Physiol.Scand.*, 19, 43.
164. R W Berliner (1959) *Rev.Mod.Phys.*, 31, 342.
165. R K Crane (1977) *Rev.Physiol.Biochem.Pharmacol.*, 78, 99.
166. I C West (1980) *Biochim.Biophys.Acta*, 604, 91.
167. J C Skou (1957) *Biochim Biophys. Acta*, 23, 394.
168. R W Albers (1967) *Ann.Rev.Biochem.*, 36, 727.
169. R L Post, C Hegyvary and S Kume (1972) *J.Biol.Chem.*, 247, 6530.
170. P L Jørgensen (1982) *Biochim.Biophys.Acta.*, 694, 27.
171. H V Rickenberg, G N Cohen, G Buttin and J Monad (1956) *Ann.Inst.*
Pasteur., 91, 829.
172. P Mitchell (1963) *Biochem.Soc.Symp.*, 22, 142.
173. P Mitchell (1966) *Biol.Rev.*, 41, 445.
174. P Mitchell (1970) in "Membranes and Ion Transport", Vol 1, ed,
E E Bittar, Wiley-Interscience, New York and London, 192.
175. E Pavlasova and F M Harold (1969) *J.Bacteriol.*, 98, 198
176. I C West and P Mitchell (1973) *Biochem.J.*, 132, 587.
177. I R Booth, W J Mitchell and W A Hamilton (1979) *Biochem.J.*, 182, 687.
178. D Zilberstein, S Schuldiner and E Padan (1979) *Biochemistry*, 18, 669.
179. D A T Dick, D J Fry, P N John and A W Rogers (1970) *J.Physiol.*
(London), 231, 19.
180. S B Horowitz and I R Fenichel (1970) *J.Cell Biol.*, 47, 120.

181. J A M Hinke (1973) Ann. N Y Acad.Sci., 204, 274.
182. A A Lev and W McD Armstrong (1975) Curr.Top.Membr.Transp., 6, 59.
183. L G Palmer and M M Civan (1977) J.Membr.Biol., 33, 41.
184. L G Palmer and M M Civan (1975) Science, 188, 1321.
185. R D Moore and R K Gupta (1980) Int.J.Quart.Chem.Biol.Symp., 7, 83.
186. R K Gupta, J L Benovic and Z B Rose (1978) J.Biol.Chem., 253, 6172.
187. R K Gupta (1979) Biochim.Biophys.Acta., 586, 189.
188. R K Gupta and R D Moore (1980) J.Biol.Chem., 255, 3987.
189. R K Gupta and W D Yushok (1980) Proc.Natl.Acad.Sci.USA, 27, 2487.
190. R K Gupta (1980) Int.J.Quart.Chem.Quart.Biol.Symp., 7, 67.
191. W D Yushok and R K Gupta (1980) Biochim.Biophys.Res.Comm., 95, 73.
192. J K M Roberts and O Jardetzky (1981) Biochim.Biophys.Acta., 639, 53.
193. M M Civan and M Shporer (1978) in "Biological Magnetic Resonance"
Vol 1, ed, L J Berliner and J Reuben, Plenum Press, London, 1.
194. H J C Yeh, F J Brindley and E D Becker (1973) Biophys.J., 13, 56.
195. R K Gupta and P Gupta (1982) Biophys.J., 37, 76a.
196. R K Gupta, P Gupta and W Negendank (1982) in "Ions, Cell
Proliferation, Cancer", [Proc.Symp.] eds, A L Boynton, W L McKeehan
and J F Whitfield, Academic Press, New York, 1.
197. R K Gupta and P Gupta (1982) J.Magn.Reson., 47, 344.
198. M M Pike, E T Fossel, T W Smith and C S Springer Jr - Special
Communication.
199. M M Pike and C S Springer Jr (1982) J.Magn.Reson., 46, 348.
200. M M Pike, D M Yermush, J A Balschi, R E Lenkinski and C S Springer
Jr (1983) Inorg.Chem., 22, 2388.
201. S C Chu, M M Pike, E T Fossel, T W Smith, J A Balschi and
C S Springer Jr (1984) J.Magn.Reson., 56, 33.
202. D Z Ting, P S Hagan, S I Chan, J D Doll and C S Springer Jr (1981)
Biophys.J., 34(2), 189.

203. M M Pike, S R Simon, J A Balschi and C S Springer Jr (1982)
Proc.Natl.Acad.Sci. USA, 79(3), 810.
204. J A Balschi, V P Cirillo, W J Le Noble, M M Pike, C E Schreiber Jr,
S R Simon, C S Springer Jr (1982) Rare Earths Med.Sci.Technol., 3,
15.
205. J A Balschi, V P Cirillo and C S Springer Jr (1982) Biophys.J.,
38(3), 323.
206. R A Iles, H N Stevens and J R Griffiths (1982) in "Progress in
Nuclear Magnetic Resonance Spectroscopy", Vol 15, parts 1/2, eds,
J W Emsley, J Feeney and L H Sutcliffe, Pergamon Press Ltd., New
York, 49.
207. D R Burton, S Forsen, G Karlstrom and R A Dwek (1979) Prog. NMR
Spectroscopy, 13, 1.
208. C C Hinckley (1969) J.Amer.Chem.Soc., 91, 5160.
209. J R Campbell (1971) Aldrichimica Acta, 4(4), 55.
210. R Von Ammon and R D Fischer (1972) Angew.Chem.Int.Ed. (English), 11,
675.
211. J Reuben (1973) "Progress in NMR Spectroscopy", 9(1), Pergamon
Press, Oxford.
212. B C Mayo (1973) Chem.Soc.Rev., 2, 49.
213. A F Cockerill, G L O Davis, R C Harden and D M Rackham (1973)
Chem.Rev., 73(6), 553.
214. J A Glasel (1973) in "Current Research Topics in Bioinorganic
Chemistry" ed, S J Lippard, Wiley, New York, 383.
215. R E Sievers (ed) (1973) "Nuclear Magnetic Resonance Shift Reagents",
Academic Press, New York.
216. J Reuben (1975) Naturwissenschaften, 62(4), 172.
217. G A Webb (1975) in "Annual Reports on NMR Spectroscopy" Vol 6A, ed,
E F Mooney, Academic Press, London and New York, 2.

218. B D Flockhart (1976) *CRC Crit.Rev.Anal.Chem.*, 6(1), 69.
219. K A Kime and R E Sievers (1977) *Aldrichima Acta*, 10(4), 54.
220. J Reuben (1979) in "Handb.Phys.Chem. Rare Earths", 4, 515, ed, K A Gschneidner Jr and LeRoy Eyring.
221. K G Orrell (1970) in "Annual Reports on NMR Spectroscopy", Vol 9, ed, G A Webb, Academic Press, London and New York, 1.
222. G A Elgavish and J Reuben (1981) *J.Magn.Reson.*, 42(2), 242.
223. F Inagaki and T Miyazawa (1982) *Prog.Nucl.Magn.Reson.*, 14(2), 67-111.
224. H N Cheng and H S Gutowsky (1980) *J.Phys.Chem.*, 84(9), 1039.
225. R J P Williams (1982) *Struct. Bonding (Berlin)*, 50, 79.
226. J K M Saunders and D H Williams (1970) *Chem.Commun.*, 422.
227. J Briggs, G H Frost, F A Hart, G P Moss and M L Staniforth (1970) *Chem.Commun.*, 749.
228. R E Rondeau and R E Sievers (1971) *J.Amer.Chem.Soc.*, 93, 1522.
229. D H Templeton and C H Dauben (1954) *J.Amer.Chem.Soc.*, 76, 5237.
230. P Laszlo (1967) *Prog. NMR Spectroscopy*, 3, 231.
231. R Foster and C A Fyre (1969) *Prog. NMR Spectroscopy*, 4, 1.
232. J Reuben (1973), *J.Amer.Chem.Soc.*, 95, 3534.
233. G A Elgavish and J Reuben (1976) *J.Amer.Chem.Soc.*, 98, 4755.
234. J Reuben (1977) *J.Amer.Chem.Soc.*, 99, 1765.
235. R E Lenkinski, G A Elgavish and J Reuben (1978) *J.Magn.Reson.*, 32, 367.
236. B L Shapiro and M D Johnston Jr (1972) *J.Amer.Chem.Soc.*, 94, 8185.
237. H M McConnell and R E Robertson (1958) *J.Chem.Phys.*, 29, 1361.
238. K Tori and Y Yoshimura (1973) *Tetrahedron Lett.*, 3127.
239. J J Uebel, C Pacheco and R M Wing (1973) *Tetrahedron Lett.*, 4383.
240. J Reuben (1973) *J.Magn.Reson.*, 11, 103.
241. R M Golding, R O Pascual and S Ahn (1982) *J.Magn.Reson.*, 46, 406.

242. R M Golding, Paper presented as ISMAR Conference, Chicago, September 1983.
243. R K Harris (ed) (1973) "Nuclear Magnetic Resonance - Specialist Periodical Reports", Vol 2, The Chemical Society, London, Ch.10.
244. R E Crammer and R Dubois (1973) J.Chem.Soc.Chem.Comm., 936.
245. W De W Horrocks jun (1974) J.Amer.Chem.Soc., 96, 3022.
246. H N Cheng and H S Gutowsky (1978) J.Phys.Chem., 82, 914.
247. W De W Horrocks jun (1977) J.Magn.Reson., 26, 333.
248. H A Bergen and R M Golding (1977) Austral.J.Chem., 30, 2361.
249. C L Honeybourne (1977) in "Nuclear Magnetic Resonance - Specialist Periodical Reports", Vol 6, 122, The Chemical Society, London; (1978) ib. Vol 7, 260; (1979) ib. Vol 8, 224.
250. G A Webb (1970) in "Annual Reports on NMR Spectroscopy", Vol 3, ed, E F Mooney, Academic Press, London and New York, 211.
251. S P Sinha (1967) "Europium", Springer-Verlag, Berlin.
252. F Inagaki and T Miyazawa (1982) in "Progress in NMR Spectroscopy", Vol 14, ed, Emsley, Freeney and Sutcliffe, 67.
253. (a) J A Wolhoff and J T G Overbeek (1959) Rec.Trav.Chim., 78, 759.
(b) M M Taqui Khan and P Rabindra Reddy (1974) J.Inorg.Nucl.Chem., 36, 607.
254. C C Bryden, C N Reilley and J F Desreux (1981) Anal.Chem., 53, 1418.
255. K G Morallee, E Nieboer, J F C Rossotti, R J P Williams and A V Xavier (1970) J.Chem.Soc. D, 1132.
256. C M Dobson, R J P Williams and A V Xavier (1974) J.Chem.Soc., Dalton Trans., 1762.
257. W D Horrocks and E G Hore (1978) J.Amer.Chem.Soc., 100, 4386.
258. C F G C Geraldes (1979) J.Magn.Reson., 36, 89.
259. J Lettvin and A D J Sherry (1977) J.Magn.Reson., 28, 459.

260. D A Gansow, A R Kavsar, K M Triplett, J J Weaver and E L Yee (1977) J.Amer.Chem.Soc., 99, 7807.
261. D A Gansow, K M Triplett, T T Peterson, R E Bolto and J D Roberts (1980) Org.Magn.Reson., 13, 77.
262. J J Dechter and G C Levy (1980) J.Magn.Reson., 30, 207.
263. W H Bearden, V M Cargin and W R Robertsen (1981) Org.Magn.Reson., 15, 131.
264. T J Wenzel, M E Ashley and R E Sievers (1982) Anal.Chem., 54, 615.
265. C R Malloy, T W Smith, J Delayre and E T Fossel (1983) Inorg.Chem., 22, 2388 (reference 265 cited therein).
266. K M Brindle, F F Brown, I D Campbell, C Gratwohl and P W Kuchel (1970) Biochem.J., 180, 37.
267. H Degani and G A Algavish (1978) FEBS Lett., 90, 357.
268. G A Elgavish (1982) Rare Earths Mod. Sci. Technol., 3, 193.
269. M K Hayer and F G Riddell (1984) Inorg.Chim.Acta., 92, L37.
270. F T Wall and R H Doremus (1954) J.Amer.Chem.Soc., 76, 868.
271. D R Davies and D E C Corbridge (1958) Acta.Cryst., 11, 315.
272. E Giesbrecht and L F Audrieth (1958) J.Inorg.Nucl.Chem., 6, 308.
273. P J Brophy, M K Hayer and F G Riddell (1983) Biochem.J., 210(3), 961.
274. E D Becker (1980) "High Resolution NMR - Theory and Chemical Applications", 2nd Ed., Academic Press, New York.
275. Jifi Koryta (1982) "Ions, Electrodes and Membranes", John Wiley & Sons, New York.
276. A D Bangham, M W Hill and N G A Miller (1974) in "Methods of Membrane Biology", 1, ed, E Korn, Plenum Press, London, 1.
277. D Papahadjopoulos (1978) Ann.N.Y. Acad.Sci., 308.
278. H J Müller-Eberhard (1975) Ann.Rev.Biochem., 44, 697.
279. B de Kruijff and R A Demel (1974) Biochim.Biophys.Acta., 339, 57.
280. M S Bretscher (1973) Science, 181, 622.

281. A D Bangham (1972) *Ann.Rev.Biochem.*, 41, 753.
282. D A Haydon and S B Hladky (1972) *Quart.Rev.Biophys.*, 5, 187
283. S C Kinsky (1972) *Biochim.Biophys.Acta.*, 265, 1.
284. D Chapman (1973) in "Biological Membranes", Vol.2, eds, D Chapman and D F H Wallach, Academic Press, London and New York.
285. P Mueller and D O Rudin (1969) in "Current Topics in Bioenergetics, Vo. 3", ed, D R Sanadi, Academic Press, New York and London.
286. A D Bangham (1968) in "Progress in Biophysics and Molecular Biology", eds, J A V Butler and D Noble, Pergamon Press, Oxford.
287. C L Khetrapal, A C Kurwar, A S Tracey and P Diehl (1975) in "NMR Basic Principles and Progress", Vol 9, ed, P Diehl, E Fluck and R Kosfeld, Berlin-Heidelberg, New York: Springer, 5.
288. L T Mimms, G Zanpighi, Y Nozaki, C Tanford and J A Reynolds (1981) *Biochemistry*, 20, 833.
289. F A Henn and T E Thompson (1960) *Ann.Rev.Biochem.*, 38, 341.
290. J W Nichols, M W Hill, A D Bangham and D W Deamer (1977) *Biochim.Biophys,Acta.*, 596, 393.
291. J W Nichols and D W Deamer (1980) *Proc.Natl.Acad.Sci., USA*, 77, 2038.
292. N R Clement and J M Gould (1981) *Biochemistry*, 20, 1534.
293. C M Biegel and J M Gould (1981) *Biochemistry*, 20, 3474.
294. P Schlieper and E DeRobertis (1977) *Biochim.Biophys,Res.Commun.*, 75, 886.
295. E M Choy, D F Evans and EL Cussler (1974) *J.Amer.Chem.Soc.*, 96, 7085.
296. J B Smith and E Rozengurt (1978) *Proc.Natl.Acad.Sci., USA*, 75, 5560.
297. R Sandeaux, P Seta, G Jeminet, M Alleaume and C Gavach (1978) *Biochim,Biophys.Acta.* 511, 499.
298. J Sandström (1982) "Dynamic NMR Spectroscopy", Academic Press, London.

299. H Degani and G A Elgavish (1978) FEBS Lett., 90, 357.
300. B G Cox, Private communication.
301. R T Hamilton and M Nilsen-Hamilton (1980) Biochim.Biophys.Res. Commun., 95(1), 140.
302. S McLaughlin, N Mulrime, R Grisalfi, G Vaio and A McLaughlin (1981) J.Gen.Physiol., 77, 445 and references therein.
303. O Söderman, G Arvidson, G Lindblom and K Fontell (1983) Eur.J.Biochem., 134, 309 and references therein.
304. S Forsen and R A Hoffmar (1963) J.Chem.Phys., 39, 2892.
305. S Forsen and R A Hoffmar (1963) Acta.Chem.Scand., 17, 1787.
306. S Forsen and R A Hoffmar (1964) J.Chem.Phys., 40, 1189.
307. R A Hoffman and S Forsen (1966) J.Chem.Phys., 45, 2049.
308. G A Morris and R Freeman (1978) J.Magn.Reson., 29, 433.
309. D E Dishong, C J Diamond, M I Cinoman and G W Gokel (1983) J.Amer.Chem.Soc., 105, 586.
310. S P Bag, Q Fernando and H Freiser (1962) Inorg.Chem., 1, 887.
311. E Riegel and M C Reinhard (1926) J.Amer.Chem.Soc., 48, 1334.
312. H Betz and U Weiser (1976) Eur.J.Biochem., 62, 65.
313. A D Bangham and R W Horne (1964) J.Mol.Biol., 8, 660.
314. H Fernandez-Moran (1962) in "The Interpretation of Ultrastructure", ed, R J C Harris, Academic Press, London and New York.